UNIVERSITÉ D'ORLÉANS

ÉCOLE DOCTORALE
SANTE, SCIENCES BIOLOGIQUES ET CHIMIE DU VIVANT

Unité de recherche Amélioration, Génétique et Physiologie Forestières
INRA Val de Loire

THÈSE présentée par:

Amra ŠEĆEROVIĆ

Soutenue le: **29 novembre 2016**

Pour obtenir le grade de: **Docteur de l'université d'Orléans**
Discipline/ Spécialité: Biologie (Physiologie cellulaire et moleculaire des plantes)

Identification and characterization of molecular players potentially responsible for the mechanical properties of tension wood

THÈSE dirigée par:

Gilles PILATE	Directeur de recherche, AGPF, INRA Val de Loire
Annabelle DEJARDIN	Chargée de recherche, AGPF, INRA Val de Loire

RAPPORTEURS:

Simon HAWKINS	Professeur, Université de Lille
Nathalie LEBLANC	Maitre de conférences, PIAF, Université Blaise Pascal

---

JURY:

Eric LAINE	Professeur, Université d'Orléans, Président du jury
Simon HAWKINS	Professeur, Université de Lille
Nathalie LEBLANC	Maitre de conférences, PIAF, Université Blaise Pascal
Carole ASSOR	Chargée de recherche, IATE, Montpellier
Annabelle DEJARDIN	Chargée de recherche, AGPF, INRA Val de Loire
Gilles PILATE	Directeur de recherche, AGPF, INRA Val de Loire

ACKNOWLEDGMENTS

Firstly, I would like to thank to the jury members **Simon Hawkins** and **Nathalie Leblanc-Fournier** for kindly accepting to evaluate work presented in this thesis.

I further acknowledge **Gilles Pilate** and **Annabelle Déjardin** for the given opportunity and confidence in making this thesis under their supervision in AGPF research unit. I thank you, Gilles, for friendly and attentive supervisory approach along my thesis. Annabelle, I am sincerely grateful for the opportunity to make the first scientific steps with you, as for the accomplishment of the further one, all by virtue of your kindness, reasonableness and professionalism. I finally thank both of you for the given time and willingness to discussions, as for punctilious and valuable advices, which have shed a new light on my scientific perspectives.

I further thank to colleagues from AGPF unit for their contribution to experiments preformed in frame of this thesis.

I acknowledge **Marie-Claude Lesage Descauses** for the kind hospitality in the laboratory of molecular biology, where most of my work was performed. I express my gratitude for your enormous help at the end of my thesis, as for in work given confidence, liberty and severity, your professionalism and care about (foreign) students.

I thank to **Françoise Laurans** who kindly enabled performance of experiments in the laboratory of histology, as for transmission of the acquired knowledge. I equally thank to **Véronique Laine Prade** for technical help in the same laboratory.

To **Nathalie Boizot** I thank for the assistance in the laboratories of proteomics and biochemistry, always accompanied with her smile and great kindness.
I equally thank to platform Genobois headed by **Jean-Paul Charpentier** and associated laboratories of biochemistry and spectroscopy in frame of which the experiments were executed with notable technical assistance of **Kevin Ader**.

My sincerest acknowledgment goes to **Vincent Segura** for substantial contribution to results through the statistical analyses and, moreover, for encouragements, numerous discussions and the given advices during my thesis.

I sincerely thank to **Jean-Charles Leplé** for providing and analysing RNA sequencing data, as for the great willingness for discussions and sharing of knowledge.

Many thanks to **Nassim Belmokhtar** for allowing me to perform his newly developed saccharification test and, above, encouragements and shared moments always so full of positive energy and laugh.

I also thank to **Frédéric Millier** for the preparation of wood samples for biomechanical measurements, to **Jean-Charles Gaudin** for the essays of heterologous protein expression, **Jean-Léandre Haton** for the informatical assistance and **Franck Rogeon** for the assistance in bibliography research.

Work on this thesis required a great amount of time spent in the greenhouse. Many thanks to **experimental unit** headed by **Patrick Poursat** for the assistance in care of plants, providing of material and technical maintenance of the greenhouse. Equally, I thank to **Jacky Despras** and **Jonathan Riant** for the help with construction and installation of tilting supports.

Multidisciplinary collaboration accomplished through the project Stress In Trees allowed me to meet and to work with the scientist from the domain of biomechanics. I thank to **Bruno Clair** as head of the project for incentive discussions, willingness for organization of biomechanical measurements and for kind hospitality of unforgettable expedition to French Guiana. I equally thank to **Tancrède Alméras** for the great contribution in setting, performance and analysis of biomechanical experiments. I am equally thankful for having in the frame of the project the opportunity to meet **Olivier Arnould** and **Carole Assor**. To PhD student **Barbara Ghislain**, I thank for the cheerful moments spent during the annual meetings of the project.

I sincerely thank to **Eric Badel** and PhD student under his supervision **Benjamin Niez** for preforming the biomechanical measurements at PIAF unit in Clermont-Ferrand.

I would also like to thank to colleagues with who I did not have an opportunity to share working tasks, but to spent pleasant moments in discussions at AGPF unit: **Vanina Guerin**, **Bénedicte Le Guerroué**, **Corrine Buret**, **Céline Ridel**, **Yves Rousselle**, **Christian Breton**, **Marie-Anne Lelu-Walter**, **Marc Villar**, **Catharine Bastien** and **Jean-Charles Bastien**.
Special thanks to **Véronique Jorge**, **Leopoldo Sanchez-Rodriguez** and **Facundo Muñoz** for cheerful moments and fruitful discussions during lunch breaks and for the encouragements during my thesis.

I would certainly not forget the former PhD students **Fernanda Guedes** and **Wassim Lakhal** for pleasent and sincere friendship at the beginning of my thesis, so as **Josipa Atlija**, **Monika Tunjić** and **Erica Lupi** for all the enjoyable time during their internships at INRA. Josipa, thank you for being so supportive and caring.

I would also like to thank to the present PhD students at AGPF with the sincere wishes for successful completion of their theses: **Alexandre Marchal**, **Cathy Bouffartigue**, **Florian Gautier**, **Marie Pegard**, **Mesfin Gebreselassie** and **Thibaud Chauvin**.

Three years of work on this thesis and life in France allowed me to raise the new educational level not only regarding science, then equally French culture. Along the way, I have had the fortune to meet people with who I spent enjoyable and unforgettable time.

Thank you **Marija Mazor** for spreading the positive energy, your support and care, numerous moments of sincere joy, laugh, mind-opening discussions and travels. It has been my pleasure for being able to share this brave and rich journey in France with you.
Modar, realizing the moment that we are communicating on language neither one of us spoke shortly before, have been such a joyful and unforgettable fulfillment. Thank you for being a loyal friend and support along the way.
Marija Ćosić, if there was no so many times mentioned karma, I would be deprived of the precious time that I spent with you in the exchange of knowledge, thoughts and laughs in everyday moments. I thank you and I wish you the greatest luck in accomplishment of your scientific dreams.

Without our friendship, **Arnaud**, this experience would definitively be impoverished. Thank you for being an honest, supportive and attentive friend, and most of all thank you for many unforgettable and entertaining moments, so as for the precious moments of life reviewing.

I also thank to **Anthony Venon** for his gentleness and unforgettable experiences, **Rafiou** for support and memories, **Antoine** for being such great dance partner and friend, **Souleymane** for support and kind friendship, **Estelle Ancelet**, **Sebastien Lehmann** and **Mercedes Roman Dobarco** for their kindness and shared moments.

Special thanks to **Sylvie Doisneau** who ennobled this experience with her great energy, French language and culture.

I would also like to thank to families Buret, Dowkiw, Lehmann, Marks and Venon for hosting me in their homes while being far from my own…

Although not mentioned, I keep in my heart all those people I met along the way and shared equally fulfilling moments in France.

Matija, for raising a new level of my life - thank you.

To my longtime friends in Croatia, **Elvana**, **Jadranka**, **Jelena**, **Lidija**, **Maja**, **Nina** and **Tea**, I thank for their support and patience along these three years.

*I express the greatest acknowledgement to my parents **Mirsada** and **Džavid** for their unconditional support, understanding and sacrifice given to my brother and me. Our accomplishments are a reward for your diligence, modesty and kindliness in life. With all the love and respect, I thank you mom, for all these years you have been continuously breathing for us. To my brother **Kenan** and his wife **Elma**, I sincerely thank for the momentous support and sentimental care during my thesis.*

*I dedicate this work to my beloved grandmother **Hajrija**, persistent in the belief and spread of learning as a life-long process.*

TABLE OF CONTENTS

LIST OF PRINCIPAL ABBREVIATIONS

AGP	Arabinogalactan protein	**MIR**	Middle InfraRed
ANR	Agence Nationale de la Recherche	**MS**	Murashige and Skoog
At	*Arabidopsis thaliana*	**NW**	Normal wood
BGAL	Beta-galactosidase	**OW**	Opposite wood
bp	Base pairs	**PCR**	Polymerase chain reaction
cDNA	Complementary DNA	**PCW**	Primary cell wall
CESA	Cellulose synthase	**Pta**	*Populus tremula x alba*
CMF	Cellulose microfibril	**Ptr**	*Populus trichocarpa*
CML	Compound middle lamella	**RG-I**	Rhamnogalacturonan-I
COBL	Cobra-like	**RNA**	Ribonucleic acid
CTL	Chitinase-like	**RNAi**	Interference RNA
DNA	Deoxyribonucleic acid	**RT**	Reverse-transcription
Eg	*Eucalyptus grandis*	**RT-PCR**	Reverse transcription polymerase chain reaction
FLA	Fasciclin-like arabinogalactan	**RT-qPCR**	Reverse transcription quantitative polymerase chain reaction
G	Gelatinous	**S1/S2**	Secondary cell wall layer 1 and 2
INRA	Institut National de la Recherche Agronomique	**T-DNA**	Transfer DNA
KOR	Korrigan	**TW**	Tension wood
Lus	*Linum usitatissimum*	**WT**	Wild-type

PREFACE

The work presented in this thesis was wholly conducted in AGPF (Amélioration Génétique et Physiologie Forestières) research unit at INRA Val de Loire in Orléans in France. It was financed from the ANR Blanc project Stress In Trees ANR-12-BS09-0004. Most experiments relied on the greenhouse facilities of GBFOR Experimental Unit and the XYLOBIOTECH technical facility of XYLOFOREST platform (ANR-10-EQPX-16). The project is based on multidisciplinary approach in molecular physiology and biomechanics, and aims in deciphering mechanism of tensile stress generation in tension wood, using poplar and simarouba as the biological models.

The thesis is divided in chapters:

- "Introduction" concerning the bibliographic study about tension wood, objectives of the thesis and experimental strategy;
- "Materials and methods" used in the experimental work;
- "Results" concerning the first draft of article about chitinase-like protein intended for submission in a journal, other obtained results in the studies of fasciclin-like arabinogalactan proteins, beta-galactosidase and simarouba, and discussions following each part of the results
- "General discussion", which ends with proposed model of molecular regulation of the tensile stress generation in the G-layer, based on the results presented in the thesis.

The scientific productions resulted from the work presented in this thesis are listed on the next page.

Article

Šećerović A, Lesage-Descauses MC, Laurans F, Segura V, Belmokhtar N, Leplé JC, Niez B, Badel E, Almeras T, Clair B, Déjardin A, Pilate G, ***PtaCTL2*** **encodes chitinase-like protein required for cellulose structure, secondary cell wall organization and mechanical strength of poplar stems,** intended for submission in Journal of Experimental Botany

Oral communications

Šećerović A, Lesage-Descauses MC, Lainé-Prade V, Laurans F, Leplé JC, Segura V, Badel E, Clair B, Pilate G, Déjardin A, **Effects of *CTL2* down-regulation on tension wood formation in GM poplars**, XIV International Cell Wall Meeting, Chania, Greece, 13-17 June 2016

Šećerović A, Guedes F T P, Lesage-Descauses M-C, Millet N, Lainé-Prade V, Laurans F, Leplé JC, Déjardin A, Pilate G, **β-galactosidase: un role dans les couches G du bois de tension?**, Congrès Réseau Français des Parois, Amiens, France, 07-09 July 2014

Poster communication

Šećerović A, Guedes F T P, Lesage-Descauses M-C, Millet N, Lainé-Prade V, Laurans F, Leplé JC, Déjardin A, Pilate G; **β-galactosidase: a function in tension wood G-layers?**, Biotechnocentre, Seillac, France, 09-10 October 2014

INTRODUCTION

Bibliographic study

1. GROWING INTEREST FOR WOOD

Roughly, 3 trillion of trees on Earth (**Crowther *et al.*, 2015**) play an indispensable role in the ecosystem through the exchange of carbon dioxide and oxygen. Trees are principally made of roots, which withdraw the nutrients and water from soil, and of trunk, which harbours branches and leaves in search for light and the execution of photosynthesis. The trunk and branches are made of wood, which provides mechanical support and conducts water and nutrient transport from the roots to the crown.

Trees are an inexhaustible source of scientific researches because of their interactions with other species, such as the symbiosis of roots with fungi, or physiological regulatory mechanisms of growth control and adaptation to the environment, as to biotic and abiotic stresses. Humans exploit trees for commercial use of wood. The outstanding mechanical properties make wood a desirable material for timber industry, the reputable energetic values an effective heating source, and the high lignocellulosic content a desirable biomass for paper production. Lately, a downtrend of sustainable wood resources reinforced efforts for their preservation. On the other side, the accelerated development of techniques has put a focus on adaptation of wood properties intended for production of the second-generation biofuels, as the case for lignin-deficient poplars (**van Acker *et al.*, 2013**).

1.1. Poplar as a model for wood studies

Poplar/cottonwood/aspen are angiosperm trees, which belong to the Salicaceae family and *Populus* genus. The genus comprises up to 35 species native to the temperate and boreal regions of Europe, China, southern Canada and northern America (**Isebrands and Richardson, 2014**). Poplar trees are well adapted to the alluvial soils and require a high amount of water for their growth. The native poplar species in Europe are *Populus alba*, *Populus nigra* and *Populus tremula* (**Fig. 1**). The species commonly used in plantation for wood production in France are interamerican (*Populus trichocarpa* x *Populus deltoides*) and euramerican (*P. nigra* x *P. deltoides*) hybrid poplars. In cultivation, poplars are reputable for an easy propagation and rapid juvenile growth. Soft and flexible wood of poplar is valuable as a pulp resource for paper production, and is exploited as wrapping and lining material in food and timber industry, respectively (http://www.peupliersdefrance.org/n/les-utilisations-du-peuplier/n:1137).

Poplar is widely used as a tree model in biological studies because of its fast growth, easy vegetative propagation, the availability of genetic and genomic resources and the availability of techniques for genetic transformation. These characteristics were crucial for the choice of North-American poplar species *Populus trichocarpa* as the first sequenced tree genome (**Tuskan *et al.*, 2006**). The genome (v3.0) is available on Phytozome portal (https://phytozome.jgi.doe.gov/pz/portal.html#). In addition, gene expression data from *P. trichocarpa* and *P. tremula* are available through The Populus Genome Integrative Explorer (**Sundell *et al.*, 2015**).

The genome of poplar is organized in 19 chromosomes. Its size (422.9 Mb) and compactness are convenient for genomic researches, often compared with those conducted on the widely used plant model - *Arabidopsis thaliana*. The genome sequencing facilitated molecular studies of the xylem development in trees (reviewed in **Ye and Zhong, 2015**) and the genetic control of wood adaptive traits (reviewed in **Plomion *et al.*, 2016**).

Genetic engineering is an invaluable tool used to unravel functions of numerous genes potentially involved in wood formation. It is as well beneficial in direct targeting of biomass composition (i.e. lignin), which represents an improvement of economic

interest (**Pilate *et al.*, 2002**). However, the generation of gene-targeted mutants is still more successful in Arabidopsis than in woody plants as poplar. Some tools for the large population mutagenesis have been particularly restricted in trees due to their outcrossing, high heterozygosity, tree massiveness or late fertilization (**Busov *et al.*, 2005a**). The most common transformation system for gene-targeted modifications in trees is the T-DNA transfer via *Agrobacterium tumefaciens*. However, transformation protocols have been raised only for a small number of poplar genotypes (**Busov *et al.*, 2005b**). One example is the transformation protocol for the *P. tremula* x *P. alba* hybrid 717-1B4 clone (**Leplé *et al.*, 1992**). Recently, CRISPR/Cas9-mediated mutagenesis was reported as a prospective and highly efficient system in the generation of targeted mutations in stable transgenic poplars (**Fan *et al.*, 2015**).

Figure 1. *Populus nigra* and *Populus alba* growing wild in nature (photo credits: *M. Villar* and *M. Sabatti*)

1.2. Wood properties

1.2.1. Formation and structure

Xylogenesis

Wood is a vascular tissue formed during the secondary growth of stem in a multistep process called xylogenesis (**Fig. 2**). In angiosperm/hardwood trees, cells of the meristematic vascular cambium divide towards the inner parts of the trunk to generate secondary xylem composed of three cell types. After completing their expansion and elongation, cells start depositing secondary cell walls in which lignin gets progressively incorporated. Lignification is rapidly accompanied by the loss of cellular content and programed cell death (**Déjardin *et al.*, 2010**).

High number of transcription factors regulate each step of wood formation, from cambial activity to secondary wall biosynthesis. A significant progress has been made in their identification and functional characterization (reviewed in **Ye and Zhong, 2015**).

Cell types

Xylem is formed of axially orientated fibres and vessels and radially orientated parenchyma ray cells (**Fig. 2**). Each cell type has their specific functions, which contribute to the growth and life of the tree. The rays have function as a temporary reserve storage during the winter and in intercommunication between the phloem and xylem. This is also the only cell type, which may remain alive for several years before the cell death (**Déjardin *et al.*, 2010**). The vessels are the largest cells in diameter and have function in water conduction over long distances. The fibers are the most abundant cell type, which provide stiffness to wood and mechanical support to tree (**Déjardin *et al.*, 2010**).

Cell walls and layers

The xylem cells are composed of the primary cell wall (PCW) deposited while young cells undergo division and expansion, and the thick lignified secondary cell wall (SCW) made of three layers called S1, S2 and S3. The S2-layer accounts for the majority of the cell wall and is important for the physical and mechanical properties of wood (**Barnett and Bonham, 2004**). The property is linked to the parallel arrangement and orientation of cellulose microfibrils at an angle much lower in the S2-layer than in the S1- and S3-layers in which the angle is almost perpendicular to the longitudinal fiber axis. In the primary cell wall, cellulose microfibrils are arranged randomly within the cell wall (**Plomion *et al.*, 2001**). The alternation of high and low angles between the layers increases rigidity and mechanical strength of the cell wall (**Déjardin *et al.*, 2010**). The cells are linked to each other by firstly deposited pectic middle lamella, which gets heavily lignified in woody cells (**Plomion *et al.*, 2001**).

The cell walls are principally formed of cellulose microfibrils (CMF) entrapped in amorphous matrix made of hemicelluloses and lignin (**Déjardin *et al.*, 2010**). All the components get assembled into the cell wall network by physical interactions, enzymatic ligations and crosslinking reactions. The cell wall (CW) formation is regulated for synthesis and transport of CW precursors and CW polymer biosynthetic enzymes, and the assembly of components into the cell wall (**Kumar *et al.*, 2016a**).

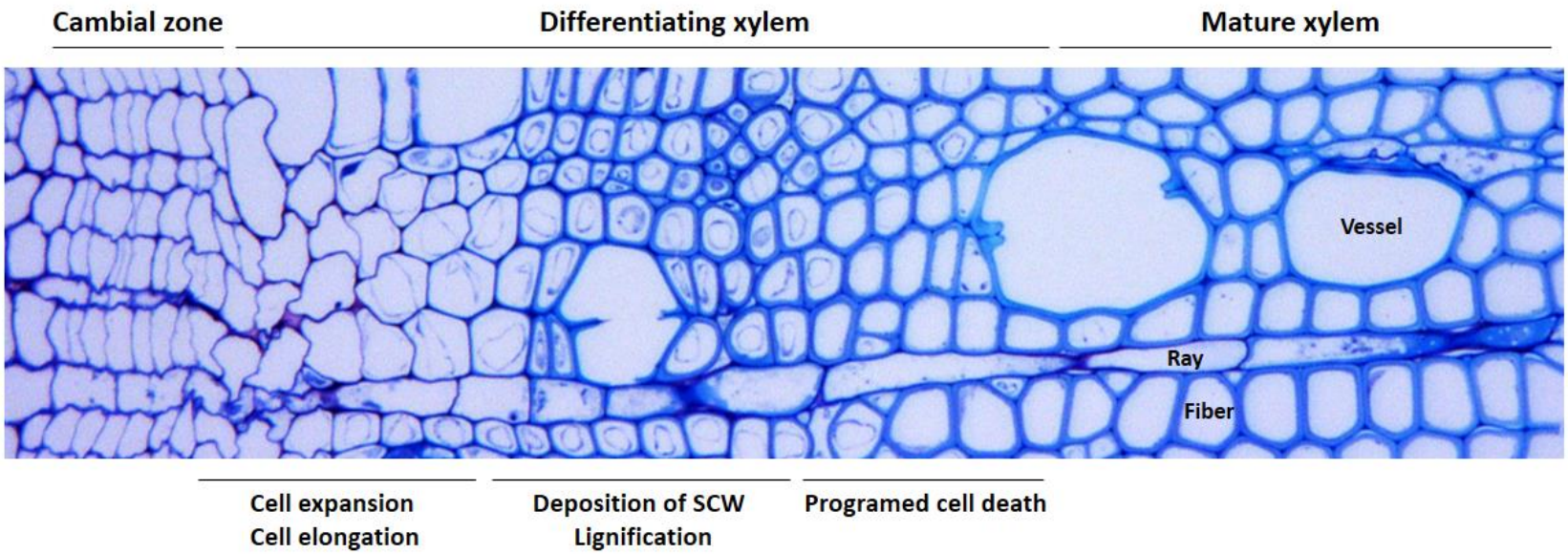

Figure 2. Wood formation visible on the stem cross-section of poplar (*P. tremula* x *P. alba*). The expansion and elongation of cells is initiated from cambial tissue. These cells have only primary cell wall. Once shaped, cells undergo deposition and progressive lignification of the secondary cell wall. Finally, programed cell death leads to formation of mature cells. Xylem (wood) is formed of the three types of specialized cells: vessels, rays and fibers.

1.2.2. Chemical composition

Lignin

Lignin is a heterogeneous polymer made from the *p*-hydroxylphenyl (H), guaiacyl (G), and syringyl (S) units. Polymerisation of the units is in the cell wall catalysed by oxidative enzymes peroxidase and/or laccase. Proportion of the units significantly varies between species and cell wall types. In the secondary cell walls, lignin is mostly constituted of the G and S units, while it contains the H unit in small amounts (**Kumar *et al.*, 2016a**). Lignin is in the secondary cell wall interspersed between cellulose microfibrils to provide the cell wall with: i) compression strength important for the mechanical properties, ii) hydrophobicity important for water conduction, iii) resistance to pathogens. Lignin constitute approximately 20% of the cell wall content (**Mellerowitz and Gorshkova, 2012**).

Cellulose

The major wood component is cellulose, which accounts for around 40% of the total cell wall content (**Baba *et al.*, 2009**). Cellulose is a structure of linear β-1,4-glucan chains, which get synthesized at the plasma membrane by cellulose synthase complex (CSC). The complex is made of CESA proteins organized in hexameric rosettes, which get assembled in Golgi bodies and transported to plasma membrane (**McFarlane *et al.*, 2014**). In poplar, CESA family consists of 18 proteins (**Djerbi *et al.*, 2005**) and four of them make CSC, which synthesize cellulose in secondary cell wall (**Aspeborg *et al.*, 2005**).

As previously stated, cellulose microfibrils are in the secondary cell wall deposited under an angle with respect to the longitudinal fiber axis. What controls such deposition of microfibrils is still insufficiently understood. However, it is known that cellulose microfibrils coalign with cortical microtubules, which make the cytoskeleton. It was suggested that other factors as extracellular matrix of polysaccharides or proteins may also guide the cellulose deposition (**McFarlane *et al.*, 2014**).

Cellulose microfibrils can crystallize into larger macrofibrils through inter- and intramolecular hydrogen bonds and Van der Waals forces (**McFarlane *et al.*, 2014**). The aggregation into the crystalline structure stiffen the cell wall, but also promotes

cell wall flexibility. Crystalline cellulose has a very limited accessibility to water and chemicals, which are expected to target amorphous cellulose and crystalline surface (**Wagberg and Annergren, 1997**).

Hemicelluloses

Hemicelluloses are the structurally variable polysaccharides synthesized in the Golgi apparatus and transported and submitted to modifications in the cell wall (**Kumar *et al.*, 2016a**). They are essentially amorphous and can be easily removed by alkaline treatment after elimination of lignin (**Heredia *et al.*, 1995**).

Xyloglucan is the most abundant hemicellulose in the primary cell walls of dicots. It is strongly associated with cellulose microfibrils via hydrogen bonds and is thought to represent the major load-bearing structure of growing plant cell walls, probably in association with extensins (**Pauly and Keegstra, 2016**). Another function prescribed to xyloglucan is a spacer polymer, which prevents the formation of cellulose superaggregates, or as an adapter, which interfaces between cellulose and other polymers (**Pauly and Keegstra, 2016**). It consists of a β-1,4-linked glucan backbone substituted with xylosyl residues, which may be further substituted with a diverse array of glycosyl and non-glycosyl residues. Their structures vary among plant species, tissue and cell types, and developmental stage of a cell (**Pauly and Keegstra, 2016**).

Xylan is dominant hemicellulose in the secondary cell walls of angiosperms (**Mellerowicz and Gorshkova, 2012**) and the most abundant sugar after cellulose. It is synthesized in the Golgi apparatus by coordinated action of synthetic transmembrane enzymes with activity towards substrates synthesized in cytosol and Golgi lumen (**Rennie and Scheller, 2014**). Xylan is made of a backbone of β-(1,4)-linked xylose residues decorated in dicots with α-(1,2)-glucuronic acid and 4-O-methyl-glucuronic acid (**Kumar *et al.*, 2016a**). The substitutions of xylan affect its solubility and conformations important for crosslinking of cellulose microfibrils coated by xylan. Glucuronic acid of xylan may covalently bind to lignin via ester bounds (**Rennie and Scheller, 2014**).

Mannan is the dominant hemicellulose in the secondary cell wall of gymnosperms (**Mellerowicz and Gorshkova, 2012**). In the plant cell walls, its function is imparting cell wall rigidity. It has industrial application as gelling agent and stabilizer (**Pauly *et al.*, 2013**). Mannan is a structure of linear β-(1,4)-mannose chain. It often comes in a complex with other monosaccharides to form variable structures as galactomannans, glucomannans and galactoglucomannans (**Kumar *et al.*, 2016a**). The mannan itself and galactomannan consist of a backbone made of only β-1,4-linked mannose, while glucomannan and galactoglucomannan have both the β-1,4-linked mannose and glucose units in their backbones. The mannosyl residue can be substituted with α-1,6-linked galactosyl residue (only the case for galactomannan and galactoglucomannan) or O-acetylated at the O-2 and O-3 positions (**Pauly *et al.*, 2013**). A higher degree of substitution is associated with the increased polymer solubility (**Pauly *et al.*, 2013**).

Pectins

Pectins are complex polysaccharides, water soluble when highly esterified, chemically soluble when linked with ionic bonds to calcium or covalently to hemicelluloses, celluloses or proteins (**Heredia *et al.*, 1995**). In plant cell walls, the most abundant pectins are homogalacturonans (HG), type-I rhamnogalacturonans (RG-I) and type-II rhamnogalacturonans (RG-II). The pectins influence cell wall charge and porosity, and have functions as ligands for cell wall sensors responding to modified cell wall mechanics or pathogen attack (**Anderson, 2016**).

Homogalacturonan is the most abundant form of pectin in primary cell walls of eudicots. It is a structure of unbranched α-1,4-linked galacturonic acid chains, which can be decorated with xylose, apiose or acetyl groups at the O-2 and O-3 positions (**Anderson, 2016**). The carboxyl groups of galacturonic acid can be methyl-esterified and negatively charged when de-methyl-esterified, thus affecting the chemistry of homogalacturonan (**Anderson, 2016**).

Rhamnogalacturonan-I (RG-I) pectin is formed of a backbone made of repeating α-(1,4)-galacturonic acid and α-(1,2)-rhamnose. The side chains attached to the

backbone may be composed of α-(1,4)-arabinan, β-(1,4)-galactan or type-I arabinogalactan (β-(1,4)-galactose linked to α-(1,5)-arabinose).

Rhamnogalacturonan-II (RG-II) is structurally complex pectin constituted of homogalacturonan-like backbone modified with four different side chains formed of 12 different monosaccharide units (**Anderson, 2016**).

Proteins

Cell wall proteins have function in cell wall structure, modifications of cell wall components, cell wall signalling and interactions with plasma membrane proteins (**Jamet, 2006**). They may be bound to plasma membrane forming a plasma membrane-cell wall continuum (**Kumar *et al.*, 2016a**). The binding is facilitated by GPI anchor attached to C-terminus of a protein.

Expansins are important group of structural cell wall proteins, which exist in plants in two families. The α-expansins target tight-contact zone of cellulose microfibrils and act as the mediators of primary cell wall loosening in a pH-dependent manner. α-expansins lack a lytic activity. The β-expansins are the group-1 grass pollen allergens, which facilitate the pollen tube invasion of the stigma by dissolving the middle lamella (**Cosgrove, 2015**).

Depending on the abundance of aminoacids or polysaccharide chains, proteins are divided in the groups of: glycine-rich proteins, proline-rich proteins, hydroxyproline-rich proteins and arabinogalactan-rich proteins (**Showalter, 1993**). Extensins and arabinogalactan proteins (AGP) from hydroxylproline–rich group of proteins will be described below.

Extensins are proteins rich in hydroxyproline and serine, usually structured in the repeating pentapeptide motif Ser-Hyp_4. Most of hydroxyproline residues are glycosylated with one to four arabinosyl residues, and some of serine residues are glycosylated with single galactose unit (**Showalter, 1993**). Some extensins form intramolecular crosslinks to modify its usually rod-like structure, and some form intermolecular crosslinks within the cell wall network, which is potentially important

for the cell growth. Extensins interact with pectin, but a functional significance of these interactions is not known (**Showalter and Basu, 2016**).

The cell walls are enriched in *arabinogalactan proteins* (AGP) constituted of hydroxyproline-rich core protein to which polysaccharide side chains are attached by β-links. The attachment is rich in arabinose and galactose, sometimes glucuronic acid and some other less abundant sugars. The side chains exhibit the arabinogalactan type-II glycan structure formed of β-1,3-galactan backbone on which β-1,6 galactan side chains are attached and modified by arabinose or other sugar units. The sugar attachment makes most of the AGP's weight (**Showalter, 2001**). AGPs are secreted to plasma membrane, cell walls, intracellular spaces or culture media; expressed in leaves, stems, roots, floral parts and seeds; and are found highly abundant in xylem, stylar transmitting tissue and cell suspension cultures. Functionally, AGPs were related to vegetative, cellular and reproductive growth; development and programmed cell death, and to molecular interactions and signalling (**Showalter, 2001**). In Arabidopsis, a high number of AGPs is divided into subgroups of classical AGPs, lysine-rich AGPs, arabinogalactan peptides, fasciclin-like AGPs, non-classical AGPs and nodulin-like proteins (**Li *et al.*, 2010**). The classical AGPs have C-terminal domain with glycosylphosphatidylinositol (GPI) anchor, which is likely responsible for AGPs mobility at the surface of plasma membrane and localized delivery in the cell wall. AGPs have high water-holding capacity and are subject to cross-linking to form aggregates responsible for their adhesive nature (**Showalter, 2001**). AGPs are proposed to decrease pectin alignment and crosslinking in the cell wall, thus increasing the porosity of pectin network (**Lamport *et al.*, 2005**). Some xylem-associated AGPs were linked to the secondary cell wall thickening and programmed cell death by positioning or interaction with the cell wall components or themselves at the cell surface (**Showalter, 2001**). AGPs were also proposed to have function in microfibril orientation in order to control the cell expansion (**Verbelen *et al.*, 2001**). Periplasmic AGP is a capacitor of calcium ions whose release from and recycling to the membrane regulates AGP exocytosis and plant growth (**Lamport *et al.*, 2014**).

2. TENSION WOOD

2.1. Modulation of the tree orientation

Mechanical strain in wood

While elongating their axis in the orientation towards light and negative gravity, trees are constantly exposed to growth stresses/strains. Such stresses originate from the longitudinal constrains in the stem, which are the consequence of wood natural tendency to shrink, impeded by attachment of newly formed fibers to mature fibers (**Almeras *et al.*, 2009**).

Formation of reaction wood

The growth strains get even exceeded when various environmental and mechanical loads as snow, wind or uneven ground stimulate complementary movements of stems and branches (**Fig. 3a**). On such obstructions, trees adapt their axes (reorientation) and prevent from breaking (reinforcement) by the production of atypical reaction wood. In the reaction wood, strain is up to 5 times higher than in normal wood (**Fournier *et al.*, 1994**).

Angiosperms and gymnosperms set up different kind of reaction wood mechanisms resulting in the formation of tension and compression wood, respectively. While tension wood (TW) is produced at the upper side to pull tilted stems and branches, compression wood formed at the lower side generates pushing compression force. Reaction wood is easily recognizable on stem cuts since the increased activity of vascular cambium on the reaction side causes pith eccentricity (**Fig. 3b**). A mean division rate of tension wood fibers from greenhouse-grown poplars is approximately 3 hours (**Abedini *et al.*, 2015**). As opposed to reaction side gets formed opposite wood (OW), structurally more similar to normal wood (NW). The focus in the following sections will be put on studies of tension wood as the main object of the presenting thesis.

Tilting perception

It is still poorly understood where the tilting signal is perceived and how is it transmitted to the cambium. Significant efforts have been lately devoted to decipher this mechanism. The recent pioneer study performed on woody cells showed that tilting signal is perceived in endodermal cells through sedimentation of starch-filled amyloplast. The sedimentation then causes relocalization of the auxin transport protein PIN3 toward the cambial zone on tension wood side and cortex on opposite wood side, resulting in the asymmetric cambial growth (**Gerttula *et al.*, 2015**). Apart from auxin, plant hormone gibberellin (**Nugroho *et al.*, 2013**) and ethylene (**Love *et al.*, 2009**) were shown to stimulate elongation and division of tension wood fibers, respectively.

Tension wood properties

Tension wood has different mechanical, anatomical and chemical properties than opposite wood (**Fig. 4**). In poplar, TW has an increased proportion of fibers and rays, and a decreased proportion of vessels (**Jourez *et al.*, 2001**). The main anatomical characteristic of TW is G-fiber, which was detected in around half of the dicotyledonous species (**Fischer and Stevenson, 1981**). Properties of the G-fiber will be thoroughly described in the next chapter.

The G-fiber can be also found in thorns, coiling tendrils, twining wines, contractile roots, corms, peduncles and phloem (**Mellerowicz and Gorshkova, 2012**). We could anticipate that the G-fibers of different origins may have specialized and common function in the tilting of axes by generation of high tensile strains. It should be noted that in the case of xylem fibers, it was shown that high tensile stresses are effectively generated in TW of species - which do not produce G-fibers (**Clair *et al.*, 2006a**).

Composition of tension wood

Bentum *et al.* (**1969**) observed that fibers of normal wood and tension wood contain the same amount of lignin originating from S1 and S2 layers.

A pioneering study of polysaccharide composition in TW in poplar showed that it is composed exclusively of glucose and xylose, with proportions respectively increased

for 14% and decreased for 8% in comparison to OW. Galactose was found only in traces (**Norberg and Meier, 1966**). A similar study detected small quantities of galactose, mannose and arabinose (**Timell, 1969**). The very recent monosaccharide analysis performed with advanced techniques showed that, in comparison to normal wood, TW contains increased proportions of glucose, galactose, rhamnose and galacturonic acid, and decreased proportion of xylose, mannose and glucuronic acid (**Gorshkova *et al.*, 2015**).

The modified composition can be related to transcriptional and metabolic changes detected in TW. In poplar, the analyses showed increased carbon flux to cellulose, upregulation of genes involved in pectin degradation and down-regulation of genes involved in lignin, xylan, mannan and arabinan biosynthesis (**Andersson-Gunneras *et al.*, 2006**). Similar study performed on TW from eucalyptus showed that the modified composition has an origin in downregulation of lignin and xylan biosynthesis, but might also have an origin in synthesis of unknown polysaccharides usually not occurring in wood (**Mizrachi *et al.*, 2014**).

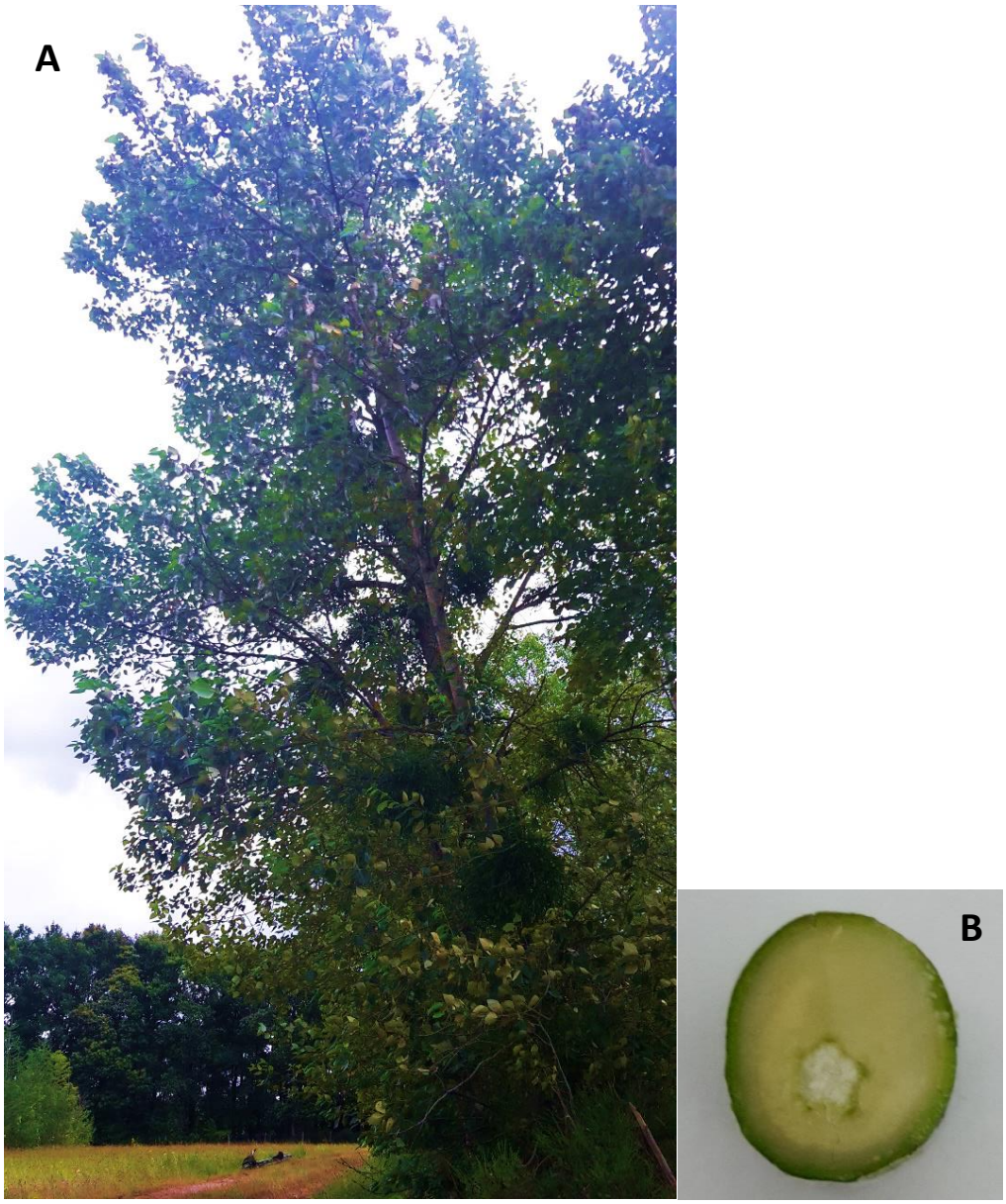

Figure 3. (A) The naturally displaced axes of *Populus trichocarpa* growing at INRA Orléans, France. In order to reorient or reinforce the axes, trees produce tension wood at the upper part of eccentric stems and branches, (B) as visible on stem section of young greenhouse-grown poplar (*Populus tremula* x *Populus alba*) tree.

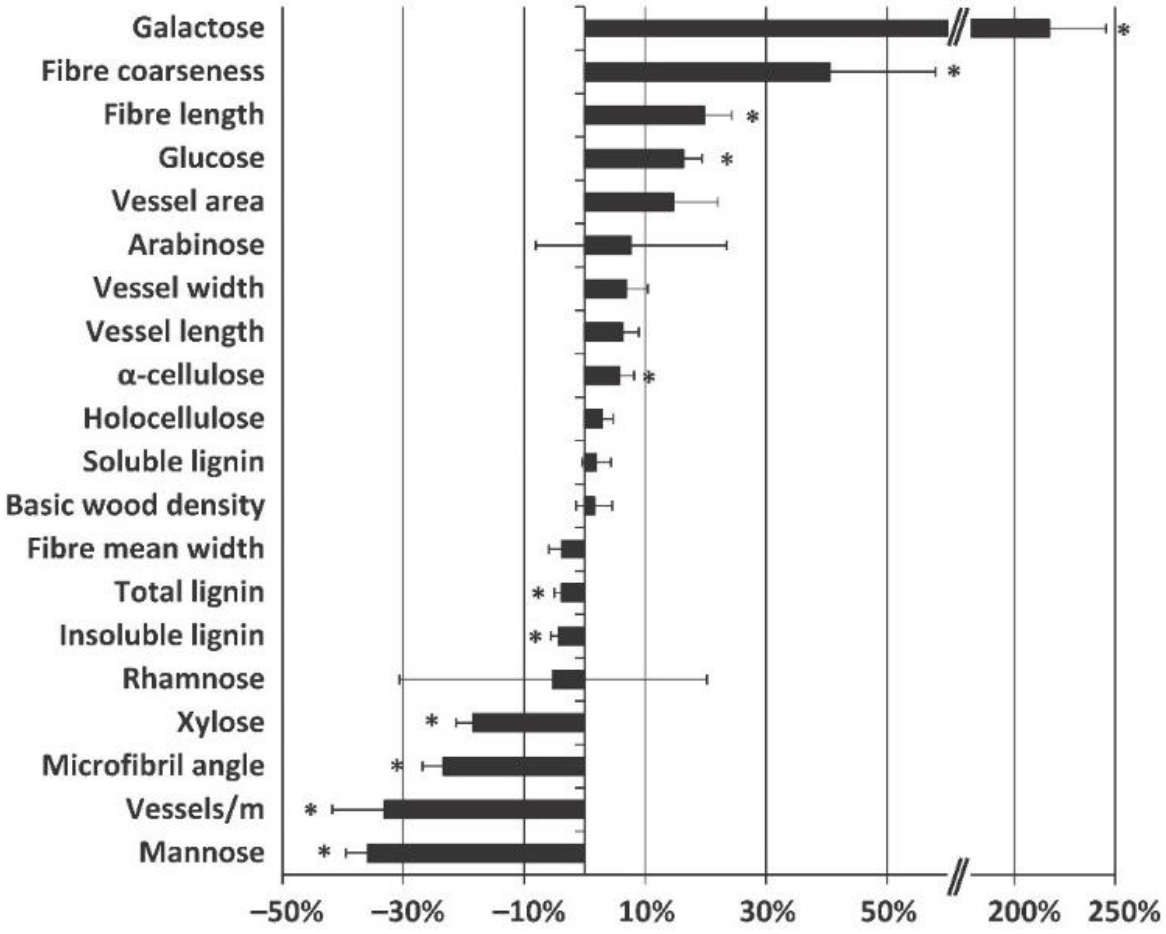

Figure 4. Relative changes of wood properties between tension and opposite wood of *Eucalyptus grandis* x *Eucalyptus urophylla*. A positive change indicates a higher value in tension wood as compared with opposite wood, and a negative change indicates a lower value in tension wood compared with opposite wood. Error bars represent standard error (n=5). Paired, two-tailed t-test: *, P≤0.05 (reprinted from **Mizrachi *et al.*, 2014**).

2.2. The G-fiber

As previously indicated, some species develop characteristic G-fibers in tension wood. The G-fibers were detected in 7 out of 21 studied tropical angiosperm trees (**Clair *et al.*, 2006a**). Despite the diversity, most of TW studies have been performed on poplar, which develops the classical G-fiber.

Letter G comes from gelatinous, as it indicates structure of G-layer – an additionnal cell wall layer deposited in G-fibers. Presence of the G-layer makes G-fibers easily distinguishable from fibers of normal and opposite wood (**Fig. 5**). The G-layer is detectable on stem cross-sections of poplar stems artificially tilted for only 1-2 days (**Abedini *et al.*, 2015**), suggesting that the synthesis of G-layer starts rapidly after stem tilting.

Due to the G-layer formation, the whole cell wall increases in thickness, while S1/S2 layers become thinner than were before deposition of the G-layer. It suggests that the G-layer replaces part of the S2 layer (**Abedini *et al.*, 2015**). Indeed, the G-layer is defined as a replacement of the S3-layer and sometimes as a partial or complete replacement of the S2-layer (**Mellerowicz and Gorshkova, 2012**).

Angiosperm trees develop diverse kinds of G-layer. For example, *Laetia procera* develops multi-layered G-layer structure (**Ruelle *et al.*, 2011**), while *Simarouba amara*, tropical species previously described to have similar fiber in TW and OW (**Ruelle *et al.*, 2011**), was recently shown to form a new type of G-layer (**Roussel and Clair, 2015**). In simarouba, the fiber during its differentiation develops the classical G-layer, while upon fiber maturation, the G-layer lignifies and decreases in thickness. Such a lignified fiber resembles to a fiber of normal wood (**Fig. 6**). In the same study, six other species were found to form as well the lignified type of G-layer.

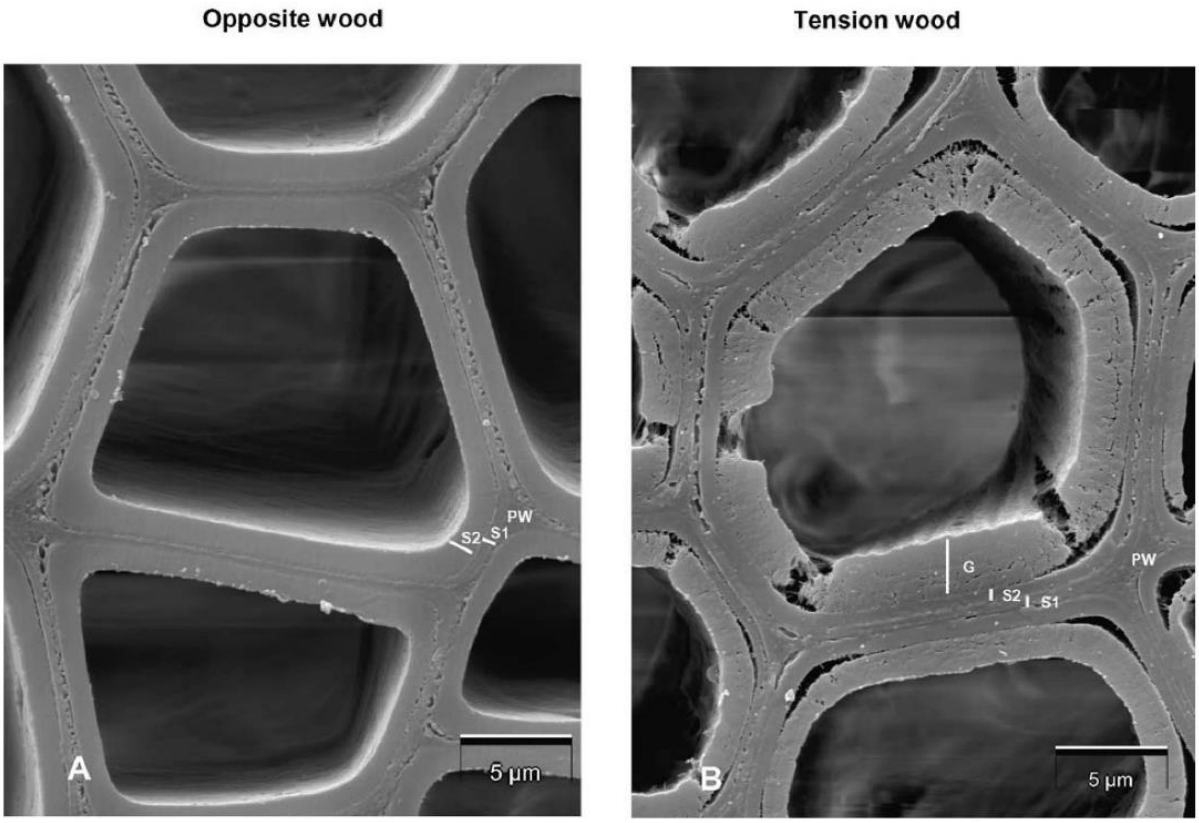

Figure 5. Transmission electron microscopy of wood cross-section from poplar (*P. tremula* x *P. alba*). A) Absence of G-layer in fibers of opposite wood B) and presence in fibers of tension wood (reprinted and text-modified from **Pilate *et al.*, 2004**). PW= primary cell wall; S1/S2= secondary cell wall layer 1 and 2; G= G-layer.

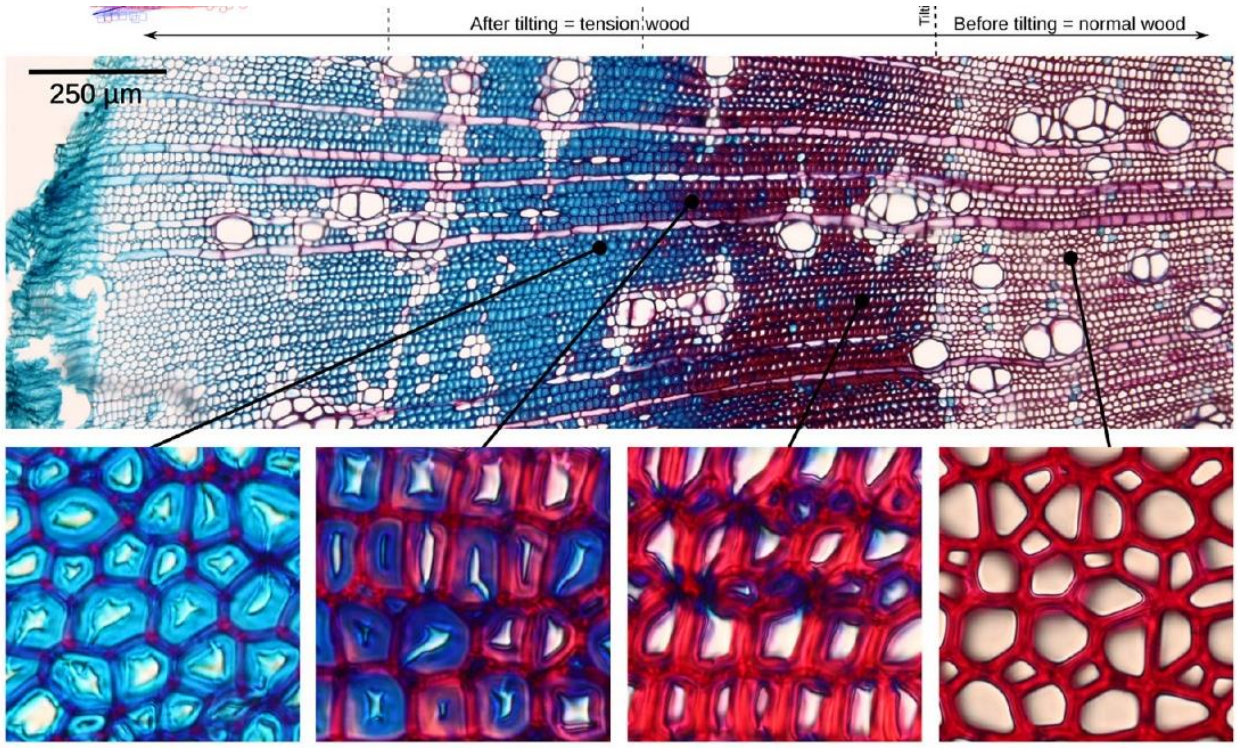

Figure 6. Safranin/Alcian blue double-staining of TW cross-section from artificially-tilted stem of *Simarouba amara*. During fiber differentiation, the classical G-layer is cellulosic and stains in blue. Upon fiber maturation, the G-layer becomes lignified and stains in red (reprinted and text-modified from **Roussel and Clair, 2015**).

2.3. Peculiar properties of the G-layer

A gel-like structure

In a pioneering study, **Norberg and Meier** (**1966**) observed a porous structure of the G-layer characterized by water-filled capillaries. Using the advanced technique of nitrogen adsorption–desorption isotherms of supercritically dried wood, it was demonstrated that matrix of the G-layer has a hydrogel structure. The structure has pores of surface 30 times bigger than in normal wood (**Clair *et al.*, 2008**).

Recently, **Chang *et al.*** (**2015**) measured mesoporosity of the cell walls during the maturation of OW and TW. It was observed that during deposition of the G-layer, mesopores increase in size and differ in shape. They concluded that such modifications are indicative of a G-layer matrix swelling during maturation.

Crystalline cellulose

In the G-layer, cellulose has highly crystalline structure (**Kaku *et al.*, 2009**). Microfibrils in the G-layer form crystalline macro-aggregates ranging in size from 35 to 40 nm, while the distance between aggregates varies from the full contact to more than 55 nm (**Clair *et al.*, 2008**).

A low microfibril angle

Orientation of CMF was found to be in close association with orientation of densely packed microtubules in G-fibers of poplar and ash (**Prodhan *et al.*, 1995**). Cellulose microfibrils are in the G-layer oriented in parallel to the axis of fiber (**Lautner *et al.*, 2012**; **Clair *et al.*, 2011**). For comparison, in S2-layer of G-fibers, angle varies between 20 and 25 degrees (**Fig. 7**) (**Clair *et al.*, 2011**).

Moreover, the orientation in the G-layer is probably related with the generation of tensile stress in cellulose microfibrils (see the next section). As stated by **Clair *et al.*** (**2011**), stress generation would be impeded in S2-layer because of the steep CMF, being 25° at outer S2-layers of NW and OW and 10° at inner S2-layer of NW (**Clair *et al.*, 2011**).

The state of tension in microfibrils

Clair *et al.* (**2006b**) were the first who established a relationship between the longitudinal macroscopic strain and the state of tension in cellulose microfibrils. Upon the stress release, values of lattice spacing of crystalline cellulose, which is a distance between glucose monomers along the cellulose microfibrils, decreased in TW and corresponded to values usually detected in wood. The observation supported the assumption that tensile stress is induced in cellulose microfibrils. **Clair *et al.*** (**2011**) later used synchrotron radiation microdiffraction to measure both the angle of microfibrils and lattice spacing in crystalline microfibrils. The measurements were performed *in planta*, in fibers of tension and normal wood. During deposition of G-layer, increase in cellulose lattice spacing is observed together with a decrease in microfibril angle, while the effect could not be detected during deposition of S2-layers in TW. These observations led to conclusion that the increase in lattice spacing happens due to a mechanical stress induced in cellulose microfibrils, which occurs rapidly after their deposition. This has been the first direct evidence that a tensile stress is generated in cellulose microfibrils during deposition of the G-layer.

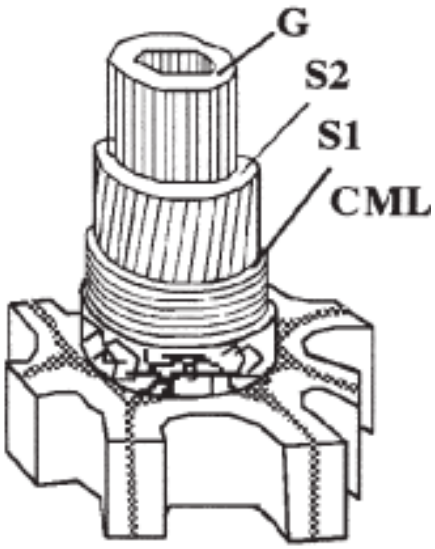

Figure 7. Cellulose microfibrils are in the G-layer orientated in parallel to the fiber axis and at 20-25° angle in the S2-layer. CML= compound middle lamella; S1, S2= secondary cell wall layer 1 and 2; G= G-layer (reprinted and text-modified from **Yamamoto, 2004**)

Particular biochemical composition

A recent immunohistolocalization revealed the presence of a number of common polysaccharide epitopes in the PCW and S1/S2 layers in both OW and TW (**Guedes, 2013**). This suggests that the differences between the biochemical composition of TW and OW fibers merely originate from the G-layer.

The total content

The G-layer may contains no or very few lignin (**Pilate *et al.*, 2004**), but it contains relatively low sugar content, which accounts for 62% of the G-layer's dry weight (**Guedes, 2013**). The rest of G-layer content is still unknown, although it was speculated to originate from proteins and mineral ions (**Guedes, 2013**). One study identified 72 proteins in the isolated G-layers of poplar (**Kaku *et al.*, 2009**), but the results should be taken with caution since among these proteins, a number appeared related to lignin biosynthesis and cytoskeleton proteins, suggesting that the G-layers were probably contaminated with cellular contents.

Glucose

Glucose is the most abundant monosaccharide in the G-layer. A pioneering study showed that the isolated G-layers contain 98.5% of glucose (**Norberg and Meier, 1966**). An another study also detected high content (89%) of glucose (**Nishikubo *et al.*, 2007**) and the most recent analysis showed that glucose makes 72% of the G-layer's total sugar content (**Guedes, 2013**). All the analyses were performed on sonicated G-layers, which get easily isolated because of the weak attachment of the G-layer to the S2-layer. However, the latter two analyses involved advanced technique of high resolution gas chromatography, which provides more precise results than paper chromatography used in the analysis from 1966. The analysis from Guedes (2013) was performed in our laboratory and in collaboration with the biochemical platform BIBS from INRA Nantes (France).

Non-cellulosic polysaccharides

Nishikubo *et al.* (**2007**) reported that the G-layer contains more than 10% of non-cellulosic polysaccharides, most of which represent xylose, mannose, fucose, galactose, arabinose and rhamnose. The analysis from **Guedes** (**2013**) revealed rather high non-cellulosic content, since cellulose accounted for only 60% of the total

sugar content. They detected the same non-cellulosic monosaccharides and within similar values as Nishikubo and colleagues, except for galactose, which accounted for 20%.

Using immunolocalization, in the G-layer were localized epitopes of xyloglucan (**Nishikubo *et al.*, 2007**; **Kaku *et al.*, 2009**), AGP (**Bowling and Vaughn, 2008**), RG-I pectin (**Arend 2008**, **Bowling and Vaughn, 2008**), mannans and xylans (**Kim and Daniel 2012**). In the very recent study performed in my laboratory at INRA Orléans, distribution of polysaccharides was evaluated during TW fiber differentiation (**Guedes, 2013**). This extensive research involved high number of antibodies recognizing different classes of non-cellulosic polysaccharides. The analysis revealed a new insight into structures present in the G-layer (**Fig. 8**), sometimes contradictory to the previous observations. It is the case for xyloglucans, which were previously localized in the G-layer (**Nishikubo *et al.*, 2007**), but the extensive analysis with 29 antibodies could not detect xyloglucan epitopes in the G-layer (**Guedes, 2013**). The same result was obtained after enzymatic removal of pectin, which could mask the xyloglucan epitopes. Additionally, digestion of polysaccharides from the G-layer with β-1,4-xylanase and β-1,4-glucanase suggest that xylose and glucose from the G-layer did not originate from xyloglucan (**Guedes, 2013**).

AGP and RG-I

In the same study, a high number of antibodies was found to bind AGP and RG-I epitopes, which is in consistence with previous observations (**Lafarguette *et al.*, 2004**; **Arend, 2008**; **Bowling and Vaughn, 2008**).

Several antibodies detected AGP epitopes only in the differentiating G-layer (CCRC-M7, JIM14, JIM16, JIM15), while two antibodies (JIM8 and Mac207) bound their AGP epitopes in both differentiating and mature G-layers (**Guedes, 2013**). This suggests that AGPs either are modified during G-layer maturation or that their epitopes get hinder by some other structures. The labelling of JIM14 antibody was already reported in the G-layer of poplar (**Lafarguette *et al.*, 2004**), and JIM14 and CCRC-M7 antibodies in sweetgum (**Bowling and Vaughn, 2008**).

RG-I pectin may be present in the G-layer with long side chains with respect to the backbone, as suggested by a rather low rhamnose to galactose ratio. Moreover,

significant differences in labelling during G-layer development were detected with LM5 antibody, which recognizes β-1,4-galactan side chain (**Fig. 9**; **Guedes, 2013**). LM5 firstly bound the whole thickness of the developing G-layer. While the G-layer was under growth, labelling was restricted to the outer and inner sides of the G-layer, to be finally detected only at the outer side of mature G-layer. Strong labelling of differentiating G-layer with LM5 antibody was also reported in willow by **Gritsch *et al.*** (**2015**), while the labelling of the outer side of mature G-layer was reported by **Arend *et al.*** (**2008**). On the contrary, signal of RU1 antibody, which recognizes RG-I backbone progressively increased during the G-layer differentiation, being very strong in mature G-layer (**Fig. 9**). The changes in labelling intensities suggest that RG-I structure is modified during the G-layer maturation. As suggested by Guedes (2013), this may be due to enzymatic elimination of RG-I side chains by a beta-galactosidase, which makes RG-I backbone accessible to RU1 antibody. Alternatively, the modifications may result from the formation of RG-I complex between the side chains, which would impede binding of LM5, as proposed by **Gorshkova *et al.*** (**2015**). In addition, LM6 antibody directed against α-1,5-arabinan and CCRC-M7 antibody against arabinosylated β-1,6-galactan, both present on RG-I and AGP, labelled differentiating and not mature G-layer. The changes in their labelling also support the hypothesis about modifications of RG-I structure (**Guedes, 2013**).

Other structures

Antibody JIM19 directed against extensins (JIM19) bound specifically the G-layer (**Guedes, 2013**). In the G-layer were also localized epitopes of partially methyl-esterified homogalacturonan (JIM7), glucurunoxylan (CCRC-M119), mannans (LM21) and acetylated glucomannans (CCRC-M170). In several other studies, G-layer was labelled by antibody LM21, which binds mannans (**Kim and Daniel, 2012**; **Gritsch *et al.*, 2015**) and antibody CCRC-M38, which binds de-esterifed homogalacturonan (**Gritsch *et al.*, 2015**).

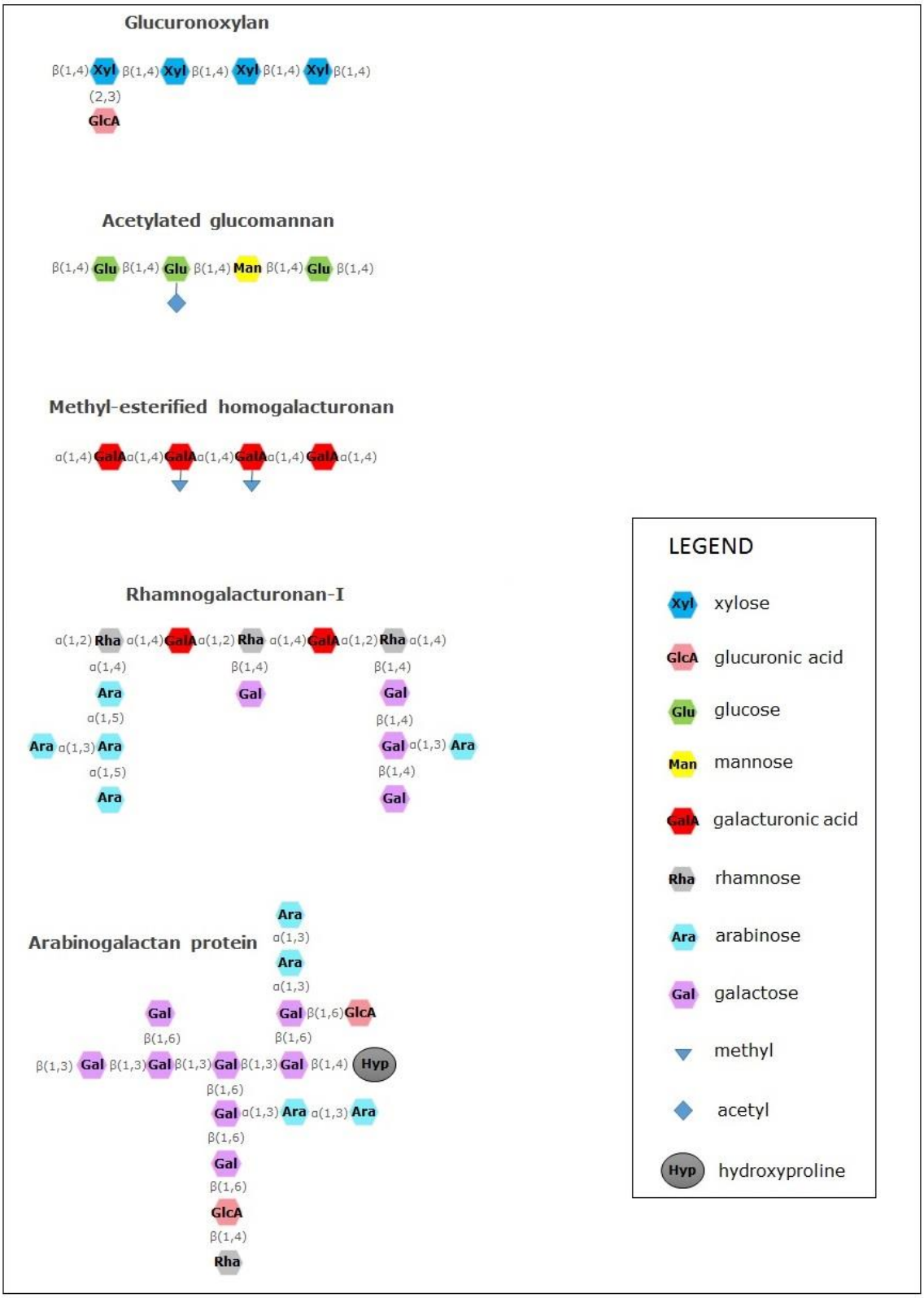

Figure 8. Schematic structures of polymers whose epitopes were localized in the G-layer of poplar

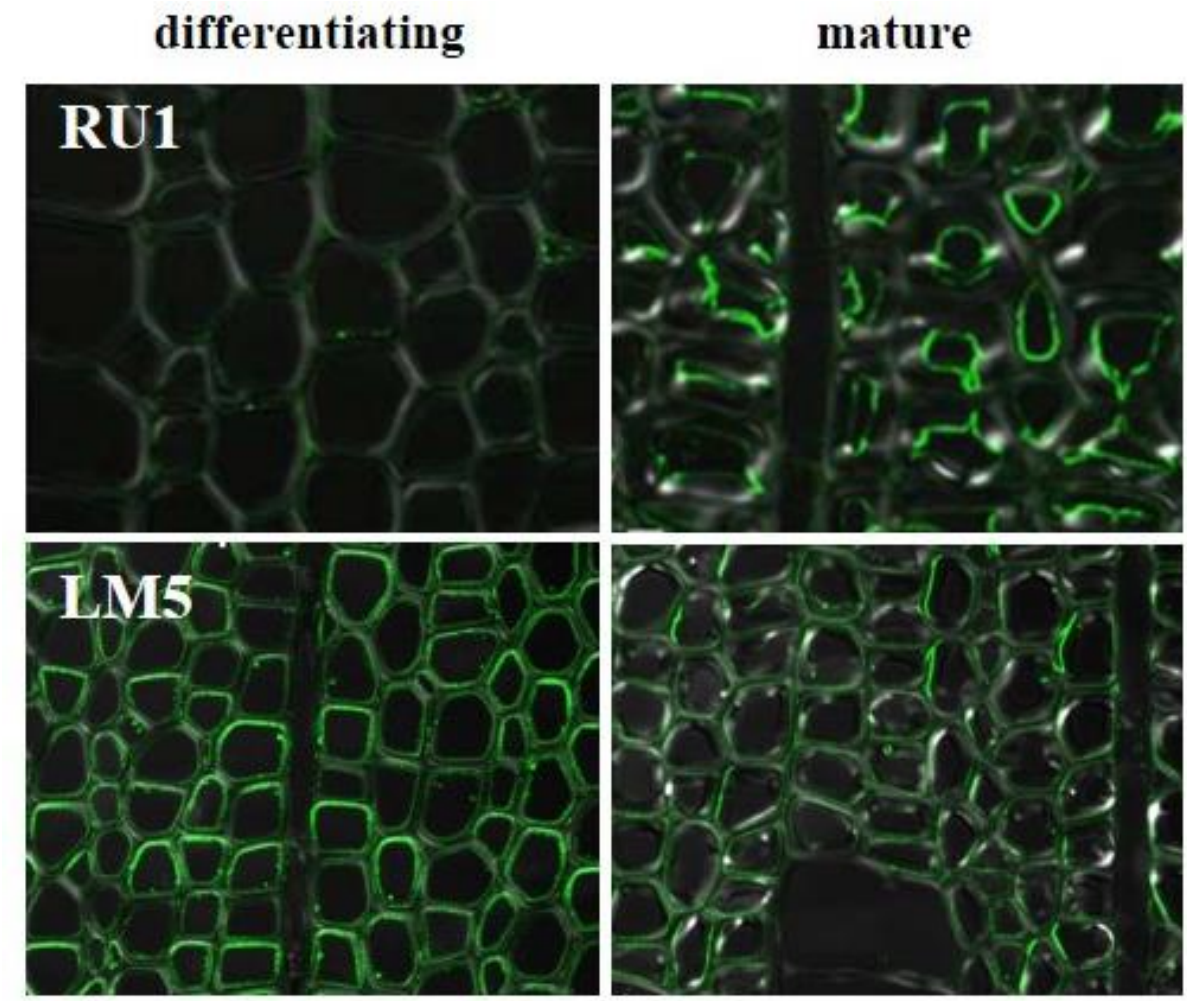

Figure 9. From differentiating to mature G-fibers of TW: increase in labelling of inner G-layer by RU1 antibody specific to RG-I backbone and progressive restriction of labelling to outer G-layer by LM5 antibody specific to β-(1,4)-galactan side chains (reprinted and modified from **Guedes**, **2013**)

2.4. Molecular players potentially important for the G-layer properties

As presented in the previous chapters, the G-layer is characterized with particular properties, which are thought to be related to a specialized function in the generation of tensile stress (**Mellerowicz and Gorshkova, 2012**; **Chang *et al.*, 2015**; **Guedes, 2013**). AGPF laboratory at INRA Orleans aims in deciphering a relation between molecular properties and generation of tensile stress in the G-layer. To date, the research involved studies of transcriptional changes in TW (**Déjardin *et al.*, 2004**), lignin (**Pilate *et al.*, 2004**), fasciclin-like arabinogalactan proteins (**Lafarguette *et al.*, 2004**), monosaccharide composition in the G-layer and polysaccharide distribution along differentiating TW fibers (**Guedes, 2013**). The latest research, partially conducted within the project Stress In Trees, particularly approached in the identification of molecules potentially responsible for the G-layer properties. This thesis was conducted within the same project with the aim to continue in identification of molecular players in the G-layer. Research performed in frame of the thesis has put in focus only several molecular players - beta-galactosidase, fasciclin-like arabinogalactan proteins and chitinase-like protein. Further chapters have the aim to justify their choice according to current findings about their putative functions in plants, particularly during xylem development.

2.4.1. Beta-galactosidase

Beta-galactosidase (BGAL) is an enzyme potentially responsible for the modification of RG-I pectin in the G-layer, which was detected as progressive decrease of immunosignal of beta-(1,4)-galactan side chains and increase of RG-I backbone signal (**Guedes, 2013**). Debranching of RG-I may be related with a gel formation in the G-layer, since the action of beta-galactosidase (AtBGAL6) on side chains of RG-I pectin was shown to increase its hydrophilic potential necessary for the seed hydration (**Macquet *et al.*, 2007**). Moreover, an epitope of beta-galactosidase was localized in the G-layer of poplar and G-type walls of hemp phloemic fibres (**Mokshina *et al.*, 2012**). In addition, *in situ* incubation of poplar xylem sections with Gal-resorufin revealed higher beta-galactosidase activity in the cell walls of TW than in NW (**Gorshkova *et al.*, 2015**).

Flax develops phloemic fibers, which have remarkable similarities with the G-fibers of tension wood. Remodelling of phloemic G-fibres during which galactan-rich layer (Gn-layer) turns to cellulose-rich layer (G-layer) involves hydrolysis of high-molecular mass galactans. The modification is related to beta-galactosidase enriched within developing flax fibres, localized in secreted Golgi vesicles and gelatinous SCWs, and encoded by *LuBGAL1* and/or *LuBGAL2* (**Roach *et al.*, 2011**; **Mokshina *et al.*, 2012**). Down-regulation of *LuBGAL1* and *LuBGAL2* increased the content of cell wall-associated galactans, decreased the ability of Gn- conversion to G-layer and reduced cellulose crystallinity and stem strength (**Roach *et al.*, 2011**).

Beta-galactosidases (BGAL) are involved in the hydrolysis of terminal non-reducing beta-D-galactose residues (CAZy.org). In plants, they are found as a part of isofunctional families of glycoside hydrolases GH35 and GH42. Beta-galactosidase families were predicted in various plant species as Arabidopsis, rice, tomato, flax and chickpea (**Hobson and Deyholos, 2013**).

Beta-galactosidases have putative function in the cell wall biogenesis and remodelling, degradation of cell wall components during cell expansion, cell senescence, fruit ripening and storage mobilization (**Martin *et al.*, 2013**). The activity of beta-galactosidase is highly correlated to the formation of secondary cell walls. β-(1,4)-galactosidase activity was partially detected in the innermost secondary cell walls of sclerenchyma cells in Arabidopsis (**Banasiak *et al.*, 2014**). Several

BGALs were identified as highly-expressed in wood-forming xylem of poplar (**Aspeborg *et al.*, 2005**). Transcripts of one BGAL were enriched in the transition between elongation and secondary cell wall deposition in hypocotyl of flax (**Roach and Deyholos, 2008**).

Cell wall targets of beta-galactosidase activity may be carbohydrates RG-I pectins, galactomannans and xyloglucans; arabinogalactan proteins and galactolipids (**Ahn *et al.*, 2007**). Based on recombinant protein activity, members of the largest a1 subgroup from Arabidopsis were functionally characterized as cell wall exo-galactanases, with activities toward β-(1,4)- and β-(1,3)-galacto-oligosaccharides, except for *AtBGAL12*, which also cleaved β-(1,6)-galactosyl substrates (**Ahn *et al.*, 2007**; **Gantulga *et al.*, 2008**; **Gantulga *et al.*, 2009**). Interestingly, LusBGAL1 and LusBGAL2 are homologous to this group. BGAL from radish (*Raphanus sativus*), also homologous to the a1 subgroup, was shown to specifically cut beta-(1,3)-galactosyl and beta-(1,6)-galactosyl residues of arabinogalactan protein, suggesting that structurally similar beta-galactosidases may have a specific function in different plant species (**Kotake *et al.*, 2005**).

2.4.2. Fasciclin-like arabinogalactan protein

Arabinogalactan proteins are glucuronic acid carriers, which potentially interact with negatively charged galacturonic acid of pectins (**Lamport *et al.*, 2014**). Interactions with AGPs decrease pectin alignment and crosslinking in the cell wall and increase the porosity of pectin network (**Lamport *et al.*, 2005**). In primary cell walls of Arabidopsis, **Tan *et al.*** (**2013**) evidenced the covalent link of AGPs to pectins and arabinoxylans in a complex structure. The interactions of AGPs with RG-I pectin may therefore influence the mesoporosity changes detected during the G-layer development (**Chang *et al.*, 2015**). AGPs responsible for the gel structure would likely be retained between cellulose microfibrils, as detected for type II arabinogalactans in tension wood of poplar (**Gorshkova *et al.*, 2015**).

Fasciclin-like arabinogalactan proteins (FLA) belong to a subgroup of AGPs with fasciclin domain (**Fig. 10**). It has been firstly reported in *Drosophila melanogaster* as a domain involved in cell adhesion (**Gaspar *et al.*, 2001**). However, the exact function of FLA domain in plants is not known.

From the comparison of EST distribution and expression analysis in poplar, expression of FLA was detected in TW (**Déjardin *et al.*, 2004**) and ten FLA genes were reported as differentially expressed in TW (**Fig. 11**; **Lafarguette *et al.*, 2004**). Several FLAs were also found up-regulated in TW of eucalyptus (**Mizratchi *et al.*, 2015**).

MacMillan *et al.*, 2015 raised an idea of conserved sub-group A of FLAs, which is involved in secondary cell wall development and important for stem mechanical properties. Moreover, several reported mutant phenotypes (listed in the following text) indicate the group's involvement in the orientation of cellulose microfibrils. FLAs are prominent candidates for a role in control of the axial orientation of cellulose microfibrils in the G-layer (**MacMillan *et al.*, 2015**). In Arabidopsis, the double knockout of the group-A members *FLA11* and *FLA12* did not affect stem cell morphology, but it decreased polysaccharide and increased lignin content, increased microfibril angle and decreased stem tensile strength and stiffness (**MacMillan *et al.*, 2010**). Several FLAs from eucalyptus, homologous to the group-A, were highly expressed in stems and overexpression of one (EgrFLA2) led to 3-fold reduction of CMF angle (**MacMillan *et al.*, 2015**). GhFLA5 from cotton, which has common

structural characteristics with the group-A, is highly expressed in fibers and was proposed to contribute to fiber strength by affecting cellulose synthesis and orientation of microfibrils (**Liu *et al.*, 2013a**). In poplar, modification of TW-specific PtaFLA6 reduced stem flexural strength for 10-12% and flexural stiffness for 19-23%, reduced lignin and crystalline cellulose content, affected the expression of nine *FLA* homologous genes and genes involved in lignin and cellulose synthesis (**Wang *et al.*, 2015**).

FLAs were also shown to have function other than in secondary cell wall development. AtFLA1 is involved in the early stages of lateral root and shoot development in tissue culture (**Johnson *et al.*, 2011**). AtFLA3 was reported as involved in microspore development and cellulose deposition during pollen formation (**Li *et al.*, 2010**). GhFLA1 from cotton is involved in fibre initiation and elongation through the modulation of the biosynthesis of primary cell wall components (**Huang *et al.*, 2013**).

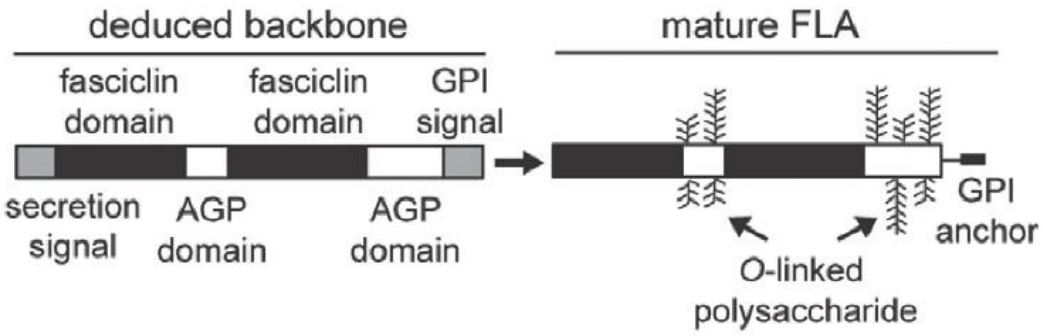

Figure 10. Schematic of a representative FLA containing two AGP domains and two FLA domains before and after post-translational modifications. Deduced proteins include an N-terminal secretion signal, two FLA domains, two AGP domains and a C-terminal signal sequence for addition of a GPI-anchor. Mature FLAs are predicted to be extensively modified post-translationally with peptidyl proline (Pro) modified to hydroxyproline (Hyp), the addition of O-linked oligo/poly-saccharide chains to Hyp residues, and the addition of a C-terminal GPI-anchor (reprinted from **Johnson *et al.*, 2011**).

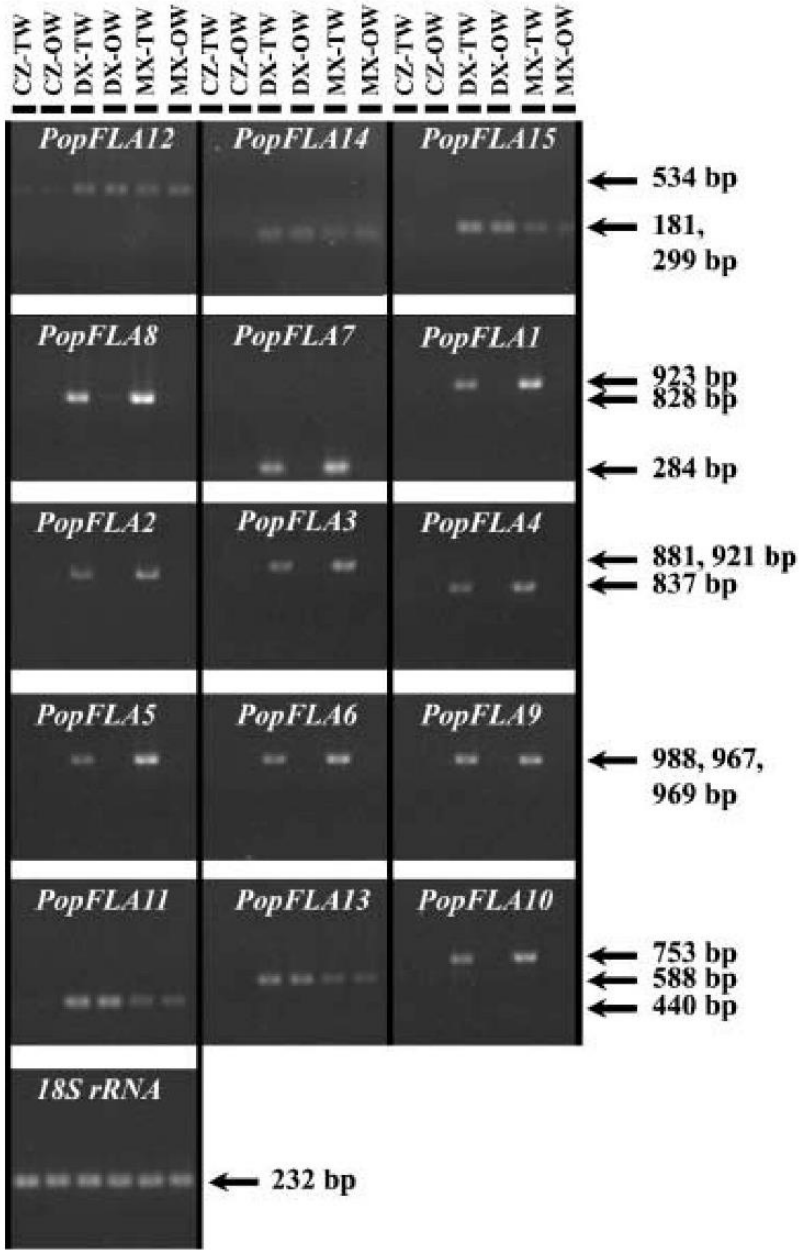

Figure 11. Semi-quantitative polymerase chain reaction (PCR) on reverse transcribed cDNAs from cambial (CZ), differentiating xylem (DX) and mature xylem (MX) of opposite and tension wood. PopFLA1-10 are differentially expressed in DX and MX of TW, while PopFLA11-15 are expressed in DX and MX of both OW and TW (reprinted and text-modified from **Lafarguette *et al.*, 2004**)

2.4.3. Chitinase-like protein

Chitinase-like proteins (CTL) arised from the evolutionary gene duplication events and mutations of classical chitinases (**Kesari *et al.*, 2015**). The classical chitinases are generally known as pathogen-induced enzymes, which cleave β-(1,4)-linked *N*-acetylglucosamine (GlcNAc) in chitin - the main component of fungal cell walls and invertebrate exoskeletons. However, chitinases were also shown to have function in cell development (**Takemoto *et al.*, 1997**), embryogenesis (**De Jong *et al.*, 1992**) and hydrolysis of acylated chitooligosaccharide signals known as Nod factors, which trigger development of root nodules (**Staehelin *et al.*, 1994**). Chitinases from pine embryogenic tissues were shown to bind arabinogalactan protein (**Domon *et al.*, 2000**), while the addition of chitinase enhanced AGP's activity in embryogenic cell culture of carrot (**van Hengel *et al.*, 2001**).

Transcripts of a chitinase-like gene were found abundant in opposite and tension wood of poplar (**Déjardin *et al.*, 2004**). Expression of *AtCTL2* is in Arabidopsis detected exclusively in xylem cells and interfascicular fibers known to have secondary cell walls (**Hossain *et al.*, 2010**). AtCTL2 has a close homolog named AtCTL1. The both CTL proteins are structurally similar (64,2%) and have likely a function in the synthesis of different cell wall types (**Hossain *et al.*, 2010; Sanchez-Rodriguez *et al.*, 2012**). Based on their co-expression with *CESA* genes, which encode proteins involved in cellulose synthesis, AtCTL1 and AtCTL2 were associated with primary and secondary cell wall, respectively (**Persson *et al.*, 2005**). Based on phenotypes of mutants, **Sanchez-Rodriguez *et al.*** (**2012**) described the function of AtCTL1 and AtCTL2 as non-essential for cellulose biosynthesis, but conjunctive with cellulose synthase machinery. It was proposed that they contribute to cellulose crystallinity and CMF assembly, with the secondary effect on microfibrils and cross-links with hemicelluloses.

A group of highly expressed chitinase-like genes in phloemic G-fibers of flax was shown divergent from all other chitinase groups (**Mokshina *et al.*, 2014**). However, members of this group are non-homologous to AtCTL1 and AtCTL2.

3. TOWARDS A MODEL OF THE TENSILE STRESS GENERATION

High mesoporosity, matrix composition and axially orientated cellulose microfibrils forming large crystalline aggregates are properties of G-layer likely important for a mechanism of generation of high longitudinal constrains in TW.

A significant step forward has been made in the last two decades to elucidate the exact mechanism behind the tensile strain generation and transmission. Global scientific investigations have been mostly directed towards macroscopic mechanical properties, micro properties as microfibril angle and mesoporosity, so as molecular properties like composition, functional gene/protein analyses and transcriptional modifications. Even in the absence of a complete and precise molecular-physiological-mechanical background, researchers were continuously proposing models in an attempt to explain how the tensile stress gets generated and transmitted. Neither one hypothesis still gives a conciliated model, which would precisely explain the mechanism. Some of the proposed models will be discusses in the further text.

During the cell maturation, cells divided from cambium expand and undergo longitudinal contraction. Boyd (1972) proposed that origin of the expansion is in deposition of lignin and hemiceluloses between cellulose matrix, while for Bamber (1987), the expansion is a consequence of cellulose crystallization in cell wall (from **Jourez, 1997**).

Bamber (**2001**) pointed that cellulose microfibrils behave in G-layer as stretched springs which generate longitudinal tension. The absence of lignin is proposed to facilitate maximum generation of the tensile stress, in opposite to compression wood in which the high lignin content serves to maximize the compressive force by bonding to the cellulose microfibrils.

Goswami *et al.* (**2008**) assumed that a transfer of the tensile stress to adjacent S2-layers must exist to explain a generation of maturation stress. In their experiment, microfibril angle increased in S2-layer after removal of the G-layer. They proposed that a swelling of the G-layer generates forces, which are transmitted transversally to S2-layer and to whole fiber. However, this model is not satisfactory since it can be supposed that a force would be equally dispersed to lumen.

Mellerowicz *et al.* (**2008**) proposed xyloglucan as a crucial player in a mechanism of tensile stress generation in the G-layer. In their hypothesis, xyloglucans would be entrapped between cellulose microfibrils, which form aggregates. The entrapment would then cause tensioning of cellulose macrofibrils and a generation of longitudinal stress. Xyloglucans and XET activity were also proposed to be involved in cross-links between G- and S2-layer. However, despite multiple experiments, we failed to find the evidence of xyloglucan presence within the G-layer (**Guedes, 2013**).

Based on the previously published hypotheses (**Clair *et al.*, 2006b**; **Mellerowicz *et al.*, 2008**; **Goswami *et al.*, 2008**), **Mellerowicz and Gorshkova** (**2012**) proposed a combinatorial mechanism in which the entrapment of matrix polysaccharides between cellulose microfibrils would cause their tensioning, longitudinal shrinkage of inner and outer G-layer and radial pressure on adjacent S-layers.

Gorshkova *et al.* (**2015**) refined the hypothesis from 2012, proposing entrapment and water retention of hydroscopic molecules as RG-I, beta-galactosidase-released galactans or acidic arabinogalactans. According to their hypothesis, the entrapment would limit the interactions between microfibrils and cause their longitudinal tensioning (**Fig. 12 a, b**).

Almeras *et al.* (**2012**) proposed that a pressure caused by matrix swelling might be responsible for tensioning of cellulose microfibrils. The hypothesis now has a foundation in observation of **Chang *et al.*** (**2015**), who detected increase in mesoporosity during the G-layer differentiation, which is, by them, indicative of G-layer matrix swelling (**Fig. 12 c**).

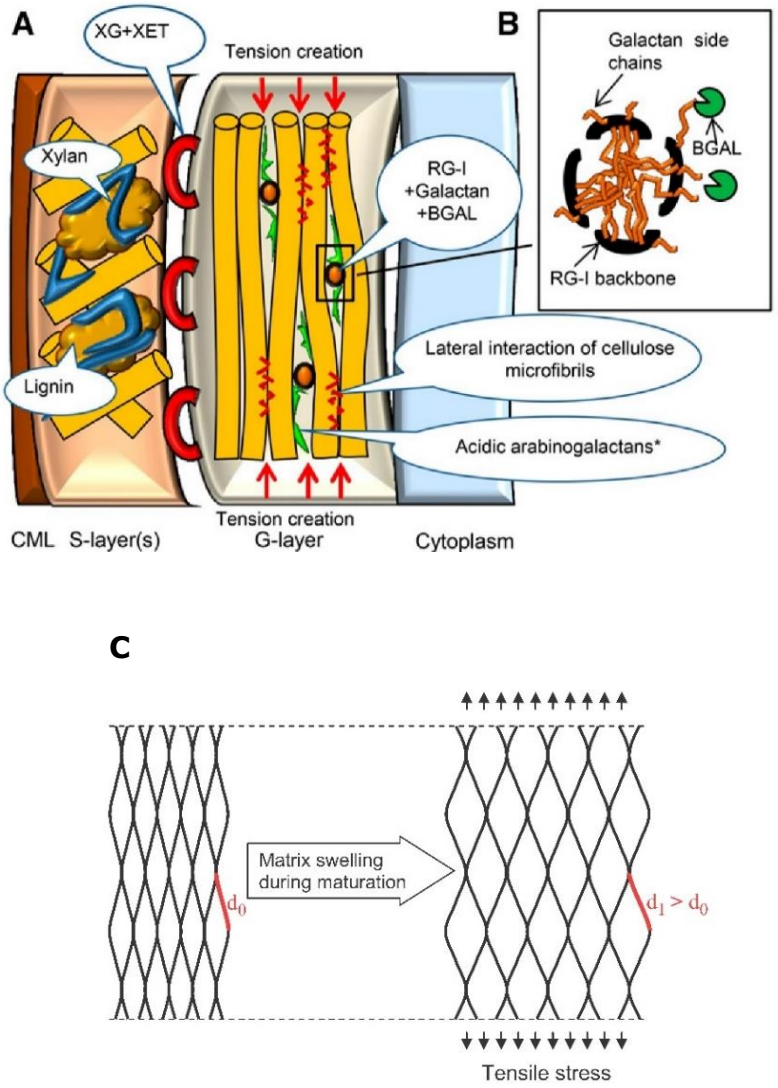

Figure 12. Proposed mechanisms of tensile stress generation: (**A**) In the G-layer, RG-I with galactan side-chains, β-1,4-galactan and acidic arabinogalactans get entrapped between laterally interacting cellulose microfibrils. Beta-galactosidase (BGAL) modifies RG-I to make polymer more compact and to provide conditions for lateral interaction with CMF. Xyloglucan and XET are involved in cross-links between the G-layer and S2-layer in which CMF are orientated helicoidally and separated by xylan and lignin to impede the interactions between CMFs. (**B**) Proposed spatial structure of RG-I in which β-1,4-galactan side chains interact laterally to associate molecules of RG-I (reprinted and text-modified from **Gorshkova *et al.*, 2015**). (**C**) Model of longitudinal tensile stress generation caused by a swelling pressure of gelatinous matrix within the cellulose microfibril network (reprinted from **Chang *et al.*, 2015**)

INTRODUCTION

Objectives and strategy

In the introduction of the thesis, I approached the current findings about tension wood properties and hypothesized mechanisms of a tensile stress generation. Understanding of this mechanism is the main objective of ANR Blanc Stress In Trees project, which began in 2013 and is scheduled to finish in 2017. The project is multidisciplinary and involves molecular physiologist from AGPF at INRA Orleans and biomechanists from LMGC at University of Montpellier and EcoFog in French Guiana. A base of the project makes the hypothesis of tensile stress generation, which was raised from the previous results and models of the project partners (Clair *et al.*, 2008; Clair *et al.*, 2011. Almeras *et al.*, 2012). The hypothesis says that, during the G-layer differentiation, hydrophilic matrix molecules would be deposited between paralleled cellulose microfibrils and initiate formation of a gel, which would swell during the G-layer maturation. The swelling would generate forces able to place the microfibrils under tension by their transversal stretching and longitudinal tensioning. In favor of the hypothesis goes the recent observation of changes in mesoporosity during the G-layer maturation (Chang *et al.*, 2015).

The recent work conducted in my laboratory within the same project raised a number of G-layer matrix components with a potential in a gel formation (Guedes, 2013). The components localized in the study were presented in the chapter devoted to the G-layer composition. This thesis have had an aim to continue identyfing molecular players important for the G-layer properties and decrypting a molecular mechanism underlying generation of tensile stress. Towards the aim, three potential molecular players were selected to study: beta-galactosidase (BGAL), fasciclin-like arabinogalactan protein (FLA) and chitinase-like protein (CTL). Current findings about the molecules, stated in the introduction of this thesis, support the idea that a BGAL might be responsible for the RG-I modifications in the G-layer and consequentially formation of a gel. FLAs may have a function in orientation of cellulose microfibrils or a gel-like structure in the G-layer. Finally, CTL imposed as a prominent candidate for a function in control of cellulose crystallinity, which is of particular interest because of the highly crystalline cellulose structure in the G-layer. In addition, CTL may co-operate with FLA in formation of a gel.

Objective of my thesis was to clarify function of these molecules primarly by functional characterization of transgenic RNAi lines modified for the expression of one or two of

their genes. In addition, epitopes of RG-I pectin and arabinogalactan proteins, previously localized in the G-layer of poplar (Guedes, 2013), were as well localized in fibers of simarouba, which develop different type of the G-fiber. Comparison between their localization was used to evaluate if RG-I and AGPs are molecules important for properties of different types of the G-layer and if they are involved in a common mechanism of tensile stress generation, potentially shared across species. Latter is actually the main objective of the Stress In Trees project in which poplar and simarouba have been used as species for evaluation of the hypothesis.

The objective of my thesis was accomplished following the experimental strategy of:

1) Identification of beta-galactosidase (BGAL), chitinase-like protein (CTL) and fasciclin-like arabinogalactan (FLA) families in poplar, Arabidopsis and flax

2) Expression profiling of BGAL, CTL and FLA family in normal, tension and opposite wood

3) Identification of candidate *BGAL*, *CTL* and *FLA* genes

4) Expression analysis of *BGAL*, *CTL* and *FLA* genes in different tissues and organs of poplar; in tension and opposite wood of poplar stems tilted in different duration

5) Production and characterization of RNAi transgenic poplar trees modified for the expression of selected *BGAL*, *CTL* and *FLA* genes

6) Localization of RG-I and AGP structures in fibers of simarouba and comparison to localization in fibers of poplar

MATERIALS & METHODS

I. PLANT MATERIAL

1.1. Poplar

Plant origin and manipulations

The model poplar genotype species used for all experiments was INRA clone 717-1B4 (*Populus tremula* x *Populus alba*). Plants were multiplied *in vitro* by vegetative micropropagation from stem nodes and grown *in vitro* during 6-8 weeks. Some of these plants were used for the genetic transformation described in the next chapter, and some served as control plants for the characterization of the newly-generated transgenic plants. Propagated plants were then acclimatized in the greenhouse. The growth conditions were regulated at 16h of light and temperature between 20°C and 25°C. The formation of opposite and tension wood was induced artificially by tilting pots and/or rod-attached stem at 25-35° angle.

Only seeds used in the analysis of tissues and organs were collected from one field-grown poplar tree at INRA Orléans.

For diverse experiments performed on poplar trees, growing and tilting periods, type of collected sample and number of plant replicates are given in **Tab. 1**.

Experiment	Age (months)	Tilting period (DBS)	Samples	Biological replicates
Gene expression - tilted stems	4	1, 3, 7, 15, 25	Scratched xylem of OW and TW	2
Gene expression of BGAL family	4	7, 15	Scratched xylem of OW and TW	3
Gene expression - tissues and organs	2.5	/	Apex, leaves, lower xylem, lower phloem, roots	3
Beta-galactosidase activity	4	90	Half stem from the upper face containing TW and half stem from the lower face containing OW (MUG); Stem sections (X-Gal + Safranin/Alcian-blue)	3
Immunolocalization	4	20	Cut TW sections embedded in resin	1

Table 1. Details on poplar material used in diverse experiments. DBS=days before sampling

Sampling for diverse use

Tension and opposite wood were collected from upper and lower parts of the stem, respectively. Wood was collected from debarked stems. To obtain a sample enriched in OW or TW, stem was split in two parts in the middle of pith. To obtain young xylem, wood was scratched with blade. Phloem, apex, leaves and roots were collected as complete tissues or organs. The plant material was immediately frozen in liquid nitrogen and stored at -80°C until use. Only the seeds were stored at 4°C prior manipulation. When used, seeds were firstly liberated from cotton of catkins and, either directly ground, or germinated in Petri dish on humid paper pad during 48 h and then ground.

To obtain a fine powder, complete tissues were ground in cryogenic jars with balls in Retsch® MM 400 mixer mill, 2 times per 30 s with frequency of 30 rotations per minute. To obtain fine powder from scratched xylem, samples were ground with pestle in a mortar.

Acclimatization and sampling of transgenic lines for screening

The plants were acclimatized in the greenhouse, first for 3 weeks in a plant propagator and then repotted and grown for 2 months in 2L pots with fertilized soil. Upon repotting, the plants were attached to a rod and tilted at 25° angle to produce OW and TW.

The acclimatization of the plants in 1 to 3 biological replicates was carried out in 6 batches grown in equally lasting, but different periods of the year, for the reason of:

1. Two transformation experiments started within a 2 month interval, resulting with a time-shift in the plant availability for acclimatization in the greenhouse
2. Impossibility to acclimatize a high number of plants in the specified greenhouse dedicated to genetically modified plants

Prior sampling, the plants were measured for height and stem diameter, marked for upper (tension wood) side of the stem and detached from the rod. The leaves were removed and the stem was cut 3 cm above base. The first fragment, 5 cm long, was sampled and stored at -20°C for observations of wood anatomy. The

second 25cm long fragment was debarked, the young xylem was scratched, directly placed in liquid nitrogen and ground in mortar with pestle. The ground powder was stored at -80°C prior RNA extraction and semi-quantitative RT-PCR gene expression analysis. The modification of gene expression was semi-quantitatively estimated in the transgenic lines. The wood phenotype was observed on Safranin/Alcian blue stained stem cross-sections. The analyses were carried out in comparison to wild-type poplar clone 717-1B4.

Acclimatization and sampling of selected transgenic lines

6 wild-types and 41 plants corresponding to biological replicates of transgenic lines selected for detailed analysis were grown in the greenhouse conditions for a total of 4.5 months: the first 3 weeks in a plant propagator, followed by 6 weeks in 2L pots and finally 10 weeks in 5L pots. During the last period, the stem was tilted and attached between 2 rods under 35° angle to produce tension and opposite wood (**Fig. 13**). The soil was fertilized and watered automatically with a water-supply system. The elongating shoots were regularly attached to the rods.

Figure 13. Experimental setup in the greenhouse: poplar trees artificially tilted between two rods at 35° angle to produce tension and opposite wood

Prior sampling, the trees were measured for height and marked for points corresponding to ¼ and ½ of stem height. TW was marked along the upper side of a tilted stem. The stems were detached and cut 2 cm from the basis. The diameter was measured after sampling at the cutting point. After leaf removal, the spring-backed stem was immediately photographed from upper perspective. The stem was then sampled for different analyses (**Fig. 14**), first at ¼ and ½ points to keep respective fragments E and H precisely above marked points. The lengths of the fragments to sample, estimated from the average tree height, were adjusted according to the individual height of the tree, with respect to the marked points. Leaves from the apex of one repetition per transgenic line and 3 wild-types were sampled in a tube, put in liquid nitrogen and stored at -80°C. The **fragments A, E** and **H** for histological analyses were put on ice and later stored at -20°C. The fragment B for measurement of wood elastic properties was debarked and preserved in 30% ethanol prior analyses. The **fragment C** for measurement of cellulose ultrastructure was separated in OW and TW and reshaped in wood fragments 10-20 mm long, 3-4 mm wide and 1-2 mm thick. The fragments were dried at room temperature for 2 weeks. The young xylem of **fragment D** was scratched for RNA extraction, from TW and OW sides of the debarked stem, put directly in a mortar with liquid nitrogen, ground with a pestle and stored in cryogenic tubes and then at -80°C. The **fragment F** for protein extraction was sampled only for BGAL7 lines and wild-types, separated into OW and TW and stored at -80°C. **Fragment G** used for wood biochemistry was debarked and separated in OW and TW, cut in small parts with guillotine and dried at 40°C for 4 days. Dried wood was further ground in Retsch MM 400 mixer mill in jars with 25 mm ball mills, 30 s twice for 1.5 g of wood, 30 rotations per min. The upper parts of **fragment E** were used for fixation in LR White resin following the protocol described later in the text, only for one biological tree replicate of T1 and T2 lines, showing a median height, chosen 2 weeks before sampling.

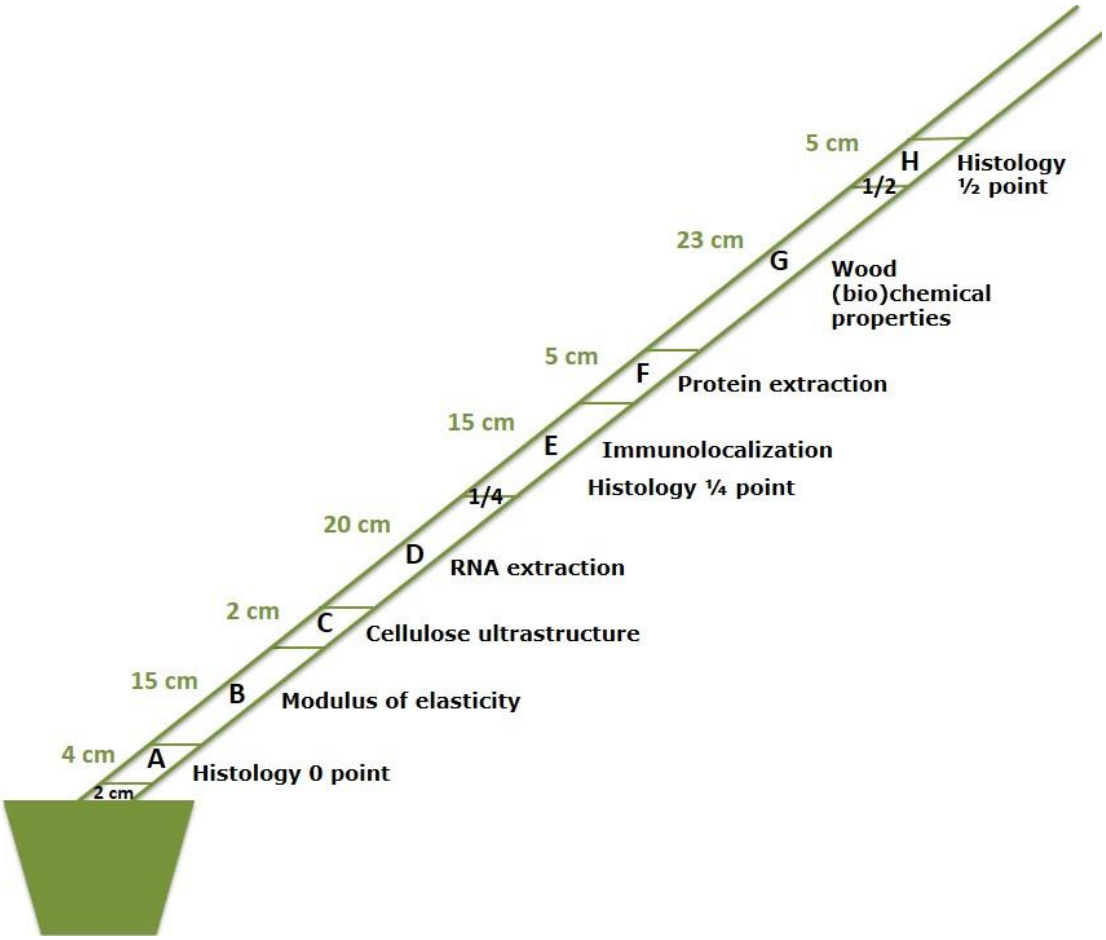

Figure 14. Scheme of sampling of fragments A-H from stems of transgenic poplar trees

1.2. Genetically modified poplars

RNAi technology was used to silence expression of selected candidate genes (*CTL2*, *BGAL7)* or clusters of genes in the large FLA family (*FLA1*, *FLA14)*. cDNA sequences of *FLA1* and *FLA14* genes (*P. tremula* x *P. alba*) were first retrieved from NCBI GenBank (http://www.ncbi.nlm.nih.gov/genbank/) and sequences of *CTL2* and *BGAL7* (*P. trichocarpa*) from JGI Phytozome (https://phytozome.jgi.doe.gov/pz/portal.html#). Their accession numbers and gene models are given in **Tab. 2**. In order to find a sequence as specific possible, the selected genes were aligned first with poplar genome in BLAST search on JGI Phytozome and then with the closest homologs in a multisequence alignment perfomed with Clustal Omega tool (http://www.ebi.ac.uk/Tools/msa/clustalo/). The sequences corresponding to *CTL2* and *BGAL7* genes were chosen as gene-specific. Alignment of fifteen FLAs reported in **Lafarguette *et al.*** (**2004**) showed that FLAs are highly homologous to each other. We therefore selected sequence of *FLA1* to be specific for cluster of six genes differentially expressed in tension wood (cluster 1592, **Lafarguette *et al.*, 2004**). The sequence of *FLA14* was chosen as specific to the group of non-differentially expressed genes *FLA11-15* (**Lafarguette *et al.*, 2004**). The selected sequences were between 95 and 170 bp long. Their corresponding primers for amplification are given in **Tab. 2**.

The genetically modified poplar trees were obtained in several steps:

1) production of RNAi vector constructs for gene expression modification
2) transformation of poplar internodes with construct-carrying *Agrobacterium*
3) plant regeneration

Production of RNAi vectors

Different templates from *P. tremula* x *P. alba* (CTL2: plasmid clone JXO0018 G10; FLA1: plasmid clone pta XM0028 A2; FLA14: plasmid clone pta 5XO0024D6; BGAL7: RT-obtained cDNA from tension wood tissue) were amplified in PCR reaction with primers (**Tab. 2**) corresponding to attR recombination sites and gene specific sequences. AttR ends flanking the sequence of interest are necessary for BP recombination into first pDONR 221 entry vector and then for LB recombination into destination/expression vector pHellsgate8 (**Annex I** of materials and methods) (**Helliwell *et al.*, 2002**). The both steps were conducted using TOPO

TA Cloning kits and Gateway Clonase II Technology. Plasmids from spectinomycin-resistant colonies were isolated with NucleoSpin Plasmid kit (Macherey-Nagel). Plasmid DNA was verified for orientation of intron with the respect to the *35S* promoter, first by enzymatic restriction analysis and then by sequencing. The isolated plasmid was further electroporated into *Agrobacterium tumefaciens* strain C58 (pMP90) using Bio-Rad electroporation apparatus under pulsing settings for *Agrobacterium*. Bacterial culture was grown for 2 days at 28°C on MYA medium with antibiotics rifampicin (50 µg/ml) and gentamycin (20 µg/ml) for selection of bacteria, and spectinomycin (75 µg/ml) for vector selection.

Primer	**GenBank accession/ Gene model**	**Primer sequence (5'-3')**	**Amplicon (bp)**
attB1_FLA1	AY607753	GGGGACAAGTTTGTACAAAAAAGCAGGCT **CTCAGGCACCAGCAGTGGTTGC**	155
attB2_FLA1		GGGGACCACTTTGTACAAGAAAGCTGGGT **TTCTCCAGGATTTTGGTGACGTTGG**	
attB1_FLA14	AY607766	GGGGACAAGTTTGTACAAAAAAGCAGGCT **GTCAGAGAGCCCTGATGATG**	176
attB2_FLA14		GGGGACCACTTTGTACAAGAAAGCTGGGT **GATATTGCAACAACAGTACCAACAA**	
attB1_CTL2	Potri.010G141600	GGGGACAAGTTTGTACAAAAAAGCAGGCT **ATGGAGGCCAAATGGTGTTTTCTTG**	228
attB2_CTL2		GGGGACCACTTTGTACAAGAAAGCTGGGT **TTGCAGCAATAAGCAGACAAGC**	
attB1_BGAL7	Potri.002G080700	GGGGACAAGTTTGTACAAAAAAGCAGGCT **AACCGTTGCCTTCAACACTG**	152
attB2_BGAL7		GGGGACCACTTTGTACAAGAAAGCTGGGT **TTTCCATTGTTCAATTGAATCAAAT**	

Table 2. Primers used to generate attB-flanked gene sequences for recombination into donor vector. The bold part of the sequences corresponds to the gene specific sequence. The amplicon size corresponds to the predicted size of attB-gene PCR product.

Plant transformation and regeneration

T-DNA transformation of poplar clone INRA 717-1B4 (*P. tremula x P. alba*) by *A. tumefaciens*, so as plant regeneration, were carried out in *in vitro* conditions, according to the slightly modified protocol described by **Leplé *et al.*** (**1992**).
The protocol consists of five steps:

1) pre-culture of internode explants and *Agrobacterium* culture
2) incubation of explants with *Agrobacterium* suspension
3) co-culturing
4) selection of transformed cells (green calli)
5) regeneration of transgenic plants

A. tumefaciens C58 (pMP90) harboring pHellsgate8 binary vector was **pre-cultured** on MYA medium with antibiotics for selection for 2 days at 28°C. Poplar internodes were sampled from *in vitro* 8-10 week old 7171-1B4 plants, wounded and pre-cultured on MS medium (3% agar) with auxin NAA (10 mM) and cytokinin 2-ip (5 mM), for 2 days at 24°C in darkness. The internodes were further **incubated** within a bacterial suspension prepared at OD_{660} 0.25-0.3 in liquid MS medium, under shaking at 190 rpm for 16 h in darkness. After this incubation step, the internodes were **co-cultured** with *Agrobacterium* on MS medium (3% agar) with hormones, in darkness, for 2 days at 24°C. The explants were then **decontaminated** from bacteria by washing, 5 times in water with agitation 125 rpm. The decontaminated explants were cultured on MS medium (3% agar) with antibiotics cefotaxime (250 mg/L) and ticarcillin (500 mg/L) for inhibiting bacteria development, and kanamycin (50 µg/ml) for **selection** of transformed cells. The explants were first grown for 2 weeks in darkness and then exposed to light. When resistant green calli reached a size of few millimeters, they were isolated and grown on MS medium (3% agar) with antibiotics and thidiazuron (0.1 µM) to induce shoot growth. The calli were then transferred every 2 weeks during 2 months on new medium with progressively declining concentration of thidiazuron. The shoots **regenerated** from a single callus represented one individual transgenic line. The elongated shoots were grown on MS medium (2% agar) to induce rooting for 2 months. The sufficiently enlarged young plants were micropropagated from nodes on MS medium (2% agar) to obtain genetically

identical clones. The plants were grown for 6 weeks before acclimatization in the greenhouse, which is described in chapter concerning poplar.

Selection of transgenic lines

Around 50% of all the produced transgenic plants were screened for the semi-quantitative estimation of gene down-regulation and for histological observations. The percentage of the screened lines and the number of positive lines are given in **Fig. 15**. For each gene construct, based on this screening, we were able to find at least 2 down-regulated transgenic lines on which we focused for detailed characterization (**Fig. 15**). These lines were named T1 and T2. In addition, we selected a third line, named T3, as an additional control, showing no changes in target gene expression in comparison to WT.

Transgenic lines	*FLA1*	*FLA14*	*CTL2*	*BGAL7*
Production	21	21	12	8
Screening	48%	52%	42%	50%
Downregulated lines: Non down-regulated lines	3:7	4:7	5:0	2:2
Characterization	3 (T1, T2, T3)	3 (T1, T2, T3)	3 (T1, T2, T3)	3 (T1, T2, T3)

Figure 15. Number of produced transgenic lines, percentage of screened lines, ratio of down-regulated and non-down-regulated lines after characterization and number of lines chosen for characterization

1.3. Simarouba

Two simarouba (*Simarouba amara*) inclined trees were sampled for upper (TW) and lower (OW) wood in the forest and in the greenhouse in French Guiana, on 18th April 2013. An example of simarouba material is shown in **Fig. 16**. The adult simarouba tree, which was naturally grown and tilted in the forest, was 26cm large in diameter. A Simarouba juvenile tree grown for one year in the greenhouse was artificially double tilted at 90°, first for a period of 3.5 months until complete stem reorientation and second time on opposite side for 1.5 months.

Figure 16. Adult simarouba tree grown in wild forest of French Guiana and simarouba juvenile tree grown in greenhouse conditions (Photo credit adult simarouba: B. Clair)

II. BIOINFORMATIC ANALYSES

Alignments

BLAST sequence alignments were performed with nucleotide collection database of *P. trichocarpa* on NCBI portal (http://blast.ncbi.nlm.nih.gov/Blast.cgi) or JBI Phytozome portal (v3 of the genome, https://phytozome.jgi.doe.gov/pz/portal.html#). Clustal Omega tool (EMBL-EBI, http://www.ebi.ac.uk/Tools/msa/clustalo/) was used for multiple sequence alignments.

Construction of primers

The primer design was performed using Primer3Plus tool (http://primer3plus.com/cgi-bin/dev/primer3plus.cgi). The oligonucleotide properties were calculated with Oligo Calc tool (http://biotools.nubic.northwestern.edu/OligoCalc.html). The sequence restriction sites were verified with RestrictionMapper (http://www.restrictionmapper.org/).

Phylogenetic analysis

Gene families were predicted in the genomes of *Populus trichocarpa*, *Arabidopsis thaliana* and *Linum usitatissimum* with BioMart tool (JBI Phytozome, v11). The database was searched for gene models with the following Pfam protein domains: FLA (Pf02469), GH19-CTL (Pf00182), GH35-BGAL (Pf01301) and GH42-BGAL (Pf02449). Phylogenetic analyses were conducted with MEGA7 software (**Kumar *et al.*, 2016b**). The protein sequences were aligned with MUSCLE tool using default settings. The evolutionary history was inferred by using the Maximum Likelihood method based on the JTT matrix-based model, partial deletion (cutoff 95%), Gamma distributed rates, bootstrapping 500 replicates. Phylogenetic tree was visualized with Interactive Tree Of Life (iTOL, v3, http://itol.embl.de/).

III. TRANSCRIPTOMIC ANALYSES

3.1. RNA isolation

Total RNA was isolated from around 100 mg of ground tissue with a slightly modified protocol from **Chang et *al.*** (**1993**). Cells were lysed with 900 µl of extraction buffer (CTAB 2%, PVP40 2%, Tris-HCl 0.1M, EDTA 0.025M, NaCl 2M, Spermidine 0.344M), during 30 minutes at 65°C. RNA was extracted in two steps with a mix of chloroform and isoamylalcohol (24:1). After overnight precipitation with 2.5 M Lithium Chloride, RNA was dissolved in RNAse-DNAse free water and purified with NucleoSpin RNA Plant kit (Macherey-Nagel, France) according to manufacturer's recommendations. In order to ensure the elimination of genomic DNA, the sample was treated with DNase I (Macherey-Nagel, France) during the purification step. RNA was eluted in RNAse-DNAse free water and quantified by Nanodrop ND-1000 spectrophotometer.

3.2. RT-PCR

The synthesis of cDNA was performed in 13 µl of reverse transcription (RT) reaction composed of 2 µg of RNA, 1 µl of 500 µg/ml oligo $(dT)_{12\text{-}18}$ primer and 1 µl of dNTP mix (10 mM each), incubated at 65°C for 5 minutes. Next, 4 µl of 5X first-strand buffer, 2 µl of 0.1 M DTT and 1 µl of 200 U SuperScript II enzyme (Invitrogen, Life Technologies) were added in a total of 20 µl volume reaction, incubated for 50 minutes at 42°C. The reaction was inactivated by heating at 70°C for 15 minutes. Two µl of diluted cDNA (1/4) was amplified in Polymerase Chain Reaction (PCR) with 0.25 µl of 1 U Taq DNA polymerase (Invitrogen, Life Technologies), each gene specific primer 0.2 µM (**Tab. 3**), dNTPs 200 µM, $MgCl_2$ 1.5 mM and enzyme buffer 1X.

The primer couples for gene expression were designed with QuantPrimer tool (http://www.quantprime.de/), on the basis of the sequence specificity and a product size range between 150 and 250 bp. The primers were chosen to be gene-specific, except for BGAL for which it was not possible to find specific primers for four *BGAL* genes. Amplification of couples *BGAL10*/*BGAL11* and *BGAL12*/*BGAL13* was therefore analyzed with per one primer. Primer couples used for amplification of *FLA1* and *FLA14* were retrieved from **Lafarguette *et al.*** (**2004**). PCR amplification was carried out in conditions given in **Tab. 4**. As a control of equal

matrix loading, cDNA was amplified with primers corresponding to 18S rRNA sub-unit.

The amplicons were loaded on a 2% agarose gel and electrophoresed. The gel was stained with ethidium bromide and exposed to ultra violet light in an ultraviolet transilluminator (Fisher Bioblock Scientific).

Gene name	GenBank accession/ Gene model	Forward primer (5'-3') / Reverse primer (5'-3')	Amplicon (bp)
FLA1	AY607753	GTTTCTAGCATTATATCTTAACAAC	923
		CAGAATTATTCAACACACAATCGGC	
FLA14	AY607766	TCGCCATCAATTTAACCACA	181
		CCATTGTTTGTGTTGCCAAG	
CTL2	Potri.010G141600	AAGCATCTCCCTTCAGCACACG	202
		TGCCAACACCCATTAGGTCGAG	
BGAL1	Potri.017G057900	AGGCACATGTGTACGGTGGAAG	223
		TGAGTCTGTGCTGCAACCTTGG	
BGAL2	Potri.009G012400	CGTGTCAGAGTCTCACCCATTACC	233
		TCTTTGATCCGATGCAAGCCTTC	
BGAL3	Potri.011G044300	CAAAGCCAGGTTTACTGGAGCAG	184
		TGATTGCCATACCCGAAAGCTAC	
BGAL4	Potri.009G134400	GACTACGTCTGGTTCACCACAACC	152
		TGGCTCCCATGTGCAGAACCTATG	
BGAL5	Potri.004G174800	GCTCGCTTAAAGTGTCCAAACAAG	149
		TTTCCCAAGCAATGCTGCTCAAC	
BGAL6	Potri.013G105100	GGCAGGAATTCACCGAAGCAATC	229
		CGGCTTCCTTGAACAGATCCTACG	
BGAL7	Potri.002G080700	TGTGATGACTGGATTGCCGGATG	214
		TGGCCGAGATGAGCTTGCATAC	
BGAL8	Potri.005G180600	TCGACCACTCATGTGGTACAAGAC	206
		TGCCAGTCGGTTTGAGGAAAGC	
BGAL9	Potri.005G069200	TCTGCACATGGAAGTAAGGATGCC	132
		CTCCAGGAAAGCTCCTGAATCTTG	
BGAL10_11	Potri.003G040000	TCAATGGAGTCTGTGGGACAGATG	219
		AGCACATTTGGCATTAGGAAGGC	

BGAL12_13	Potri.T154000	GCGCTACAGTTGGATTCACGAAC	199
		TGCCACTTAAGAGATTGACTGCTG	
BGAL14	Potri.001G025800	GATGCACCGCTAGATGAATATGGG	182
		AAGCAGCTCGATCCCTTCTCAG	
BGAL15	Potri.006G139100	ACCAACTTTGGACGCACGTCAG	217
		TGCTGGTGTACGTAGTCAGCTC	
BGAL16	Potri.018G062800	GGACTTGACGTCATATCAGTGGTC	158
		GACTGGCAAATGTGGTCTTGTACC	
BGAL17	Potri.004G159800	ACAACCATTGACATGGTACAAGGC	184
		AGGCCGGAATGTAGCCGAATAG	
BGAL18	Potri.007G018100	CAATCAACAGGCCATGCTGTGC	179
		TCATAGTGTCCACCCACATTCGG	
BGAL19	Potri.005G232600	CAGCAATGGTCTTACCAGGTTGG	182
		CTGCGCATGTCCAAAGCCAATG	
BGAL20	Potri.003G038500	GAATGGGCATGAACCTTCACCAG	228
		GTGAACTTCTGCATTTGAGCCTTG	
BGAL21	Potri.001G200400	AATGGCCAGCTATCTGGGACTG	224
		TTCTGCCAGGACAAGTCCATCC	
BGAL22	Potri.006G144500	GCGGTTTATAACACGGCAAGGC	187
		ACCACAAGTAGTCTGTGGCATCC	
BGAL23	Potri.007G099800	TCGTGGAGAAAGCTGGGATTTGG	239
		GCCATTTCCAGATGCACTACCTTG	
18S		CTTCGGGATCGGAGTAATGA	
		GCGGAGTCCTAGAAGCAACA	

Table 3. Primers used in semi-quantitative RT-PCR analyses

Initial denaturation	95°C, 5 min				
Gene	***FLA1***	***FLA14***	***CTL2***	***BGAL7***	***18S***
No of cycles	25/20/20	25/20/22	20/20/20	30/35/35/35	20
Denaturation	95°C, 30 s	95°C, 30 s	95°C, 30 s	95°C, 30 s	95°C, 30 s
Annealing	57°C, 45 s	57°C, 45 s	57°C, 45 s	59°C, 45 s	60°C, 45 s
Elongation	72°C, 1.5 min	72°C, 30 s	72°C, 30 s	72°C, 30 s	72°C, 30 s
Final extension	72°C, 15 min				

Table 4. Amplification conditions used in RT-PCR kinetic expression study (orange), screening (green) and characterization (purple) of transgenic lines and BGAL family expression study (blue)

3.3. RT-qPCR

Two µg of RNA was reverse-transcribed into cDNA in a reaction performed with 10 µl of 2x reaction mix and 2 µl of 200 U/µl SuperScript III enzyme (Invitrogen, Life Technologies). The reaction was incubated for 50 min at 42°C and then 5 min at 85°C. To remove remaining RNA template, the synthesized cDNA was treated with 2 units of RNAase H for 20 min at 37°C. 2 µl of cDNA matrix (diluted 1/2) was amplified in Real-Time Polymerase Chain Reaction with 6 µl of SYBR Green master mix (Invitrogen, Life Technologies) and each gene-specific primer 0.2 µM (**Tab. 5**), in total volume reaction of 12 µl. The reaction was performed twice for each sample, in Twin-Tec Real-time plates (Eppendorf, Germany) on MasterCycler Realplex Epgradient apparatus (Eppendorf), under the following amplification conditions: initial denaturation for 2 min at 95°C, 40 cycles conducted of a denaturation step for 15 s at 95°C and an annealing/elongation step for 30 s at 60°C. In order to verify the specificity of amplification, the melting curve was formed by heating the reaction from 60°C to 95°C. Primers were designed for amplicon length of approximately 200 bp. Housekeeping gene encoding ubiquitin was used for normalization. The efficiency of the amplification reaction was evaluated in qPCR reaction from a serial dilutions of cDNA pool.

The relative quantification of gene expression was calculated as $\mathbf{2^{-\Delta Ct}}$, where ΔCt represents:

- in expression study performed on tissues and organs: a difference between Ct value normalized with the signal of endogenous control (*UBC* gene) and lowest Ct value (seeds) normalized with the same signal
- in the expression analysis performed on transgenic lines: a difference between Ct value of gene and Ct value of endogenous control (*UBC* gene)

Gene	GenBank accession or Gene model	Forward primer (5'-3') Reverse primer (5'-3')
FLA1	AY607753	CTGCAGCTTCTGTGGATGTA
		AGCTACAAAATCATACAAACTGGAT
FLA4	Potri.013G014200	CCACTACCTTTGCTCAGACGTCAC
		CGTTTGTGATGCCGTGTGGTTG
FLA8	Potri.009G012200	ATCCTGGCACCAACTGACAACG
		TCCCGGTGGTGGTGACATTTAG
FLA11	Potri.016G088700	AGCCGGAAATAGTGCTGATGGC
		TTCTCGGGCTTTGAAGGTGCAG
FLA13	Potri.006G129200	CCCGCTAAATGTGACAACATCAGG
		TTTGACCCTGCAGGAGCTTTGG
FLA14	AY607766	TCGCCATCAATTTAACCACA
		CCATTGTTTGTGTTGCCAAG
CTL1	Potri.014G146600	TGTGGCACACGCTGTTGGATTC
		CAGTAGCGACTCCATAACCACAGG
CTL2	Potri.010G141600	AAGCATCTCCCTTCAGCACACG
		TGCCAACACCCATTAGGTCGAG
BGAL7	Potri.002G080700	TGTGATGACTGGATTGCCGGATG
		TGGCCGAGATGAGCTTGCATAC
CESA8A	Potri.011G069600	TCGACAGGCTATCTGCAAGGTATG
		AGTCCACAGCAAGGATGGAAAGG
CESA7A	Potri.006G181900	ACTGGTGTCAGATCAAGACCTGTG
		TTTCTTTGCGTCCCATCTTGCG
CESA4	Potri.002G257900	ACCTTGCATGCCAAAGATGAGC
		GGAAAGCCACACACATGACAAGC
KOR	Potri.003G151700	TCGTTGCTGCTGGTCTATTGGTTG
		TCGGAAGCTTTCCCGATCTTTGAG
COBL4	Potri.015G060100	TGTCACCTGCACCTACTCACAG
		TGGGATTCCTTCGAGTTACTCTTG
UBC	Potri.003G136200	TGTTAAGTGATGGCATCGAAACGG
		TTGTCCTGAAAGCAACCTTAGGAG

Table 5. Primers used in relative quantitative RT-qPCR analyses

IV. BETA-GALACTOSIDASE ACTIVITY

4.1. Localization with X-Gal substrate

Fresh 50 µm-thick wood sections were cut with a Leica RM2155 microtome and placed in a plate with wells containing 200 mM citrate-phosphate buffer, pH 5.0. The sections were pretreated with chilled 90% acetone, 3 times under vacuum and for 30 min at 4°C. Prior reaction, the samples were rinsed with citrate-phosphate buffer, 3 times per 10 minutes. The sections were then incubated in 500 µl of reactive medium composed of 1mM 5-bromo-4-choloro-3-indolyl-beta-D-galactopyranoside (X-Gal, Thermo Fisher Scientific) dissolved in dimethylformamide, 100 mM citrate-phosphate buffer, pH 8.0; 0.5 mM potassium ferrocyanide and 0.5 mM potassium ferricyanide. The reactive medium was infiltrated 3 times under vacuum. The reaction was carried out over-night at 4°C in darkness. Next day, the sections were rinsed 3 times per 10 minutes with citrate-phosphate buffer and once for 10 minutes with water. The sections were fixed on a glass slide in Aquatex. Photos were taken with Leica M205 FA stereomicroscope.

4.2. Quantification with MUG substrate

150 mg of ground opposite and tension wood was mixed with 800 µl of cold extraction buffer composed of 25mM citric acid/50mM Na_2HPO_4 buffer (pH 5.45), 1mM $MgCl_2$ and 50mM β-mercaptoethanol. The extraction was performed by mixture grinding with Retsch MM 400 mixer mill using Qiagen tube carrier, for 1 min at frequency 20 rotations per sec. Supernatant was separated by centrifugation, 10 min at 18 000 x g and 4°C. The concentration of proteins was determined in a Bradford reaction. Reaction with MUG was performed with 5 µg of proteins adjusted with extraction buffer to 500 µl and 55 µl of 10 mM 4-methylumbelliferyl-β-D-galactopyranoside (MUG) substrate. Reaction was incubated at 37°C with agitation at 850 rpm. 100 µl of reaction mix was sampled after 0, 30 and 60 min; and incubated with 900 µl of 200 mM Na_2CO_3. The fluorescence of released 4-methylumbelliferone (MU), excited at 460 nm and emitted at 355 nm, was detected with Fluroskan Ascent microplate fluorometer. The concentrations were calculated according to MU standard in range from 0 to 10 nm/ml.

V. WOOD CHARACTERIZATION

5.1. Wood anatomy

Safranin/Alcian-blue staining

1% safranin and 1% alcian blue were prepared in 50% and 100% ethanol, respectively. Safranin/alcian blue double staining was performed on fresh wood 30 µm cross-sections, prepared with Leica RM2155 microtome. The sections were incubated for 6 min in 2.6% bleach, washed in water, incubated per 1 min in 50% and 25% ethanol, 3.5 min in 1% safranin and 6 min in 1% alcian blue. After each staining, sections were rinsed in 100% ethanol. The stained cross-sections were fixed on glass slides with Canada balsam and cover slips, and observed under Leica DMR optical microscope. Pictures were taken with Leica DFC 320 camera.

5.2. Immunohistolocalization

Fixation and embedding

Opposite and tension wood sections (3 mm) of poplar and simarouba were fixed in a solution of 2.5% paraformaldehyde and 0.1% glutaraldehyde dissolved in 0.1 M citrate-phosphate buffer, pH 6.8. The sections were further rinsed in 0.1 M citrate-phosphate buffer, dehydrated in a gradient of ethanol (25%, 50%, 70%) and embedded in medium grade LR White resin (London Resin Company Ltd, UK). The embedded samples were cut as semi-thin sections (0.8 µm) with a diamond knife (Diatome, Switzerland) installed on a Leica ultracut R microtome. The cut sections were fixed on silanized slides (Dako Cytomation, France) heated at 55°C. The fixed cuts were used for methylene blue/Azur II staining and immunohistolocalization study.

Methylene blue/Azur II staining

1% methylene blue solution was prepared in 1% of sodium tetraborate, while 1% Azur II solution was prepared in distilled water. Cut sections were fixed on glass slide by heating at more than 100°C. The sections were first treated with 1% periodic acid, for 5 min at room temperature and then rinsed with water. The sections were further covered with droplets of equilibrated volumes of methylene blue and Azur II. The slides were warmed at 50°C up to 2 min, not allowing the

sample to dry. The sections were rinsed with water and fixed with Canada balsam and cover slip.

Epitope detection

Resin-embedded wood sections were first rehydrated for 10 minutes with water and then incubated with 1x TBS-Tween (Diapath). The sections were saturated with droplets of 1x TBS-Tween BSA 3% blocking buffer, for 1h in darkness. The immunoreaction was performed by incubating the cross-sections with droplets of primary antibody diluted to optimal concentration in 1x TBS-Tween BSA 0.3%, overnight at 4°C in darkness. Next day, the sections were washed with 0.05 M TBS (Biosciences) and incubated for 1h in darkness with corresponding 20nm gold-conjugated secondary antibody (British Biocell International, UK), diluted 50 x in 0.05 M TBS, and then rinsed, 3 times with 0.05 M TBS and 3 times with distilled water. The visualization of gold particles was enhanced with Silver Enhancing kit (British Biocell International, UK). The sections were stained for 40 sec with droplets of 1/120 diluted methylene blue/Azur II stain and observed under Leica DMR optical microscope. The zones of observations in simarouba are given in **Fig. 17**. The same protocol was conducted on poplar sections fixed for thesis of F. Guedes (2013). The poplar sections were used as a control of the obtained results and for comparison of labelling to simarouba. The zones of observations were the same as for cellulosic TW fiber and OW fiber of simarouba, except that poplar fibers have secondary cell wall with S1 and S2 layers, which were not distinguished and were studied as one layer.

All the incubations were conducted in a moist chamber to prevent sample drying. The list of used antibodies, corresponding antigens and epitopes, primary antibody dilutions and immunization species are given in **Tab. 7**.

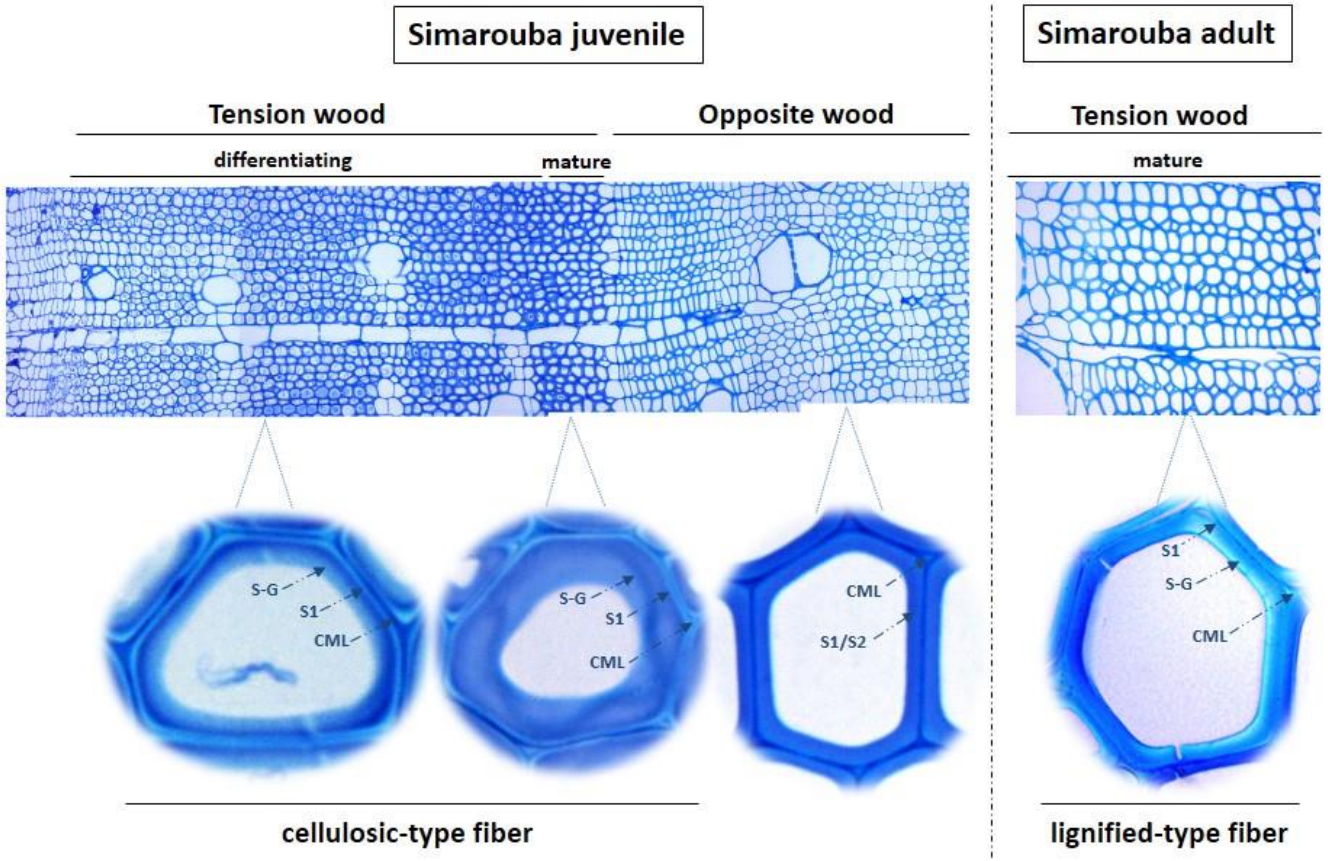

Figure 17. Observation zones of simarouba fibers in immunohistolocalization study: cellulosic-type fibers in differentiating and mature tension wood of simarouba juvenile tree, lignified-type fiber in mature tension wood of adult simarouba, fibers of mature opposite wood in simarouba juvenile tree. Cell wall layers of fibers: CML= compound middle lamella (middle lamella + primary cell wall); S1= secondary cell wall layer 1; S1/S2= secondary cell wall layer 1 and 2; S-G= secondary cell wall layer 2/gelatinous-type layer

Antibody	Antigen	Epitope	Dilution	Immunization
LM5	RG-I	β-(1,4)-Gal	1/30	Rat
RU1	RG-I	(1,2)-Rha-(1,4)-GalA-	1/3	Mouse
PopFLA1	AGP	Unknown	1/100	Rabbit
JIM14	AGP	Unknown	1/10	Rat
JIM16	AGP	Unknown	1/10	Rat
Mac207	AGP	β-GlcA-α-(1,3)-GalA-(1,2)-Rha	1/10	Rat
LM6	RG-I/AGP	α-(1,5)-L-Ara	1/20	Rat
CCRC-M7	RG-I/AGP	Arabinosylated β-(1,6)-D-Gal	1/10	Mouse

Table 7. Antibodies used in immunolocalization study, antigens and their characterized epitopes, dilution of primary antibody and immunization system. Rha - rhamnose; GalA - galacturonic acid; Gal – galactose; Ara – arabinose.

5.3. Wood chemical properties

Middle Infrared spectroscopy

A small quantity of ground wood was exposed to Middle Infrared (MIR) light of wavelength 400 to 4000 cm-1, in attenuated total reflectance (ATR) mode of PerkinElmer Spectrum 400 FT-IR spectrometer. The spectra were captured and analyzed in range between 800 and 1800 cm-1, with reads every 1 cm-1. In order to improve signal quality, the raw spectra were first statistically pretreated in R program for smoothing and normalization. The spectra were further subjected to principal component analysis (PCA) for comparison between wild type and transgenic lines.

5.4. Cellulose ultrastructure

X-ray diffractometry

Wood sections were cut with blade to 10-20 mm length, 3-4 mm width and 1-2 mm thickness. The beam was in X-ray diffractometer positioned perpendicular to the surface of wood sample. The interferences were projected on diffractogram as diffraction peaks of Miller's index 002 associated with the crystalline plan of atoms in wood. An angle of cellulose microfibrils was calculated as 0.6*T where the T parameter corresponds to the half-surface of a peak. An anisotropic index was calculated as a ratio between the maximal intensity and the baseline of diffraction peak.

Annex I: Map of pHellsgate8 vector for RNAi gene silencing

(snapgene.com/resources/plasmid_files/plant_vectors/pHELLSGATE_8/)

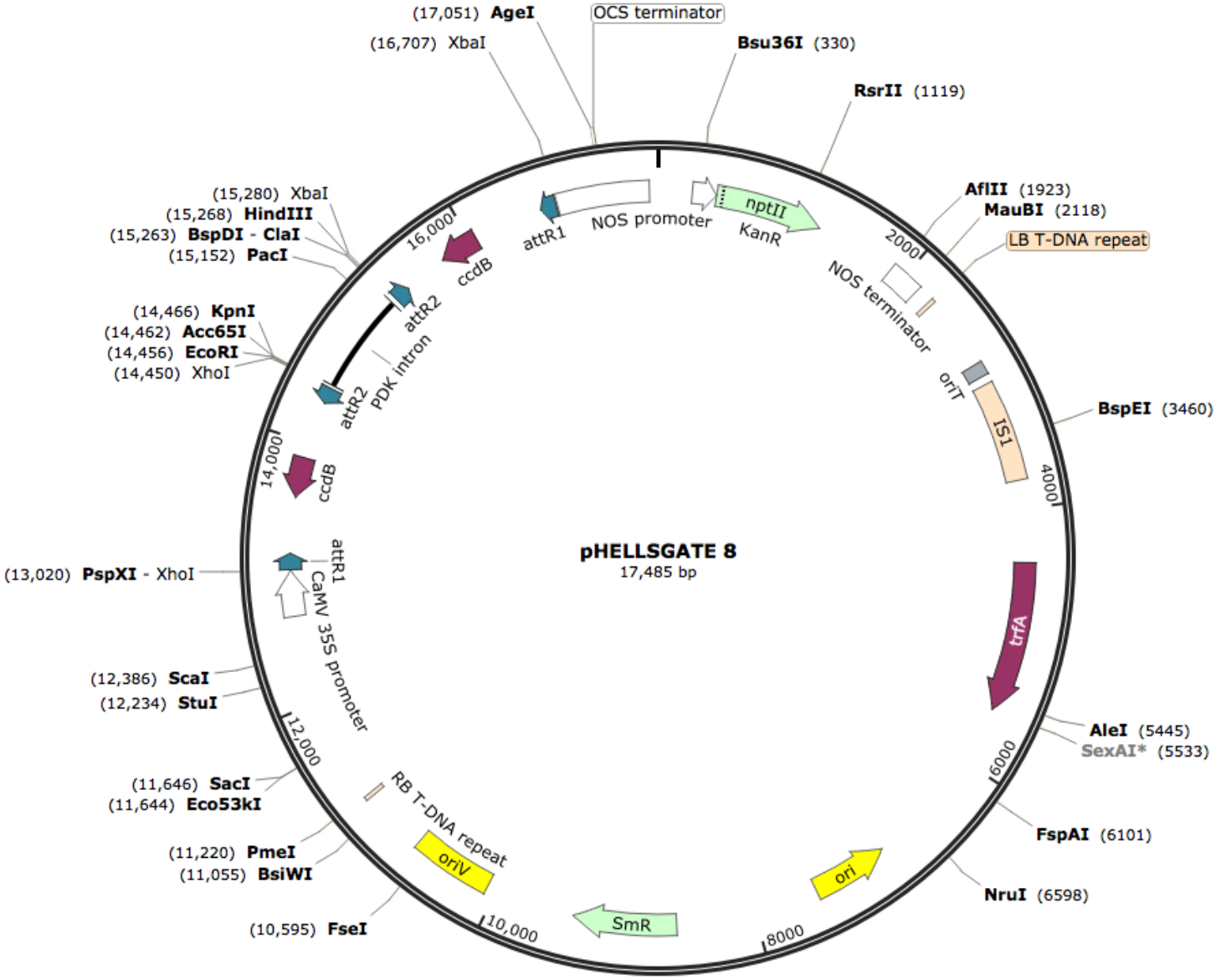

RESULTS

Identification and characterization of molecular players in tension wood of poplar

1. Article: CHITINASE-LIKE PROTEIN

PtaCTL2 encodes chitinase-like protein required for cellulose crystalline structure, secondary cell wall organization and mechanical strength of poplar stems

A Šećerović[1], MC Lesage-Descauses[1], F Laurans[1], V Segura[1], N Belmokhtar[1], JC Leplé[1], Niez B[2], E Badel[2], T Almeras[3], B Clair[4], A Déjardin[1], G Pilate[1]

[1] Unité Amélioration, Génétique et Physiologie Forestières, INRA Val de Loire, 45075 Orléans cedex 2, France

[2] Physique et Physiologie Intégratives de l'Arbre Fruitier et Forestier, INRA Site de Crouël, 63039 Clermont-Ferrand cedex 2, France

[3] Laboratoire de Mécanique et Génie Civil, Université de Montpellier 2, 34090 Montpellier, France

[4] Ecologie des Forêts de Guyane, Campus Agronomique, 97387 Kourou, French Guiana

ABSTRACT

Two chitinase-like proteins (CTL) from Arabidopsis were reported to have function in cellulose synthesis and structure. We characterized in poplar hybrid *Populus tremula* x *Populus alba* PtaCTL2, which is a homolog of Arabidopsis CTL related to secondary cell wall. *PtaCTL2* had high expression in wood and low expression in other tissues and organs of poplar. Characterization of PtaCTL2 RNAi transgenic poplars revealed modifications of wood chemical properties related to hemicelluloses and lignin, reduced cellulose content and altered crystalline cellulose structure. We further showed that the modifications weakened mechanical properties of stems, which were brittle, had reduced wood density and more frequent cracks on stem cross-sections. The modifications of biochemical and mechanical properties were examined in straight-growing and tilted trees, and demonstrated in opposite and normal wood, so as in tension wood, which has particular cellulose structure.

INTRODUCTION

Chitinases are widely spread enzymes, which are known to degrade chitin structure formed of β-(1,4)-linked units of N-acetylglucosamine (**Adrangi and Faramarzi, 2013**). The chitinase activity is employed by plants in the defense system against chitin-containing pathogens (**Kesari *et al.*, 2015**). The chitinases belong to the structurally diversified families of glycosyl hydrolases (GH) 18 and 19 (**Kesari *et al.*, 2015**). GH19 family is found primarily in plants, while GH18 family can be found in various organisms (**Mokshina *et al.*, 2014**). Chitinase-like proteins (CTL) have structural similarities with GH18 and GH19 families, but their functions seem far from the classical enzymatic activity (**Kesari *et al.*, 2015**). The substitutions in protein domains responsible for the chitinase activity and chitin binding raised their novel functions in cell wall development (**Kesari *et al.*, 2015**; **Hermans *et al.*, 2010**), as it was reported in Arabidopsis, cotton and rice.

OsCTL1 is Golgi-targeted integral membrane protein ubiquitously expressed in rice. Its mutation reduced thickness of secondary cell walls, mechanical strength of culms and leaves and cellulose content in internodes, while it elevated content of xylose and arabinose (**Wu *et al.*, 2012**). In Arabidopsis, a function of AtCTL1 has been exhaustively reported from phenotypes of its mutants (**Zhong *et al.*, 2002**; **Kwon *et al.*, 2007**; **Hermans *et al.*, 2010**). The *elp1* mutation in AtCTL1 caused severe cell wall effects as increased and shape-modified pith cells, length-reduced cortical and epidermal cells; and endodermal cells and pith cells with ectopic lignin deposition (**Zhong *et al.*, 2002**). The mutation of AtCTL1's close homolog AtCTL2 caused only slight lignin increase in hypocotyls of dark-grown seedlings, while there were no modifications of plant growth or cell wall development (**Hossain *et al.*, 2010**).

Based on the co-expression with *CESA* genes, AtCTL1 and AtCTL2 were associated with the cellulose synthesis in primary and secondary cell walls, respectively (**Persson *et al.*, 2005**). It is in accordance with the ubiquitous expression of *AtCTL1* and the expression of *AtCTL2*, which was restricted to stems, anthers and stigmata (**Hossain *et al.*, 2010**). The preferential expression in cells with secondary cell walls was also reported for two cotton paralogs GhCTL1 and GhCTL2 (**Zhang *et al.*, 2004**). AtCTL1 and AtCTL2 are highly homologous proteins and functionally important for cellulose synthesis, cellulose organization and

interaction with hemicelluloses in the cell wall (**Sanchez-Rodriguez *et al.*, 2012**).

Tension wood fibers of angiosperm trees develop the additional secondary cell wall layer called G-layer. The G-layer has particular properties characterized with highly crystalline cellulose structure and cellulose microfibrils oriented in parallel to the fiber axis (**Clair *et al.*, 2006**). During the G-layer development, the microfibrils generate high tensile stresses, giving rise to the outstanding mechanical properties of tension wood required for the reorientation of axes and reinforcement of stems and branches, displaced by tree weight or environmental loads as wind (**Clair *et al.*, 2011**). Matrix of the G-layer has been extensively studied in a search for molecules, which may be implicated in a mechanism of tensile stress generation (**Kim and Daniel, 2012**; **Gritsch *et al.*, 2015**; **Gorshkova *et al.*, 2015**). The matrix is, among other components, constituted of arabinogalactan proteins (AGP) (**Bowling and Vaughn, 2008**). AGPs were demonstrated to bind chitinases from embryogenic pine tissues (**Domon *et al.*, 2000**), and AGPs modified by chitinase were reported as important for somatic embryo development (**van Hengel *et al.*, 2001**). A group of fasciclin-like arabinogalactans (*FLA*) genes was also shown to be expressed differentially in tension wood, when compared to opposite wood (**Lafarguette *et al.*, 2004**).

Bast fibers of flax develop a cell wall layer remarkably similar to the G-layer of poplar, and these fibers are enriched in transcripts of a group of CTLs, which was in a phylogenetic analysis shown to be distinct from other CTL groups (**Mokshina *et al.*, 2014**). In poplar, a high number of transcripts of a chitinase-like gene homologous to AtCTL2 was detected in differentiating tension and opposite wood, and not in cambial wood tissue (**Déjardin *et al.*, 2004**). However, a function of chitinase-like proteins and their significance for wood formation stay, up to date, undetermined.

In the present study, CTL family from poplar was predicted and compared in a phylogenetic analysis with CTL families from flax and Arabidopsis. Additionally, the CTL poplar family was studied in expression analysis in wood. The study of chitinase-like protein was further focalized on CTL2, which had the highest expression in wood and is homologous to CTL2 from Arabidopsis related to secondary cell wall. The down-regulation of *PtaCTL2* did not alter plant growth and wood anatomy of RNAi transgenic poplars, but the phentoype strongly suggested the importance of PtaCTL2 for secondary cell wall properties. *PtaCTL2* transgenic

poplars had altered wood chemical properties, cellulose and xylose content and crystalline cellulose structure. The modifications of wood properties as well reflected on stem mechanical properties of transgenics. Finally, the results suggested that PtaCTL2 is equally important for properties of tension wood, opposite and normal wood.

RESULTS

Phylogenetic analysis of CTL family

We predicted chitinase and chitinase-like genes (commonly named CTLs) in genomes of Arabidopsis (At), poplar (Ptr) and flax (Lus). Genomes are available on JBI Phytozome (v11) website, where we used BioMart tool to filter proteins with Pf00182 domain conserved for GH19 family. The research was restricted on GH19 chitinases for reason of: i) the characterized Arabidopsis CTLs possess GH19 signature (**Hermans *et al.*, 2010**), ii) GH19 chitinases have different structure than GH18 chitinases (**Kesari *et al.*, 2015**). The tool predicted 21 CTLs in poplar, 37 in flax and 14 in Arabidopsis. Their gene models are given in supplementary **Tab. I-1**.

PtrCTL1 and PtrCTL2 were named because of their homology with well characterized homologs from Arabidopsis AtCTL1 and AtCTL2 (**Sanchez-Rodriguez *et al.*, 2012**). The remaining CTLs from poplar and Arabidopsis were annotated according to the falling order in groups A, B and C. The groups were formed according to the phylogenetic relationship between LusCTLs, as presented in **Mokshina *et al.*** (**2014**). The phylogenetic tree and grouping of CTLs from Arabidopsis, flax and poplar is shown in **Fig. I-1.**

Most of CTLs from poplar were predominantly falling into group-B (52%), while the majority of CTLs from Arabidopsis (64%) and flax (65%) were sharing homology with the group-C. One group of CTLs from flax was particularly expanded within the group-C. The smallest and the most divergent group of CTLs was group-A. The group clearly divided in 2 clades, each represented with AtCTL1 or AtCTL2, which were described functionally in Arabidopsis (**Sanchez-Rodriguez *et al.*, 2012**). AtCTL2, protein related with secondary cell wall (**Hossain *et al.*, 2010**) was grouped in the same clade as PtrCTL2, LusCTL1 and LusCTL2. The group of flax CTLs (LusCTL19, LusCTL20, LusCTL21), potentially involved in development of flax G-fibers (**Mokshina *et al.*, 2014**), was classified within group-C. A

multisequence alignment of the group-A reveled that all members have conserved signature sequence of GH19 chitinases (**Fig. I-2**). On the contrary, the amino acid residues assigned to the chitinase catalytic activity and substrate binding were highly substituted in the sequences of group-A members. Although the motifs were similar among the examined CTLs, one substituted motif (S-K-T-S) was conserved among members of the same clade (AtCTL2, PtrCTL2, LusCTL1 and LusCTL2) and AtCTL1. Existence of the cleavage site in signal peptide was predicted for all members of group-A, except for AtCTL2, LusCTL1 and LusCTL6.

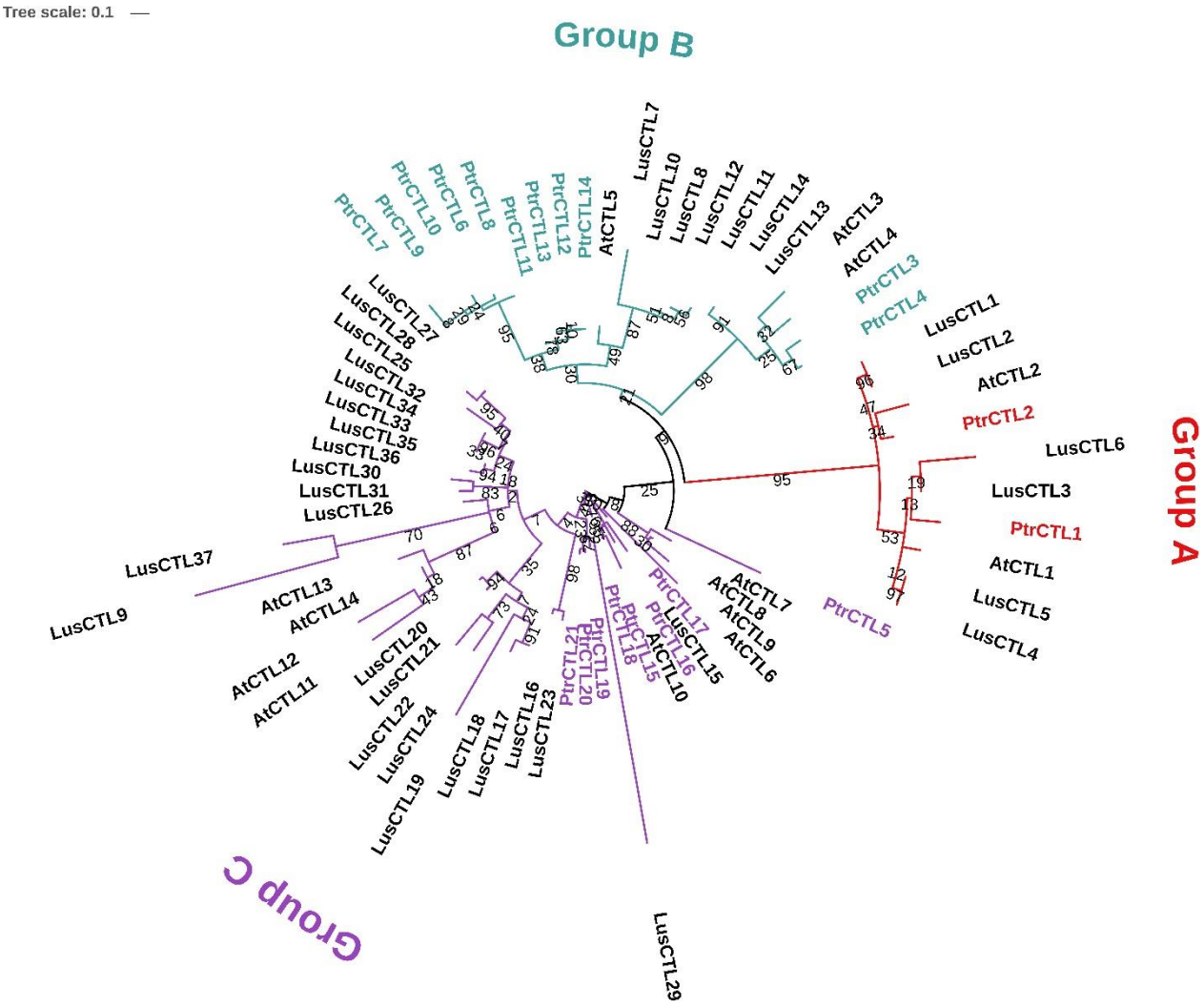

Figure I-1. Phylogenetic tree of aligned CTL GH19 protein family predicted from genomes of *Arabidopsis thaliana* (At), *Linum usitatissimum* (Lus) and *Populus trichocarpa* (Ptr). The members were attributed to groups A, B and C according to Mokshina *et al.* (2014). The evolutionary history was inferred by using the Maximum Likelihood method based on the JTT matrix-based model in the analysis conducted in MEGA7 software.

Figure I-2. Multiple sequence alignment of CTLs from flax (Lus), Arabidopsis (At) and poplar (Ptr). The amino acid residues colored in blue indicate chitinase 19_1 (C-x(4,5)-F-Y-[ST]-x(3)-[FY]-[LIVMF]-x-A-x(3)-[YF]-x(2)-F-[GSA]) and chitinase 19_2 signature ([LIVM]-[GSA]-F-x-[STAG](2)-[LIVMFY]-W-[FY]-W-[LIVM]) sequences. The amino acid residues colored in red putatively bind the substrate in class I of GH19 chitinases where they should be, in the order: HETT, W, S, YN, Q, K, N, R. The residues colored in green are essential for catalytic activity in class I chitinases where they should be, in the order: E, E, Q. The residues were assigned according to Hermans *et al.* (2010). The putative secretion signal was predicted with SignalP 4.1. Two residues colored in grey mark the predicted cleavage site.

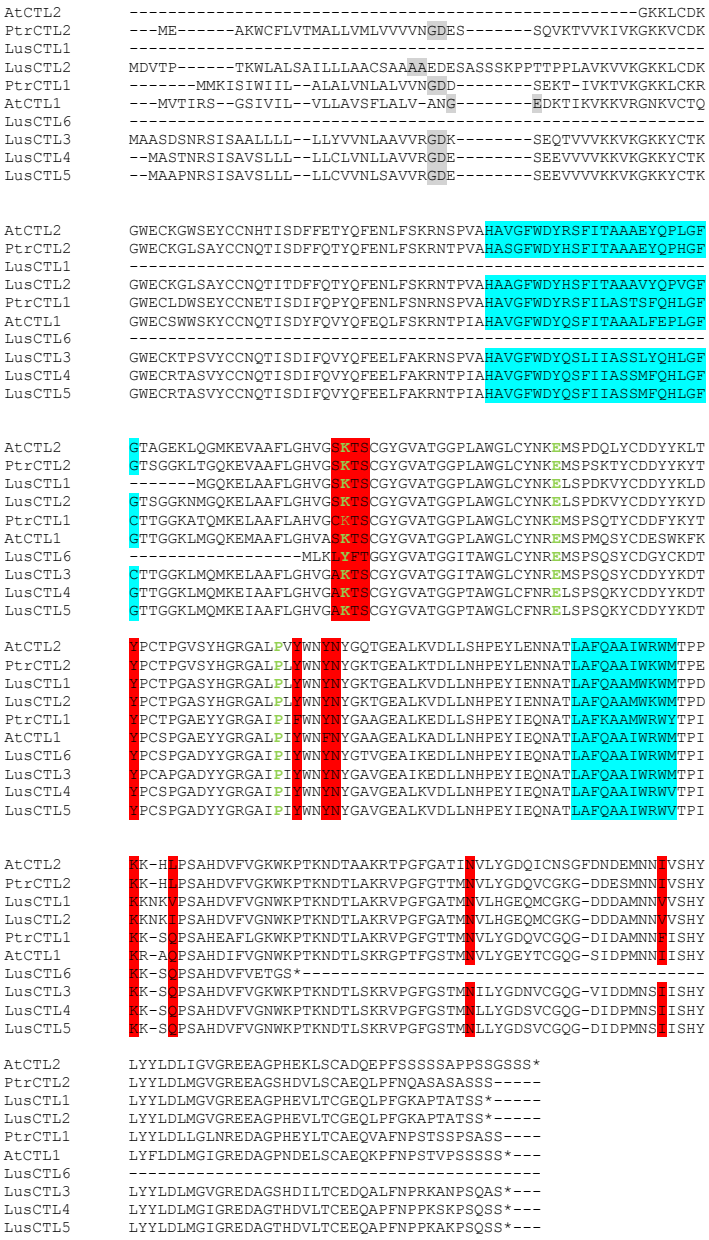

Expression profile of poplar GH19 chitinase-like family in wood

CTL family from poplar was profiled in the analysis of gene expression in normal wood (NW), opposite wood (OW) and tension wood (TW). The expression was detected for only 9 out of 21 genes (**Fig. I-3**). However, for the majority of genes expression was close to zero. Only *PtrCTL1* and *PtrCTL2* were notably expressed in wood - *PtrCTL2* having approximately 12-fold higher expression than *PtrCTL1*. For both genes, there was no significant difference in expression between OW and TW and no evident difference in expression between NW and TW or OW.

A functional study of chitinase-like proteins was continued for only one gene and was further performed in poplar model *P. tremula* x *P. alba*. We chose to study CTL2, based on its high expression in wood and homology with *AtCTL2* gene highly expressed in cells with secondary cell wall (**Hossain *et al.*, 2010**).

To examine the expression of *PtaCTL2* within other tissues and organs of poplar, we performed RT-qPCR analysis in apex, leaves, xylem, phloem, roots, seeds and germinated seeds. Among the analyzed tissues and organs, the expression of *PtaCTL2* was notably the highest in xylem (**Fig. I-4**). The expression was 10-40 times lower in leaves, apex, phloem and roots. In seeds and germinated seeds, *PtaCTL2* had expression close to zero.

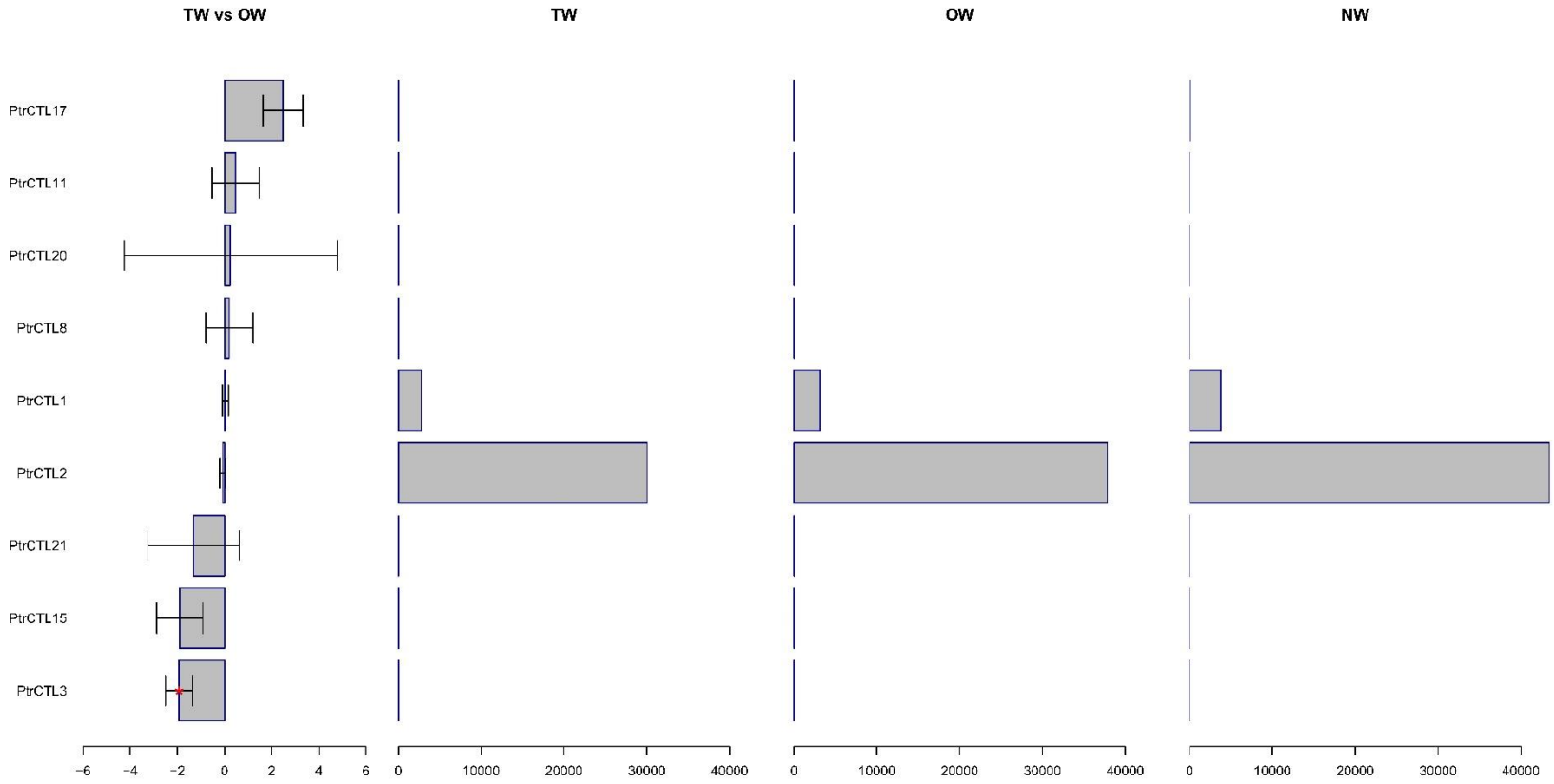

Figure I-3. Expression of *CTL* gene family in tension wood (TW), opposite wood (OW) and normal wood (NW). The expression was detected for 9 out of 21 genes of the family. The first column shows relative log2 ratio of gene expression in TW and OW, and the t-test of statistical significance. Bars represent standard errors. The remaining columns show absolute gene expression in TW, OW and NW.

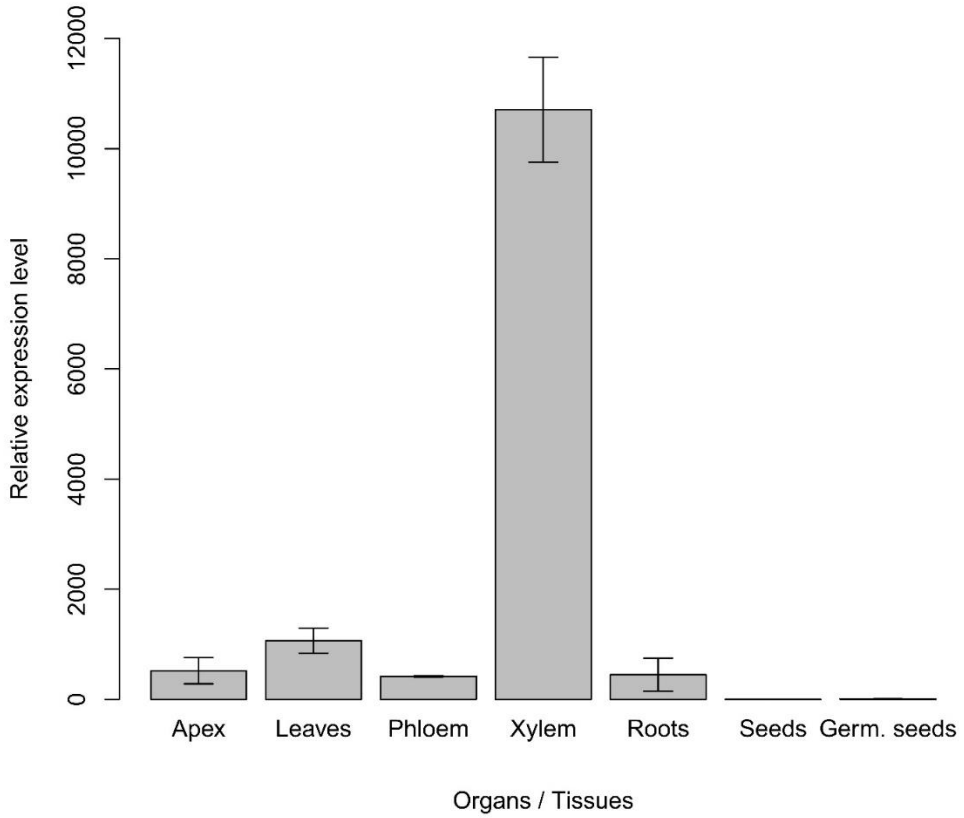

Figure I-4. Relative expression level of *PtaCTL2* in various tissues and organs of poplar. The expression was normalized according to *UBC* and lowest value detected in seeds. Bars represent standard error, where: n= 3 technical repetitions of different pulls from 1 tree (seeds/germ.seeds) or 6 trees (all other organs/tissues). Germ. seeds = germinated seeds.

Production of RNAi transgenic lines

To study a function of PtaCTL2, we produced transgenic RNAi poplar trees and analysed their traits. A 170 bp-long sequence specific for *PtaCTL2* was cloned into pHellsgate 8 gene-silencing vector (**Helliwell *et al.*, 2002**) to produce a *CaMV 35S*-driven hairpin CTL2 construct in transgenic poplar lines. We obtained 12 transgenic lines and screened 5 of them for the gene expression. All the screened lines showed to be down-regulated when compared to wild-type, and 2 lines were selected for the following characterization. The selected transgenic lines were named T1 and T2 and each was represented with 3 biological tree replicates. In the semi-quantitative RT-PCR analysis, both lines exhibited in OW and TW lower expression of *PtrCTL2* in comparison to wild-type (**Fig. I-5**).

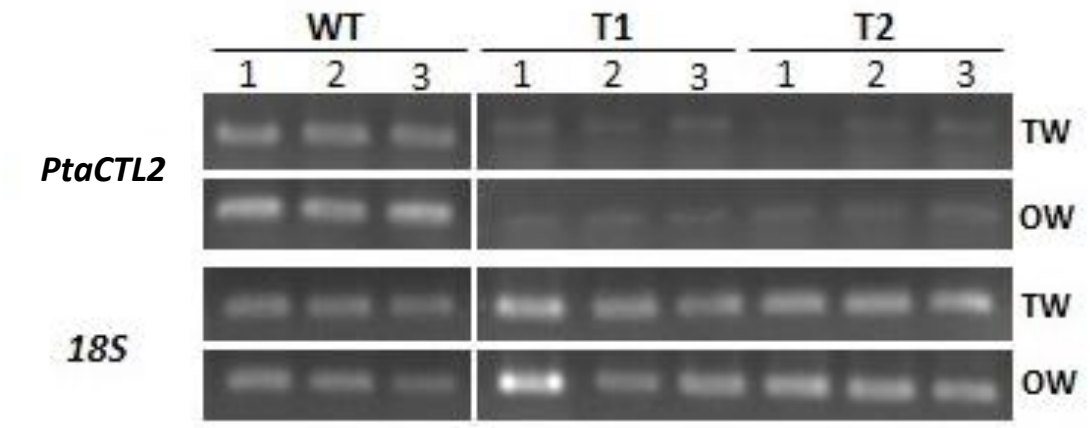

Figure I-5. RT-PCR expression analysis of *PtaCTL2* in opposite wood (OW) and tension wood (TW) of 3 biological replicates. In comparison to wild-type (TW), the expression was down-regulated in CTL2 transgenic lines T1 and T2. Amplification of *18S* was used as a control of equal RNA loading in RT-PCR reaction.

Traits of transgenic trees

Growth phenotype

Tree height and diameter were measured after four months of growth in the greenhouse. Stems were tilted within the last two months to produce tension wood. There were no significant difference for height and diameter between wild-types and transgenic trees (**Fig. I-6**). During growth in the greenhouse conditions, transgenic trees did not show any apparent phenotype defects in plant development as modifications in size of leaves or shape of leaves and stems (data not shown). However, when sampled, stems of transgenic trees were brittle at stem cutting point (data not shown).

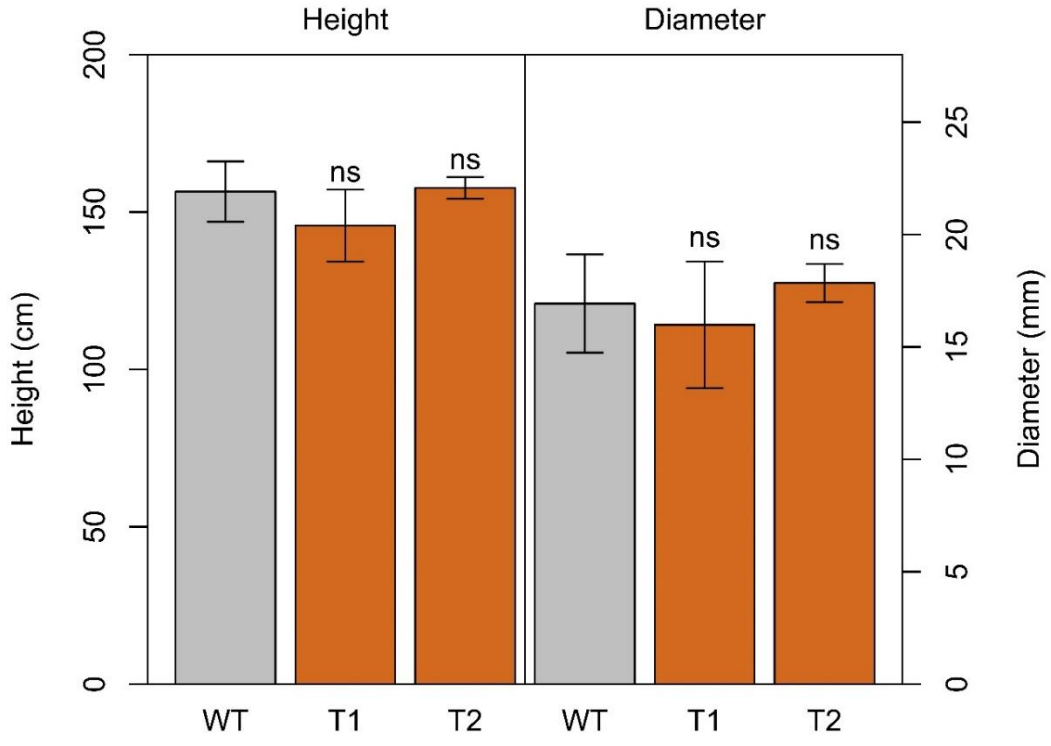

Figure I-6. Height and diameter of wild-type (WT) and CTL2 transgenic lines T1 and T2 grown in the greenhouse conditions for 4 months. Bars represent standard errors, where: n=6 biological replicates (wild-type), n=3 biological replicates (T1, T2). The statistically significant difference between WT and transgenic lines was calculated from Welch's t-test, where: ns= non-significant.

Wood anatomy

Wood anatomy was studied on stained stem cross-sections on which it was possible to distinguish NW formed around the pith, and OW and TW formed on two sides after stem tilting. In transgenic lines, all the wood types were properly formed (**Fig. I-7a**). However, TW was more frequently torn apart in transgenic lines than in wild-type (**Fig. I-7a, I-7b**). The effect appeared in a consequence of cutting of stem slices with microtome and complemented the observation of brittle stems during tree cutting. Hence, the fragility of stems in both cases seemed to be related with modifications of stem mechanical properties. The splitting was observed particularly in zones close to vessels (**Fig. I-7b**).

Cell wall development was studied in resin-embedded cross-sections. Only in one zone of mature wood of transgenic lines, fibers surrounding vessels did not develop the G-layer (**Fig. I-7c**). In other zones of TW, as in NW and OW, cell wall development was not altered (**OW**; **Fig. I-7d**). Even though we did not measure the thickness, cell walls of OW and TW fibers looked thinner in transgenics when compared to WT fibers (**Fig. I-7c, I-7d**).

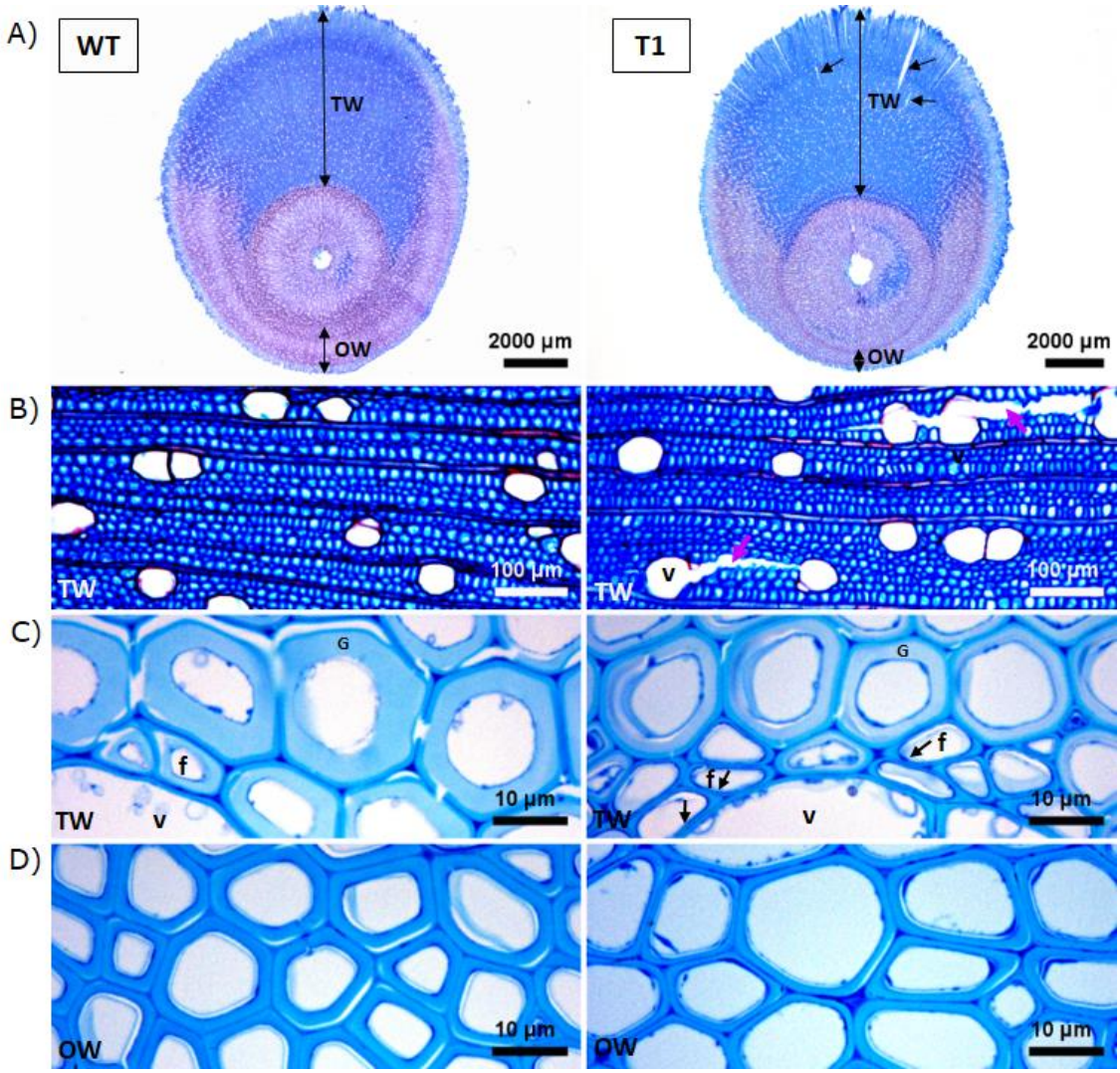

Figure I-7. Comparison of wood anatomy between wild-type (WT) and CTL2 transgenic line T1. The figures are representative of observations performed on transgenic lines T1 and T2.

A) Cross-section of basal stem stained with safranin/alcian blue. Zones out of the ring of normal wood surrounding the pith: tension wood (TW) stained in blue and opposite wood (OW) stained in purple. Arrows: more frequent splitting of TW in T1 line upon cutting of fresh stems with microtome

B) Mature TW stained with safranin/astra blue stain. Arrows: detail of torn wood nearby vessels (v) in T1 line

C) Mature TW stained with methylene blue/azur II stain with thinner cell wall in fibers of T1 line. Arrows: fibers (f) surrounding vessels (v) with undeveloped G-layers (G) in T1 line

D) Mature OW stained with methylene blue/azur II stain with thinner cell wall in fibers of T1 line.

Biomechanical properties

Mechanical properties of stems were estimated from measures of stem modulus of elasticity (MOE) and wood density. In wild-type, MOE was lower in TW than in NW and OW, which had around the same measure of MOE. In transgenics, MOE was lower in OW of only one line when compared to wild-type (**Fig. I-8**). Although the other transgenic line showed the same trend, the difference was not significant, probably due to a high variability between individual trees. Wood density was higher in TW than in OW (**Fig. I-8**), as reported in one study performed on wild-type plants (**Jourez *et al.*, 2001**). The increased wood density in TW is presumably related to the thicker secondary cell wall in G-fibers. Wood of transgenics was less dense than of wild-type (**Fig. I-9**). The level of reduction was of the same range between wood types.

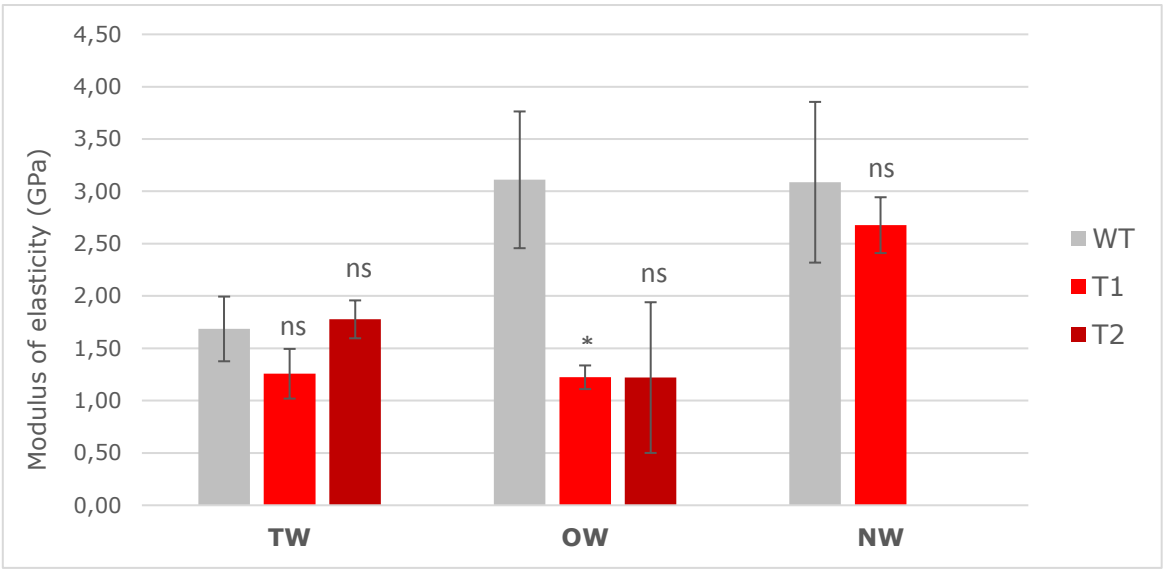

Figure I-8. Young's modulus of elasticity of tension wood (TW), opposite wood (OW) and normal wood (NW) from wild-type (WT) and CTL2 transgenic lines T1 and T2. Bars represent standard errors, where: n=5 (WT), n=3 (transgenic lines, with the exception for T2-OW where n=2). The statistically significant difference between wild-type and transgenic lines was calculated from Welch's t-test, where: *** p-value 0-0.001, ** p-value 0.001-0.01, * p-value 0.01-0.05, ns= non-significant.

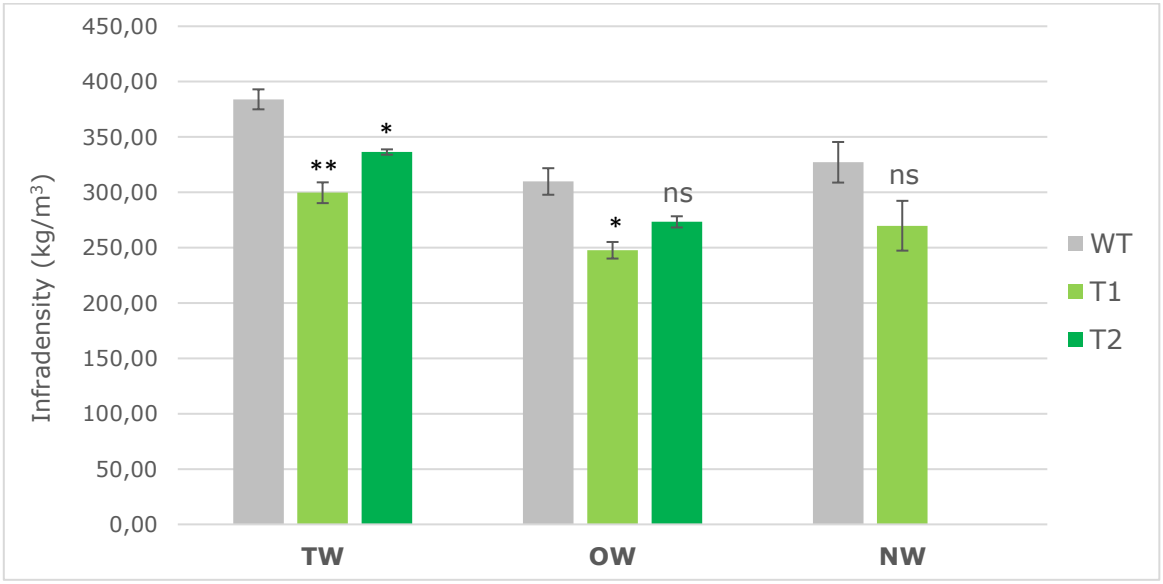

Figure I-9. Infradensity of tension wood (TW), opposite wood (OW) and normal wood (NW) of wild-type (WT) and CTL2 transgenic lines T1 and T2. Bars represent standard errors, where: n=5 (WT), n=3 (T1/T2-TW, T1-NW), n=2 (T1/T2-OW, WT-NW). The statistically significant difference between wild-type and transgenic lines was calculated from Welch's t-test, where: *** p-value 0-0.001, ** p-value 0.001-0.01, * p-value 0.01-0.05, ns= non-significant.

Wood biochemical properties

Wood absorbance of middle infrared light was recoreded in an attempt to differentiate chemical properties of wild-type from transgenic trees. The peaks captured at 1236 and 1738 cm^{-1} of wavelength clearly differentiated TW samples as they were higher than peaks from other samples. These peaks were in TW assigned to perpendicular xylose-based polysaccharides of different orientation to that measured in NW or OW (**Olsson *et al.*, 2011**; **Chang *et al.*, 2014**). The differentiation of peaks also revealed unexpected overlapping of several spectra originating from different wood types. Indeed, PCA analysis showed that the overlapping have origin in modification of wood from transgenics, samples of which were strongly shifted on the first axis (**Fig. I-10**). TW samples of transgenics were shifted to the middle of axis and grouped with OW and NW of wild-type. OW samples of transgenics were shifted to the right side of the axis and grouped with NW of transgenics. The strong shift clearly evidenced modifications in wood chemical properties of transgenic lines. The origin of the 50% of variances contributing to the modifications detected on the first axis were assigned to peaks of origin attributed to cellulose, lignin and hemicelluloses (**Fig. I-11, Tab. I-2**).

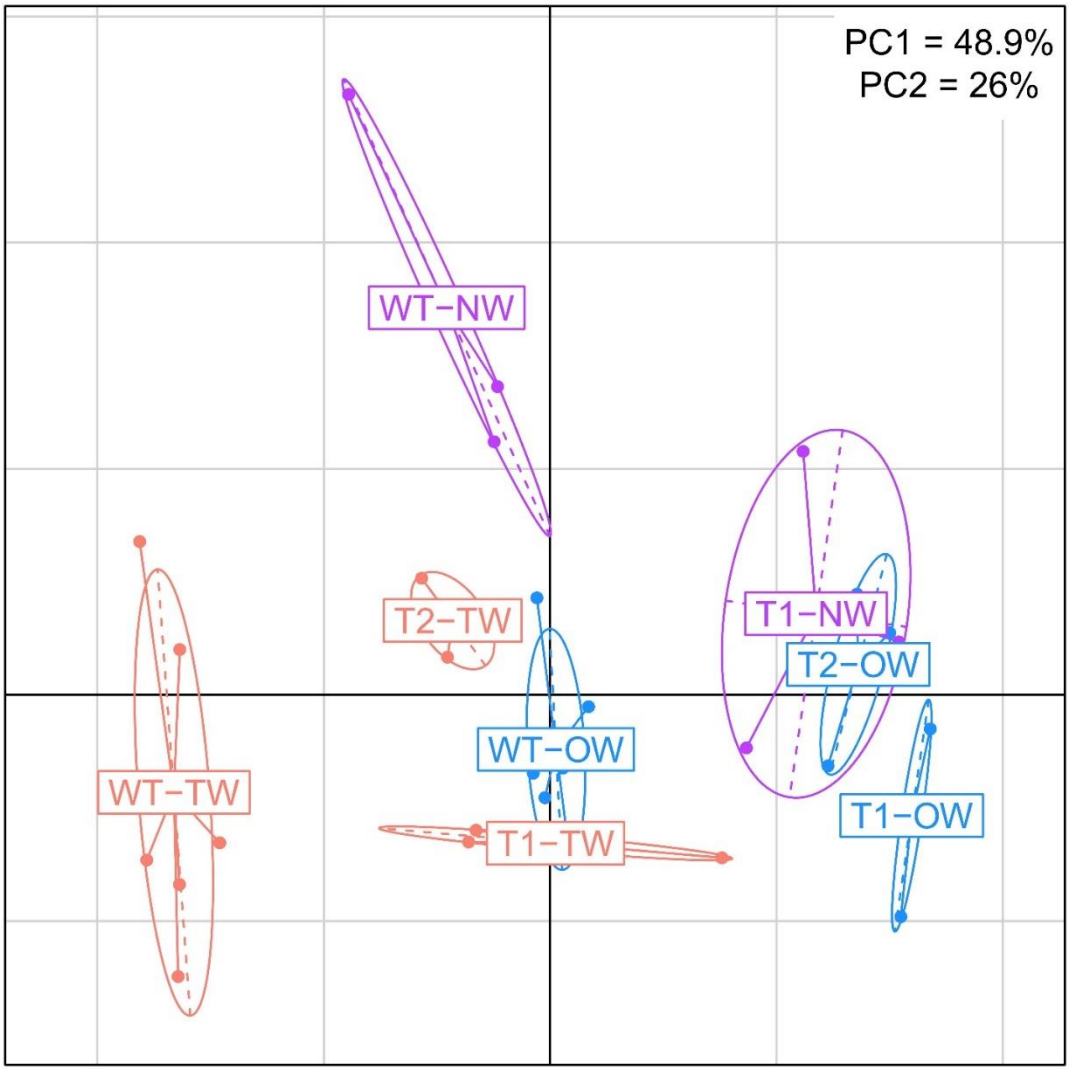

Figure I-10. Graph of principal component analysis of normalized FT-MIR spectra of normal wood (NW), opposite wood (OW) and tension wood (TW) from wild-type (WT) and CTL2 transgenic lines T1 and T2. Number of biological tree replicates (shown with dots): n=6 (WT), n=3 (transgenic lines). Contributions (%) of the first (PC1) and the second (PC2) principal components to the variances are shown on the graph.

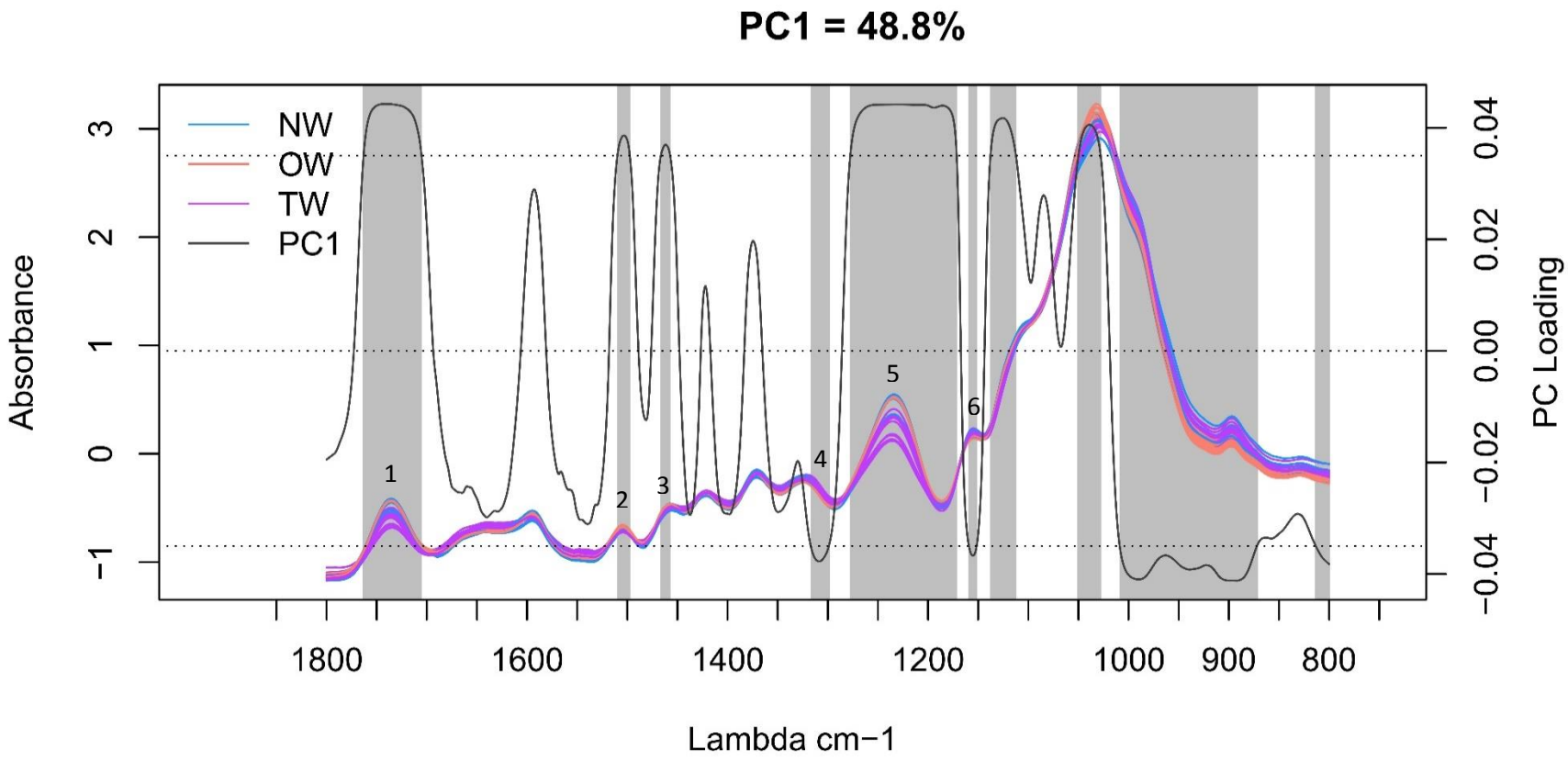

Figure I-11. Ensemble of spectra from wild-type and transgenic lines colored according to the wood type: normal wood (NW), opposite wood (OW) and tension wood (TW). Areas in grey show significant contribution of peak to the first principal component (PC1) in the PCA graph (Fig. 9). Numbers of the peaks are attributed to chemical groups in Table I-2.

Table I-2. Assignment of the peaks from FT-MIR spectra (Fig. 10) to chemical groups, according to Olsson *et al.* (2011).

No of peak	Wave number (cm^{-1})	Chemical group
1	1738	Xylan
2	1501	Lignin
3	1460	Xylan
4	1312	Cellulose
5	1236	Xylan
6	1158	Cellulose

We further studied if the modifications in chemical properties could be related to content of the major cell wall components as glucose, xylose and lignin. Transgenic lines had the higher glucose content and the lower xylose content, while there were no modifications of the lignin content (**Figures I-12, I-13, I-14**). As expected, TW had higher content of glucose than OW and NW, as it is the wood enriched in glucose (**Norberg and Meier, 1966**). The glucose decrease in transgenics varied in TW between 12-15%, in OW 13-23% and was 20% in NW.

In comparison to wild-type, transgenic lines had elevated content of xylose. The difference was statistically non-significant for 2 transgenic samples and the significance could not be calculated for one line due to insufficient quantity of wood material. However, the statistically significant increase detected in 2 transgenic samples and the increase trend in all other samples lead to a conclusion that transgenics have elevated xylose content.

The total lignin content was 6-7% higher in OW and NW than in TW, which is in agreement with previous observations (**Gorshkova *et al.*, 2015**). There were no difference in lignin content between wild-type and transgenics.

The modifications had an impact on wood saccharification efficiency expressed as a glucose content released after wood hot water pretreatment and enzymatic cellulolytic reaction. In wild-type, TW yielded more glucose than other wood types (**Fig. I-15**). Enzymatic glucose liberated from NW, OW and TW of transgenics was significantly lower than glucose liberated from wood of wild-types, with a difference exceeding for more than 100 µg/mg. Moreover, decrease in TW of transgenic lines brought the level of released glucose to the levels in OW and NW of wild-type, which is in accordance with the PCA grouping.

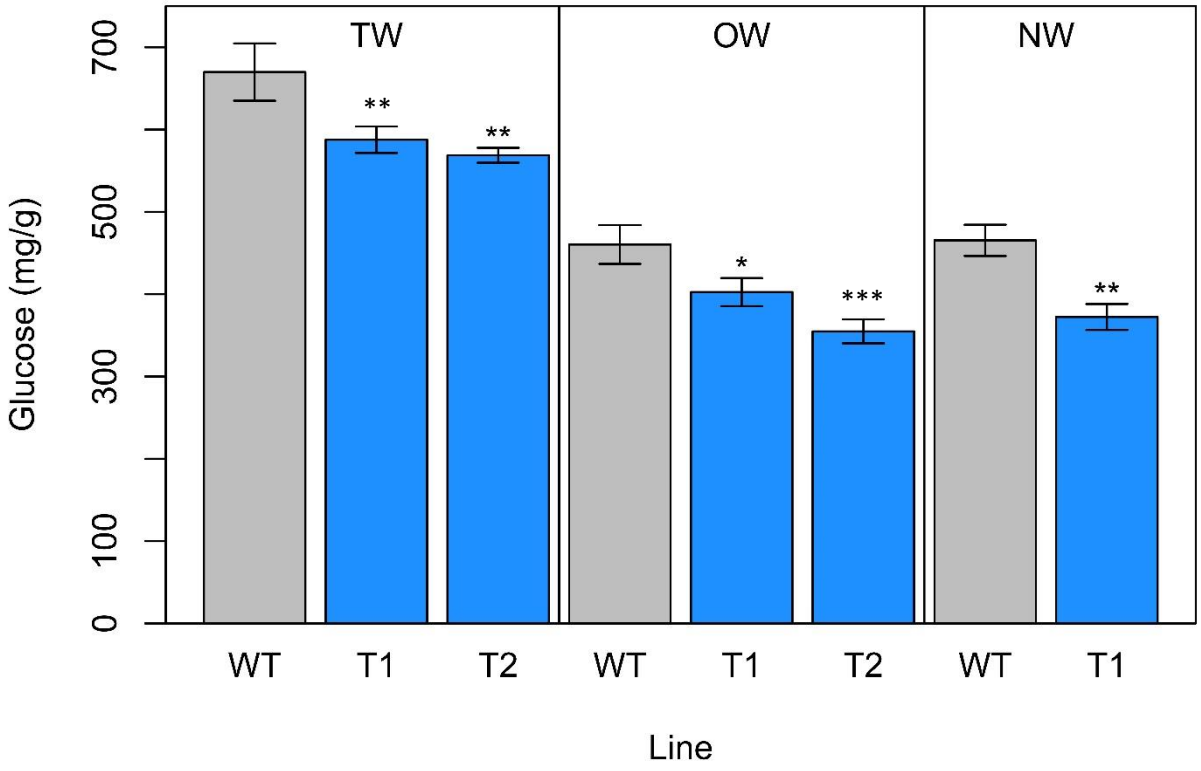

Figure I-12. Glucose content in tension wood (TW), opposite wood (OW) and normal wood (NW) of wild-type (WT) trees and CTL2 transgenic lines T1 and T2. Bars represent standard errors, where: n=6 biological replicates (WT-TW), n=4 (WT-OW), n=3 biological replicates (T1-TW, T1-NW, T2-TW, T2-OW, T2-NW), n=2 biological replicates (T1-OW). The statistically significant difference between wild-type and transgenic lines was calculated from Welch's t-test, where: *** p-value 0-0.001, ** p-value 0.001-0.01, * p-value 0.01-0.05, ns= non-significant.

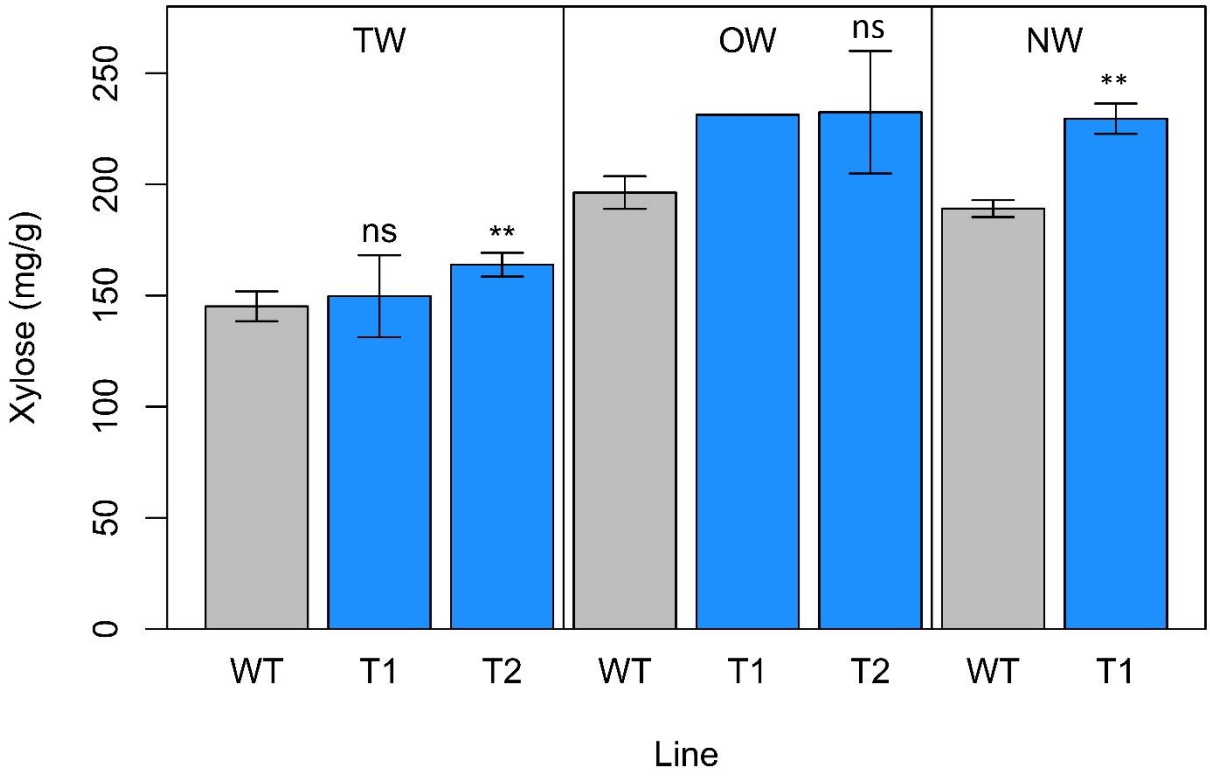

Figure I-13. Xylose content in tension wood (TW), opposite wood (OW) and normal wood (NW) of wild-type (WT) trees and CTL2 transgenic lines T1 and T2. Bars represent standard errors, where: n=6 biological replicates (WT-TW), n=4 (WT-OW), n=3 biological replicates (T1-TW, NW; T2-TW, NW, OW), n=1 biological replicate (T1-OW). The statistically significant difference between wild-type and transgenic lines was calculated from Welch's t-test, where: *** p-value 0-0.001, ** p-value 0.001-0.01, * p-value 0.01-0.05, ns= non-significant.

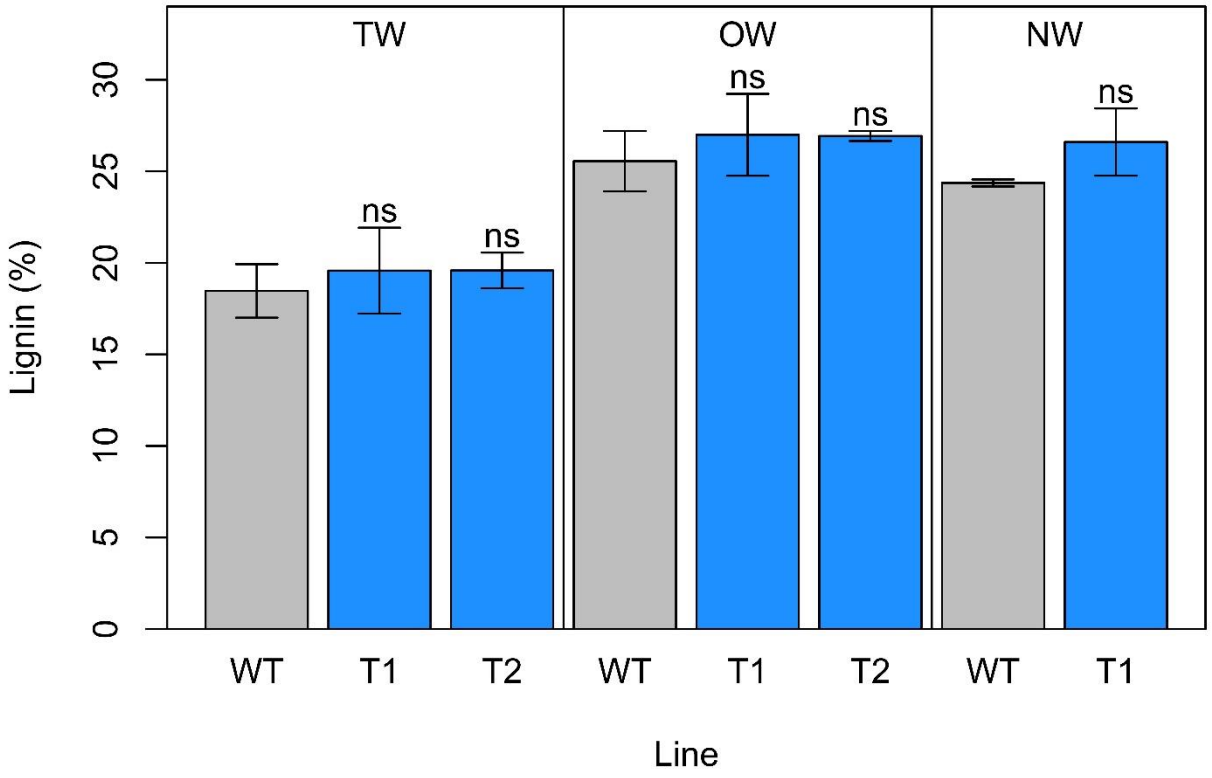

Figure I-14. Total lignin content (mol%) in tension wood (TW), opposite wood (OW) and normal wood (NW) of wild-type (WT) and CTL2 transgenic lines T1 and T2. Bars represent standard errors, where: n=6 biological replicates (WT), n=3 biological replicates (T1, T2). The statistically significant difference between wild-type and transgenic lines was calculated from Welch's test, where: ns= non-significant.

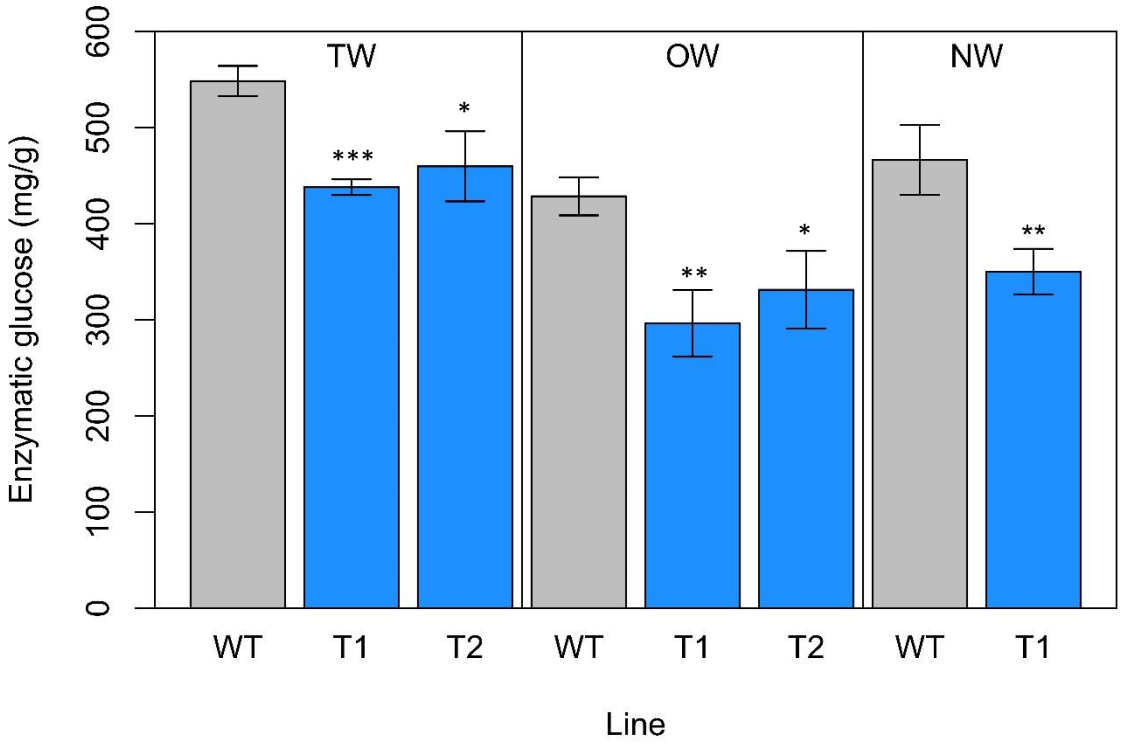

Figure I-15. Saccharification potential expressed as glucose content liberated after wood hot water pretreatment and enzymatic cellulolytic reaction. The analysis was performed in opposite wood (OW), tension wood (TW) and normal wood (NW) of wild-type (WT) and CTL2 transgenic lines T1 and T2. Bars represent standard errors, where: n=6 biological replicates (WT), n=3 biological replicates (T1, T2). The statistically significant difference between wild-type and transgenic lines was calculated from Welch's t-test, where: *** p-value 0-0.001, ** p-value 0.001-0.01, * p-value 0.01-0.05, ns= non-significant.

Cellulose ultrastructure

X-ray diffractometry was used to estimate cellulose ultrastructure - orientation of microfibrils and cellulose crystalline structure. Cellulose crystallinity was estimated from anisotropic index, which represents a ratio between maximal intensity of the diffraction peak indicative of highly organized cellulose, and baseline of the peak indicative of non-organized cellulose structure. The ratio reflects global cellulose organization where high index is the indicator of cellulose crystalline structure.

Microfibril angle and crystallinity were in all wood types reversely proportional. TW had low microfibril angle around 8° and high crystalline cellulose organization, which could be detected from high anisotropic index (**Fig. I-16**). The angle in TW was probably overestimated because of contribution of secondary cell wall layers 1 and 2 characterized with higher angles than in the G-layer (**Yamamoto, 2004**). In OW, the angle of cellulose microfibrils varied between 18° to 30°, and low anisotropic index around 2 was an indicator of amorphous cellulose organization.

TW of transgenics had modified cellulose crystalline organization detected as the decrease of anisotropic index (**Fig. I-16**). The angle of cellulose microfibril was unchanged, probably due to low sensitivity of the used method toward such small angles as it is angle in TW. OW and NW of transgenics did not have significantly modified cellulose ultrastructure.

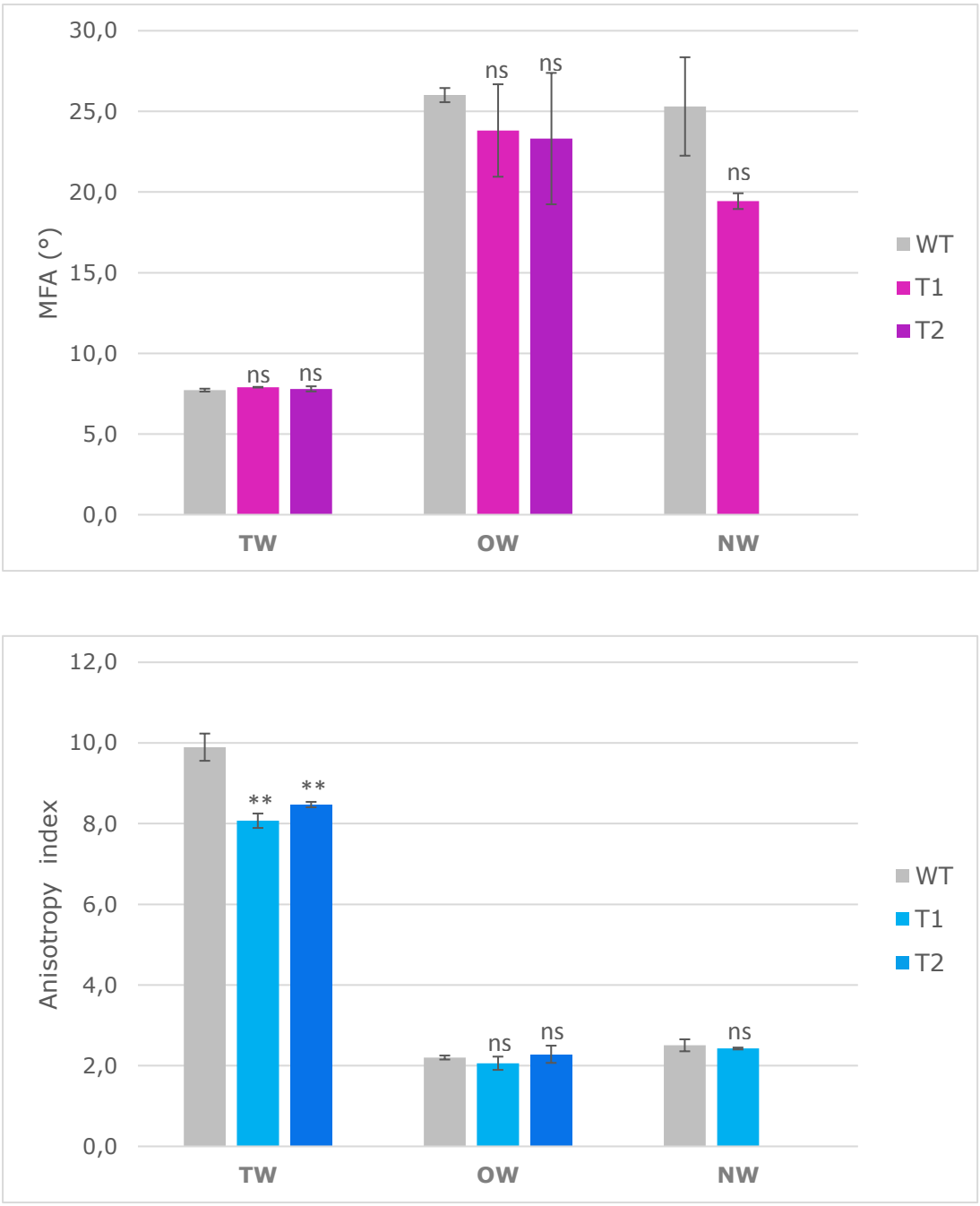

Figure I-16. Cellulose microfibril angle and anisotropic index of cellulose organization estimated from X-ray diffraction in opposite wood (OW) and tension wood (TW) of wild-type (WT) and CTL2 transgenic lines T1 and T2. Bars represent standard errors, where: n=6 (TW-WT), n=5 (OW-WT), n=3 (OW and TW of transgenic lines). The statistically significant difference between wild-type and transgenic lines was calculated from Welch's t-test, where: *** p-value 0-0.001, ** p-value 0.001-0.01, * p-value 0.01-0.05, ns= non-significant.

Expression of *PtaCTL2*-associated genes

AtCTL2 was previously shown to be highly co-expressed with genes associated to cellulose synthesis in secondary cell walls (**Persson *et al.*, 2005**). We quantified if the down-regulation of *PtaCTL2* altered the expression of some of these homologous genes and several other potential gene partners. The expression was quantified for genes encoding CESAs, FLAs, COBRA, KORRIGAN and CTL1.

PtaFLA1, *PtaFLA4* and *PtaFLA8* encode fasciclin-like arabinoglactan proteins differentially expressed in TW (**Lafarguette *et al.*, 2004**), while *PtaFLA11*, *PtaFLA13* and *PtaFLA14* were chosen as the representatives of genes non-differentially expressed between OW and TW (**Lafarguette *et al.*, 2004**). Moreover, *PtaFLA11 and PtaFLA13* are homologous to *AtFLA11* gene coregulated with *AtCTL2* in Arabidopsis (**Persson *et al.*, 2005**). *CESA4*, *CES7A* and *CESA8A* were identified in poplar as CESAs involved in cellulose synthesis in secondary cell walls (**Aspeborg *et al.*, 2005**). Names to *CESA* were given according to the nomenclature described in **Kumar *et al.*** (**2009**). *KOR* encodes a putative β-(1,4)-glucanase and its expression was detected in tension wood of poplar (**Andersson-Gunneras *et al.*, 2006**). *COBL4* encodes COBRA protein, which was shown to co-express with *CTL2* in Arabidopsis (**Persson *et al.*, 2005**).

PtaCTL2 had the highest expression in wild-type among the analyzed genes (**Fig. I-17**). The expression was same in OW and TW. *PtaCTL2* was also the sole gene significantly down-regulated in both TW and OW of transgenics. The down-regulation of *PtaCTL2* did not increase the expression level of its closest homolog *PtaCTL1*. The down-regulation of *PtaCTL2* did not alter the expression of other analyzed genes. Only *PtaFLA11* and *PtaFLA13* had decreased expression in transgenics compared to wild-type, but the difference was non-significant, probably due to a variability in the expression between individual trees.

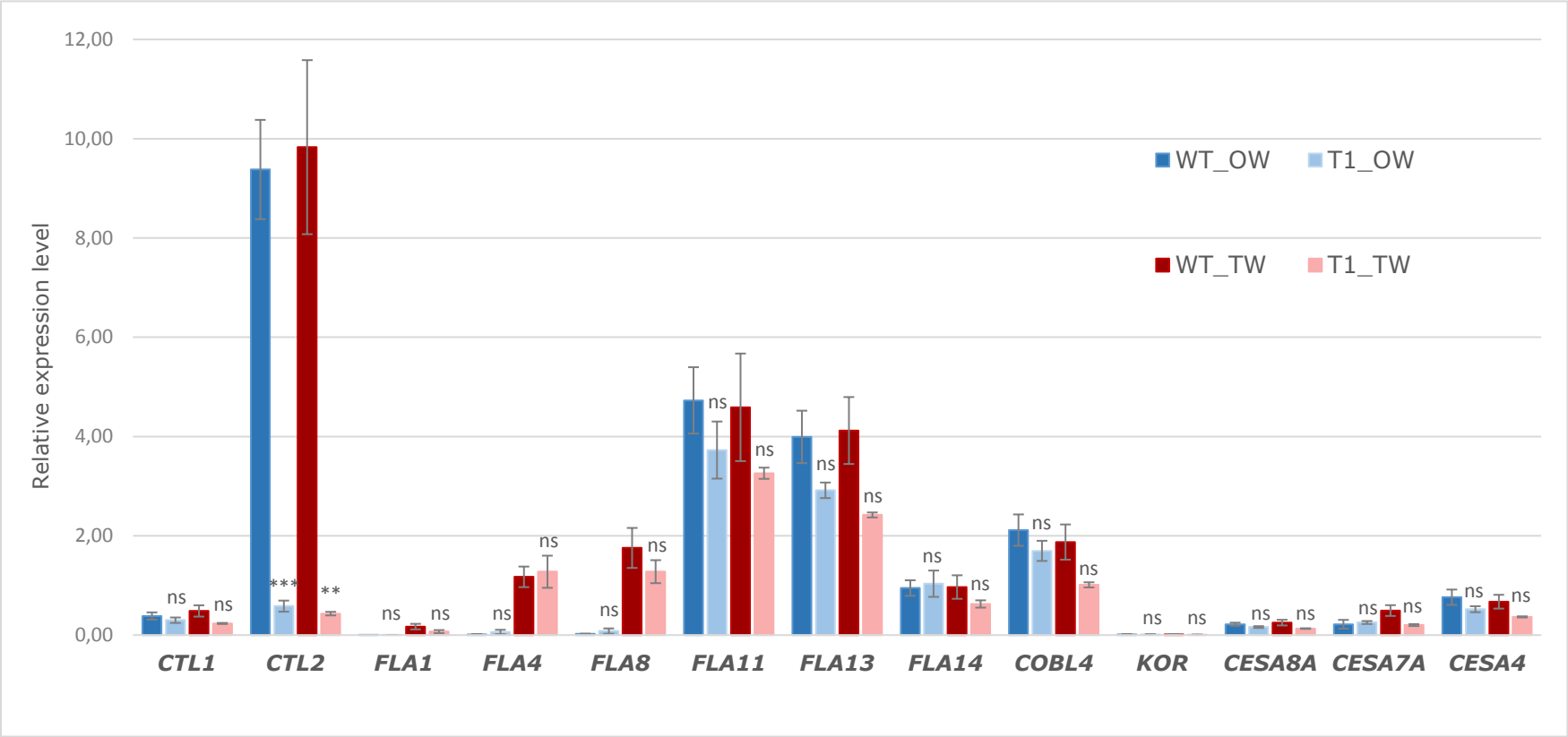

Figure I-17. Relative expression level of *CTL2* and its potential gene partners (*CTL1*, *FLA1*, *FLA4*, *FLA8*, *FLA11*, *FLA13*, *FLA14*, *COBL*, *KOR*, *CESA4*, *CESA7A*, *CESA8A*) in opposite wood (OW) and tension wood (TW) of wild-type (WT) and CTL2 transgenic line T1 in poplar. Bars represent standard error, where: n=6 biological replicates (WT), n=3 biological replicates (T1). The statistically significant difference between wild-type and transgenic line was calculated from Welch's t-test, where: *** p-value 0-0.001, ** p-value 0.001-0.01, * p-value 0.01-0.05, ns= non-significant.

DISCUSSION

The traits of transgenic RNAi poplar trees characterized in this study suggest that CTL2 from poplar has a function in cellulose synthesis and is required for crystalline cellulose structure important for complete secondary cell wall organization and biomechanical properties of poplar stems.

PtrCTL2 has a close homolog named PtrCTL1. Together with the two Arabidopsis and six flax orthologs, they made a small group of GH19 chitinases commonly named chitinase-like proteins (CTL). Sequence alignment of the group members revealed that they all have conserved motif of GH19 family and substituted amino acids in domains responsible for chitinase activity and substrate binding. The substitutions were previously demonstrated for the group members AtCTL1 and AtCTL2, leading to the conclusion that these CTLs do not possess the classical chitinase activity (**Hossain *et al.*, 2010**; **Hermans *et al.*, 2010**). From our analysis, the same conclusion may be given for the group-A members from flax, Arabidopsis and poplar, which justifies their assignment as the chitinase-like proteins. However, the statement seeks for a confirmation in enzymatic essay of CTLs with chitin substrates.

The group members *PtrCTL1* and *PtrCTL2* were the sole genes of poplar *CTL* family expressed in wood, but non-differentially expressed between TW and OW/NW. In the analyses conducted in *P. tremula* x *P. alba*, *PtaCTL2* had the notable expression in wood and low expression in other tissues and organs of poplar. Its orthologs AtCTL2 (**Hossain *et al.*, 2010**), LusCTL1 and LusCTL2 (**Mokshina *et al.*, 2012**), were shown to have equally the high expression in cells with secondary cell walls. It strongly suggests that the clade to which all these CTLs belong may be specifically involved in properties of the secondary cell wall. The same preferential function may also have to the clade homologous GhCTL1 and GhCTL2, which are highly expressed in cotton fibers (**Zhang *et al.*, 2004**).

In the present study of *PtaCTL2* RNAi lines, the notable phenotypes were detected in wood, which is formed of cells with the secondary cell wall. The down-regulation of *PtaCTL2* did not have effect on the plant growth and development. It strongly suggests that PtaCTL2 has a localized function and we showed that its modification reflects on the properties of wood. Indeed, stems of transgenics were brittle and their cross-sections had more frequent wood cracks. Such modifications were, at least partially, related to reduction in wood density and thinner cell walls in

transgenics. However, the latter needs a validation by a quantitative measurement. The wood density is proportional to mechanical strength, and it may be therefore concluded that function of PtaCTL2, among others, determines mechanical properties of stems. Similarly, mutation of *CTL1* in rice reduced mechanical strength of culms and leaves accompanied with thinner secondary cell walls (**Wu *et al.*, 2012**).

The modifications of mechanical properties in *PtaCTL2* transgenics were brought in a relation with altered wood chemical properties, demonstrated as modifications of wood FT-MIR spectra and reduction in saccharification efficiency. Both analyses are dependent on content, deposition and/or organization of cell wall components. We assigned the modified peaks of spectra to chemical bonds of cellulose, hemicelluloses and lignin, which make the main structure of the cell wall. Because of diversity of the altered chemical groups, we can conclude that wood of *PtaCTL2* transgenics had modified structure of the complete secondary cell wall.

We showed that the altered wood chemical properties, at least partially, originate from decrease in cellulose content and altered crystalline cellulose structure in the cell wall. However, we could detect the modifications of crystalline organization only in tension wood, probably because the X-ray diffractometry is a method sensitive to detect changes in only highly ordered cellulose structure, as it is in tension wood. Modifications of crystalline cellulose content were already reported in the *ctl1 ctl2* double mutant of Arabidopsis (**Sanchez-Rodriguez *et al.*, 2012**), suggesting that CTLs have function in a regulation of crystalline cellulose structure, controlled by an undetermined mechanism.

Cellulose is synthesized on plasma membrane by the cellulose synthase complex composed of CESA proteins (**McFarlane *et al.*, 2014**). In Arabidopsis, *CTL1* and *CTL2* co-express with *CESA* genes (**Persson *et al.*, 2005**). The down-regulation of *PtaCTL2* did not modify the expression of *CESA4*, *CESA7A* and *CESA8A* genes related to cellulose synthesis in secondary cell walls. Reduction in the cellulose content quantified in transgenics might be caused by a lack of posttranslational subcellular interactions between CESA and CTL2, as it was demonstrated that CTL1 co-localizes with CESA6 in unknown vesicles that move along the actin cytoskeleton (**Sanchez-Rodriguez *et al.*, 2012**). However, the significance of their interactions for cellulose synthesis is still undetermined. Alternatively, down-regulation of cellulose synthesis might be caused by a feedback response from crystalline-modified cell wall towards CESA complex. Either way, CTL is directly or

indirectly involved in cellulose synthesis in poplar, having plausibly important function as CTLs in Arabidopsis and rice, whose *ctl* mutants had reduced cellulose content (**Sanchez-Rodriguez *et al.*, 2012**; **Wu *et al.*, 2012**).

In CTL2 RNAi transgenics, *FLA* genes had tendency toward down-regulation. Interestingly, the same tendency was observed for *CTL2* in FLA RNAi transgenic lines (not published). It is therefore tempting to speculate that PtaCTL2 has co-operative function with FLAs. However, FLAs were reported to have function in a control of cellulose micorifbril angle, which was not altered in our PtaCTL2 transgenics (**MacMillan *et al.*, 2010**; **MacMillan *et al.*, 2015**). It therefore stays to determine if these two properties are regulated by same mechanism.

As the *ctl1* mutant of rice (**Wu *et al.*, 2012**), PtaCTL2 transgenics had the elevated content of xylose. Considering the tight interactions of cellulose and hemicelluloses in the cell wall, it is possible that a feedback response on reduced cellulose crystallinity would induce an up-regulation of xylose synthesis. In this case, CTL2 may directly control the crystalline cellulose structure and directly or indirectly interaction with xylose-structured hemicelluloses, as it was proposed for CTLs from Arabidopsis (**Sanchez-Rodriguez *et al.*, 2012**).

Organization of lignin in the cell wall may be only indirectly affected by the interactions of cellulose and hemicelluloses. In our study, some of the peaks contributing to the changes of FT-MIR spectra were attributed to the chemical bonds from lignin. Lignin was shown to be highly oriented in both tension and opposite wood (**Chang *et al.*, 2014**), and is therefore likely that a complete disorganization of cell wall structure caused the modification of lignin structure in PtaCTL2 transgenics. However, the modifications could not be related with the lignin content since there were no difference between transgenics and wild-type. On the contrary, Arabidopsis c*tl2* mutant had an increased lignin content (**Hossain *et al.*, 2010**). However, the increase was mild in comparison to highly elevated lignin content in *ctl1* and double *ctl1 ctl2* mutants. In these mutants, a feedback response might differently up-regulate the lignin synthesis, knowing that *AtCTL1* has ubiquitous expression related to primary cell wall (**Hossain *et al.*, 2010**; **Persson *et al.*, 2005**), which gets deposited before secondary cell wall.

The biochemical and biomechanical properties of transgenics were strongly modified within the same range in all wood types, suggesting that the effects originate preferentially from secondary cell wall layers 1 and 2, and cannot be specifically linked to the G-layer, which is absent in fibers of opposite and normal

wood. It has a firm foundation in non-differentiate expression of *PtaCTL2* between NW, OW and TW, as shown in our study.

All together, our results suggest that PtaCTL2 has a function in cellulose synthesis and is required for cellulose crystallinity and organization of the secondary cell wall in wood. We also demonstrated that the function of PtaCTL2 in wood is tightly related with the mechanical properties of stem. A determination and localization of protein interactions and activity would highlight a substrate of PtaCTL2 and reveal if the protein interacts with intracellular molecules as CESAs or cell wall components as cellulose, hemicelluloses or even AGP (FLA).

MATERIALS AND METHODS

Phylogenetic analysis

CTL family was predicted by searching for conserved GH19 domain (Pf00182) in the genomes of *Populus trichocarpa*, *Arabidopsis thaliana* and *Linum usitatissimum* with BioMart tool available on the JBI Phytozome website (v11, https://phytozome.jgi.doe.gov/pz/portal.html). The phylogenetic analyses were conducted in MEGA7 software (**Kumar *et al.*, 2016**). The protein sequences were aligned by MUSCLE tool using default settings. The evolutionary history was inferred by using the Maximum Likelihood method based on the JTT matrix-based model, partial deletion (cutoff 95%), Gamma distributed rates, bootstrapping 500 replicates. The phylogenetic tree was visualized with Interactive Tree Of Life (iTOL, v3, http://itol.embl.de/).

Plant material and sampling

Model species used in the experiments was INRA clone 717-1B4 (*P. tremula* x *P. alba*). Plants were micropropagated *in vitro* and acclimatized in the greenhouse in pots with fertilized soil, in conditions of 16h of light and temperature around 25°C. Only seeds were collected from one field-grown poplar tree at INRA Orléans. Formation of OW and TW was induced artificially by stem tilting attached to rod at 35° angle. OW and TW were sampled by xylem scratching. The scratched xylem was ground with pestle in a mortar. Apex, leaves, phloem, xylem and roots were cut as complete tissues or organs. The seeds were germinated on a humid paper pad in Petri dish for 48h at room temperature. To obtain a fine powder, the complete tissues were ground in cryogenic jars of Retsch® MM 400 mixer mill, two times 30s with frequency 30 rotations/min. The collected material was immediately frozen in liquid nitrogen and stored at -80°C before manipulation.

RNA isolation

Total RNA was isolated from 100 mg of a ground tissue following slightly modified protocol from **Chang et *al.*** (**1993**). Cells were lysed for 30 minutes at 65°C with 900 µl of extraction buffer containing 2% CTAB, 2% PVP40, 0.1M Tris-HCl, 0.025M EDTA, 2M NaCl and 0.344M spermidine. 2-fold extraction of RNA was performed with mix of chloroform and isoamylalcohol (24:1). After overnight precipitation with 2.5 M lithium chloride, RNA was purified with NucleoSpin RNA Plant kit

(Macherey-Nagel), according to manufacturer's recommendations. The sample was treated with DNase I (Macherey-Nagel) during the purification step.

RT-PCR

cDNA was synthesized in 13 µl of reverse transcription (RT) reaction composed of 2 µg of RNA, 1 µl of 500 µg/ml oligo $(dT)_{12-18}$ primer and 1 µl of dNTP mix (10 mM each), and incubated at 65°C for 5 minutes. Next, 4 µl of 5X first-strand buffer, 2 µl of 0.1 M DTT and 1 µl of 200 U SuperScript II enzyme (Invitrogen, Life Technologies) were added in a total of 20 µl volume reaction, incubated for 50 minutes at 42°C. The reaction was inactivated by heating at 70°C for 15 minutes. Two µl of diluted cDNA (1/4) was amplified in Polymerase Chain Reaction (PCR) with forward 5' AAGCATCTCCCTTCAGCACACG 3' and reverse 5' TGCCAACACCCATTAGGTCGAG 3' primers, 0.2 µM each, 0.25 µl of 1 U Taq DNA polymerase (Invitrogen, Life Technologies), dNTPs 200 µM, $MgCl_2$ 1.5 mM and enzyme buffer 1X.

The PCR amplification was carried out in conditions: initial denaturation 95°C for 5 min, 20 cycles of denaturation 95°C at 30 s, annealing 57°C for 45 s, elongation 72°C for 30c. Final extension was conducted at 72°C for 15 min. As a control of equal RNA loading, cDNA was amplified with primers corresponding to *18S* gene (forward 5' CTTCGGGATCGGAGTAATGA 3', reverse 5' GCGGAGTCCTAGAAGCAACA 3'). Amplicons were loaded on 2% agarose gel, electrophoresed, stained with ethidium bromide and visualized with ultraviolet transilluminator.

RT-qPCR

Two µg of RNA was reverse-transcribed to cDNA in a reaction performed with 10 µl of 2x reaction mix and 2 µl of 200U/µl SuperScript III enzyme (Invitrogen, Life Technologies). The reaction was incubated for 50 min at 42°C and then 5 min at 85°C. To remove remaining RNA template, the cDNA was treated with 2 U RNAase H for 20 min at 37°C. 2 µl of cDNA matrix (diluted 1/2) was amplified in Real-Time Polymerase Chain Reaction with 6 µl of SYBR Green master mix (Invitrogen, Life Technologies) and primers 0.2 µM, the same used in RT-PCR reaction, in total volume of 12 µl. The reaction was performed twice for each sample, in Twin-Tec Real-time plates (Eppendorf, Germany) on MasterCycler Realplex Epgradient apparatus (Eppendorf), in conditions: initial denaturation 2 min at 95°C and 40 cycles conducted of denaturation step (15 s at 95°C) and annealing/elongation

step (30 s at 60°C). In order to verify the specificity of amplification, the melting curve was formed by heating the reaction from 60°C to 95°C. An efficiency of the amplification was evaluated by performing qPCR reaction from serial dilutions of the cDNA pool. The relative gene expression was normalized with *UBC* gene (forward 5′ TGTTAAGTGATGGCATCGAAACGG 3′, reverse 5′ TTGTCCTGAAAGCAACCTTAGGAG 3′) and, in the study of expression in tissues and organs, the lowest Ct value corresponding to seeds.

Production of transgenic lines

The template DNA, obtained from the cDNA library prepared from wood tissues (**Déjardin *et al.*, 2004**), was amplified in the PCR reaction. The forward (GGGGACAAGTTTGTACAAAAAAGCAGGCTATGGAGGCCAAATGGTGTTTTCTTG) and reverse (GGGGACCACTTTGTACAAGAAAGCTGGGTTTGCAGCAATAAGCAGACAAGC) primers, used to generate 170 bp-long gene-specific sequence flanked with the attR recombination sites, were chosen according to the genome of *P. trichocarpa* (JBI Phytozome, v11). Using the Gateway Clonase II Technology and TOPO TA Cloning kits, the sequence was incorporated into, first pDONR 221 entry vector, and then expression vector pHellsgate8 (**Helliwell *et al.*, 2002**). Plasmids isolated with NucleoSpin Plasmid kit (Macherey-Nagel) were verified for orientation of intron with the respect to the *35S* promoter, first by enzymatic restriction analysis and then by sequencing. The plasmid was then electroporated into *Agrobacterium tumefaciens* strain C58 (pMP90). The bacterial culture harboring pHellsgate 8 binary vector was grown for 2 days at 28°C on MYA medium with rifampicin (50 µg/ml) and gentamycin (20 µg/ml) for selection of bacteria, and spectinomycin (75 µg/ml) for vector selection. Poplar (*P. tremula* x *P. alba*) internodes were sampled from *in vitro* 8-10 week old 717-1B4 plants, wounded and pre-cultured for 2 days at 24°C in darkness on MS medium (3% agar) with auxin NAA (10 mM) and cytokinin 2-ip (5 mM). The internodes were incubated with the bacterial culture within a bacterial suspension prepared at OD_{660} 0.25-0.3 in liquid MS medium, under shaking at 190 rpm for 16 h in darkness. After the incubation step, the internodes were co-cultured with *Agrobacterium* on MS medium (3% agar) with the hormones, for 2 days at 24°C in darkness. The explants were decontaminated from bacteria by several washings in water with agitation at 125 rpm. The decontaminated explants were cultured on MS medium (3% agar) with antibiotics cefotaxime (250 mg/L) and ticarcillin (500 mg/L) for

inhibiting bacteria development, and kanamycin (50 µg/ml) for selection of transformed cells, for first 2 weeks in darkness and then on light. Green calli of size a few millimeters were isolated and grown on MS medium (3% agar) with antibiotics and thidiazuron (0.1 µM). The calli were transferred every 2 weeks on a new medium with a progressively decreasing concentration of thidiazuron for 2 months. The elongated shoots regenerated from single callus, which represent one individual transgenic line, were grown during 2 months on MS medium (2% agar) to induce rooting. Sufficiently enlarged young plants were micorpropagated from nodes on MS medium (2% agar) and grown *in vitro* for 6 weeks.

Cultivation and sampling

In vitro-generated plants were grown in the greenhouse conditions for in total 4.5 months: first 3 weeks in mini-greenhouse, following 6 weeks in 2L pots and remaining 10 weeks in 5L pots. Within the last period, plants were grown tilted between 2 rods under 35° angle to produce tension and opposite wood. Soil was fertilized and watered with water-supply system. Newly grown shoots were regularly attached to rods. Prior sampling, trees were measured for height and diameter 2 cm above the soil. Stem was fragmented immediately after sampling. From the tree basis, the fragments were sampled for observation of wood anatomy on fresh stem cuts (4 cm), modulus of elasticity (15 cm), ultrastructure (2 cm), RNA extraction (20 cm), observations of wood anatomy on resin-fixed samples (15 cm) and wood biochemical properties (25 cm). Wood used for the analysis of FT-MIRS, saccharification and biochemical composition was ground in Retsch MM 400 mixer mill in jars with 25 mm ball mills, 2-fold 30 s (30 rotations/min) for 1.5 g of wood. For all analyses, except FT-MIRS, the ground wood was sieved to obtain size of particles between 50 and 1000 µm.

Mechanical measurements

Measures of Young's modulus of elasticity were performed on fresh wood samples collected on TW and OW side of tilted stems and unspecified zone of non-tilted stems. Wood was sampled according to calibrated specimen of size 3x2x40 mm respective to radial, tangential and longitudinal axis of stem. The mechanical tests were carried out on the basis of a conventional method of 3-point flexion in central sample point using a micromechanical plate (Microtest Tensile placement 2kN Dual Leadscrew, DEBEN, England) with applied force of 2000 N. The modulus was

calculated as $(L^3/48I)*\alpha$, where α represents a slope of a curve expressing force in dependence of displacement of the central point, L is a distance between the end points of a sample and I is sample volume.
Infradensity was expressed as a ratio of dried mass to saturated volume of wood. The volume was calculated from difference in mass of wood-immersed and empty water container measured on precise balance (d=0.1 mg; BP210S, Sartorius, Germany). The mass of dried wood was measured after 48h of a sample drying at 104°C.

Safranin/alcian blue staining

1% safranin and 1% alcian blue were prepared in 50% and 100% ethanol, respectively. Safranin/alcian blue double staining was performed on fresh wood 30 µm cross-sections, prepared with Leica RM2155 microtome. The sections were incubated for 6 min in 2.6% bleach, washed in water, incubated per 1 min in 50% and 25% ethanol, 3.5 min in 1% safranin and 6 min in 1% alcian blue. After each staining, sections were rinsed in 100% ethanol. The stained cross-sections were fixed on glass slides with Canada balsam and cover slips, and observed under the Leica DMR optical microscope. Pictures were taken with Leica DFC 320 camera.

Fixation and resin embedding of stem sections

Opposite and tension wood sections (3 mm) were cut with blade and fixed in a solution of 2.5% paraformaldehyde and 0.1% glutaraldehyde dissolved in 0.1 M citrate-phosphate buffer, pH 6.8. The sections were further rinsed in 0.1 M citrate-phosphate buffer, dehydrated in a gradient of ethanol (25%, 50%, 70%) and embedded in medium grade LR White resin (London Resin Company Ltd, UK). The embedded samples were cut as semi-thin (0.8 µm) cross-sections with a diamond knife (Diatome, Switzerland) installed on a Leica ultracut R microtome. The cut cross-sections were fixed on silanized slides (Dako Cytomation, France) heated at 55°C.

Methylene blue/azur II staining

1% methylene blue solution and 1% Azur II solution were prepared in 1% sodium tetraborate and distilled water, respectively. Fixed cross-sections were first treated with 1% periodic acid, for 5 min at room temperature and then rinsed with water. The sections were next covered with droplets of equilibrated volumes of methylene

blue and azur II. The slides were warmed at 50°C up to 2 min, not allowing the sample to dry. The sections were rinsed with water and fixed with Canada balsam and cover slip.

FT-MIR spectroscopy

A small quantity of ground wood was exposed to Middle InfraRed (MIR) light of wavelength 400 to 4000 cm-1, in attenuated total reflectance (ATR) mode of FT-IR spectrometer (PerkinElmer Spectrum 400). The spectra were captured and analyzed in range between 800 and 1800 cm^{-1}, with reads every 1 cm^{-1}. In order to improve signal quality, the raw spectra were first statistically pretreated by smoothing and normalization. The analyzed spectra were then subjected to principal component analysis (PCA) in R program.

Saccharification test

Saccharification test was conducted in 96-wells micro plates with canals (Hastelloy) within steps of pretreatment and enzymatic hydrolysis. 5 mg of ground and sieved wood was distributed in a microplate with fine feed robot (Labman), mixed with 300 µl of water and covered with thermo-resistant tape. The microplates were stacked between membranes, placed in 7.5 L reactor (PARR) and pretreated with hot water vapor for 40 min. The cooled-down micro plates were centrifuged for 10 min at 6000 rpm at 4°C. Saccharification was performed with 40 µl of enzymatic cellulolytic solution diluted in 1M sodium acetate buffer, pH 5 to concentration 8.75 mg/ml. The reaction was incubated at 50°C during 70 h without agitation. The microplates were centrifuged for 15 min at 6000 rpm. 200 µl of supernatant was separated and measured on spectrometer for the absorbance at 510 nm. Quantity of glucose was calculated from a glucose standard and expressed as a difference between supernatant and enzymatic solution.

Biochemical analysis

300 mg of ground and sieved wood powder was first dried and treated with 96% ethanol to eliminate nonstructural carbohydrates and polyphenols like flavonoids; and with water to eliminate soluble compounds like proteins and tannins. The wood powder free from extractives was hydrolyzed with 5 ml of 72% sulfuric acid, for 2h at room temperature and agitation 250 rpm. The second hydrolysis was performed with 3% sulfuric acid, for 1 hour at 120°C. The hydrolysis gave insoluble

residue used for lignin dosage and soluble filtrate used for both lignin and sugar dosage. Lignin content was analyzed following Klason method. Insoluble Klason lignin was determined from the mass of dried hydrolyzed powder and was expressed per gram of wood powder free from extractives. Soluble lignin was determined from the absorbance of diluted hydrolyzed filtrate measured at 205 nm wavelength with UV spectrophotometer. Total lignin content was expressed as the sum of insoluble Klason and soluble lignin, each calculated for 2 technical repetitions. 25 ml of filtered hydrolysate was neutralized with 1 g of calcium carbonate to obtain pH around 7. The neutralized hydrolysates were agitated during 16h at 4°C. The mixture was first centrifuged during 15 min at 13 000 g and 4°C to separate the supernatant, and then purified with Chromafil Xtra PET-45/25 (Macherey-Nagel) filter, controlling the pH between 6 and 8. Sample (20 µl) was injected in HPCL apparatus with EC 250/4.6 Nucleodur 100-5 NH2-RP column (Macherey-Nagel) and eluted with 25% of water and 75% of acetonitrile. Elution was identified with ELSD detector (drift tube temperature 50°C, N2 gas pressure: 3.5 bars, gain 5, filter 6s). Quantities of glucose and xylose were calculated from the calibration curves obtained with 2.5, 5, 10, 20 and 40 µg of glucose and xylose. The quantities of glucose or xylose were expressed per gram of wood free from extractives.

Cellulose ultrastructure

Wood sections were cut with blade to 10-20 mm length, 3-4 mm width and 1-2 mm thickness. The beam was in X-ray diffractometer positioned perpendicular to the surface of wood sample. The interferences were projected on diffractogram as diffraction peaks of Miller's index 002 associated with the crystalline plan of atoms in wood. An angle of cellulose microfibrils was calculated as 0.6*T where the T parameter corresponds to the half-surface of a peak. An anisotropic index was calculated as a ratio between the maximal intensity and the baseline of diffraction peak.

REFERENCES

Adrangi S, Faramarzi MA. 2013. From bacteria to human: A journey into the world of chitinases. Biotechnology Advances **31**, 1786-1795.

Aspeborg H, Schrader J, Coutinho PM, Stam M, Kallas A, Djerbi S, Nilsson P, Denman S, Amini B, Sterky F, Master E, Sandberg G, Mellerowicz E, Sundberg B, Henrissat B, Teeri TT. 2005. Carbohydrate-active enzymes involved in the secondary cell wall biogenesis in hybrid aspen. Plant Physiology **137**, 983-997.

Bowling AJ, Vaughn KC. 2008. Immunocytochemical characterization of tension wood: gelatinous fibers contain more than just cellulose. American Journal of Botany **95**, 655-663.

Chang S., Puryear J., Cairney. 1993. A simple and efficient method for isolating RNA from pine trees. Plant Molecular Biology Report **11**: 113-116

Chang SS, Salmen L, Olsson AM, Clair B. 2014. Deposition and organisation of cell wall polymers during maturation of poplar tension wood by FTIR microspectroscopy. Planta **239**, 243-254.

Clair B, Almeras T, Pilate G, Jullien D, Sugiyama J, Riekel C. 2011. Maturation Stress Generation in Poplar Tension Wood Studied by Synchrotron Radiation Microdiffraction. Plant Physiology **155**, 562-570.

Clair B, Almeras T, Yamamoto H, Okuyama T, Sugiyama J. 2006. Mechanical behavior of cellulose microfibrils in tension wood, in relation with maturation stress generation. Biophysical Journal **91**, 1128-1135.

Dejardin A, Leple JC, Lesage-Descauses MC, Costa G, Pilate G. 2004. Expressed sequence tags from poplar wood tissues - a comparative analysis from multiple libraries. Plant Biology **6**, 55-64.

Domon JM, Neutelings G, Roger D, David A, David H. 2000. A basic chitinase-like protein secreted by embryogenic tissues of Pinus caribaea acts on arabinogalactan proteins extracted from the same cell lines. Journal of Plant Physiology **156**, 33-39.

Gorshkova T, Mokshina N, Chernova T, Ibragimova N, Salnikov V, Mikshina P, Tryfona T, Banasiak A, Immerzeel P, Dupree P, Mellerowicz EJ. 2015. Aspen tension wood fibers Contain beta-(1->4)-galactans and acidic arabinogalactans retained by cellulose microfibrils in gelatinous walls. Plant Physiology **169**, 2048-2063.

Gritsch C, Wan Y, Mitchell RAC, Shewry PR, Hanley SJ, Karp A. 2015. G-fibre cell wall development in willow stems during tension wood induction. Journal of Experimental Botany **66**, 6447-6459.

Helliwell CA, Wesley SV, Wielopolska AJ, Waterhouse PM. 2002. High-throughput vectors for efficient gene silencing in plants. Functional Plant Biology **29**, 1217-1225.

Hermans C, Porco S, Verbruggen N, Bush DR. 2010. Chitinase-Like Protein CTL1 Plays a Role in Altering Root System Architecture in Response to Multiple Environmental Conditions. Plant Physiology **152**, 904-917.

Hossain MA, Noh H, Kim K, Koh E, Wi S, Bae H, Lee H, Hong S. 2010. Mutation of the chitinase-like protein-encoding AtCTL2 gene enhances lignin accumulation in dark-grown Arabidopsis seedlings. Journal of Plant Physiology **167**, 650-658.

Jourez B, Riboux A, Leclercq A. 2001. Anatomical characteristics of tension wood and opposite wood in young inclined stems of poplar (Populus euramericana cv 'Ghoy'). Iawa Journal **22**, 133-157.

Kesari P, Patil DN, Kumar P, Tomar S, Sharma AK, Kumar P. 2015. Structural and functional evolution of chitinase-like proteins from plants. Proteomics **15**, 1693-1705.

Kim JS, Daniel G. 2012. Distribution of glucomannans and xylans in poplar xylem and their changes under tension stress. Planta **236**, 35-50.

Kumar M, Thammannagowda S, Bulone V, Chiang V, Han KH, Joshi CP, Mansfield SD, Mellerowicz E, Sundberg B, Teeri T, Ellis BE. 2009. An update on the nomenclature for the cellulose synthase genes in Populus. Trends in Plant Science **14**, 248-254.

Kumar S, Stecher G, Tamura K. 2016. MEGA7: Molecular Evolutionary Genetics Analysis Version 7.0 for Bigger Datasets. Molecular Biology and Evolution **33**, 1870-1874.

Kwon Y, Kim S, Jung M, Kim M, Oh J, Ju H, Kim K, Vierling E, Lee H, Hong S. 2007. Arabidopsis hot2 encodes an endochitinase-like protein that is essential for tolerance to heat, salt and drought stresses. Plant Journal **49**, 184-193.

Lafarguette F, Leple JC, Dejardin A, Laurans F, Costa G, Lesage-Descauses MC, Pilate G. 2004. Poplar genes encoding fasciclin-like arabinogalactan proteins are highly expressed in tension wood. New Phytologist **164**, 107-121.

MacMillan CP, Mansfield SD, Stachurski ZH, Evans R, Southerton SG. 2010. Fasciclin-like arabinogalactan proteins: specialization for stem biomechanics and cell wall architecture in Arabidopsis and Eucalyptus. Plant Journal **62**, 689-703.

MacMillan CP, Taylor L, Bi Y, Southerton SG, Evans R, Spokevicius A. 2015. The fasciclin-like arabinogalactan protein family of Eucalyptus grandis contains members that impact wood biology and biomechanics. New Phytologist **206**, 1314-1327.

McFarlane HE, Doring A, Persson S. 2014. The Cell Biology of Cellulose Synthesis. Annual Review of Plant Biology, Vol 65 **65**, 69-+.

Mokshina N, Gorshkova T, Deyholos MK. 2014. Chitinase-like (CTL) and

cellulose synthase (CESA) gene expression in gelatinous-type cellulosic walls of flax (Linum usitatissimum L.) bast fibers. PLoS ONE **9**, e97949.

Nishikubo N, Awano T, Banasiak A, Bourquin V, Ibatullin F, Funada R, Brumer H, Teeri TT, Hayashi T, Sundberg B, Mellerowicz EJ. 2007. Xyloglucan endo-transglycosylase (XET) functions in gelatinous layers of tension wood fibers in poplar - A glimpse into the mechanism of the balancing act of trees. Plant and Cell Physiology **48**, 843-855.

Olsson AM, Bjurhager I, Gerber L, Sundberg B, Salmen L. 2011. Ultra-structural organisation of cell wall polymers in normal and tension wood of aspen revealed by polarisation FTIR microspectroscopy. Planta **233**, 1277-1286.

Persson S, Wei HR, Milne J, Page GP, Somerville CR. 2005. Identification of genes required for cellulose synthesis by regression analysis of public microarray data sets. Proceedings of the National Academy of Sciences of the United States of America **102**, 8633-8638.

Sanchez-Rodriguez C, Bauer S, Hematy K, Saxe F, Ibanez AB, Vodermaier V, Konlechner C, Sampathkumar A, Ruggeberg M, Aichinger E, Neumetzler L, Burgert I, Somerville C, Hauser MT, Persson S. 2012. CHITINASE-LIKE1/POM-POM1 and Its Homolog CTL2 Are Glucan-Interacting Proteins Important for Cellulose Biosynthesis in Arabidopsis. Plant Cell **24**, 589-607.

van Hengel AJ, Guzzo F, van Kammen A, de Vries SC. 1998. Expression pattern of the carrot EP3 endochitinase genes in suspension cultures and in developing seeds. Plant Physiology **117**, 43-53.

Wu B, Zhang B, Dai Y, Zhang L, Shang-Guan K, Peng Y, Zhou Y, Zhu Z. 2012. Brittle Culm15 Encodes a Membrane-Associated Chitinase-Like Protein Required for Cellulose Biosynthesis in Rice. Plant Physiology **159**, 1440-1452.

Yamamoto H. 2004. Role of the gelatinous layer on the origin of the physical properties of the tension wood. Journal of Wood Science **50**, 197-208.

Zhang DS, Hrmova M, Wan CH, Wu CF, Balzen J, Cai W, Wang J, Densmore LD, Fincher GB, Zhang H, Haigler CH. 2004. Members of a new group o f chitinase-like genes are expressed preferentially in cotton cells with secondary walls. Plant Molecular Biology **54**, 353-372.

Zhong RQ, Kays SJ, Schroeder BP, Ye ZH. 2002. Mutation of a chitinase-like gene causes ectopic deposition of lignin, aberrant cell shapes, and overproduction of ethylene. Plant Cell **14**, 165-179.

Supplementary Table I-1. Predicted genes of CTL GH19 family in poplar, Arabidopsis and flax

Species	Gene	Gene model	Gene	Gene model
Populus trichocarpa	*PtrCTL1*	Potri.014G146600	*PtrCTL12*	Potri.009G141700
	PtrCTL2	Potri.010G141600	*PtrCTL13*	Potri.009G142200
	PtrCTL3	Potri.014G111800	*PtrCTL14*	Potri.T175200
	PtrCTL4	Potri.002G186500	*PtrCTL15*	Potri.013G125000
	PtrCTL5	Potri.004G182100	*PtrCTL16*	Potri.019G093700
	PtrCTL6	Potri.009G142100	*PtrCTL17*	Potri.019G093800
	PtrCTL7	Potri.009G141800	*PtrCTL18*	Potri.013G125100
	PtrCTL8	Potri.009G142300	*PtrCTL19*	Potri.019G094000
	PtrCTL9	Potri.009G142000	*PtrCTL20*	Potri.019G093900
	PtrCTL10	Potri.T175300	*PtrCTL21*	Potri.019G094100
	PtrCTL11	Potri.004G182000		
Arabidopsis thaliana	*AtCTL1*	AT1G05850	*AtCTL8*	AT2G43590
	AtCTL2	AT3G16920	*AtCTL9*	AT2G43580
	AtCTL3	AT4G01700	*AtCTL10*	AT3G54420
	AtCTL4	AT1G02360	*AtCTL11*	AT2G43600
	AtCTL5	AT3G12500	*AtCTL12*	AT1G56680
	AtCTL6	AT2G43570	*AtCTL13*	AT2G43620
	AtCTL7	AT3G47540	*AtCTL14*	AT2G43610
Linum usitatissimum	*LusCTL1*	Lus10016872.g	*LusCTL20*	Lus10010866.g
	LusCTL2	Lus10037737.g	*LusCTL21*	Lus10024366.g
	LusCTL3	Lus10037428.g	*LusCTL22*	Lus10035618.g
	LusCTL4	Lus10037430.g	*LusCTL23*	Lus10035620.g
	LusCTL5	Lus10041278.g	*LusCTL24*	Lus10003231.g
	LusCTL6	Lus10041282.g	*LusCTL25*	Lus10035621.g
	LusCTL7	Lus10041829.g	*LusCTL26*	Lus10024369.g
	LusCTL8	Lus10041830.g	*LusCTL27*	Lus10035624.g
	LusCTL9	Lus10028378.g	*LusCTL28*	Lus10003227.g
	LusCTL10	Lus10028377.g	*LusCTL29*	Lus10000217.g
	LusCTL11	Lus10041831.g	*LusCTL30*	Lus10035625.g
	LusCTL12	Lus10000193.g	*LusCTL31*	Lus10003226.g
	LusCTL13	Lus10038026.g	*LusCTL32*	Lus10024368.g
	LusCTL14	Lus10009968.g	*LusCTL33*	Lus10010861.g
	LusCTL15	Lus10000453.g	*LusCTL34*	Lus10010862.g
	LusCTL16	Lus10003230.g	*LusCTL35*	Lus10003587.g
	LusCTL17	Lus10024367.g	*LusCTL36*	Lus10032794.g
	LusCTL18	Lus10010863.g	*LusCTL37*	Lus10010860.g
	LusCTL19	Lus10010864.g		

2. FASCICLIN-LIKE ARABINOGALACTAN PROTEIN

FLA protein families from poplar, Arabidopsis and flax were identified and aligned in a phylogenetic analysis. FLA family of poplar was further studied in expressional analysis in TW, OW and NW. To understand a function of FLAs in tension wood formation, we selected to study FLA1, which is differentially expressed in TW in comparison to OW (**Lafarguette *et al.*, 2004**). In parallel, we also studied FLA14, which has non-differentiate expression between TW and OW (**Lafarguette *et al.*, 2004**). Such approach was used in order to understand what differentiate two groups of FLAs with different expression profile. FLA1 and FLA14 were first studied in expression analysis in different plant tissues and organs, and then in wood from stems of different tilting duration. Their function was further studied in FLA1 and FLA14 RNAi transgenic lines characterized for growth, chemical properties, cellulose ultrastructure and expression of potential gene partners.

2.1. FLA family

2.1.1. Phylogenetic analysis

Based on presence of fasciclin domain (Pf02469), poplar genome (*P. trichocarpa*) was predicted to contain 48 FLAs. Names of the first 15 PtrFLA from poplar were given according to **Lafarguette *et al.*** (**2004**), while the remaining genes were assigned according to falling order in groups A to D. Poplar FLA family was compared in a phylogenetic analysis to FLA family from Arabidopsis consisted of 21 genes (**Johnson *et al.*, 2003**) and LusFLA family from flax predicted to consist of 42 genes (**Table II-1**). According to the FLA family from Arabidopsis (**Johnson *et al.*, 2003**), FLAs were classified into 4 groups named A, B, C and D. The classification is based on the number and homology of fasciclin-like domains, position of arabinogalactan region and presence of the GPI anchor signal.
Most of PtrFLAs (58%) and LusFLAs (43%) were attributed to the group-A (**Fig. II-1**). One clade of the group-A was made of only FLAs from poplar. The clade consisted of 14 FLAs among which were 6 FLAs (FLA1-6) previously reported to have differentiate expression in TW when compared to OW (**Lafarguette *et al.*, 2004**).

In Arabidopsis, most of FLAs were attributed to group-A (29%) and group-C (33%). Group-D was scattered in the phylogenetic tree, likely due to structural diversity of group-D members, as reported in Arabidopsis (**Johnson *et al.*, 2003**).

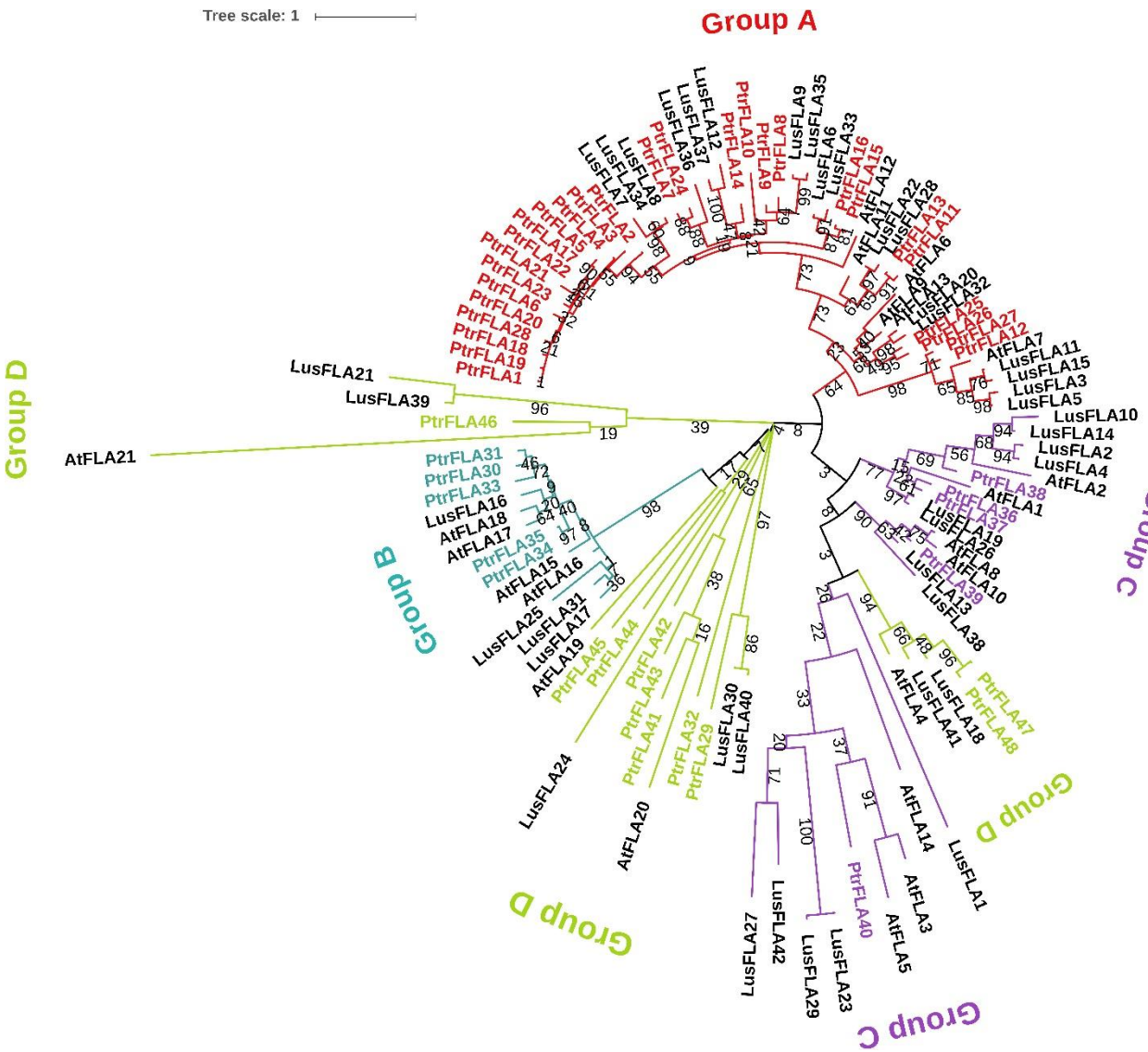

Figure II-1. Phylogenetic tree of FLA protein family from *Arabidopsis thaliana* (At), *Linum usitatissimum* (Lus) and *Populus trichocarpa* (Ptr). Members were attributed to groups A, B, C and D according to Johnson *et al.* (2003). The evolutionary history was inferred by using the Maximum Likelihood method based on the JTT matrix-based model in the analysis conducted in MEGA7 software.

2.1.2. Expression analysis in wood

RNA sequencing data were used to study expression of PtrFLA family in NW, OW and TW. The expression of different levels could be detected for 39 out of 48 genes (**Fig. II-2**). Ten *FLA*s had high expression in all three wood types. Notably the highest expression had *FLA15*. Ten *FLAs* had significantly differentiate expression in TW compared to OW. Their expression was very low in OW and NW. Expression of only one gene, *FLA16*, was shown to be higher in OW than in TW.

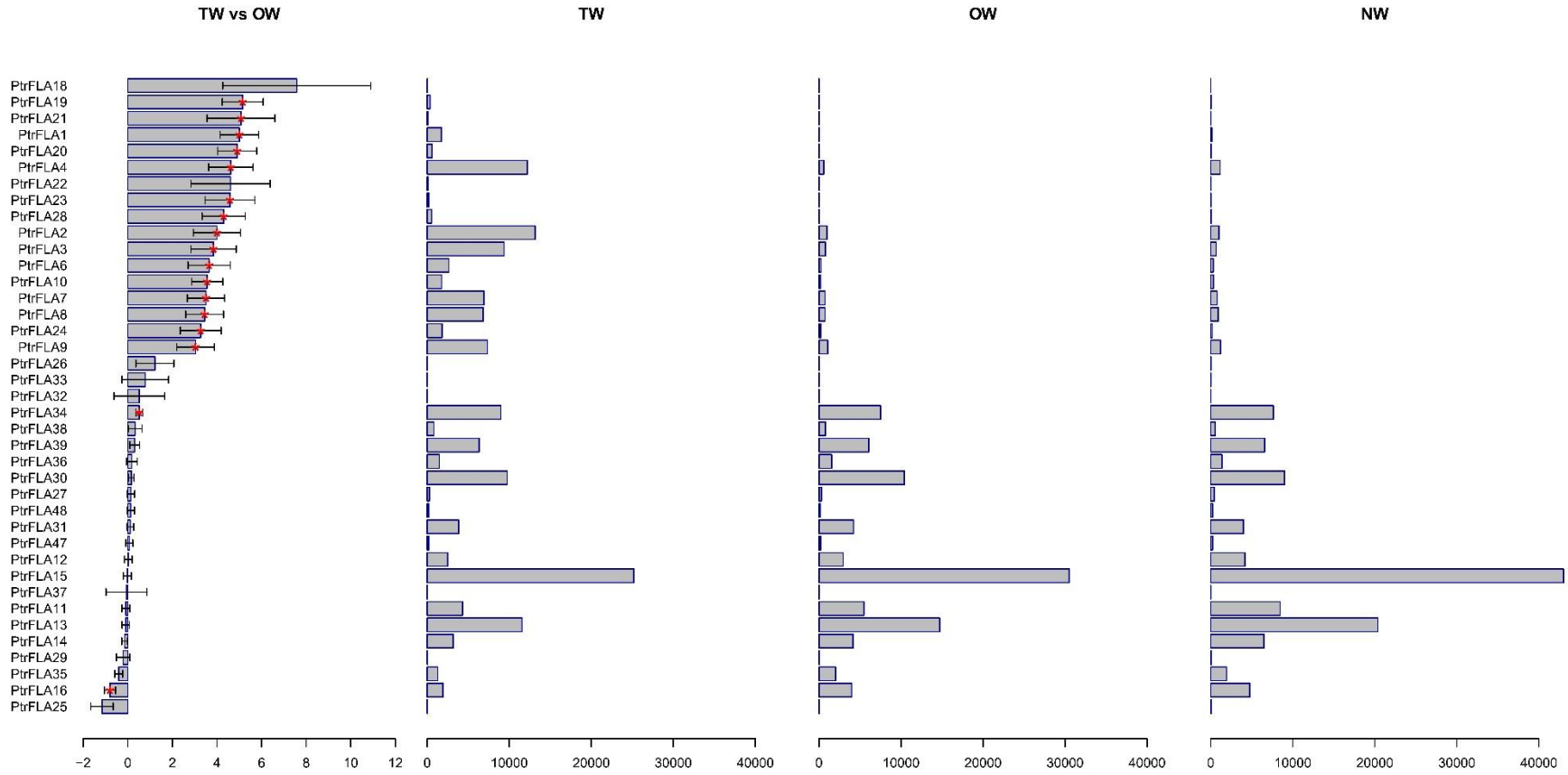

Figure II-2. Expression of *FLA* gene family in tension wood (TW), opposite wood (OW) and normal wood (NW). Expression was detected for 39 out of 48 genes. First column shows relative log2 ratio of gene expression in TW and OW. The ratio was examined for statistical significance with t-test, where: * p-value 0.01-0.05. Bars represent standard errors. The remaining columns show absolute gene expression in TW, OW and NW.

2.2. Characterization of FLA1 and FLA14

The study was focalized on two family members: FLA1 and FLA14. Such strategy was used in order to understand what differentiate the group of FLAs specific to tension wood from FLAs continuously expressed in wood. According to the expression of fifteen FLAs reported by **Lafarguette *et al.*** (**2004**), FLA1 was chosen as representative of FLAs specifically expressed in TW and FLA14 of group of non-differentially expressed FLAs. The identified FLAs were studied in expressional analyses and from traits of FLA RNAi transgenic poplars.

2.2.1. Expression profile of *FLA1* and *FLA14*

Tissues and organs

The expression analysis in various poplar tissues and organs (apex, leaves, xylem, phloem, roots, seeds and germinated seeds) was conducted in quantitative real-time reverse-transcription PCR (qRT-PCR) reaction (**Fig. II-3**). Relative quantitative expression of *FLA14* was in all tissues higher than the expression of *FLA1*. In xylem, the expression of *FLA14* was approximately twice the expression of *FLA1*. Between the analyzed tissues, the expression of *FLA1* was notably the highest in xylem and very low in other tissues and organs. The expression of *FLA14* was the highest in xylem, approximately 20-30 fold higher than in other tissues.

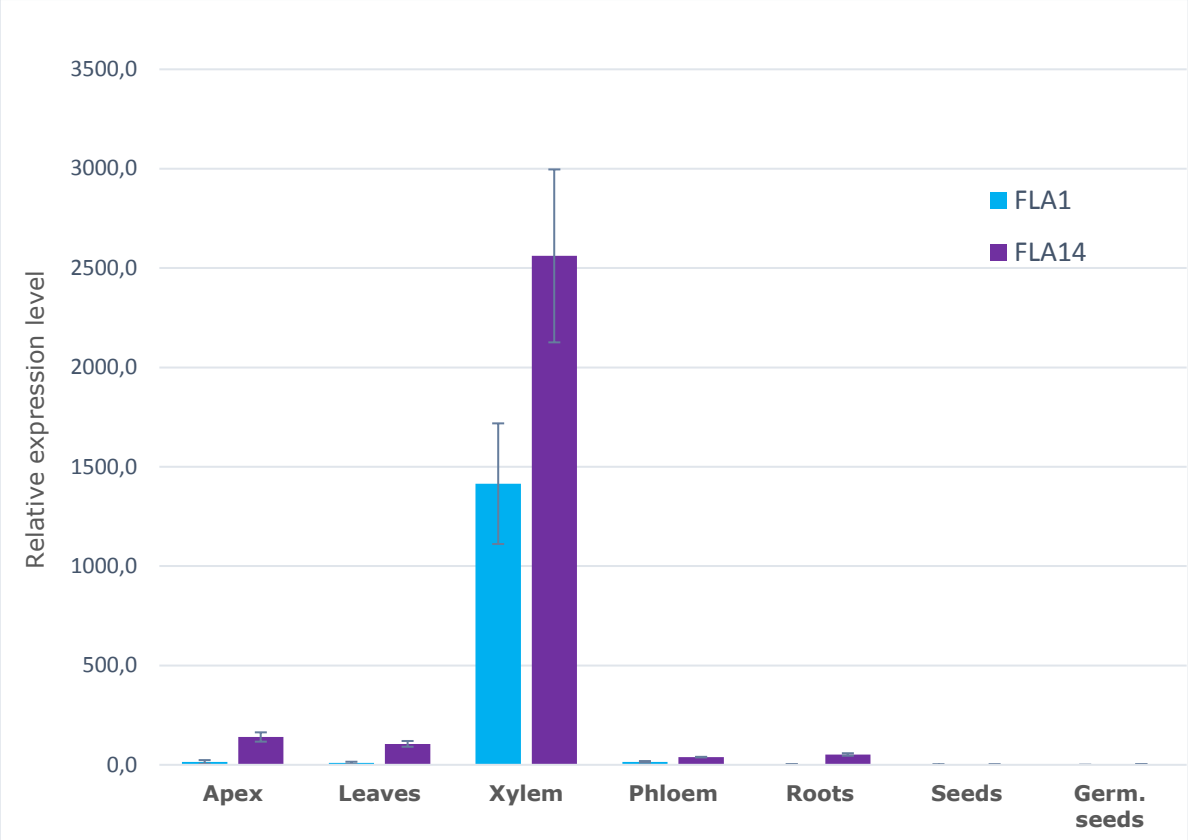

Figure II-3. Relative quantitative expression of *FLA1* and *FLA14* in different plant tissues and organs of poplar. Bars represent standard error: n= 3 technical repetitions of different pulls from 1 tree (seeds/germ.seeds) or 6 trees (for all other tissues/organs). Germ. seeds= germinated seeds.

OW and TW from stems of different tilting duration

The expression of *FLA1* and *FLA14* was analyzed in the collection of OW and TW tissues sampled 0, 1, 3, 7, 14 and 25 days after stem tilting. At day 0, wood was collected from straight growing trees on two sides corresponding to OW and TW of tilted stems. The analysis was performed on 2 biological replicates in semi-quantitative reverse-transcription PCR (RT-PCR) reaction (**Fig. II-4**). cDNA was amplified in low number of amplification cycles (20) to avoid saturation of DNA signal. Equal RNA loading in the reaction was verified by amplification of *18S* gene. The signal of *FLA1* amplification could not be detected in OW from any stem of different tilting duration. The signal of *FLA1* amplification was low in TW collected at day 0 and the highest in TW from stems tilted for 3, 7 and 14 days. The expression level decreased in TW from stems titled for 25 days, when compared to stems tilted for shorter time.

The expression of *FLA14* was higher than the expression of *FLA1* amplified in the same number of amplification cycles. The intensity of DNA band was slightly different between individual trees. The expression of *FLA14* could be detected in OW and TW collected from stems of all tilting durations. There were no apparent difference between the expression of *FLA14* in OW and TW of differently tilted stems, except that the amplification signal was strongest in OW from one tree collected at day 0.

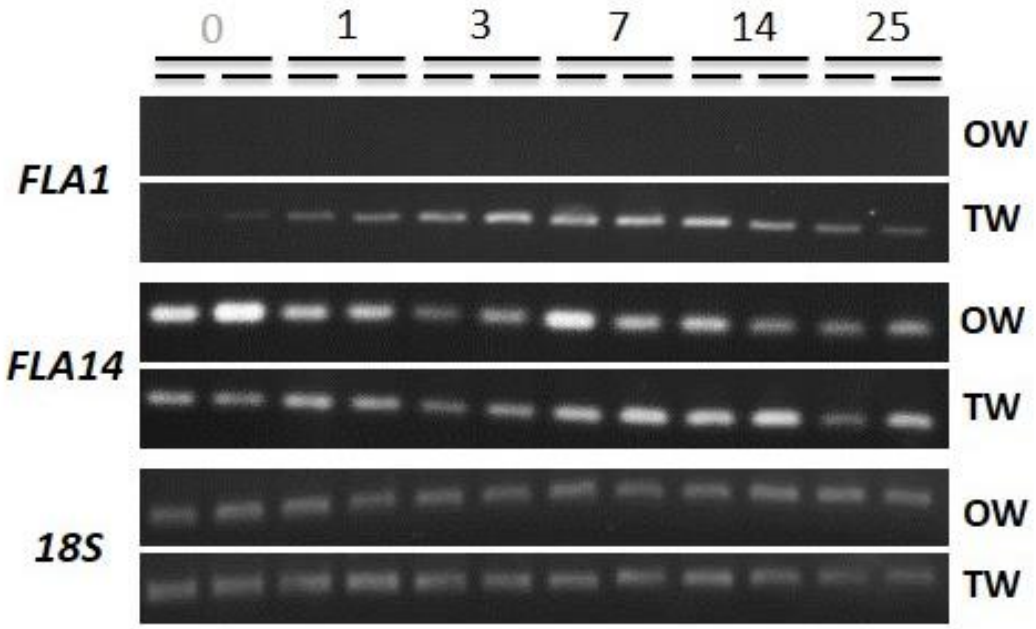

Figure II-4. Expression of *FLA1* and *FLA14* in opposite (OW) and tension (TW) wood of poplar stems tilted for 1, 3, 7, 14 and 25 days. TW and OW from 0 day correspond to the respective upper and lower xylem of straight stem sampled prior tilting. Amplification of *18S* was used as a control of equal RNA loading in RT-PCR reaction.

2.2.2. Production of FLA1 and FLA14 transgenic lines

To down-regulate the expression of *FLA1* and *FLA14*, we produced pHellsgate8 vectors (**Helliwell *et al.*, 2002**) expressing interference RNA. FLA1 sequence selected for generation of RNAi was 97 bp long and homologous to group of six genes (*FLA1-FLA6*) from the same cluster (**Déjardin *et al.*, 2004**), expressed specifically in TW (**Lafarguette *et al.*, 2004**). *FLA14* sequence was homologous to *FLA11*, *FLA12*, *FLA13* and *FLA15*, which belong to the group of genes expressed both in OW and TW (**Lafarguette *et al.*, 2004**). Such approach was used because it was not possible to find short sequence specific for the gene of interest due to high homology between FLAs.

The transformation protocol raised per 21 FLA1 and FLA14 transgenic RNAi lines. Around half of lines were screened for the gene expression in mostly one individual transgenic tree. 30% of FLA1 and 27% of FLA14 lines were shown to be down-regulated for the gene expression when compared to the expression of *FLA1* and *FLA14* in wild-types, respectively. Effects of the gene silencing were finally analyzed in 3 transgenic lines (T1, T2 and T3), each represented with 3 biological replicates. Level of the gene expression in these transgenic lines was analyzed in semi-quantitative RT-PCR reaction and compared with the expression in wild-type trees (**Fig. II-5**).

The expression of *FLA1* could not be detected in OW of wild-type and transgenic lines, which is in accordance with the expression profile of *FLA1* (**Fig. II-2, II-4**). The expression of *FLA1* was down-regulated in FLA1-T1 and FLA1-T2 lines, although not completely, as evidenced from the weak amplification signal. In both FLA1-T1 and FLA1-T2 lines, the degree of gene silencing was consistent between replicates and similar between the two lines. The expression of *FLA1* in FLA1-T3 line was not modified, when compared to wild-type.

FLA14 was down-regulated in OW and TW of only FLA14-T2 line. The expression of *FLA14* was unchanged in lines FLA14-T1 and FLA14-T3.

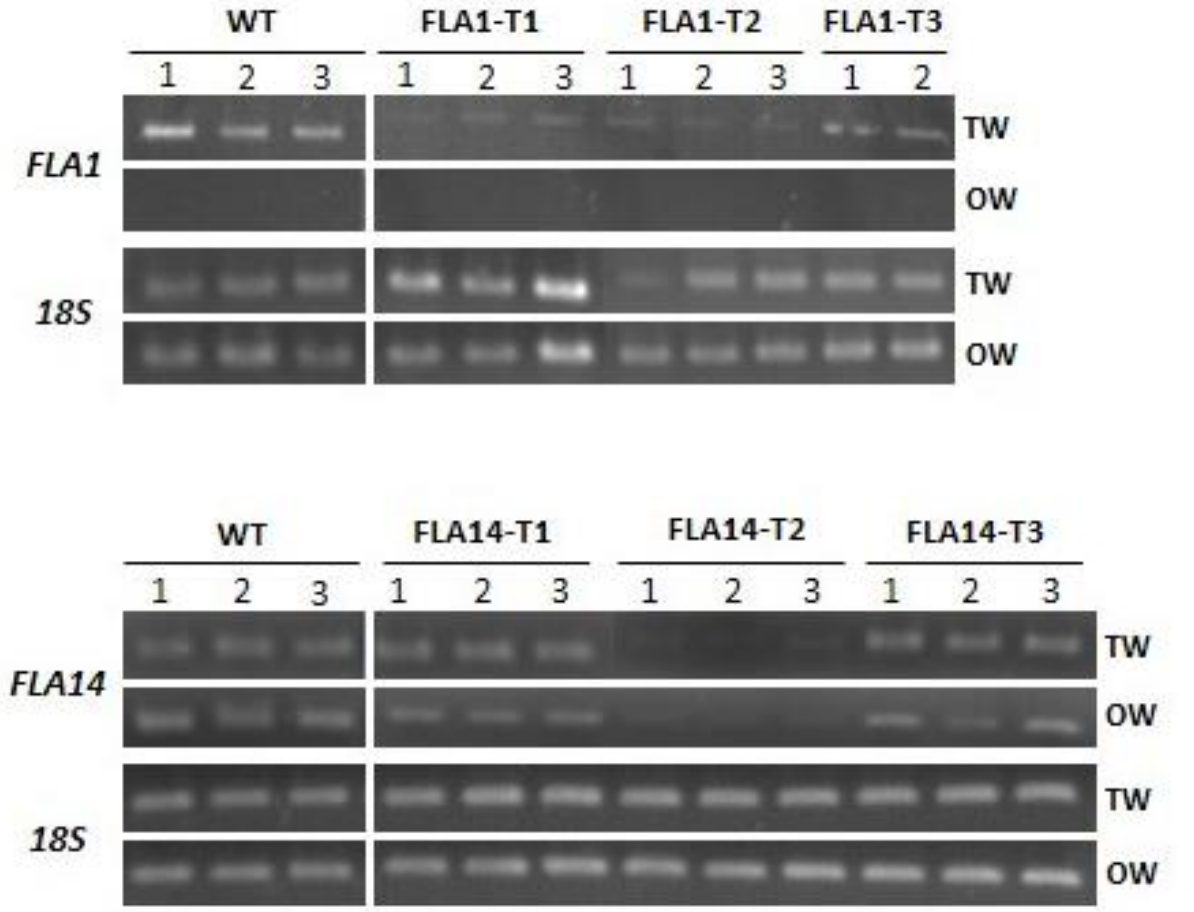

Figure II-5. RT-PCR expression analysis of *FLA1* and *FLA14* in opposite (OW) and tension (TW) wood of wild-type (WT) and FLA1 and FLA14 transgenic lines T1, T2 and T3. The analysis was performed in 3 biological replicates with the exception of FLA1-T3 line represented with only 2 replicates. *18S* was used as a housekeeping gene control of equal RNA loading in RT-PCR reaction.

2.2.3. Traits of FLA1 and FLA14 transgenic lines

Growth phenotype

Tree growth parameters were measured after 4 months of growth in the greenhouse. Any significant effect on tree height could be detected in transgenic lines FLA1-T1, FLA1-T2 and FLA1-T3 (**Fig. II-6**). FLA14-T1 line had approximately the same height as wild-type, while trees of FLA14-T2 and FLA14-T3 lines were significantly higher than wild-types (**Fig. II-6**).

Although all transgenic FLA lines had larger basal diameter than wild-type trees, the increase was not significant.

During growth in the greenhouse, none of genetically modified trees displayed phenotype different from wild-type plants (data not shown). None of lines either had modified wood anatomy or cell walls, as concluded from studies on stem cross-sections (data not shown).

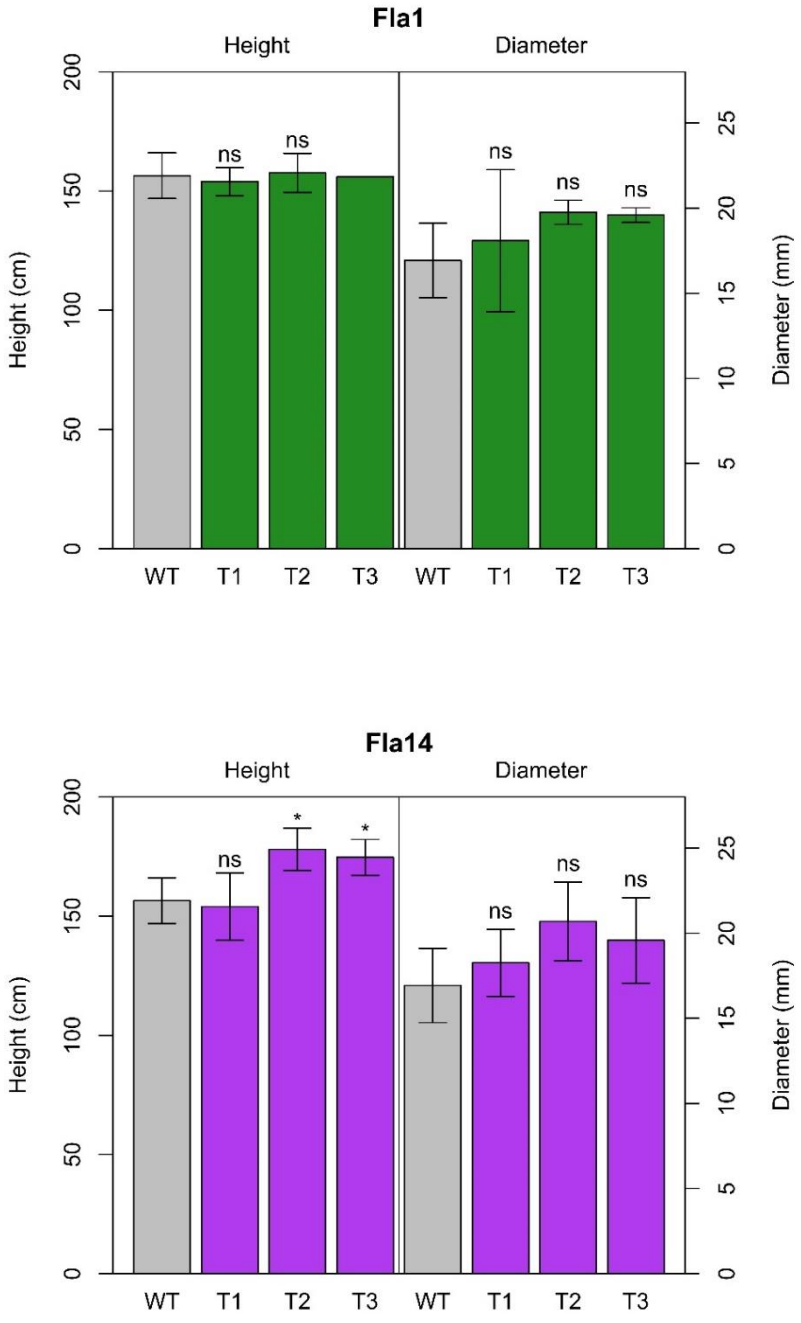

Figure II-6. Tree height and diameter of wild-type (WT), FLA1 and FLA14 transgenic lines T1, T2 and T3 grown in greenhouse conditions for 4 months. Bars represent standard errors; n=6 biological replicates (wild-type); n=3 biological replicates (T1, T2, T3), with the exception for FLA1-T3 line with only 1 tree. The statistically significant difference between wild-type and transgenic lines was calculated from Welch's t-test, where: * p-value 0.01-0.05, ns= non-significant.

Wood chemical properties

Chemical properties were studied from wood absorbance spectra of middle infrared (MIR) light. The spectra were statistically pretreated by normalization and analyzed in principal component analysis (PCA). In all transgenic lines and wild-types, OW and TW were separated on the first axis (**Fig. II-7, II-8**).

FLA1 lines

There were no difference between TW of wild-type and TW of transgenic FLA1 lines (**Fig. II-7**). OW of FLA1-T1 line was slightly different from wild-type and FLA1-T3 line. However, the difference could not be detected when spectra were proceeded with different statistical treatments (data not shown).

FLA14 lines

OW of wild-type was the same as OW of FLA14-T1 and FLA14-T3 lines and different from OW of FLA14-T2 line (**Fig. II-8**). There were no differences between TW of FLA14-lines and wild-type, except a mild difference for FLA14-T2 line.

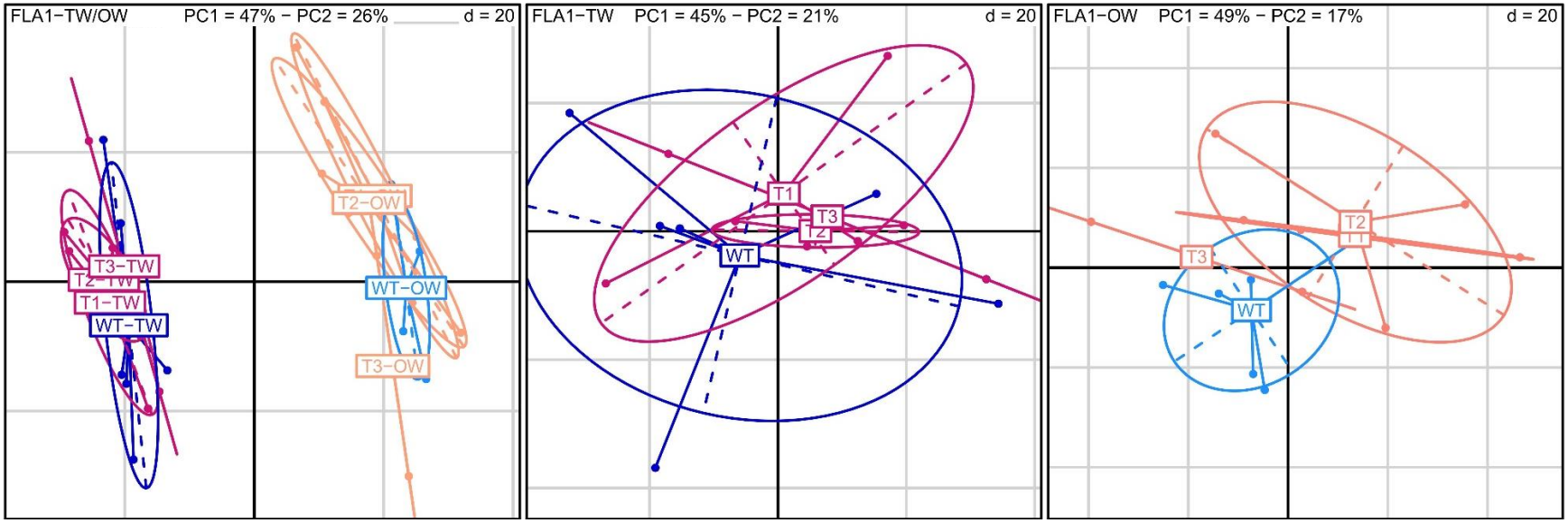

Figure II-7. Graph of principal component analysis of normalized FT-MIR spectra of opposite (OW) and tension (TW) wood from wild-type (WT) and **FLA1 transgenic lines T1, T2 and T3**. Number of biological tree replicates: n=6 (WT), n=3 (T1, T2), n=2 (T3).

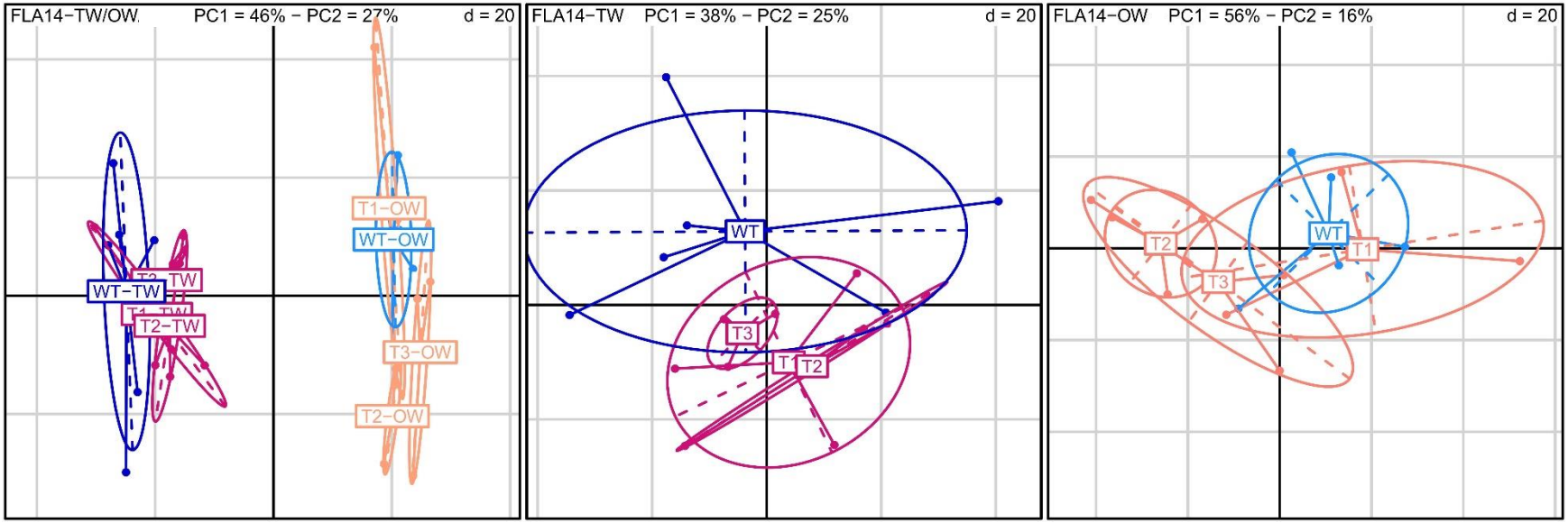

Figure II-8. Graph of principal component analysis of normalized FT-MIR spectra of opposite (OW) and tension (TW) wood from wild-type (WT) and **FLA14 transgenic lines T1, T2 and T3**. Number of biological tree replicates: n=6 (WT), n=3 (T1, T2, T3)

Cellulose ultrastructure

Microfibril angle and cellulose organization were estimated from X-ray diffraction in OW and TW of wild-types and transgenic lines FLA1 and FLA14.

Anisotropic index represents ratio between maximal intensity of diffraction peak, which is indicative of quantity of highly organized cellulose, and baseline of a peak-indicative of non-organized cellulose structure. The ratio reflects global cellulose organization and is an indicator of cellulose crystallinity. A high index indicates highly organized crystalline structure and/or poor amorphous zones. It may also be indicative of larger crystals and/or highly aggregated cellulose.

In wild-types and transgenic lines, cellulose microfibril angle and crystallinity were inversely proportional. TW had low microfibril angles and high cellulose organization, while OW had high microfibril angles and more amorphous cellulose structure.

In TW, average cellulose microfibril angle was around 8° and was most likely overestimated, because the X-ray diffraction is not sensitive to very low angles, so as because of contribution of S-layers with higher angles of cellulose microfibrils.

FLA1 lines

In TW of FLA1-T1 and FLA1-T2 transgenic lines, the anisotropic index was lower than in wild-types and indicated alterations of crystalline cellulose structure (**Fig. II-9**). FLA1-T2 also had modified microfibril angle. However, the increase was mild in comparison to the average angle in wild-type. There were no modifications of angle in FLA1-T1 line. Cellulose ultrastructure was not altered in FLA1-T3 line.

OW of all transgenic lines had unmodified cellulose structure when compared to OW of wild types.

FLA14 lines

FLA14-T2 had altered cellulose crystalline structure only in TW, while the angle was unchanged in both TW and OW (**Fig. II-10**). Lines FLA14-T1 and FLA14-T3 had cellulose ultrastructure as wild-types in both OW and TW.

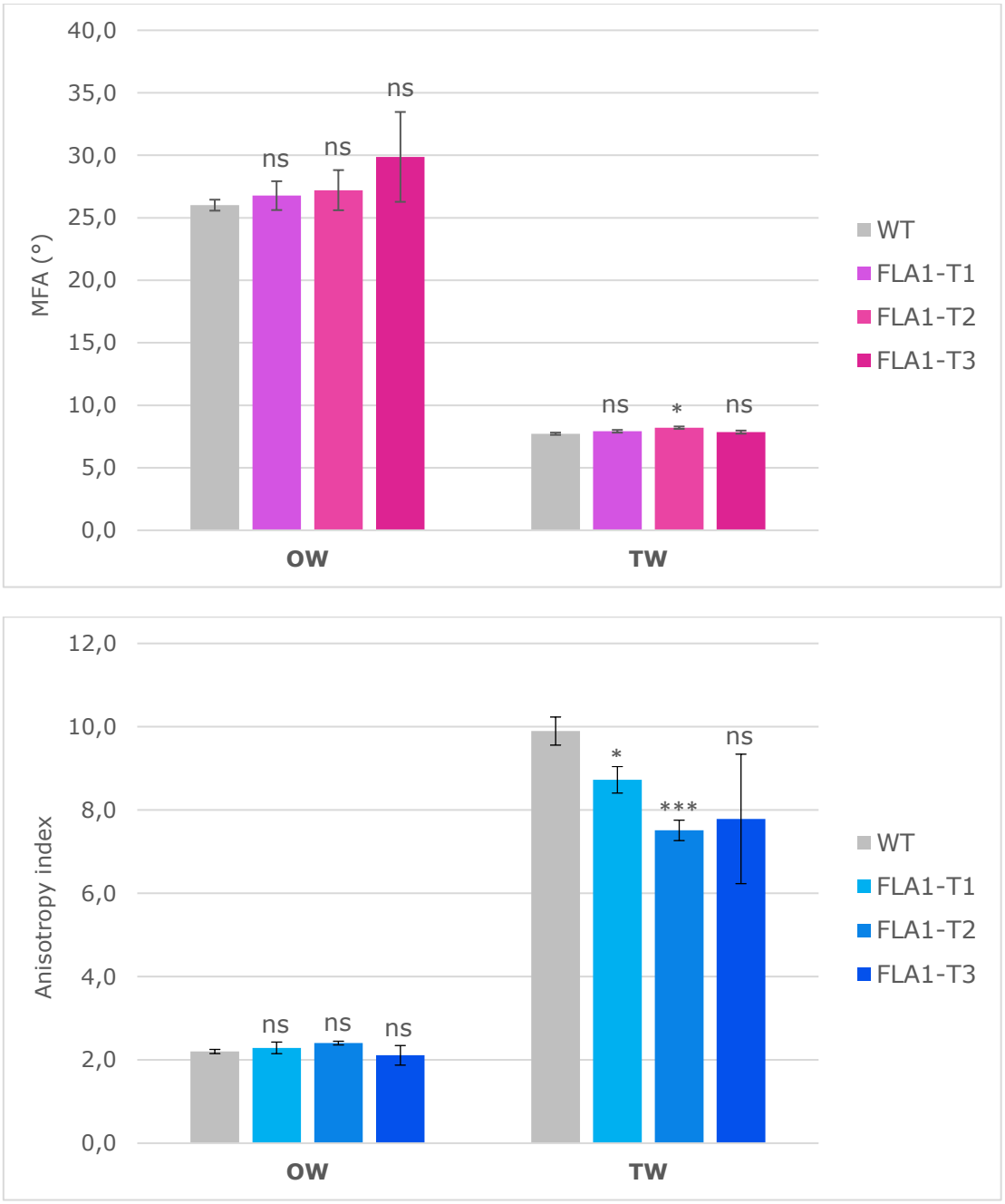

Figure II-9. Cellulose microfibril angle and anisotropic index of cellulose crystallinity estimated from X-ray diffraction in opposite wood (OW) and tension wood (TW) of wild-type (WT) and **FLA1 transgenic lines T1, T2 and T3**. Bars represent standard errors, where: n=6 (OW-WT), n=5 (TW-WT), n=3 (OW and TW of transgenic lines). The statistically significant difference between wild-type and transgenic lines was calculated from Welch's t-test, where: *** p-value 0-0.001, ** p-value 0.001-0.01, * p-value 0.01-0.05, ns= non-significant.

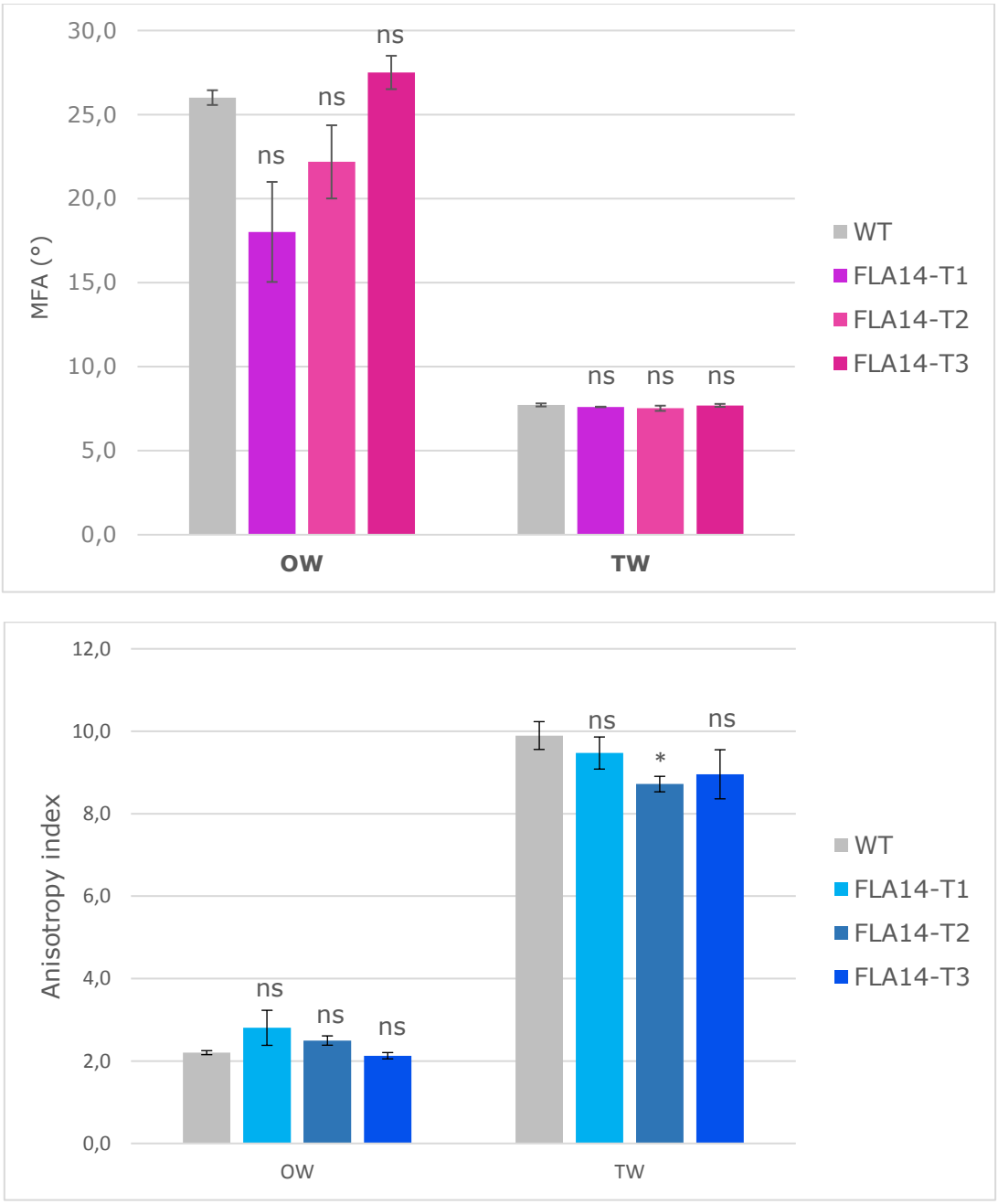

Figure II-10. Cellulose microfibril angle and anisotropic index of cellulose crystallinity estimated from X-ray diffraction in opposite wood (OW) and tension wood (TW) of wild-type (WT) and **FLA14 transgenic lines T1, T2 and T3**. Bars represent standard errors, where: n=6 (OW-WT), n=5 (TW-WT), n=3 (OW and TW of transgenic lines). The statistically significant difference between wild-type and transgenic lines was calculated from Welch's t-test, where: *** p-value 0-0.001, ** p-value 0.001-0.01, * p-value 0.01-0.05, ns= non-significant.

Effects on the expression of genes associated with *FLA*s

We quantified in FLA transgenics the expression of FLAs differentially expressed in TW (FLA1, FLA4, FLA8) and FLAs non-differentially expressed between OW and TW (FLA11, FLA13, FLA14) (Lafarguette et al., 2004). In Arabidopsis, two FLA genes were shown to co-express with genes related to cellulose synthesis as secondary cell wall CESAs, chitinase-like protein (CTL) and COBRA (Persson *et al.*, 2005). Therefore, we quantified their homologs from poplar: CESA4, CESA7A, CESA8A (Asperborg et al., 2005), COBL4, CTL1 and CTL2. In addition, we analyzed the expression of KORRIGAN, which gets expressed in tension wood of poplar (Andersson-Gunneras *et al.*, 2006).

FLA1-T1 line

The down-regulation of *FLA1* modified the expression of *FLA8* in TW, *CESA1* in OW; *FLA4*, *FLA13* and COBL4 in OW and TW (**Fig. II-11**). Although *FLA11* and CTL2 showed down-regulation trend, the difference between transgenic and wild-type was not significant.

FLA14-T2 line

The down-regulation of *FLA14* modified the expression of *FLA1*, *FLA4* and *FLA8* in TW, *FLA13* and *CESA1* in OW; *COBL4* in TW and OW (**Fig. II-12**). *FLA11* and *CTL2* showed tendency toward down-regulation, but it was non-significant when compared to level of the gene expression in wild-type.

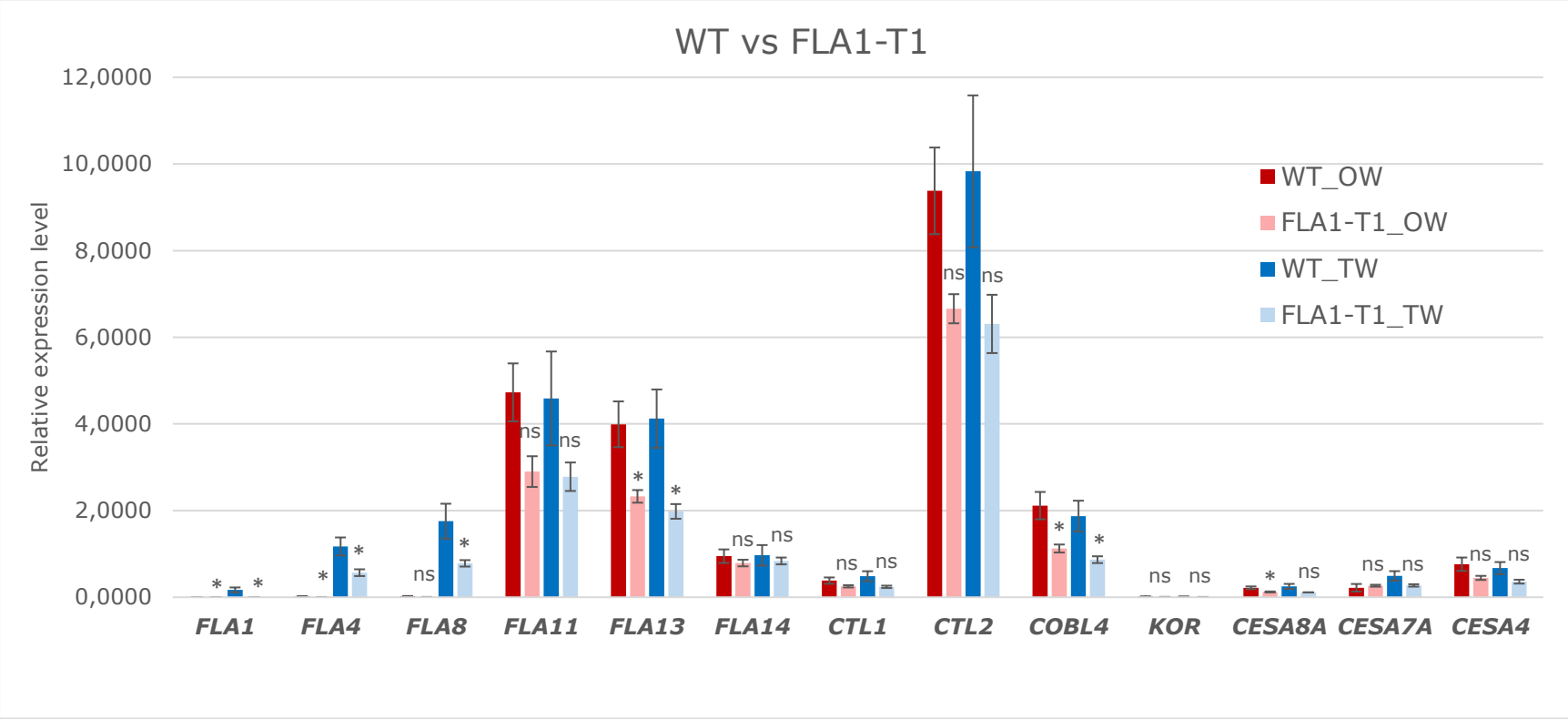

Figure II-11. Relative quantitative expression level of *CTL1*, *FLA1*, *FLA4*, *FLA8*, *FLA11*, *FLA13*, *FLA14*, *CTL1*, *CTL2*, *COBL4*, *KOR*, *CESA8A*, *CESA7A* and *CESA4* in opposite wood (OW) and tension wood (TW) of wild-type (WT) and **FLA1-T1 transgenic line**. Bars represent standard error, where: n=6 biological replicates (WT), n=3 biological replicates (T1). The statistically significant difference between wild-type and transgenic line was calculated from Welch's t-test, where: *** p-value 0-0.001, ** p-value 0.001-0.01, * p-value 0.01-0.05, ns= non-significant.

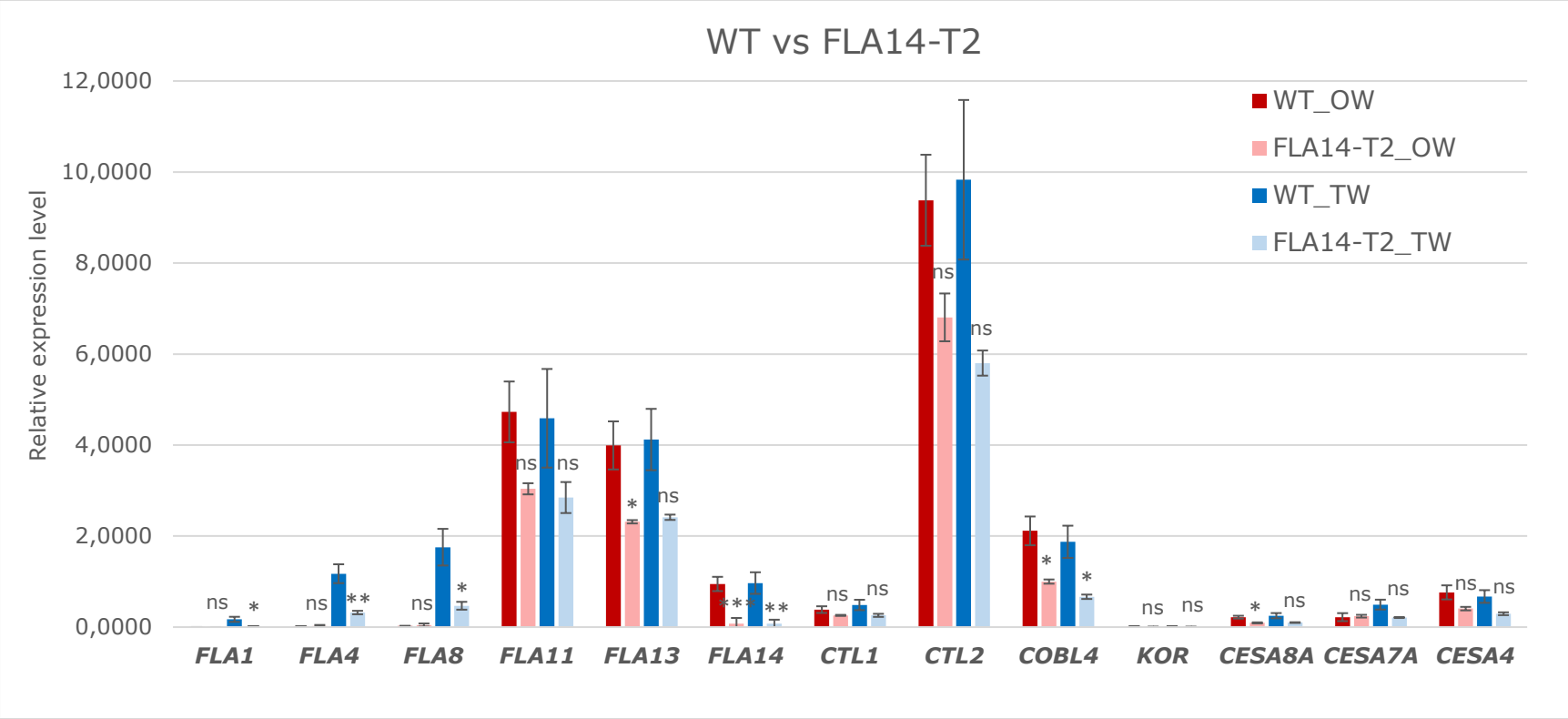

Figure II-12. Relative quantitative expression level of *FLA1*, *FLA4*, *FLA8*, *FLA11*, *FLA13*, *FLA14*, *CTL1*, *CTL2*, *COBL4*, *KOR*, *CESA8A*, *CESA7A* and *CESA4* in opposite wood (OW) and tension wood (TW) of wild-type (WT) and **FLA14-T2 transgenic line**. Bars represent standard error, where: n=6 biological replicates (WT), n=3 biological replicates (T2). The statistically significant difference between wild-type and transgenic line was calculated from Welch's t-test, where: *** p-value 0-0.001, ** p-value 0.001-0.01, * p-value 0.01-0.05, ns= non-significant

Annex II-1. Predicted genes of *FLA* family in poplar, Arabidopsis and flax

Species	Gene	Gene model	Gene	Gene model
Populus trichocarpa	*PtrFLA1*	Potri.019G121200	*PtrFLA25*	Potri.013G120600
	PtrFLA2	Potri.013G151400	*PtrFLA26*	Potri.019G093300
	PtrFLA3	Potri.013G151500	*PtrFLA27*	Potri.002G223300
	PtrFLA4	Potri.013G014200	*PtrFLA28*	Potri.019G122600
	PtrFLA5	Potri.019G123200	*PtrFLA29*	Potri.010G192300
	PtrFLA6	Potri.013G151300	*PtrFLA30*	Potri.008G012400
	PtrFLA7	Potri.012G015000	*PtrFLA31*	Potri.010G244900
	PtrFLA8	Potri.009G012200	*PtrFLA32*	Potri.012G006200
	PtrFLA9	Potri.004G210600	*PtrFLA33*	Potri.019G008400
	PtrFLA10	Potri.009G012100	*PtrFLA34*	Potri.006G200300
	PtrFLA11	Potri.016G088700	*PtrFLA35*	Potri.016G066500
	PtrFLA12	Potri.014G162900	*PtrFLA36*	Potri.001G367900
	PtrFLA13	Potri.006G129200	*PtrFLA37*	Potri.011G093500
	PtrFLA14	Potri.001G320800	*PtrFLA38*	Potri.014G168100
	PtrFLA15	Potri.015G129400	*PtrFLA39*	Potri.014G071700
	PtrFLA16	Potri.012G127900	*PtrFLA40*	Potri.001G037800
	PtrFLA17	Potri.019G121300	*PtrFLA41*	Potri.017G111600
	PtrFLA18	Potri.019G120900	*PtrFLA42*	Potri.008G127500
	PtrFLA19	Potri.019G122800	*PtrFLA43*	Potri.008G128200
	PtrFLA20	Potri.019G123100	*PtrFLA44*	Potri.019G049600
	PtrFLA21	Potri.019G120800	*PtrFLA45*	Potri.T118500
	PtrFLA22	Potri.019G121100	*PtrFLA46*	Potri.013G152200
	PtrFLA23	Potri.019G123000	*PtrFLA47*	Potri.006G174900
	PtrFLA24	Potri.015G013300	*PtrFLA48*	Potri.018G097000
Arabidopsis thaliana	*AtFLA1*	At5g55730	*AtFLA12*	At5g60490
	AtFLA2	At4g12730	*AtFLA13*	At5g44130
	AtFLA3	At2g24450	*AtFLA14*	At3g12660
	AtFLA4	At3g46550	*AtFLA15*	At3g52370
	AtFLA5	At4g31370	*AtFLA16*	At2g35860
	AtFLA6	At2g20520	*AtFLA17*	At5g06390
	AtFLA7	At2g04780	*AtFLA18*	At3g11700
	AtFLA8	At2g45470	*AtFLA19*	At1g15190
	AtFLA9	At1g03870	*AtFLA20*	At5g40940
	AtFLA10	At3g60900	*AtFLA21*	At5g06920
	AtFLA11	At5g03170		

Species	Gene	Gene model	Gene	Gene model
Linum usitatissimum	*LusFLA1*	Lus10000415.g	*LusFLA22*	Lus10019929.g
	LusFLA2	Lus10001178.g	*LusFLA23*	Lus10020158.g
	LusFLA3	Lus10001733.g	*LusFLA24*	Lus10020296.g
	LusFLA4	Lus10001752.g	*LusFLA25*	Lus10021247.g
	LusFLA5	Lus10002273.g	*LusFLA26*	Lus10022517.g
	LusFLA6	Lus10002978.g	*LusFLA27*	Lus10024089.g
	LusFLA7	Lus10002979.g	*LusFLA28*	Lus10026499.g
	LusFLA8	Lus10002984.g	*LusFLA29*	Lus10026957.g
	LusFLA9	Lus10002985.g	*LusFLA30*	Lus10028268.g
	LusFLA10	Lus10006391.g	*LusFLA31*	Lus10029353.g
	LusFLA11	Lus10006399.g	*LusFLA32*	Lus10033651.g
	LusFLA12	Lus10007404.g	*LusFLA33*	Lus10036111.g
	LusFLA13	Lus10009235.g	*LusFLA34*	Lus10036112.g
	LusFLA14	Lus10012344.g	*LusFLA35*	Lus10036113.g
	LusFLA15	Lus10012351.g	*LusFLA36*	Lus10036114.g
	LusFLA16	Lus10013604.g	*LusFLA37*	Lus10036115.g
	LusFLA17	Lus10016194.g	*LusFLA38*	Lus10038004.g
	LusFLA18	Lus10016554.g	*LusFLA39*	Lus10039717.g
	LusFLA19	Lus10016617.g	*LusFLA40*	Lus10040220.g
	LusFLA20	Lus10017696.g	*LusFLA41*	Lus10040821.g
	LusFLA21	Lus10018505.g	*LusFLA42*	Lus10041630.g

2.3. Discussion

In this study, *FLA* genes from three plant species were first identified and submitted to a phylogenetic analysis. An expression analysis of *FLA* genes was further carried out in wood from *P. tremula* x *P. alba*. Two FLA genes with different expression profiles were selected for the production and characterization of RNAi transgenic poplar trees (**Déjardin *et al.*, 2004**; **Lafarguette *et al.*, 2004**). The aim was to understand what differentiate FLAs specifically expressed in tension wood from those continuously expressed in wood. The transgenic trees were analyzed for growth, wood anatomy, wood chemical properties, cellulose ultrastructure and expression of the gene potential partners. The multilevel characterization revealed significant modifications of only cellulose ultrastructure and the expression of *COBL4*, *CESA8* and homologous *FLA* genes.

Poplar has a high number of *FLA* genes

FLA family was predicted in poplar, flax and Arabidopsis genomes. The analysis predicted 48 *FLA* genes in poplar. It is thirteen genes more than it was identified in the recent poplar's genome-wide analysis of FLA family (**Zang *et al.*, 2015**). A reason for the higher number of *FLA*s is likely in the fact that we identified genes based on the presence of only fasciclin domain, while the study of Zhang and colleagues discriminated genes for a presence of fasciclin domain, AGP-like glycosylated regions and N-terminal signal, might leading to a different total number of FLAs. Additionally, from a verification of the missing genes and their positioning within the phylogenetic tree obtained in our analysis, it can be concluded that Zhang and colleagues did not involve in their analysis all potential paralogous genes. Indeed, they state the analysis of "non-redundant FLAs", although it is not clear on which basis were FLAs discriminated for redundancy. Even though a deep structural analysis has not been performed in the present study, we could detect from the phylogenetic clustering a high number of potential paralogous *FLA* genes. The duplication events in the *P. trichocarpa* genome (**Tuskan *et al.*, 2005**) may likely be the cause for both the high number of FLAs predicted in poplar and potential functional redundancy of some of them. However, a thorough structural analysis of FLAs, as the one provided by **Zang *et al.*** (**2015**), is needed to reveal a relationship between predicted genes.

The high number of FLAs is not necessary related to the poplar's biological complexity as perennial species undergoing secondary growth. Almost the equal number of 42 *FLAs* was predicted in the genome of flax (*Linum usitatissimum*), which is an annual plant. Arabidopsis, another annual plant, was predicted to have almost twice less FLAs (21), which is in accordance to the previous phylogenetic analysis (**Johnson *et al.*, 2003**). Therefore, the number of *FLA* genes might be rather explained from the evolutionary history of these species.

FLA proteins differ in structure regarding the number of fasciclin-like domains, the number and position of arabinogalactan regions and the presence of a GPI anchor signal in C terminal. According to their structure, FLAs were classified into 4 groups in Arabidopsis (**Johnson *et al.*, 2003**). We grouped FLAs from poplar, flax and Arabidopsis according to the proposed classification. Both in poplar and flax, FLA genes were predominantly expanded within the group-A. Moreover, one sub-clade of the group-A was formed of 14 FLAs only from poplar. Without a phylogenetic comparison between more species, we can only speculate about the sub-clade's specificity for poplar. Interestingly, recent analysis of the FLA family in eucalyptus (*E. grandis*) revealed that, first, the genome contains only 18 FLAs, and second that, unlike poplar, eucalyptus does not have this specifically expanded sub-clade (**MacMillan *et al.*, 2015**). Some of poplar's genes from the sub-clade may be associated with a specific function in tension wood, since six *FLA* genes were shown to be differentially up-regulated in TW when compared to OW (**Lafarguette *et al.*, 2004**). Raising evidences support the idea that plants contain conserved types of FLAs with one fasciclin domain (mostly members of the group-A), which are specialized for secondary cell wall and stem-specific properties (**MacMillan *al.*, 2015**). It was evidenced from effects in *fla11* and *fla12* mutants of Arabidopsis (**MacMillan *et al.*, 2010**), induced somatic sector analysis of eucalyptus xylem fibers modified for *EgFLA2* and tobacco stems modified for *EgFLA3* (**MacMillan et *al.*, 2015**).

FLA genes from poplar are expressed in wood and some specifically in tension wood

Unpublished RNA sequencing data were used to profile the expression of FLA family in OW, NW and TW of poplar. One quarter of *FLA* genes had the same expression in OW, NW and TW. *FLA15* from the group-A had the highest expression. Among the genes expressed in wood, four belonged to the group-B and three to the group-C, suggesting that wood formation and/or wood properties get determined by structurally different FLAs.

The analysis also revealed that some *FLA* genes are specifically expressed in tension wood. The differentiate expression in tension wood was already reported for ten *FLA* genes (**Déjardin *et al.*, 2004**; **Lafarguette *et al.*, 2004**; **Andersson-Gunneras *et al.*, 2006**). Nine of them were detected in our analysis and the expression of one could not be detected at all, probably due to its low expression and the fact that the analyses were performed in wood of trees grown in a different time period.

FLA genes specifically expressed in TW likely play a function in the G-layer structure. Indeed, in a study performed in my laboratory, FLA1 was localized specifically in the G-layer (not published), while other immunolocalization studies evidenced the presence of AGP structures in the G-layer (**Lafarguette *et al.*, 2004**; **Bowling and Vaughn, 2008**). To differentiate TW-specific FLAs from wood-expressed FLAs, we selected to study FLA1 and FLA14, which have different expression profiles. FLA1 was chosen as a representative of the TW-specific group and FLA14 was chosen as a representative of the group of non-differentially expressed genes between OW and TW (**Lafarguette *et al.*, 2004**).

The analysis performed in different tissues and organs of poplar showed that both *FLA1* and *FLA14* have high expression in xylem (wood) and low expression in apex, leaves, phloem, roots, seeds and germinated seeds. It strongly suggests their importance in secondary cell wall development, which is consistent with the group-A's functional assignment. *FLA14* had 2-fold higher expression than *FLA1*, as detected in both the semi-quantitative and quantitative analyses.

The expression was also examined in TW and OW of stems tilted from 0 to 25 days. While *FLA14* had a uniform expression, the expression of *FLA1* was the highest in TW of stems tilted from 3 to 15 days. It indicates that the expression

of *FLA1* is regulated fast after the stem tilting, as it was previously shown for many other genes - including FLAs (**Azri *et al.*, 2014**).

RNAi technology is not efficient in precise targeting of selected FLAs

For the reason of high number of FLAs and their potential functional redundancy, it is hard to generate single FLA mutants with detectable phenotypes. Indeed, there are only few reported FLA mutants of Arabidopsis. Hence, we chose sequences according to the homology and the expression of the previously published group of 15 *FLA*s in poplar. **Déjardin *et al.*** (**2004**) reported in poplar a cluster of six homologous genes (*FLA1-FLA6*) and four other FLAs (*FLA7-FLA10*) to be differentially expressed in TW in comparison to OW (**Lafarguette *et al.*** (**2004**). Five other FLAs (*FLA11-FLA15*) were reported as non-differentially expressed between TW and OW. To study the TW-specific group, we generated RNAi lines inserting a *FLA1* sequence, which will likely silence the cluster of six *FLA* genes. To study FLAs non-differentially expressed between OW and TW, we inserted a *FLA14* sequence, which likely will silence the expression of *FLA11 to FLA15*. The differentially in TW and continuously in wood expressed *FLA*s were studied in order to understand what differentiate these two groups.

We investigated in one down-regulated FLA line the expression of several *FLA* genes from the both studied groups. The down-regulation of *FLA1* also modified the expression of *FLA4*, *FLA8* and *FLA13*, while the down-regulation of *FLA14* modified the expression of *FLA1*, *FLA4*, *FLA8* and *FLA13*. Several other FLAs also had tendency towards down-regulation, but the high variability between replicates revoked statistical significance. The antisense expression of *FLA6* from poplar also down-regulated the expression of other 9 FLA homologs (**Wang *et al.*, 2015**), confirming difficulties in precise targeting of selected genes.

As an alternative to RNAi technology imposed the CRISPR-CAS9 method as a prominent and highly efficient system in generation of targeted mutations (**Fan *et al.*, 2015**). It would be then reasonable to focus research of FLA function in transgenics obtained with such tool. However, creation of novel strategies still requires information about redundancy of FLAs genes. A wide transcriptomic analysis of the FLA family in FLA RNAi lines is therefore necessary to highlight if the down-regulation of non-targetes FLAs have origin in a co-regulation between

FLAs or only the most homologous genes were altered by unspecific recognition of interference RNA.

Incomplete gene down-regulation in FLA RNAi lines

42% and 57% of screened transgenic lines had modified expression of *FLA1* or *FLA14*, respectively. However, the gene expression was strongly, but not completely silenced in studied FLA lines, as it could be estimated from the semi-quantitative RT-PCR analysis. The incomplete down-regulation is likely related to the size of fragment used for the generation of RNAi, which was around 100 bp long and 2-fold smaller than size of 300 bp recommended by **Helliwell *et al.*** (**2003**). It should be noted that we could not follow the recommendation because it would increase a possibility of down-regulation of non-targeted FLAs.

Down-regulation of *FLA*s alters cellulose ultrastructure in tension wood

The effects were studied in two down-regulated FLA1 lines and one down-regulated FLA14 line. Although the initial idea was to characterize two down-regulated transgenic lines, additional verification of FLA14 T1-line did not confirm the gene silencing observed after the initial screening. One reason might be in different time frames in which plants for screening and characterization were grown, or likely because the screening analysis was performed on only one tree. In addition, we included in our analysis one non-down-regulated transgenic line to show that potential effects in down-regulated lines originate from the modification of gene expression.

The gene down-regulation did not affect the growth of FLA1 transgenic lines in the greenhouse conditions, neither did it alter wood anatomy or cell wall development, as it could be determined with the used techniques. The same case was for transgenic poplars, which expressed antisense sequence of FLA6 (**Wang *et al.*, 2015**).

A significant increase in height was detected in two FLA14 lines: one down-regulated and one selected as non-down-regulated. Possible explanations for the surprising effect in one unsilenced transgenic are: a) the height of a tree results from a long term gene expression, which may be different at the moment of sampling and during the whole growth period b) the gene expression was verified

only in xylem and it might be down-regulated in other parts of the tree, c) the T-DNA insertion in another gene can modify tree growth. The latter seems as the most plausible explanation since the down-regulated gene has the highest expression in xylem and its down-regulation was verified in three biological replicates. Certainly, it would be of interest to verify T-DNA insertion site in lines affected for growth.

From the PCA analysis of MIR spectra, which gives a good overview on wood chemical properties, slight modifications in OW could have been observed in FLA1 down-regulated lines when compared to WT and the non-down-regulated line. A slightly stronger difference was detected in OW and TW of down-regulated FLA14 line. Altogether, the differences were mild and could not firmly distinguish down-regulated transgenic lines from their wild-types and non-down-regulated lines.

Further ultrastructural analysis of wood revealed the more significant modifications in transgenics: FLA1 lines had modified cellulose crystalline structure in two lines and cellulose microfibril angle in one line, while FLA14 line had modified crystallinity. In both cases, the modification could be detected only in TW. The method of X-ray diffractometry is robust and fast, but indirect in measurements of crystallinity and microfibril angle. Tension wood has highly crystalline structure and it is probably easier to detect modifications of such structure with the used method. From the other side, angle of cellulose microfibrils is in general low in TW. The method overestimates such angles, which is the reason why we detected in TW angle of around 8 degrees. The increase of angle detected in only one FLA1 line was very slight and might not give a real image.

However, cellulose ultrastructure in FLA transgenics was evidently altered for crystalline properties in TW. Function of FLAs was already correlated with cellulose structure in the microfibril angle-modified Arabidopsis *fla11/fla12* mutants (**MacMillan *et al.*, 2010**) and transgenic eucalyptus systems (**MacMillan *et al.*, 2015**). Owing to the altered cellulose structure in transgenics, it would be interesting to investigate potential modifications of cellulose content, which were reported in the previously specified transgenics. Certainly, mechanical properties firmly related to cellulose structure should be also investigated with measures of stem modulus of elasticity.

We used a molecular approach to investigate in one down-regulated line the expression of genes reported to have function in cellulose synthesis and structure. Both FLA1 and FLA14 transgenic lines had reduced expression of *COBL4* gene

encoding COBRA protein and *CESA8* gene encoding one of the proteins of the cellulose synthase complex. In Arabidopsis, *COBL4* and *CESA8* genes co-expressed with *FLA11* and *FLA12*, which are homologous to poplar's *FLA11* and *FLA13* (**Persson *et al.*, 2005**). The down-regulation of *COBL4* in FLA transgenic lines is significant in a way that COBRA has function in regulation of cellulose crystallinity (**Liu *et al.*, 2013b**), which is the property modified in our FLA transgenics.

Towards a function of FLA in tension wood

The results of expression profiling and alterations of cellulose ultrastructure presented in this thesis suggest an importance of FLAs for wood properties. From the expressional analysis in crystalline cellulose-modified FLA transgenics, function of FLA was brought in a relation with *COBL4* gene encoding COBRA protein. Function of one COBRA was already assigned to control of cellulose crystallinity in cell walls of rice (**Liu *et al.*, 2013b**). COBL4 and FLA(s) might therefore have, among other proteins, cooperative function in control of cellulose crystallinity in the G-layer. However, we were not able to determine which *FLA* gene(s) may perform the function, since the down-regulation of TW-expressed group of FLAs also down-regulated wood-expressed group of FLAs and reversed. Taking into account the non-differentiate expression between OW and TW of *COBL4* and some FLAs, their function might be important for crystallinity of secondary cell wall in general. Another prominent candidate for a cooperation with FLAs is chitinase-like protein encoded by *CTL2*, as the study of CTL2 transgenic lines performed in the frame of this thesis showed that CTL2 regulates cellulose crystallinity in TW. Interestingly, CTL2 had tendency toward down-regulation in both FLA1 and FLA14 transgenic lines.

From the phenotypes of Arabidopsis mutants and eucalyptus transgenics, several FLAs from the group-A were brought in a relation with the cellulose microfibril angle (**MacMillan *et al.*, 2010**; **MacMillan *et al.*, 2015**). We could also observe a slight increase in TW microfibril angle in one RNAi-FLA1 transgenic line. Since the angle is highly oriented in the G-layer, it would be tempting to speculate that FLAs specifically expressed in TW would regulate this property. Interestingly, function of a COBRA protein from Arabidopsis was assigned to control of the

microfibril angle (**Roudier *et al.*, 2005**). It is then possible that FLAs and COBRA have multiple function in both orienting the angle and controlling the crystallinity.

AGPs are highly hydrophilic molecules (**Showalter, 2001**) and it would be possible that FLAs secreted in the G-layer, in interaction with other matrix components, have function in formation of structures responsible for a gel-like properties. It would be therefore interesting to measure wood mesoporosity in FLA transgenics, as performed by Chang and colleagues (2015).
In addition, investigations with, for example, fractioned immuno-chromatography (**Cornuault *et al.*, 2014**), would be of a great interest in revealing co-localization of FLAs with other structures detected in the G-layer as RG-I pectins, glucuronoxylans and glucomannans (**Guedes, 2013**).
Altogether, FLAs likely play a diverse function in the G-layer. As proposed in the text above, further investigations are necessary to approach a precise function and targets of FLAs, particularly in revealing a function of TW-specific FLAs.

3. BETA-GALACTOSIDASE

Beta-galactosidase activity was localized and quantified in TW and OW. In search for a *BGAL* gene potentially responsible for the higher activity detected in TW, BGAL family from poplar was compared in a phylogenetic analysis with flax and Arabidopsis, and analyzed for expression in OW and TW. One gene specifically expressed in TW, was further studied in the expression analysis and from characterization of *BGAL7* transgenic RNAi lines.

3.1. Beta-galactosidase activity

3.1.1. Localization with X-Gal substrate

In order to examine beta-galactosidase (BGAL) activity, cross-sections of poplar stems tilted for 3 months were incubated with a synthetic substrate X-Gal (indoxyl galactoside). When catalyzed by a beta-galactosidase, X-Gal yields galactose and 5-bromo-4-chloro-3-hydroxyindole. Once dimerized and oxidized, the indole compound turns to a blue insoluble product. The blue staining can be visualized on stem cross-sections and is an indicator of beta-galactosidase activity. In parallel with the X-Gal staining, stem cuts were stained with Safranin/Alcian blue to determine wood zones (TW, OW and NW) for comparison with the localization of BGAL activity (**Figure III-1**).

After an overnight incubation with X-Gal substrate, the strong blue staining was localized only in TW (**Figure III-1**). When observed with larger objectives, staining could be also detected in rays across the complete cross-section (data not shown). The most intensive blue staining was detected in newly deposited mature TW, while it progressively weakened in older wood close to zone of NW.

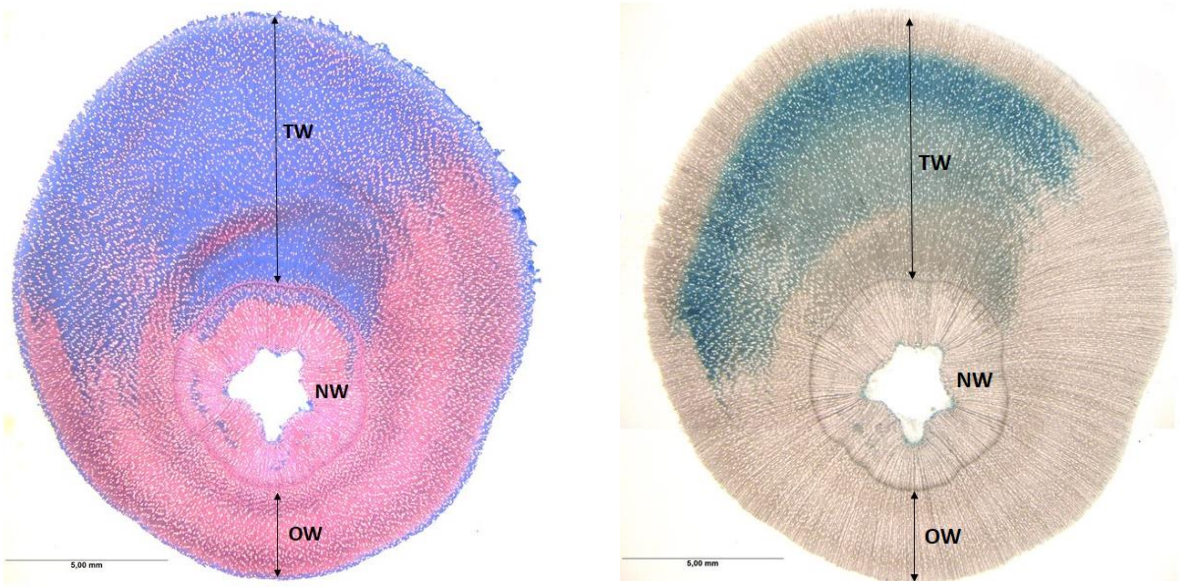

A) B)

Figure III-1. Beta-galactosidase activity in wood

A) Stem cross-section stained with safranin/alcian blue to determine wood zones
B) Blue staining localized on stem cross-section as an indicator of beta-galactosidase activity in a consequence of reaction with X-Gal substrate

TW= tension wood; OW=opposite wood; NW= normal wood. Bar= 5 mm

The figure shows one representative tree of 3 biological replicates.

3.1.2. Quantification with MUG substrate

Reaction with MUG substrate is an assay to quantify beta-galactosidase activity. It is based on enzymatic reaction between beta-galactosidase and artificial substrate MUG (4-Methylumbelliferyl-D-Galactopyranoside). When proceeded by a beta-galactosidase, the substrate releases fluorescent compound MU (4-Methylumbelliferone), which can be detected spectrophotometrically and quantified from MU standards. The reaction was performed with proteins extracted from OW and TW.

BGAL activity could be detected in both OW and TW (**Fig. III-2**). The concentration of released MU substrate in TW was twice the concentration in OW.

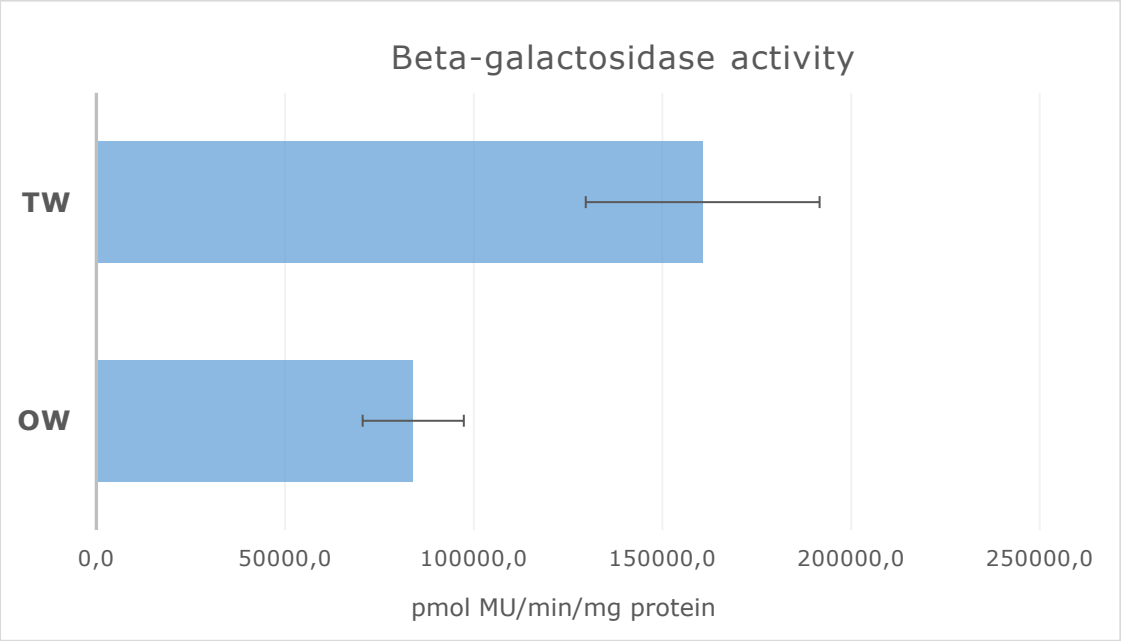

Figure III-2. The concentration of fluorescent MU (4-Methylumbelliferone) released from MUG (4-Methylumbelliferyl-D-Galactopyranoside) substrate in a reaction with proteins extracted from opposite wood (OW) and tension wood (TW). The concentration is a measure of beta-galactosidase activity. Bar represent standard error, where: n=3 biological replicates (OW), n=2 biological replicates (TW).

3.2. BGAL family

3.2.1. Phylogenetic analysis

Based on the presence of conserved domains GH35 (Pf01301) and GH42 (Pf02449), BGAL family in poplar (*Populus trichocarpa*) was predicted to have 23 gene members. BGAL family was compared in a phylogenetic analysis with BGAL families from Arabidopsis and flax constituted of 18 and 43 gene members, respectively. BGALs from all three species were annotated and classified into 8 groups according to **Hobson and Deyholos** (**2013**) (**Fig. III-3**). For the analyzed species, either one BGAL was assigned to group-A3, which was then omitted from the phylogenetic analysis. The most of BGALs were assigned to group-A1, which was constituted of 6 poplar, 6 Arabidopsis and 14 flax members. Group-D was the most divergent group of BGALs.

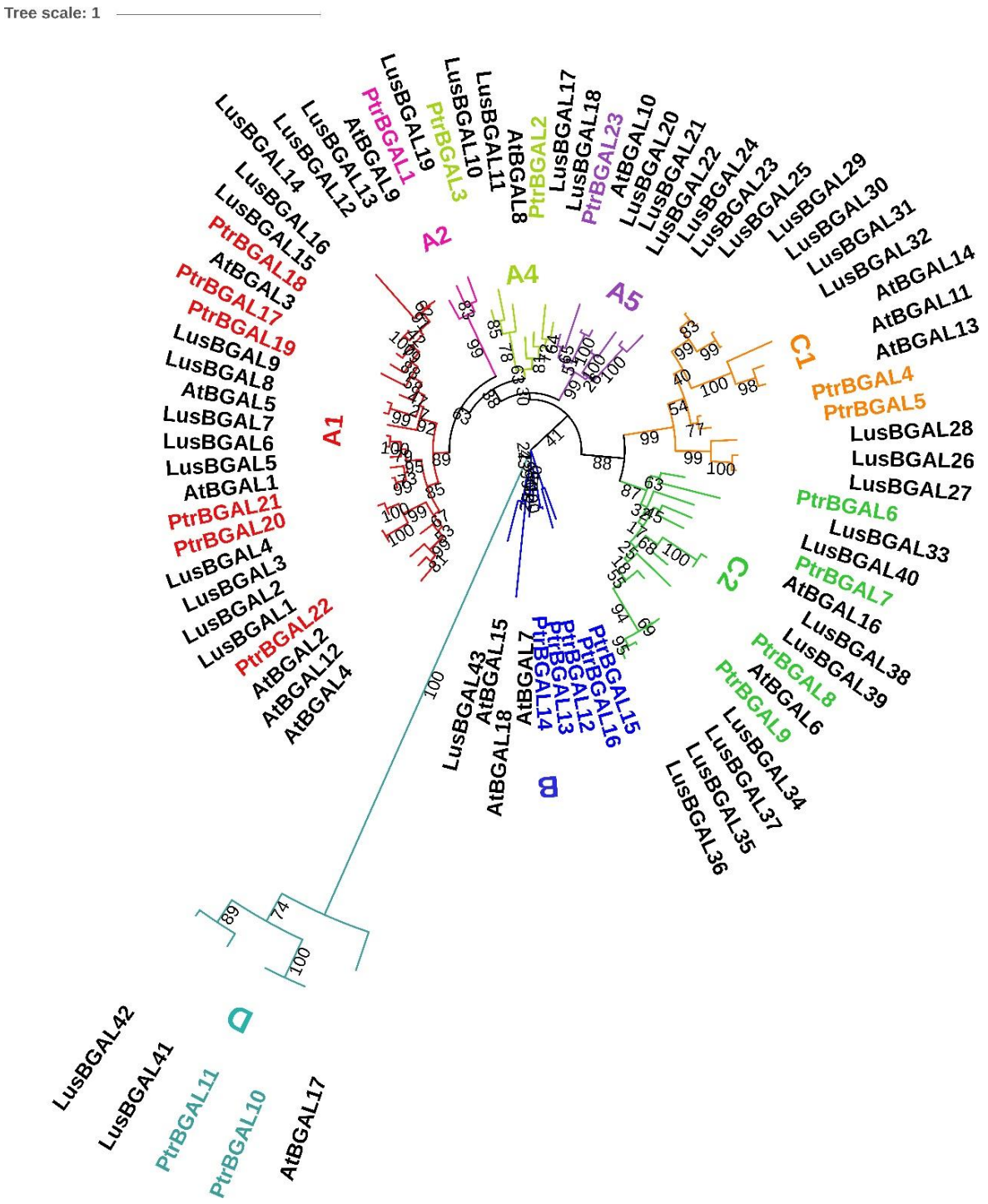

Figure III-3. Phylogenetic tree of BGAL protein family predicted from genomes of *Arabidopsis thaliana* (At), *Linum usitatissimum* (Lus) and *Populus trichocarpa* (Ptr). The members were attributed to groups according to Hobson and Deyholos (2013). The evolutionary history was inferred by using the Maximum Likelihood method based on the JTT matrix-based model in the analysis conducted in MEGA7 software.

3.2.2. Semi-quantitative expression analysis in OW and TW

BGAL family from poplar was profiled for expression in OW and TW in semi-quantitative PCR analysis. cDNA was amplified in 35 amplification cycles in order to increase a possibility of detection of amplification signal. The uniform amplification signal of *18S* gene confirmed equal loading of RNA in reverse-transcription reaction (**Figure III-4**). The amplification signal was mostly consistent between biological replicates.

Out of 23 BGALs, the amplification signal was detected for 17 genes, while it could not be detected for 6 genes (*BGAL 4, BGAL6, BGAL12, BGAL13, BGAL14, BGAL16*). Out of the expressed genes, *BGAL3 and BGAL8* had faint amplification signal and could not be compared between tissues. For 14 genes (*BGAL 1, 2, 5, 9, 10, 11, 15, 17, 18, 19, 20, 21, 22, 23*), the amplification signal did not vary between TW and OW. Only one gene (*BGAL7*) had differentiate expression between TW and OW: amplification signal of *BGAL7* was detected only in TW, while the signal could not be detected in OW.

The genes for which the amplification signal was not detected were verified for their corresponding Expressed Sequence Tags (ESTs) in GenBank (NCBI). For two genes (*BGAL4* and *BGAL14*), no ESTs were found and were considered as pseudogenes. A decrease of annealing temperature of primers for remaining 3 genes (*BGAL6*, *BGAL12*, *BGAL13*) did not result in detection of amplification signal (data not shown).

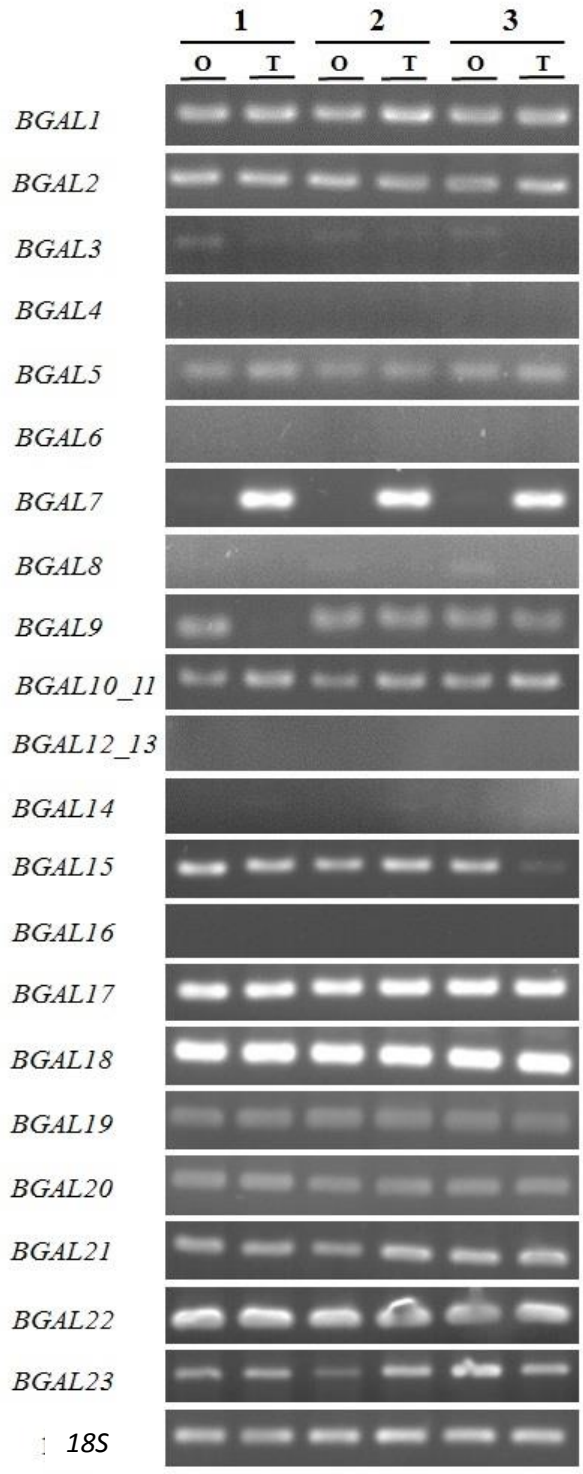

Figure III-4. Expression of *BGAL* gene family in opposite (O) and tension (T) wood of poplar. 1, 2, 3: tree biological replicates. *18S*: RNA loading control in RT-PCR reaction.

3.2.3. Quantitative expression analysis in NW, OW and TW

The expression of BGAL family from poplar was examined from RNA sequencing data of NW, OW and TW libraries. Results were consistent with the semi-quantitative analysis, since the expression was detected for 17 out of 23 genes (**Fig. III-5**). Very strong expression in all wood types had *BGAL1*, *BGAL18*, *BGAL20* and *BGAL22*. Consistent with the semi-quantitative analysis, only *BGAL7* showed significant differentiate expression in TW. *BGAL7* had lower expression than genes highly expressed in wood.

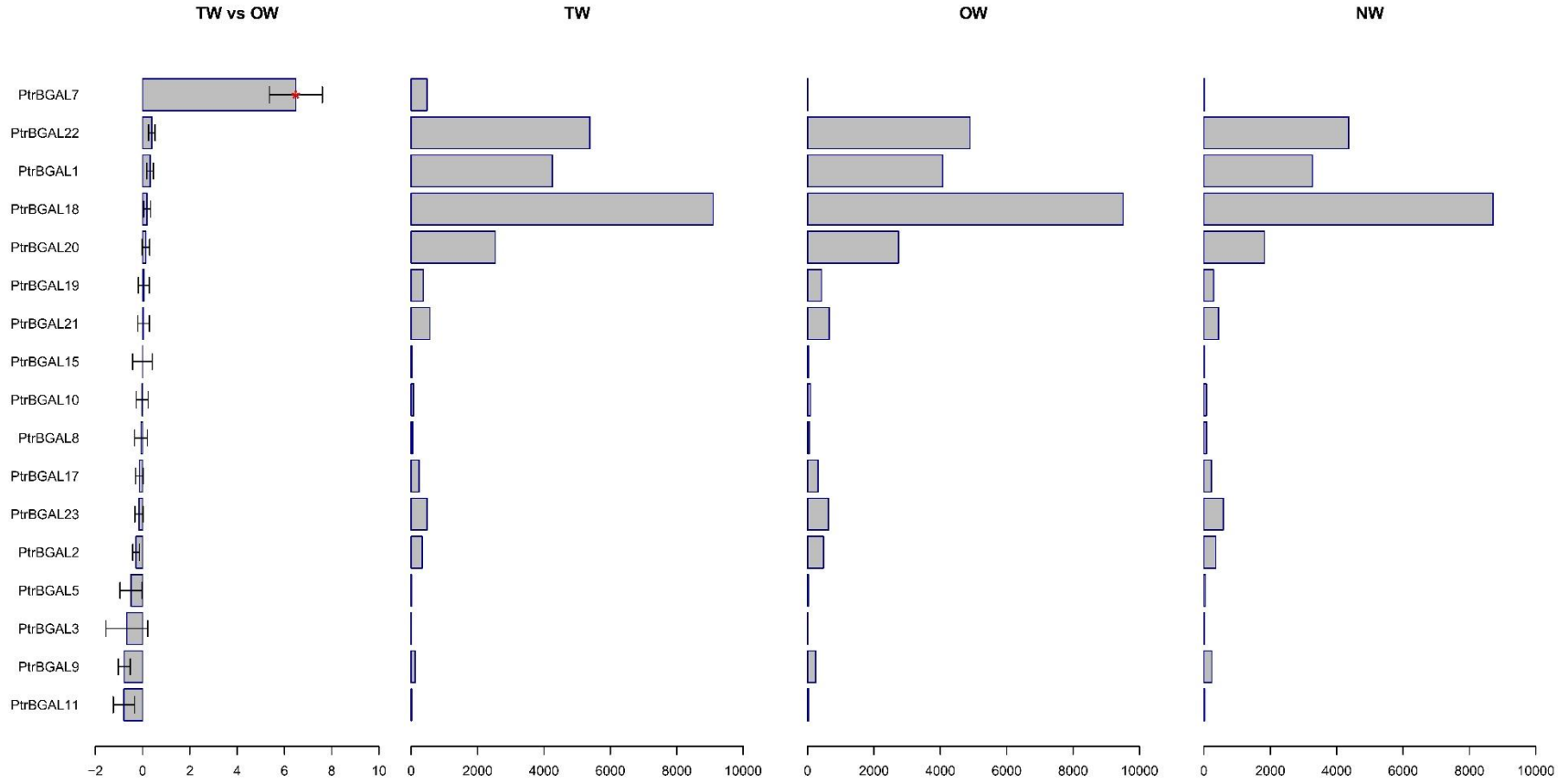

Figure III-5. Quantitative expression of *BGAL* family in tension wood (TW), opposite wood (OW) and normal wood (NW). First column shows relative log2 ratio of gene expression in TW and OW. The ratio was calculated for statistical significance from t-test, where: * p-value 0.01-0.05. Bars represent standard errors. The remaining columns show absolute gene expression in TW, OW and NW.

3.3. Characterization of BGAL7

As the sole member of *BGAL* gene family expressed differentially in TW, we chose to study *BGAL7* as a gene potentially responsible for the higher beta-galactosidase activity detected in TW. *BGAL7* was profiled for the expression in different poplar tissues/organs and wood from stems tilted for different time duration. Transgenic BGAL7 RNAi lines were characterized for growth, chemical properties and cellulose ultrastructure.

3.3.1. Expression profile of *BGAL7*

Tissues and organs

The expression of *BGAL7* was high in xylem and very low in other tissues and organs (**Fig. III-6**). Expression close to zero was detected in seeds and germinated seeds. Between other tested tissues, *BGAL7* had higher expression in phloem than in apex or leaves, though at very low levels.

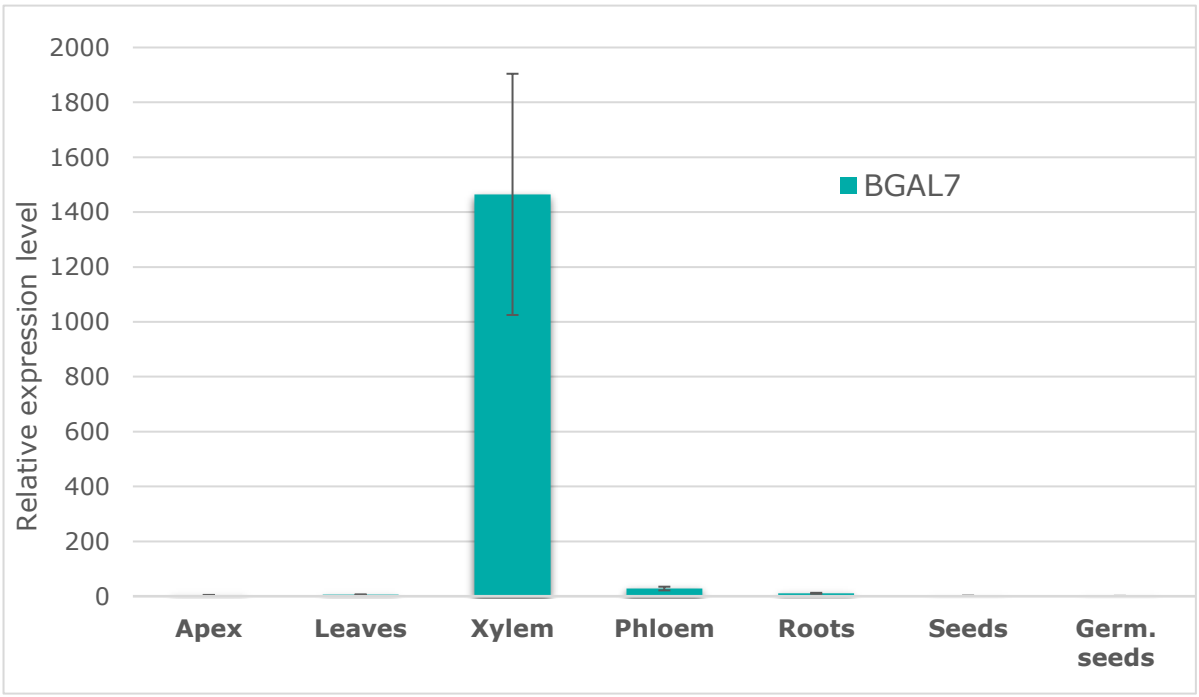

Figure III-6. Relative quantitative expression level of *BGAL7* in various plant tissues and organs of poplar. Bars represent standard error, where: n= 3 technical repetitions of different pulls from 1 tree (seeds/germ.seeds) or 6 trees (for all other tissues/organs). Germ. seeds= germinated seeds.

OW and TW from stems of different tilting duration

BGAL7 expression was analyzed in OW and TW collected from stems of two trees tilted for 0, 1, 3, 7, 14 and 25 days. Samples from day 0 were collected from straight stem on two sides corresponding to TW and OW of tilted stems.

18S amplification signal was consistent between all samples (**Fig. III-7**). A signal could not be detected in OW in any of wood samples. The amplification signal was detected in TW from stems tilted for 3, 7, 14 and 25 days, with slight variations between biological replicates. Intensity of signal was strongest in TW of stems tilted for 7 and 14 days. Progressive decrease in expression level was observed in TW of stems tilted for 25 days.

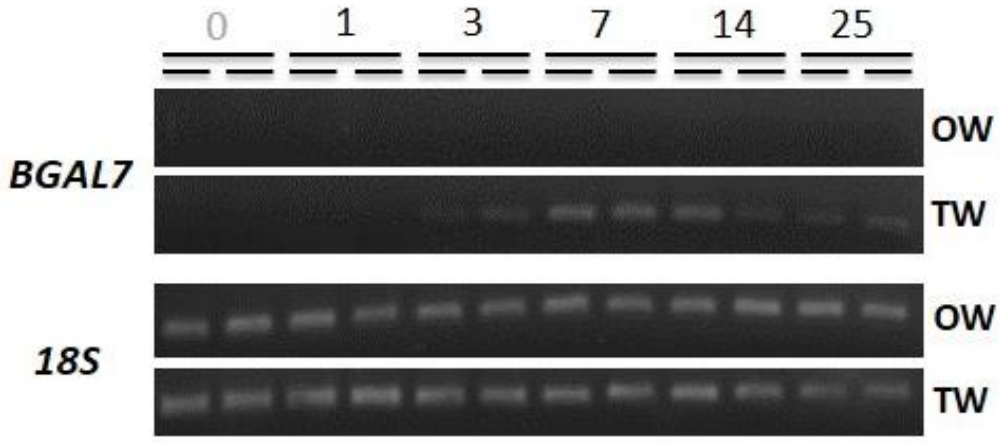

Figure III-7. Expression of *BGAL7* in opposite (OW) and tension (TW) wood from poplar stems tilted for 1, 3, 7, 14 and 25 days. TW and OW from day 0 correspond to the respective upper and lower xylem of straight stem sampled prior tilting. Analysis was for each tilting period performed in 2 biological replicates (marked with dashes). *18S* was used as a control of equal RNA loading in RT-PCR reaction.

3.3.2. Production of BGAL7 transgenic lines

For the expression of hairpin interference RNA, we used 94 bp-long BGAL7-specific sequence inserted into pHellsgate 8 vector (**Helliwell *et al.*, 2002**). The transformation raised 8 transgenic lines, out of which 4 were screened and 2 were modified for the expression of *BGAL7*. Transgenic lines T1, T2 and T3 with 3 respective tree replicates were chosen for further characterization.

In wild-type and transgenic lines, *BGAL7* amplification signal was stronger in TW than in OW (**Figure III-8**). T1 and T2 transgenic lines were down-regulated in comparison to the gene expression in TW of wild-type. The amplification signal in TW of T3 line was slightly weaker than in wild-type, but stronger than signal in T1 and T2 lines.

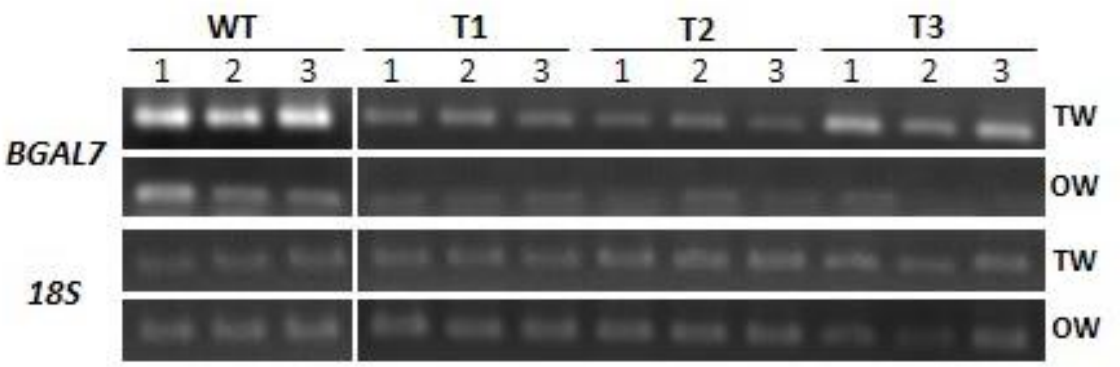

Figure III-8. Semi-quantitative expression of *BGAL7* in opposite (OW) and tension (TW) wood of wild-type (WT) and BGAL7 transgenic lines T1, T2 and T3. Analysis was performed in 3 biological replicates (1, 2, 3). *18S* gene was amplified as a control of equal RNA loading in RT-PCR reaction.

3.3.3. Traits of BGAL7 transgenic lines

Growth phenotype

Greenhouse-grown trees were measured for height and diameter after 4 months of growth. BGAL7 transgenic lines T1 and T3 showed tendency toward decrease and T2 line towards increase in height (**Figure III-9**). However, the difference was not staitistically significant. T2 line had significantly larger diameter than wild-type, while T1 and T3 lines were the same as wild-type.

Transgenic plants did not show any phenotype during growth in the greenhouse.

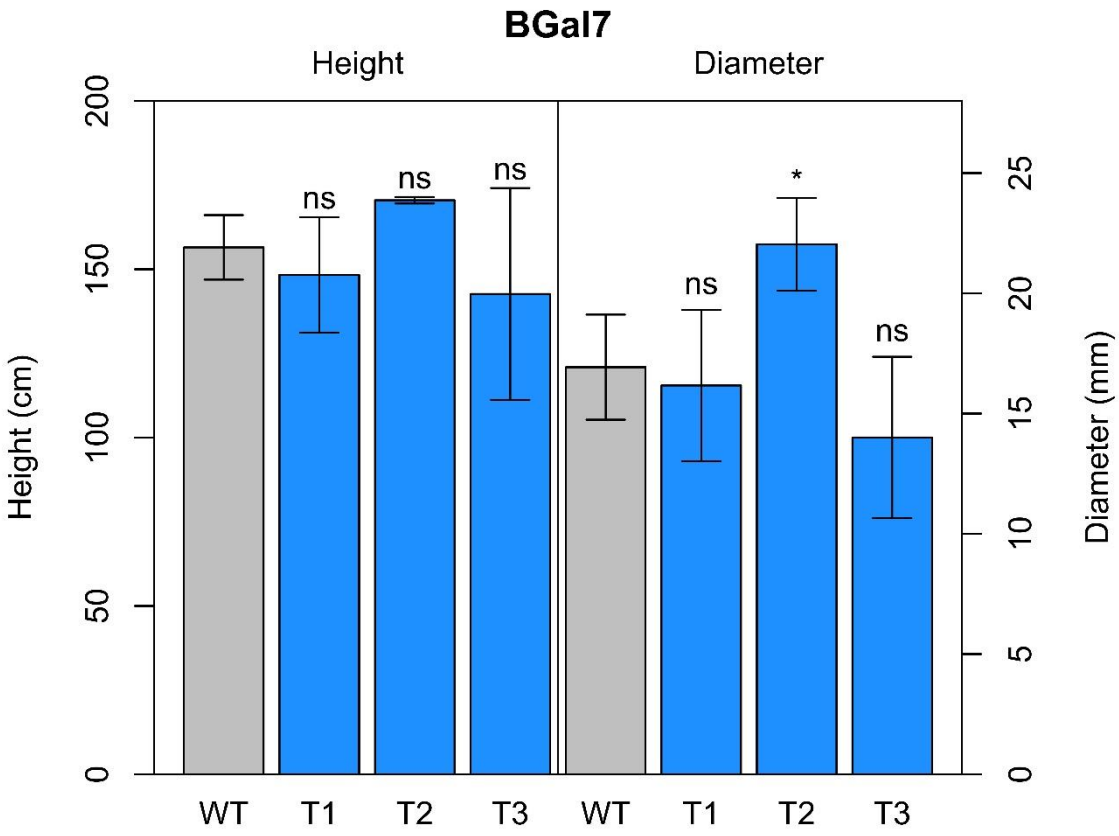

Figure III-9. Tree height and diameter of wild-type (WT) and BGAL transgenic lines T1, T2 and T3 grown in greenhouse conditions for 4 months. Bars represent standard errors, where: n=6 biological replicates (wild-type), n=3 biological replicates (T1, T2, T3). Statistically significant difference between wild-type and transgenic lines was calculated from Welch's t-test, where: * p-value 0.01-0.05, ns= non-significant.

Wood FT-MIR spectra

FT-MIR spectra of OW and TW from wild-type and transgenic BGAL7 lines were normalized and proceeded to principle component analysis (PCA). In all transgenic lines and wild-types, OW and TW were separated on the first axis (**Figure III-10**). For both wood types, there were no variances between wild type and transgenic lines T1, T2 and T3.

Cellulose ultrastructure

There was a strong correlation between cellulose microfibril angle and cellulose organization, since the organization of cellulose was higher when microfibril angle was lower and reverse (**Figure III-11**). There was no difference in microfibril angle or cellulose organization between transgenic lines and wild-type, either in OW or TW.

Other analyses

X-Gal staining of cross-sections of BGAL7 transgenic stems was not different from staining in wild-type (data not shown). The labelling with LM5 antibody, which recognizes β-(1,4)-galactan structure and RU1 antibody, which recognizes structure of RG-I backbone was the same in TW fibers of transgenic BGAL7 lines and in wild-type (data not shown).

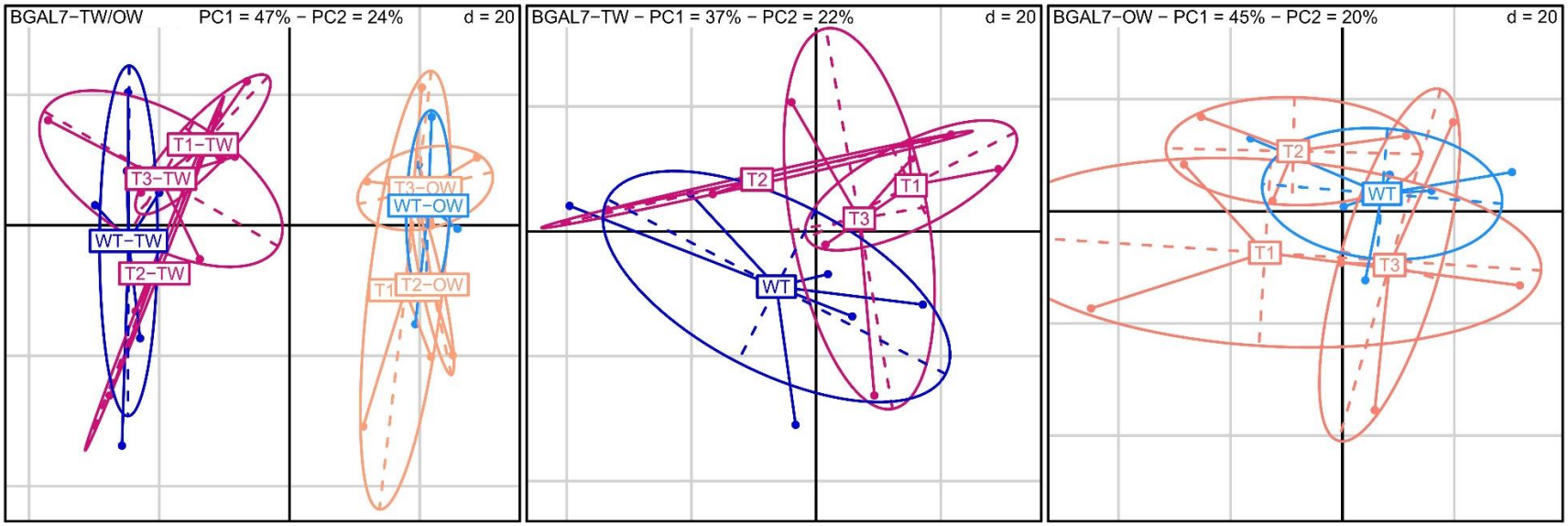

Figure III-10. Graph of principal component analysis of FT-MIR spectra of opposite (OW) and tension (TW) wood from wild-type (WT) and **BGAL7 transgenic lines T1, T2 and T3**. Number of biological replicates: n=6 (WT), n=3 (transgenic lines).

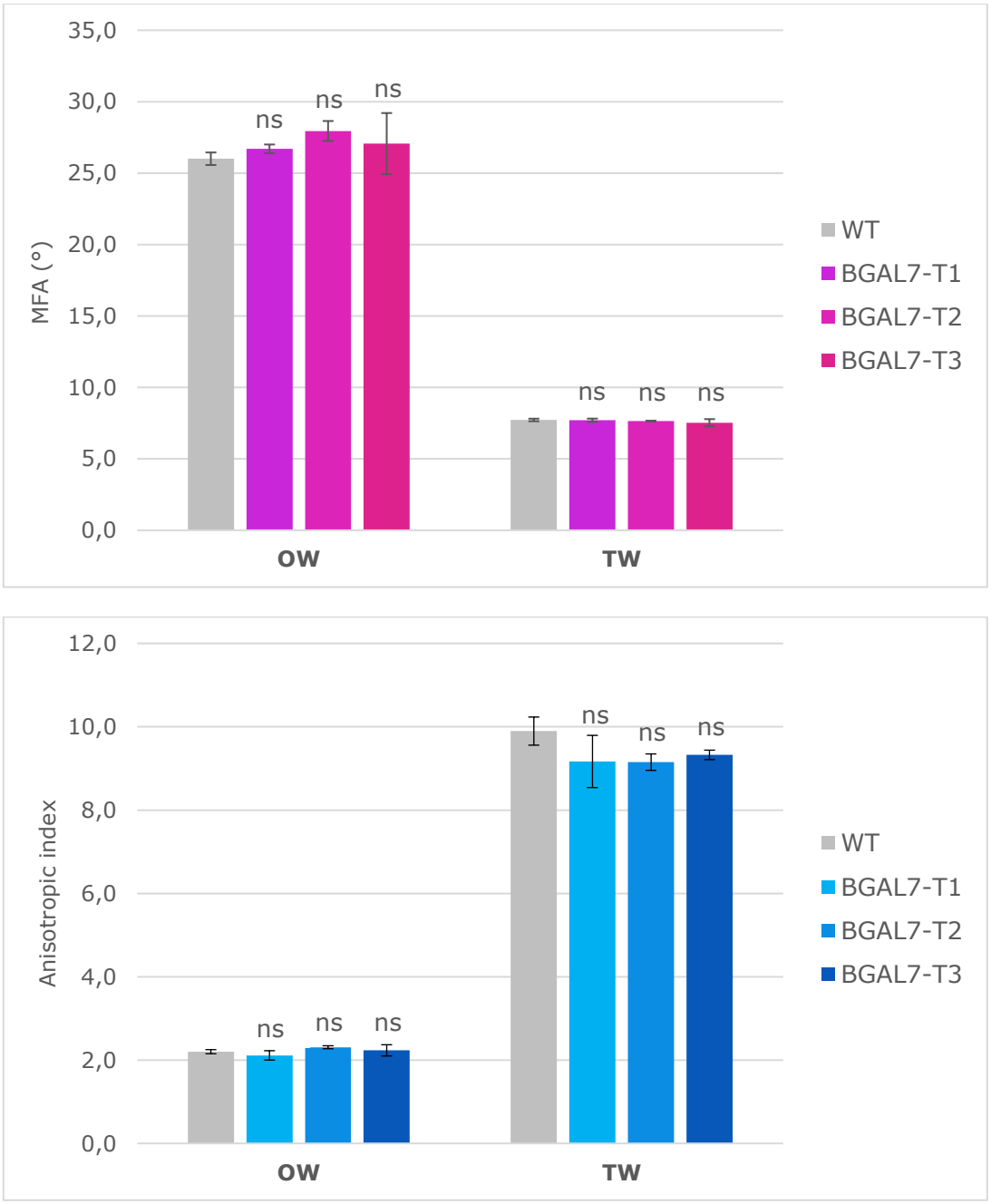

Figure III-11. Cellulose microfibril angle and anisotropic index of cellulose crystallinity estimated from X-ray diffraction in opposite wood (OW) and tension wood (TW) of wild-type (WT) and BGAL7 transgenic lines T1, T2 and T3. Bars represent standard errors, where: n=6 (OW-WT), n=5 (TW-WT), n=3 (OW and TW of transgenic lines). The statistically significant difference between wild-type and transgenic lines was calculated from Welch's t-test, where: *** p-value 0-0.001, ** p-value 0.001-0.01, * p-value 0.01-0.05, ns= non-significant.

Annex III-1. Predicted genes of *BGAL* family in poplar, Arabidopsis and flax

Species	Gene	Gene model	Gene	Gene model
Populus trichocarpa	*PtrBGAL1*	Potri.017G057900	*PtrBGAL13*	Potri.001G025700
	PtrBGAL2	Potri.009G012400	*PtrBGAL14*	Potri.001G025800
	PtrBGAL3	Potri.011G044300	*PtrBGAL15*	Potri.006G139100
	PtrBGAL4	Potri.009G134400	*PtrBGAL16*	Potri.018G062800
	PtrBGAL5	Potri.004G174800	*PtrBGAL17*	Potri.004G159800
	PtrBGAL6	Potri.013G105100	*PtrBGAL18*	Potri.007G018100
	PtrBGAL7	Potri.002G080700	*PtrBGAL19*	Potri.005G232600
	PtrBGAL8	Potri.005G180600	*PtrBGAL20*	Potri.003G038500
	PtrBGAL9	Potri.005G069200	*PtrBGAL21*	Potri.001G200400
	PtrBGAL10	Potri.003G040000	*PtrBGAL22*	Potri.006G144500
	PtrBGAL11	Potri.003G037000	*PtrBGAL23*	Potri.007G099800
	PtrBGAL12	Potri.T154000		
Arabidopsis thaliana	*AtBGAL01*	At3G13750	*AtBGAL10*	At5G63810
	AtBGAL02	At3G52840	*AtBGAL11*	At4G35010
	AtBGAL03	At4G36360	*AtBGAL12*	At4G26140
	AtBGAL04	At5G56870	*AtBGAL13*	At2G16730
	AtBGAL05	At1G45130	*AtBGAL14*	At4G38590
	AtBGAL06	At5G63800	*AtBGAL15*	At1G31740
	AtBGAL07	At5G20710	*AtBGAL16*	At1G77410
	AtBGAL08	At2G28470	*AtBGAL17*	At1G72990
	AtBGAL09	At2G32810	*AtBGAL18*	At2G04060
Linum usitatissimum	*LusBGAL1*	Lus10008974.g	*LusBGAL23*	Lus10025110.g
	LusBGAL2	Lus10028848.g	*LusBGAL24*	Lus10023977.g
	LusBGAL3	Lus10006009.g	*LusBGAL25*	Lus10023974.g
	LusBGAL4	Lus10040557.g	*LusBGAL26*	Lus10005070.g
	LusBGAL5	Lus10000701.g	*LusBGAL27*	Lus10027843.g
	LusBGAL6	Lus10015625.g	*LusBGAL28*	Lus10014126.g
	LusBGAL7	Lus10037644.g	*LusBGAL29*	Lus10005071.g
	LusBGAL8	Lus10000803.g	*LusBGAL30*	Lus10027844.g
	LusBGAL9	Lus10024292.g	*LusBGAL31*	Lus10014125.g
	LusBGAL10	Lus10006733.g	*LusBGAL32*	Lus10019784.g
	LusBGAL11	Lus10011237.g	*LusBGAL33*	Lus10008259.g
	LusBGAL12	Lus10014278.g	*LusBGAL34*	Lus10020875.g
	LusBGAL13	Lus10025980.g	*LusBGAL35*	Lus10020877.g
	LusBGAL14	Lus10020968.g	*LusBGAL36*	Lus10033500.g
	LusBGAL15	Lus10028348.g	*LusBGAL37*	Lus10033502.g
	LusBGAL16	Lus10041798.g	*LusBGAL38*	Lus10018138.g
	LusBGAL17	Lus10000271.g	*LusBGAL39*	Lus10028538.g
	LusBGAL18	Lus10036109.g	*LusBGAL40*	Lus10033427.g
	LusBGAL19	Lus10016655.g	*LusBGAL41*	Lus10015616.g
	LusBGAL20	Lus10003343.g	*LusBGAL42*	Lus10037634.g
	LusBGAL21	Lus10022645.g	*LusBGAL43*	Lus10043422.g
	LusBGAL22	Lus10025108.g		

3.4. Discussion

Beta-galactosidase was studied as a molecular player potentially responsible for the modifications of RG-I pectin structure, detected as decrease in immunosignal of β-(1,4)-galactan side chains and increase in immunosignal of RG-I backbone during the G-layer maturation (**Guedes, 2013**). The present study aimed to test if the removal of the β-(1,4)-galactan side chains by a beta-galactosidase is required for development of TW. Based on the higher BGAL activity in TW, we could conclude that activity of BGAL is important for tension wood formation. To validate our hypothesis, we selected *BGAL7* gene specifically expressed in TW to test if the gene silencing will modify TW properties. In BGAL7 RNAi lines, we could not observe any effect on the BGAL activity, wood chemical properties, G-layer formation or labelling of antibodies recognizing RG-I structure. The fact that we could not validate our hypothesis is probably related with the targeting of wrong gene. At the end of following discussion, several other *BGALs* are proposed as candidates for a novel study.

Beta-galactosidase has higher activity in TW than in OW

Beta-galactosidase activity was localized on stem cross-sections as a blue staining resulted from the enzyme activity towards an artificial X-Gal substrate consisted of galactose β-(1,3)-linked to substituted indole. The activity was detected only in TW, with the exception for rays, which were stained in both OW and TW. It is in accordance with the increased BGAL activity in the cell walls of TW tested with Gal-resorufin substrate (**Gorshkova *et al.*, 2015**). The analysis with X-Gal showed that the strong activity started from the zone of mature TW fibers. Moreover, the BGAL activity in the G-fibers co-localized with the disappearance of epitopes of β-1,4-galactan side chains at the point of fiber maturation (data not shown). The activity progressively decreased in more mature wood, which is likely related with the loss of protein's activity in dead cells as are xylem fibers. Although the staining does not allow high-resolution microscopic observations, we could assume that the staining originates from the G-layer, which makes majority of the cell wall.

We in addition quantified the BGAL activity in OW and TW with substrate which contains galactopyranoside β-(1,7)-linked to methylumbelliferyl. The activity in TW was double of the activity in OW. Surprisingly, the activity in OW was not as low as it would be expected from localization of BGAL activity on stained cross-

sections. One reason might be that the activity originates from rays, which were the only cells stained in OW and even that the most of the BGAL activity in wood originates from rays. The rays store starch during the winter and the metabolism of starch gets initiated with the restart of cambial activity at spring time. Since we performed tests in plants grown during summer in the middle of growing season, it is hard to believe that involvement in starch metabolism in wood reactivation would be a primary function of BGAL activity in rays. The rays get extended from phloem to xylem crossing the cambial zone. A recent analysis showed that gravitropic signal gets perceived in the endodermal cells tightly connected with phloem (**Gerttula *et al.*, 2015**). It would be then plausible that BGALs gets involved in a signaling pathway that takes place in rays.

Lead by the preferential activity of BGAL in rays, the difference in the activity between TW and OW would then originate only from the activity in the G-layer. However, beta-galactosidase is known as a cell wall remodeling enzyme and it should not be excluded that a mild activity is also present in PCW and/or SCW where it could not be detected with the X-Gal staining.

Only one *BGAL* gene is specifically expressed in tension wood

Further research focused on the semi-quantitative and quantitative transcriptomic analyses of BGAL family in order to find (a) candidate gene(s) responsible for the high activity in TW hypothesized to be linked with the TW properties. Most of *BGAL* genes (17 out of 23) were expressed in both TW and OW. However, as detected in the quantitative analysis, only 4 genes had notably high expression in wood and might be considered as prominent candidates for the activity in rays observed across the whole stem cross-section. Certainly, it should not be discarded that some other less expressed genes perform this activity of yet undetermined function.

Only one gene, *BGAL7*, was expressed specifically in TW. Moreover, its expression increased rapidly after stem tilting (3 days) and decreased after a longer tilting period (25 days). It suggest that the expression of *BGAL7* is regulated rapidly after tilting, which indicates its function during the formation of tension wood.

Down-regulation of *BGAL7* does not alter tension wood properties

The selected *BGAL7* is not a cell wall protein and its modification did not cause an effect on tension wood properties. Later bioinformatic analysis predicted that BGAL7 gets secreted in nucleus, peroxisome and chloroplast rather than to the cell wall (data not shown). Therefore, it is more likely that it plays an enzymatic function in metabolic or signaling pathways or modification of cell wall precursors. A significant effect on tension wood properties could not be detected in neither one transgenic lines modified for the expression of *BGAL7*. However, it should be noted that the gene modification was weak and might not be strong enough to induce some more serious effects.

Stem diameter of one transgenic line (T2) was larger than of wild-type. Trees of the same transgenic line were also higher, but due to the variability of wild-types, the difference was not statistically significant. The same trend could not be observed in the other transgenic line (T1) with the same level of gene silencing. Analysis of more than 2 gene-silenced lines would reveal if the effect is repeatable or it can be prescribed to a T-DNA insertion in gene involved in growth regulation. Wide characterization of BGAL7 RNAi lines, which involved analyses of wood anatomy, chemical properties, cellulose ultrastructure, immunolabelling of RG-I structures and X-Gal staining, suggested that the activity of BGAL7 does not have impact on tension wood properties and modification of RG-I structure in the G-layer.

Although BGAL7 was predicted in the analysis of **Hobson and Deyholos** (**2013**) as beta-galactosidase with a glycosyl hydrolase 35 domain (GH35), BGAL7 is on Phytozome portal (https://phytozome.jgi.doe.gov/pz/portal.html) described to have a glycosyl hydrolase 42 protein domain. According to the Cazy database (http://www.cazy.org/), both GH35 and GH42 families are functionally assigned as beta-galactosidases, but GH42 has also known α-L-arabinopyranosidase activity. BGAL7 might therefore have activity toward substrate different than galactose. To approach to its function, it is of certain interest to determine a substrate of BGAL7 expressed in heterologous system and compare it with substrates of other BGALs, particularly those highly expressed in xylem. Further investigations toward the protein (co)-localization(s) and transcriptomic changes in RNAi transgenics would also help to highlight its function.

Modifications of RG-I pectin in the G-layer: prospective BGALs

We were not able to validate our hypothesis by modifying the expression of *BGAL7* in tension wood. However, high BGAL activity detected in TW indicates that BGAL is the molecular player likely important for properties of TW. Since the higher activity observed in TW could not be explained with the expression of TW-specific gene *BGAL7*, it would then rather be explained with (a) post-translational modification(s) of non-differentially expressed BGAL(s). Candidates prone to such modifications are those highly expressed in wood as BGAL1, BGAL18, BGAL20 or BGAL22. The later three belong to the group-A1, which is the largest group of BGALs in poplar. The group members from Arabidopsis were functionally characterized as cell wall exo-galactanases with activities toward β-(1,4)- and β-(1,3)-galacto-oligosaccharides (**Gantulga *et al.*, 2009**). It partially corresponds to the profile of a BGAL expected to cut β-(1,4)-galactan in RG-I and not β-1,3-galactan, which cannot be normally found in side chains of RG-I pectins.

As evidenced from the phylogenetic analysis presented in this thesis, BGAL22 is homolog of LusBGAL1 and LusBGAL2, whose down-regulation in flax increased the content of cell wall-associated galactans, decreased the ability of Gn- conversion to the G-layer and reduced cellulose crystallinity and stem strength (**Roach *et al.*, 2011**). Moreover, using an antibody directed against LuBGAL1, **Mokshina *et al.*** (**2012**) localized this protein specifically in the G-layer of poplar. Further investigations of RG-I modification in the G-layer should therefore focus on BGAL22 as a prominent enzyme for an activity towards RG-I. In order to investigate if the enzymatic activity of BGAL22 towards RG-I is an important step for mechanism of microfibril tensioning in TW, it would be of interest to produce and characterize BGAL22 RNAi transgenic line. Indeed, it would be also of importance to test if a BGAL22 produced in a heterologous system would have activity towards plant cell wall pectins. Finally, activity in the G-layer may not involve an action of only one BGAL since BGAL22 may have cooperative function with other BGALs highly expressed in wood as BGAL1, BGAL18 and BGAL20. It would be then of interest to apply the same experimental strategy on all four prospective BGALs.

Localization of molecular players in tension wood fibers of simarouba in comparison to tension wood fibers of poplar

4. SIMAROUBA

Wood of simarouba undergoes modifications during maturation of TW fiber, which transforms from fiber with cellulosic G-layer to fiber with lignified G-layer (**Roussel and Clair, 2015**). We commonly named such layer as S-G layer. Epitopes of RG-I and AGP structures were immunolocalized in simarouba juvenile tree grown in greenhouse conditions, which develops cellulosic fibers, and adult simarouba grown in forest, with formed lignified fibers. In addition, the epitopes were immunolocalized in mature OW fibers of simarouba juvenile tree. Finally, labelling in the S-G layer of simarouba was compared with labelling in the G-layer of poplar.

4.1. Immunolocalization of RG-I and AGP structures in TW fibers of simarouba

Immunolabelling was studied in differentiating fibers and mature fibers of simarouba juvenile tree, while in adult simarouba it was studied only in mature fibers. Distribution of labelling was studied in different cell wall layers: compound middle lamella (CML), secondary cell wall 1 and S-G layer (Materials and methods, **Fig. 5**).

The experiment was performed with 7 antibodies, which can be classified in 3 groups according to the epitopes of their cell wall targets: LM5 and RU1 antibodies are labelling RG-I pectins; Mac207, JIM14 and PopFLA1 antibody are labelling arabinogalactan proteins; LM6 and CCRC-M7 antibodies are labelling both of the targets. Results of labelling are shown in **Table IV-1** and **Figure IV-1**.

		OW		TW								
		Mature		Differentiating			Mature					
		/		cellulosic-type fiber			cellulosic-type fiber			lignified-type fiber		
Target	**Antibody**	**CML**	**S1/S2**	**CML**	**S1**	**S-G**	**CML**	**S1**	**S-G**	**CML**	**S1**	**S-G**
RG-I	**LM5**	*	/	/	/	***	/	/	**	/	/	**
	RU1	**	*	*	/	*	*	/	***	*	/	*
AGP	**Mac207**	/	/	/	/	**	/	/	**	/	/	**
	JIM14	/	/	/	/	/	/	/	*	/	/	/
	PopFLA1	/	/	/	/	/	/	/	/	/	/	/
RG-I/AGP	**LM6**	*	/	/	/	***	/	/	***	*	/	*
	CCRC-M7	/	*	*	*	*	*	/	*	/	/	*

Table IV-1. Immunohistolocalization of RG-I pectin and AGP structures performed with 7 antibodies. The labelling was studied in the cell wall layers of fibers from: mature opposite wood (OW) of simarouba juvenile tree, differentiating and mature tension wood (TW) of simarouba juvenile tree, mature TW of adult simarouba. For a representation of the cell wall layers, see **Figure M5** of materials and methods. CML= compound middle lamella (middle lamella + primary cell wall); S1= secondary cell wall layer 1; S1/S2= secondary cell wall layer 1 and 2; S-G= secondary cell wall layer 2/gelatinous-type layer. *, **, *** = labelling of estimated intensity ranging from weak (*) to strong (***); /=labelling not detected

RG-I

LM5 antibody labelled compound middle lamella of OW. In TW, labelling of LM5 antibody was detected in S-G layer of all types of fibers, but with weaker intensity in mature cellulosic and lignified fiber than in differentiating fiber.

RU1 labelled CML and SCW in OW. In TW, labelling was detected in CML of all TW fiber types; S-G layer was labelled with weak intensity in differentiating fiber and lignified-type mature fiber, and with strong intensity in mature cellulosic-type fiber.

AGP

Mac207 labelled only S-G layer and the intensity of signal was the same between differentiating cellulosic-type fiber, mature cellulosic-type fiber and lignified-type fiber.

Labelling of **JIM14** was detected only in S-G layer of mature cellulosic-type fibers in TW.

Labelling of **PopFLA1** could not be detected in any cell wall layer of OW or TW fibers.

RG-I/AGP

In OW, **LM6** labelled only CML. In TW, strong labelling was detected in S-G layer of differentiating and mature cellulosic-type fibers. In lignified-type fiber, weak labelling was detected in CML and S-G layer.

CCRC-M7 labelled SCW of OW. In TW, labelling was detected in all cell wall layers of differentiating cellulosic-type fiber, in CML and S-G layer of mature cellulosic-type fiber and in S-G of lignified-type fiber. Labelling was in all cases weak.

Figure IV-1. Immunolabelling of tension wood fibers in poplar and simarouba with antibodies LM5, RU1, Mac207, JIM14, PopFLA1, LM6 and CCRC-M7. The type and the differentiation stage of fibers are marked on each figure.

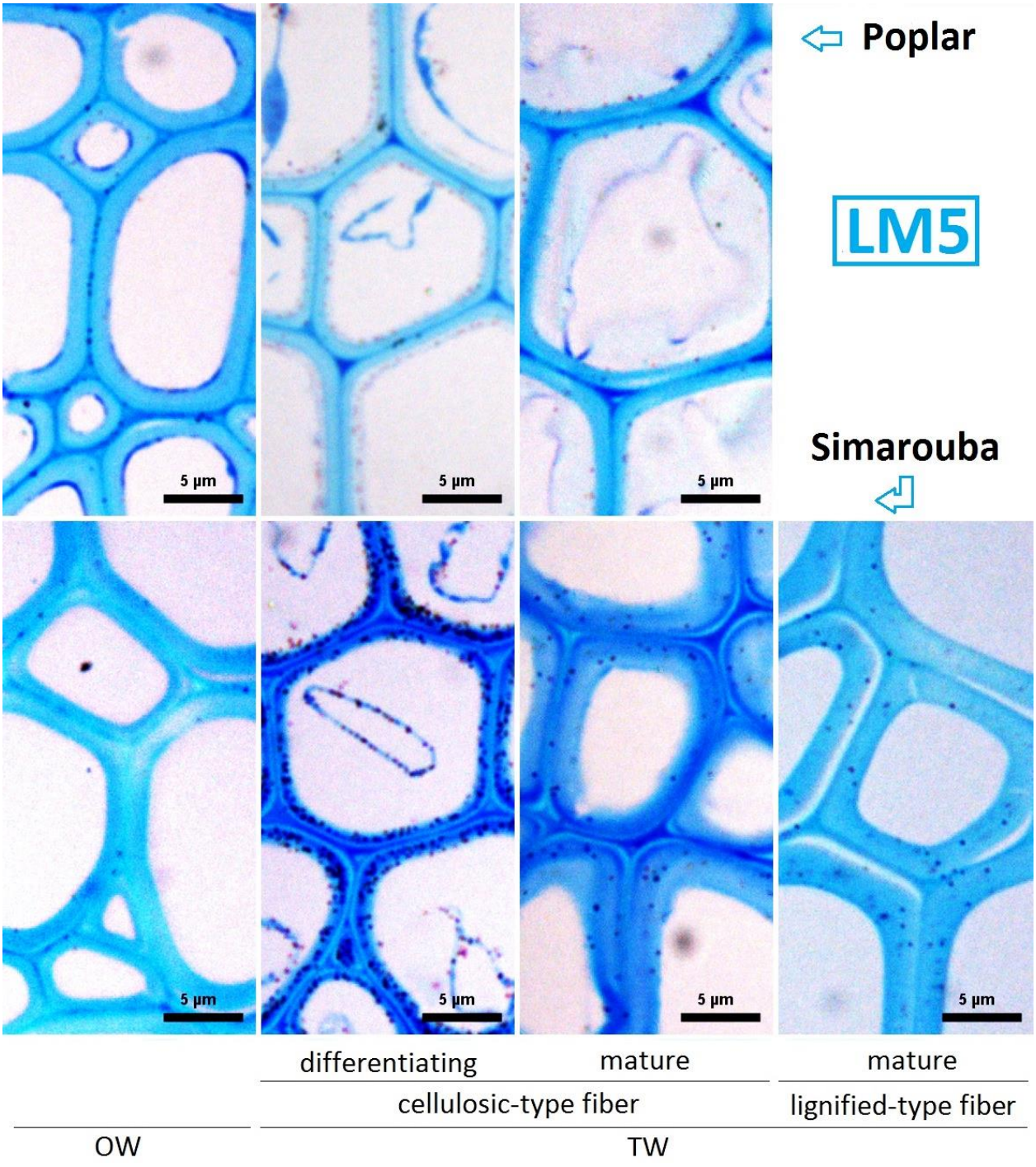

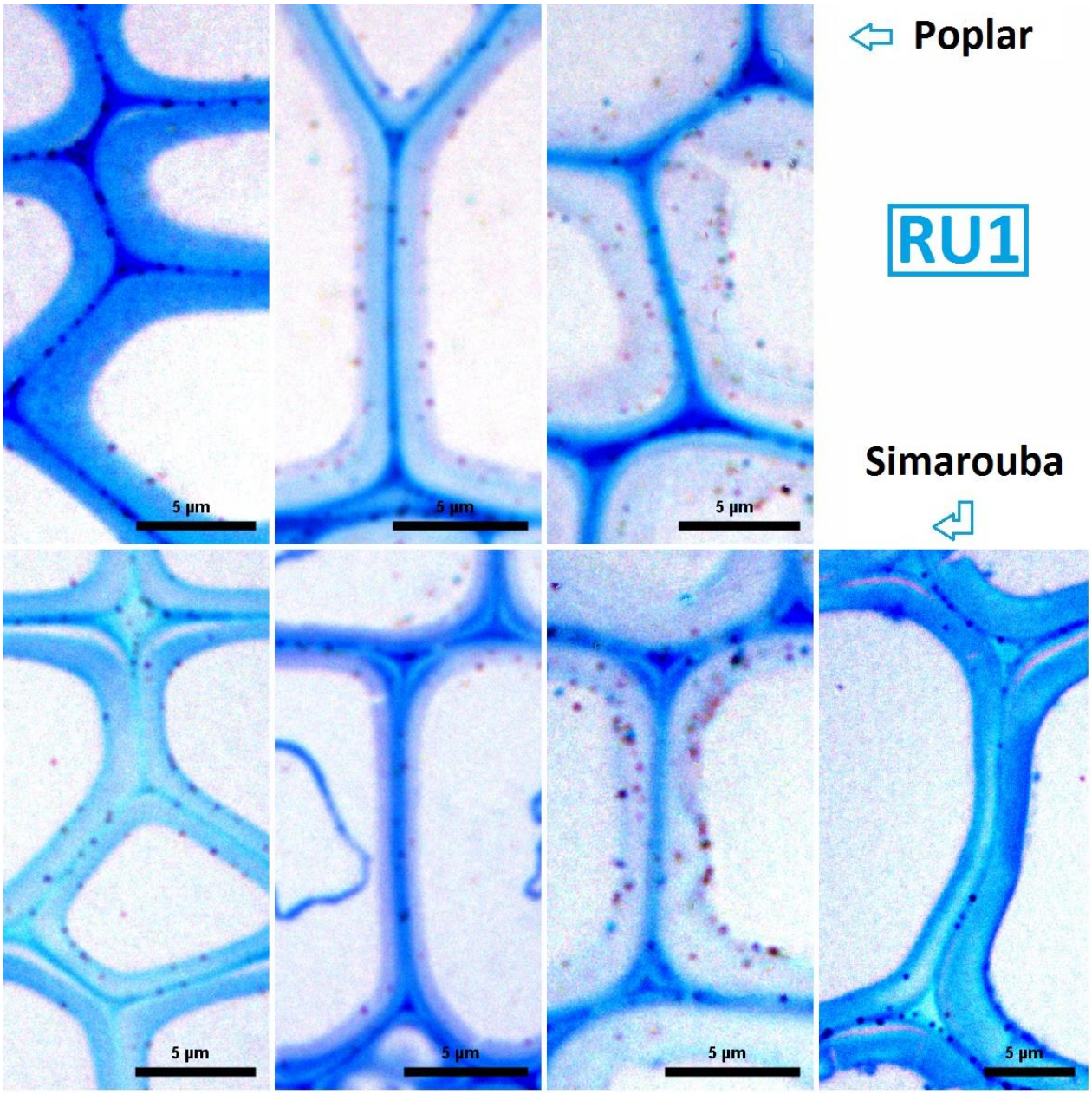
Poplar
RU1
Simarouba
5 µm
differentiating
mature
mature
cellulosic-type fiber
lignified-type fiber
OW
TW

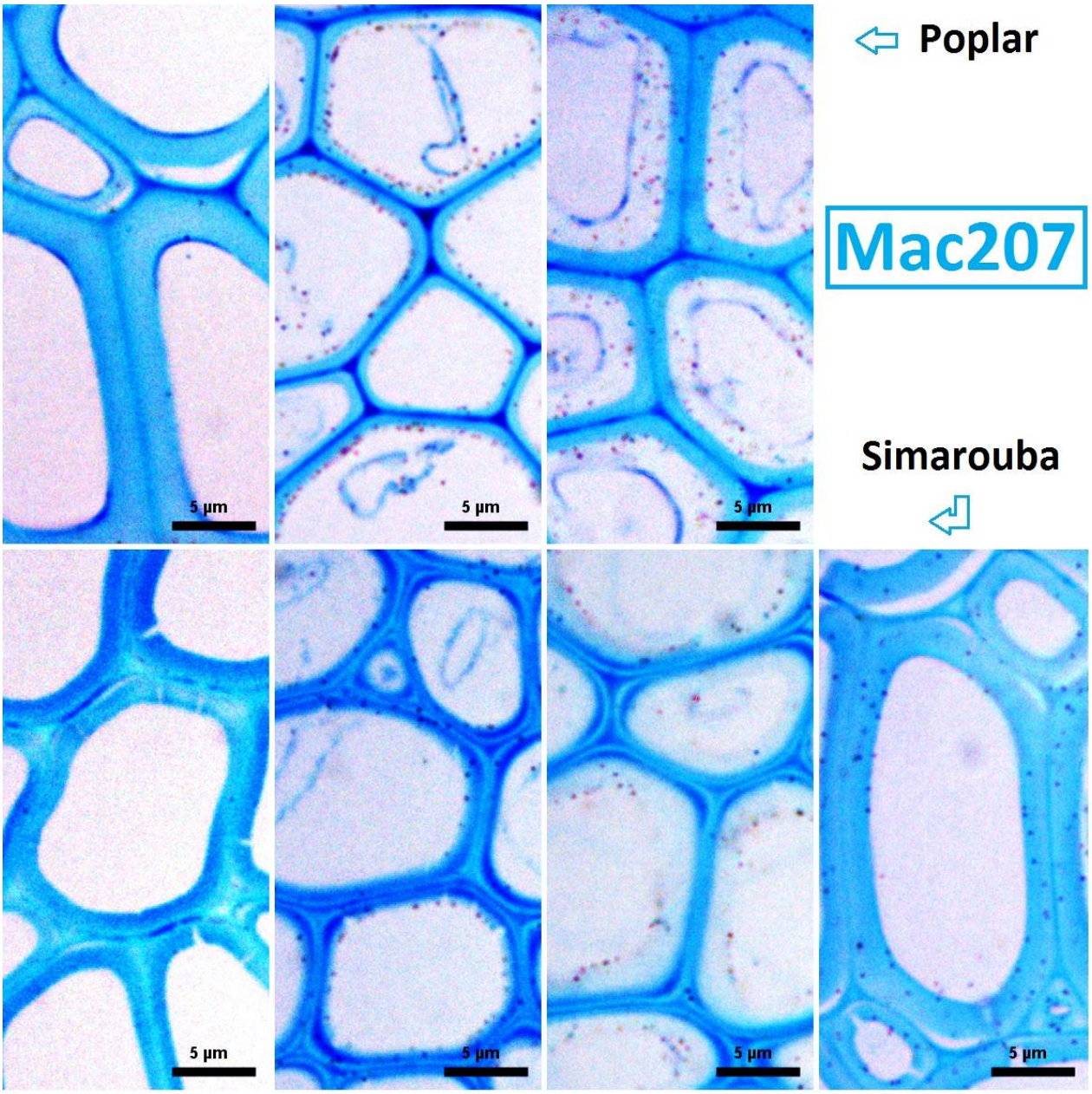
Poplar
Mac207
Simarouba
5 µm
differentiating
mature
mature
cellulosic-type fiber
lignified-type fiber
OW
TW

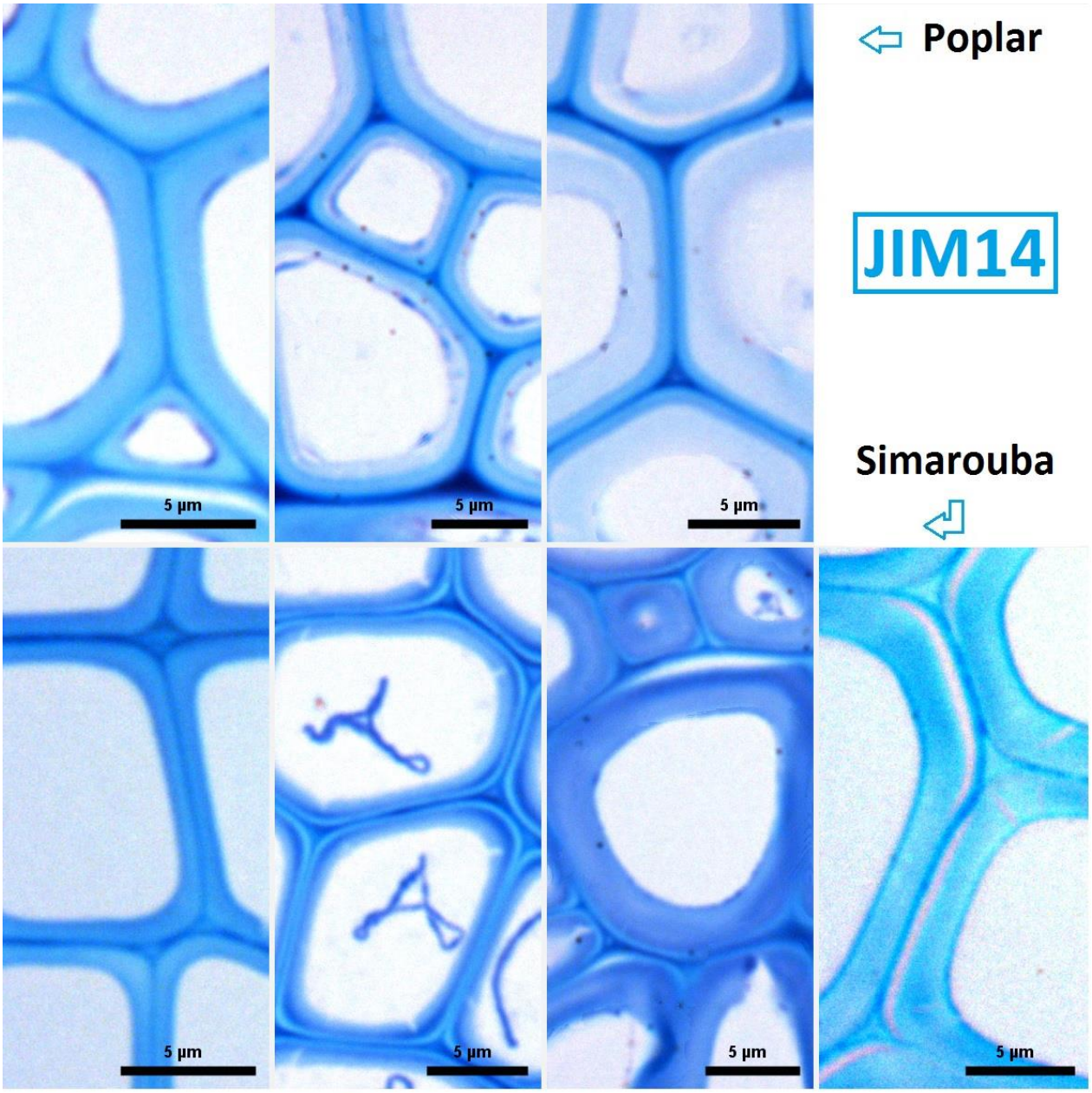
Poplar
JIM14
Simarouba
5 µm
5 µm
5 µm
5 µm
5 µm
5 µm
5 µm
5 µm
differentiating
mature
mature
cellulosic-type fiber
lignified-type fiber
OW
TW

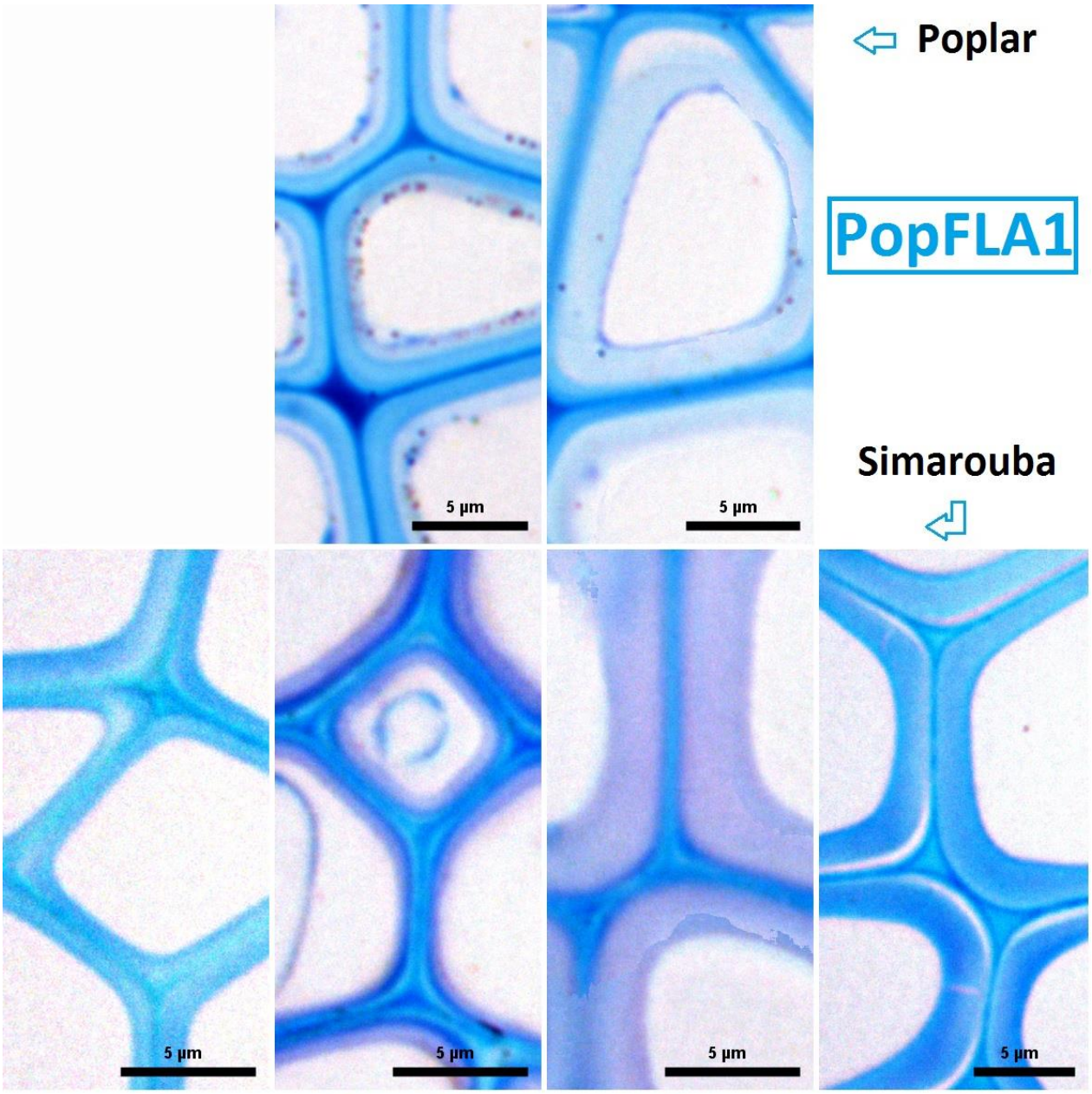
Poplar
PopFLA1
Simarouba
5 µm
5 µm
5 µm
5 µm
5 µm
differentiating
mature
mature
cellulosic-type fiber
lignified-type fiber
OW
TW

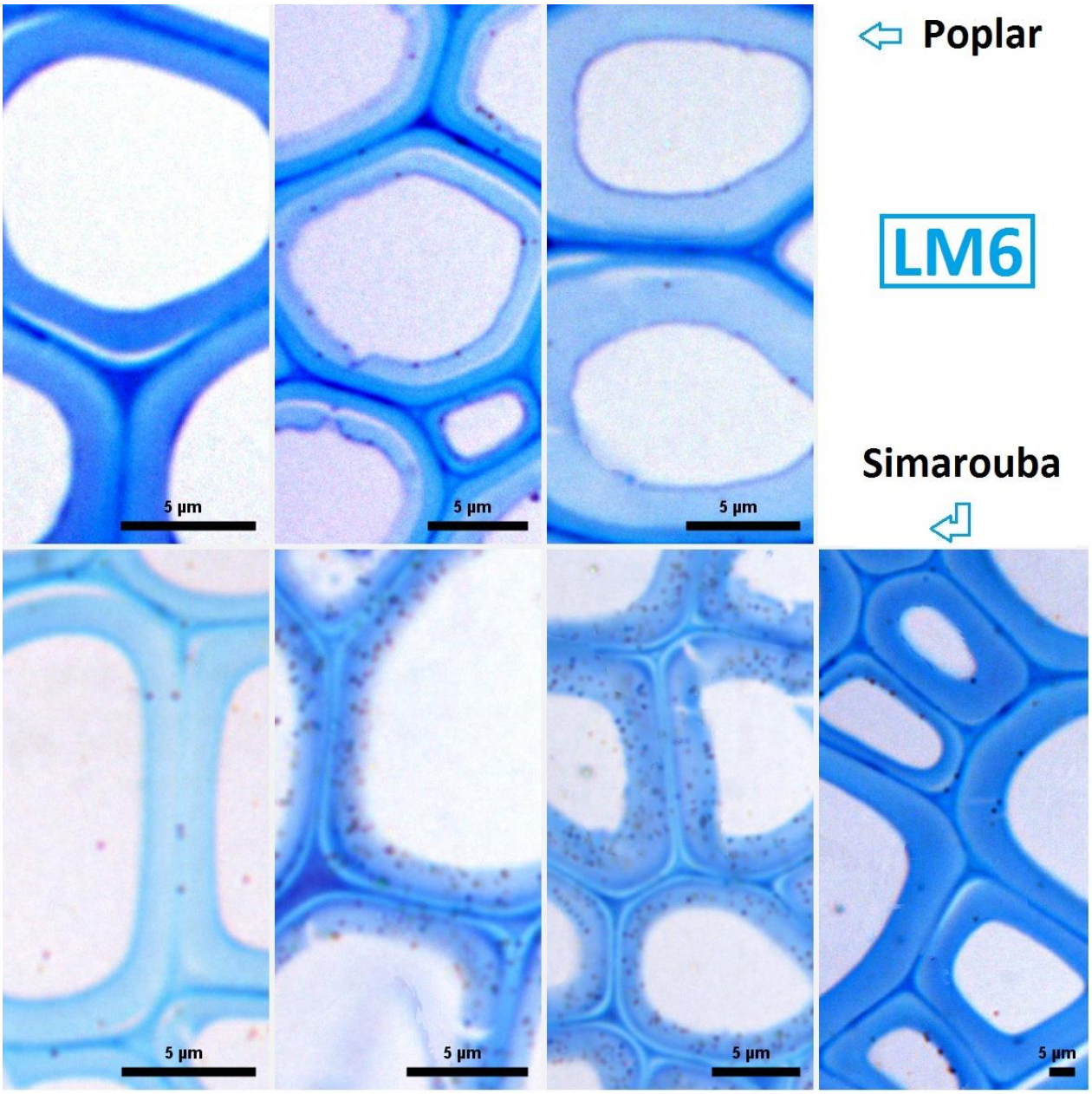
Poplar
LM6
Simarouba
5 µm
differentiating
mature
mature
cellulosic-type fiber
lignified-type fiber
OW
TW

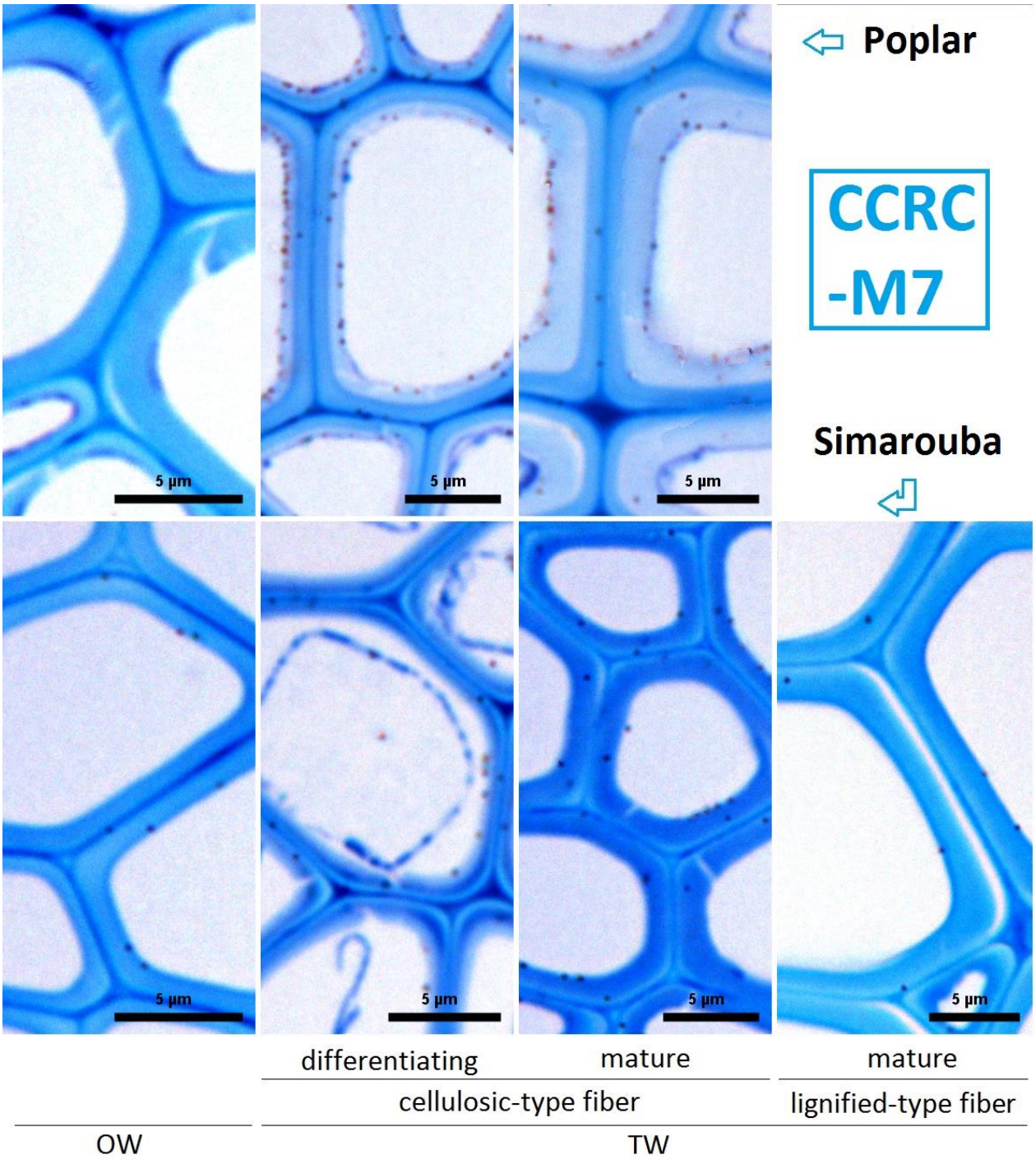
Poplar
CCRC
-M7
Simarouba
5 µm
differentiating
mature
mature
cellulosic-type fiber
lignified-type fiber
OW
TW

4.2. Comparison of immunolocalization between S-G layer of simarouba and G-layer of poplar

In parallel to the study performed on simarouba, immunolocalization was performed in TW of poplar as a control of results obtained by Guedes (2013). Labelling in simarouba was finally compared to results obtained on poplar, which is shown in **Table IV-2**.

The comparison was focalized only on G-layer of cellulosic-type fiber from poplar and S-G layer of cellulosic-type. For simarouba, the intensity of labelling in cellulosic-type fiber was compared with lignified-type fiber.

		Poplar	Simarouba	Poplar	Simarouba	Simarouba
		differentiating TW fiber		mature TW fiber		
		cellulosic-type		cellulosic-type		lignified-type
Target	Antibody	G-layer	S-G layer	G-layer	S-G layer	S-G layer
RG-I	LM5	***	***	**	**	**
	RU1	*	*	***	***	*
AGP	Mac207	***	**	***	**	**
	JIM14	*	/	*	*	/
	PopFLA1	**	/	*	/	/
RG-I/AGP	LM6	*	***	*	***	*
	CCRC-M7	***	*	**	*	*

Table IV-2. Comparison of immunohistolabeling between G-layer of poplar and S-G layer of cellulosic-type and lignified-type fiber of simarouba. CML= compound middle lamella (middle lamella + primary cell wall), S-G= secondary cell wall layer 2/gelatinous-type layer.*, **, *** = labeling of estimated intensity ranging from weak (*) to strong (***); /=labeling not detected.

Labelling of **LM5** antibody was of the same pattern in both G-layer of poplar and S-G layer of simarouba. The intensity of labelling decreased in G/S-G layer of both species upon maturation of cellulosic-type fibers and it stayed unchanged in lignified-type fiber of simarouba.

Similarly, labelling with **RU1** antibody was persistent between species, being weak in G/S-G layer of differentiating cellulosic-type fiber and strong in G/S-G layer of mature cellulosic-type fiber. Intensity of labelling was weaker in S-G layer of lignified-type fiber.

Strong labelling of **Mac207** was detected in S-G and G-layer of all fiber types, although with slightly weaker intensity in S-G layer of simarouba. Labelling in S-G layer was consistent between cellulosic and lignified-type fiber of simarouba.

There was no difference in labelling of **JIM14** antibody between poplar in simarouba. While JIM14 weakly labelled differentiating G-layer of poplar, the labelling could not be detected in differentiating S-G layer of simarouba. In mature cellulosic-type fiber, weak labelling was detected in both S-G and G-layer. Labelling could not be detected in S-G layer of lignified-type fiber.

PopFLA1 labelled only differentiate and mature G-layer of poplar, while the labelling could not be detected in S-G layer of any fiber type in simarouba.

Labelling of **LM6** was consistent between poplar and simarouba, being weak in G/S-G layer of differentiating cellulosic fiber and strong in G/S-G layer of cellulosic mature fiber. Intensity of labelling decreased in lignified-type of fiber of simarouba.

Labelling of **CCRC-M7** antibody could be detected in both species and was weaker in simarouba than in poplar. While the labelling slightly decreased during differentiation of G-layer in poplar, labelling was constantly weak in S-G layer of simarouba.

4.3. Discussion

In a number of angiosperm species, TW fibers have no G-layer (**Clair *et al.*, 2006b**), while others develop the classical G-layer as in poplar, multi-layered type as in *Laetia procera* (**Ruelle *et al.*, 2007**) or progressively lignified as in *Simarouba amara* (**Roussel and Clair, 2015**). The underlying questions are: i) what stands behind that great diversity between species, ii) are different TW types equally effective in generation of high tensile stress and iii) do they employ the same mechanism of the stress generation? The first question can be discussed in a light of different environmental conditions in which trees are growing, their divergent evolutionary history or a metabolic adaptation. An answer to the second question partially gives a study from **Clair *et al.*** (**2006a**) in which the mechanical properties were measured in species which produce and do not produce G-layer. The study showed that species without G-layer effectively generate the tensile stress, which is sometimes even higher than in species with the G-layer. For the reason of recent discovery that some species develop G-layer, which gets lignified and masks its identification in old mature wood (**Roussel and Clair, 2015**), the current classification of non-G-layer species used in the study should be reviewed. It is actually one of the goals of the project Stress In Trees, which has been studied mostly on the tropical species in French Guiana by our project partners.

Simarouba is one of the species that develops a cellulosic G-layer, which gets lignified at the point of fiber maturation, finally looking like a fiber of normal wood (**Roussel and Clair, 2015**). The immunolocalization performed in the frame of this thesis aimed at determining what differentiate two types of G-layer- lignified G-layers from simarouba and unlignified G-layers from poplar. The focus was put on localization of RG-I and AGP structures - the molecules which were studied in this thesis as candidates potentially involved in the G-layer properties and mechanism of the tensile stress generation by a gel swelling. The results showed that, apart from one antibody recognizing specifically AGP with fasciclin domain from poplar, the same structures of RG-I and AGP could be detected in the cellulosic G-layer of both simarouba and poplar. However, labelling of a number of antibodies was hindered in the lignified S-G layer of simarouba. The results were finally discussed in the light of potentially shared mechanism of tensile stress generation between the different tension wood types.

Localization of RG-I and AGP structures in the G-layer gets obstructed by lignin deposition

Immunolocalization of RG-I and AGP structures was performed with seven antibodies. The antibodies were selected according to labelling in the G-layer of poplar (**Guedes, 2013**). As a technical control, immunolocalization was performed on the same poplar samples as in Guedes (2013). The labelling in simarouba was performed for the first time. In poplar, the antibodies showed the same pattern of labelling as presented in the thesis of F. Guedes, which makes the method accurate and reliable. However, issue of the method was shown to be in the labelling noise often caused by unspecific binding of antibody or insufficient rinsing after an incubation with antibodies. However, such occasional occurrences did not prevent to raise conclusions.

Most of the antibodies showed the same pattern of labelling in the cellulosic-type of the G-layer in both simarouba and poplar. It suggests that both species incorporate the same structures (of at least AGP and RG-I) in the G-layer. However, the labelling intensity of several antibodies (LM5, RU1, Mac207) changed from differentiation to maturation of the G-layer. The changes were of the same pattern in simarouba and poplar. In addition, the labelling signal of several other antibodies (JIM14, LM6, CCRC-M7) was of different intensity in simarouba and poplar, probably due to a different number of their epitopes in the two species. Only the labelling of PopFLA1 antibody could not be detected in simarouba. This polyclonal antibody was raised in AGPF laboratory against the protein backbone of poplar FLA1 (not published). The absence of labelling in simarouba suggests either that simarouba does not have any FLA structure or contains FLAs which are too divergent from poplar to be recognized by the poplar antibodies.

Simarouba develops peculiar G-layer, which upon maturation gets lignified and finally looks like the SCW layer of normal wood (**Roussel and Clair, 2015**). Hence, we named it S-G layer. The labelling signal of several antibodies weakened (RU1, LM6) or disappeared (JIM14) in lignified S-G layer. It might be assumed that it happens due to incorporation of lignin, which masks epitopes of other matrix components. Alternatively, existing structures may get modified or differently arranged in the cell wall. AX1 antibody recognizing a structure of xylan was shown in poplar to bind heavily the S1/S2 layers and not the G-layer (**Guedes, 2013**). An additional experiment performed in my laboratory showed that AX1 binds both

the S1-layer and the S-G layer of simarouba (data not shown). However, the labelling of S-G layer with AX1 antibody was weak during the fiber differentiation and strong in the mature fibers prone to lignification. It is one confirmation that the S-G layer modifies its matrix composition upon fiber maturation, likely due to the incorporation of lignin and hemicelluloses as xylan, which consequentially hinder the labelling of some antibodies, as it could be detected for antibodies labelling AGP and RG-I. Further investigations are required to answer on underlying questions: i) what controls the lignification, ii) how it affects the tensile force and iii) what is a function of lignification.

Poplar and simarouba: different G-layer, the same mechanism?

Our study aimed to answer on the question do species which develop different type of TW employ the same mechanism of the tensile stress generation. The results obtained in the present thesis suggest that simarouba and poplar incorporate in the G-layer mostly the same structures of AGPs and RG-I, as they were immunolocalized both in the G-layer and the S-G layer, at least for the antibodies tested. These two families of molecules were studieded in the present thesis as candidates potentially involved in the generation of tensile stress in the G-layer of poplar. The obtained results have suggested that fasciclin-like arabinogalactan protein (FLA) have function in a control of cellulose crystallinity in the G-layer, which is the property likely important for the generation of tensile stress (**Clair *et al.*, 2011**). It is therefore plausible that simarouba employs FLAs for a function similar or the same as in the G-layer of poplar.

From the other hand, modifications of RG-I pectin were proposed as important for a gel formation and potential mechanism of tensile stress generation (**Guedes, 2013**). We did not succeed to validate this hypothesis since we could not detect modifications of immunosignal of RG-I lateral chains in BGAL7 transgenics. However, the high activity of beta-galactosidase was localized in mature TW fibers where the modification of RG-I was previously detected by Guedes (2013). Interestingly, we observed in simarouba as in poplar the same increase in immunosignal of RG-I backbone structure and decrease in immunosignal of β-1,4-galactan side chains during fiber differentiation. It strongly indicates that, if the modification is really crucial for a gel formation, it would be employed in the G-layer of both simarouba and poplar. The activity of beta-galactosidase was

examined on stem cross-sections of simarouba as it was performed on poplar in the frame of this thesis (data not shown). Although the results were not completely reliable since the experiment was performed in tropical conditions of F. Guiana using an inadequate equipment, we could observe in one year old simarouba tree stronger BGAL activity in TW than in OW, which was the pattern observed in poplar.

In conclusion, our current observations suggest that simarouba and poplar incorporate the same structures of AGP and RG-I in the G-layer (at least some). In addition, the RG-I structure was shown to get modified in simarouba within the same pattern as in poplar during the fiber maturation. Considering the potential of AGP and modification of RG-I in the generation of tensile stress, it could be possible that the both species employ the same mechanism of the microfibril tensioning. Further investigations should be directed toward immunolocalization of other structures localized in the G-layer of poplar as glucuronoxylan and glucomannan (**Guedes, 2013**) – molecules as well potentially related with a gel formation and mechanism of the tensile stress generation. Additionally, mechanical measurements on simarouba might reveal a significance of lignification on mechanical properties of tension wood. By far is known that, at that time classified as species without G-layer, simarouba with lignified fibers effectively generates the tensile stress (**Ruelle *et al.*, 2011**).

GENERAL DISCUSSION

Importance of (tension) wood studies

Humans rely on trees as their source of energy, timber and food. However, tree resources require an effective management in order to be preserved and exploited at the same time. Understanding of how trees function may help achieving these goals. Although most of plant physiology research is performed on Arabidopsis as the model plant, research on trees is beneficial when it concerns traits like wood formation. Poplar is a tree model widely used in wood studies and particularly wood physiological studies, as those conducted in AGPF research unit.

This thesis aims at a better understanding of tension wood formation. Tension wood is studied because it represents an impressive and important adaptive mechanism of tree secondary growth, and because it is of interest for two types of industries. In timber industry, tension wood is regarded as a defect, which decreases wood quality by causing wood twisting, while for biofuel industry it represents an enriched source of glucose for conversion to bioethanol (**Gierlinger *et al.*, 2008**). Saccharification test performed in frame of the experimental work of this thesis confirmed that tension wood yields more glucose than normal wood after the enzymatic hydrolysis. Formation of tension wood is therefore the target of genetic manipulations in direction of a gene over-expression or knockout, depending on a final use. Hence, understanding of the underlying molecular mechanism of tension wood formation is the crucial step for further actions.

Genetic engineering as a tool for studying a function of proteins potentially involved in tension wood formation

In this thesis, genetic engineering was principally used to produce RNAi transgenic poplar trees, which served as the material for studying a function of proteins potentially involved in the formation of tension wood. Transformation of poplar tissue, regeneration and growth of RNAi transgenic trees is one long experimental process and therefore requires a discerning choice of genes for their expression modifications.

Genetic engineering is advantageous because it can relate silencing of a gene or a group of genes with modifications of tension wood properties. It can then directly confirm a player's involvement in TW formation. A standard practice, also used in this thesis, is to compare effects observed in transgenics with phenotypes of

Arabidopsis mutants existing within a large collection. To evaluate proposed function of a protein, it would be of particular interest to test if the expression in Arabidopsis mutant would complement its phenotype.

In this thesis, a profound characterization of wood was carried out in the produced RNAi transgenics. However, a gene down-regulation may also have effects on other tissues, which were not examined in this study as, for example, cell wall deposition in roots.

Another advantage of the method is that it may lead to an identification of new molecular candidates affected by a gene modification, for example, based on transcriptional changes. It was the case for *COBL4* gene, which was down-regulated in FLA RNAi transgenics produced during the thesis.

The expression modification of one gene may modify the expression of many other genes, sometimes having a consequence in pleiotropic or ectopic effects. Although it was not a case in this study, the absence of a phenotype required deeper analyses as wood ultrastructure or transcriptomic changes. In the present work, such analyses were directed toward a part of lines thanks to FT-MIR spectroscopy, which was shown to be an interesting method for rapid screening of a high number of transgenics in a search for those remarkably different from their wild-types - as it was the case for CTL2 RNAi lines. The method is also of particular interest for analysis of transgenics modified for a high number of potential candidate genes, since it provides to a researcher an information, which can direct further analyses on the most interesting lines only.

The model of tensile stress generation by a gel swelling may be applied on different types of tension wood

Researches in the last two decades have significantly advanced in the understanding of tension wood mechanism. The studies performed in the frame of this thesis and the project Stress In Trees have aimed in continuation of the progress towards a model, which will explain how tension wood generates the tensile force. The project was based on the hypothesis that a G-layer matrix swells during fiber maturation and generates a force, which puts cellulose microfibrils under a tensile stress. The hypothesis now has firm foundation in the recent results partially obtained in the frame of Stress In Trees project, which demonstrated that mesoporosity changes occur in the G-layer during its development (**Chang *et al.*,**

2015). Additionally was in the G-layer of poplar localized a high number of hydrophilic matrix components (**Guedes, 2013**), which may be involved in a gel formation.

The presenting thesis have aimed in approaching the underlying molecular background, which governs formation of a gel and the G-layer properties in general. The main part of the study was performed on poplar, which develops G-fibers with classical G-layer. In poplar were studied three molecular players: fasciclin-like arabinogalactan protein (FLA), chitinase-like protein (CTL) and beta-galactosidase (BGAL). According to the literature and the results obtained during this thesis, these proteins may regulate cellulose crystallinity (CTL), cellulose microfibril angle (FLA) and/or a gel formation (BGAL, CTL, FLA) during G-layer biosynthesis.

Additionally, we performed studies on simarouba, which develops during the fiber maturation cell wall layer similar to the classical G-layer, but which upon maturation undergoes anatomical and chemical modifications (**Roussel and Clair, 2015**). We compared between poplar and simarouba localization of RG-I pectins and arabinogalactan proteins, which were proposed to be implicated in a gel formation in poplar (**Guedes**, **2013**). The obtained results demonstrated that RG-I and AGP incorporate in the G-layer of both poplar and simarouba, which indicates that these two structures may be involved in a gel formation in both species. However, absence of labelling in simarouba with PopFLA1 antibody, which recognizes epitopes of an arabinogalactan with fasciclin domain (FLA) from poplar revealed that simarouba does not have any or contains different structures of FLA. In addition, the modification of RG-I structure during the G-layer maturation, demonstrated in poplar as a change in intensities of immunosignal of RG-I backbone and β-(1,4)-galactan side chains (**Guedes, 2013**), was also evidenced in the S-G layer of simarouba. It suggest that, if important for a gel formation, the modification of RG-I would exist in both poplar and simarouba. In conclusion, if simarouba and poplar develop the gel properties thanks to, at least, AGP and modifications of RG-I pectin, it then leads to the conclusion that both species may employ the same mechanism of microfibril tensioning by a gel swelling.

Hypothesis of a gel formation by a BGAL-modified RG-I pectin stays unsubstantiated

Beta-galactosidase (BGAL) was studied as a candidate for the previously evidenced modification of RG-I pectin structure, which is potentially responsible for a gel formation and consequentially for tensioning of microfibrils by a gel swelling (**Guedes, 2013**). The removal of RG-I side branches may facilitate interactions with other molecules from the G-layer matrix as AGPs (FLA). Indeed, their covalent interactions were shown to exist in primary cell wall of Arabidopsis (**Tan *et al.*, 2013**). AGPs and RG-I may also interact with other matrix components as glucomannans and glucuronoxylans, which were localized in the G-layer (**Guedes, 2013**). However, further investigations should focalize on determination of how these components interlink together to form a gel.

From our analysis, the proposed function of BGAL was shown as prominent since of high activity of BGAL in TW fibers. However, the results of characterization of BGAL7 RNAi transgenic lines suggest that BGAL7 is not responsible for the BGAL activity in G-fibers. To validate our hypothesis, we proposed a new candidate gene *BGAL22*, based on the reported phenotype of its homologous mutant in bast fibers of flax, which suggest its involvement in galactan modifications during G-layer development (**Roach *et al.*, 2011**).

FLAs and CTL2 are important for cellulose structure of tension wood

We could detect alteration of cellulose ultrastructure in tension wood of FLA and CTL2 RNAi transgenic lines, demonstrating that these players have potential function in a control of particular cellulose organization and structure in the G-layer.

From the modifications of the gene expression in FLA transgenics, function of FLAs was brought in a relation with *COBL4* gene encoding COBRA protein and *CESA8* encoding one of the proteins of the cellulose synthase complex. Co-expression of *COBL4* with *FLA11* and *FLA12* was previously shown in Arabidopsis (**Persson *et al.*, 2005**).

The orientation of nascent microfibrils was in one model proposed to be regulated by their binding to a scaffold of cell wall polysaccharides or plasma membrane proteins orientated according to cortical microtubules or the cell wall (**Baskin, 2001**). Both the COBRA and FLA are known as GPI-anchored proteins, which

potentially bind the plasma membrane (**McFarlane *et al.*, 2014**). Bound to the membrane and oriented according to microtubules, they may control the axial orientation of microfibrils in the G-layer. Indeed, modification of the angle in *FLA* and *COBRA* mutants in Arabidopsis and eucalyptus strongly suggest their involvement in the orientation of cellulose microfibrils (**MacMillan *et al.*, 2010**; **MacMillan *et al.*, 2015**; **Roudier *et al.*, 2005**). We could also detected modification of microfibril angle in TW of one FLA1 RNAi line.

Additionally or alternatively, function of FLAs and COBRA may be important in a control of cellulose crystallinity governed from plasma membrane or directly in the G-layer upon protein release from a GPI anchor. In favor to the latter goes evidence that COBRA exist in a GPI-anchored, plasma membrane-associated and cleaved form (**Roudier *et al.*, 2005**); so as that FLAs incorporate in the G-layer, as demonstrated in AGPF laboratory (not published). We detected strong modification of crystalline structure in TW of FLA RNAi transgenics, which had modified the expression of *FLA*s and *COBL4*. Likewise, function of one COBRA was assigned to control cellulose crystallinity in cell walls of rice (**Liu *et al.*, 2013**). However, the exact controlling mechanism of cellulose organization is not known.

Results obtained in this thesis showed that chitinase-like protein encoded by *CTL2* is also important for cellulose crystallinity, since TW of CTL2 RNAi transgenics had significantly reduced crystalline organization. Modification of crystalline levels of cellulose was already reported in *ctl1 ctl2* double mutant in Arabidopsis (**Sanchez-Rodriguez *et al.*, 2012**). It is possible that CTL executes its function directly in the cell wall since bioinformatics analysis predicted that CTL2 does not have any GPI anchor, but it has a signal peptide for secretion into the cell wall (data not shown). Likewise, its close homolog CTL1 was shown to be secreted in the cell wall in Arabidopsis (**Sanchez-Rodriguez *et al.*, 2012**). Interestingly, FLAs and CTL2 showed tendency to be down-regulated in CTL2 and FLA RNAi transgenic lines, respectively. It may suggest that FLAs and CTL2 have cooperative function in the control of cellulose crystallinity in the G-layer, at least to some extent.

In CTL2 RNAi lines, the reorganization of cellulose structure was accompanied by reduction in cellulose content. CTL2 would therefore may function both in the regulation of cellulose synthesis and its crystallinity. However, the function of CTL2 would not be essential for cellulose synthesis, as proposed by Sanchez-Rodriguez *et al.* (2012), since the double knockout of *CTL2* and its close homolog *CTL1* resulted in a viable and fertile Arabidopsis plant. However, in the same study, CTL1

was shown to co-localize with CESA6 in Golgi-derivated bodies, and it stays to determine a significance of their co-localization for cellulose production. It may be possible that the decrease in cellulose content originates from a lack of CESA and CTL2 interactions or, alternatively, that reorganization of cellulose structure reduce cellulose synthesis through a feedback response.

Biomechanic measurements performed in collaboration with LMGC (Montpellier, France) and PIAF (Clermont Ferrand, France) confirmed a tight correlation of altered crystalline organization caused by down-regulation of *CTL2* with the mechanical properties of wood. CTL2 RNAi transgenic trees had lower wood densit, which is property directly linked with the wood stiffness. Additionally, stems of transgenics were brittle and had more frequent wood cracks on their cross-sections.

In the same transgenic RNAi lines, alterations of chemical properties, biochemical content and mechanical measurements were detected in TW as in NW and OW devoid of the G-layer. We could therefore conclude that the function of CTL2 is important for secondary cell wall in general, which also support the results of expressional analysis, which showed that CTL2 is equally expressed in OW and TW. Based on the same expression profile, it may be also concluded for COBL4 and some FLAs. However, wood of CTL2 RNAi transgenic lines was, beside cellulose, also altered for chemical structure associated to hemicelluloses and lignin. CTL2 therefore might have more significant function than FLAs and COBL4 important for, not only cellulose crystallinity, then organization of the complete cell wall.

The obtained results applied on a model of cellulose synthesis and cellulose microfibril tensioning in the G-layer

Altogether, the results presented in this thesis have: i) given rise to a new candidate *COBL4* with a potential function in tension wood formation, ii) advanced in the understanding of FLAs and CTL2 function in the G-layer properties and iii) affirmed BGAL as a prospective candidate for the modifications of RG-I pectin potentially leading to a gel formation. These findings are one step toward deciphering a molecular mechanism underlying establishment of the peculiar properties of G-layer and the generation of tensile stress, as it has been the aim of Stress In Trees project.

To summarize the results, I propose a model of a regulation of cellulose deposition in the cell wall and organization of the matrix components responsible for a gel formation. The model is presented in **Figure 18**. Following the model, CTL2 would interfere with CESA complex already before they both reach plasma membrane (not shown). At the plasma membrane, cellulose synthase complex track along cortical microtubules oriented in parallel to the cell axis. According to the model of Baskin (2001), microtubules would orient GPI-anchored FLA(s) and COBL4, which in turn orient the cellulose microfibrils in parallel to the fiber axis. During cellulose biosynthesis, CTL2 is directly secreted in the cell wall where it would bind deposited cellulose and control its crystalline organization interrelated with the organization of other matrix components. When cleaved from a GPI anchor, FLA(s) and COBL4 would in the cell wall perform the same or a similar function as the CTL2. Since COBL4 and CTL2 are equally expressed in TW and OW, FLA candidates for the proposed function would then rather be those with the same expression profile. COBL4, CTL2 and some FLAs would perform the same function in secondary cell wall layer 1 and 2 where cellulose is both crystalline and amorphous.

During the G-layer maturation, beta-(1,4)-galactan side chains get released from the backbone of RG-I pectin. In poplar, this activity may perform BGAL22. The modification would facilitate interactions of RG-I backbone with other matrix components as glucuronoxylans, glucomannans and some FLAs - all together stuck between the microfibrils. The modification and interactions would cause formation of a gel, whose swelling would then lead to transversal stretching and longitudinal extension of cellulose microfibrils. The model of RG-I modification and interaction with, at least AGP, can be applied on both the G-layer of poplar and the S-G layer of simarouba.

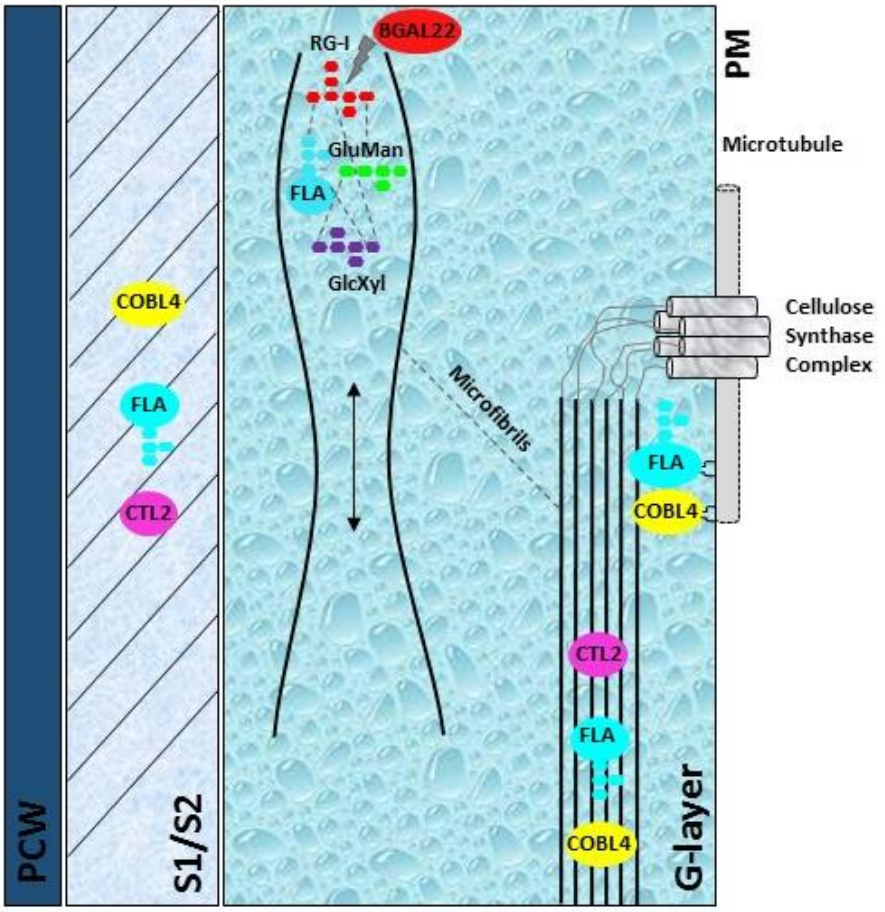

Figure 18. Schematic model representing a regulation of cellulose synthesis, deposition (right) and tensioning of cellulose microfibrils (left) in the G-layer of a TW fiber. PM=plasma membrane; GluMan=glucomannan; GlcXyl=glucurunoxylan.

REFERENCES

Abedini R, Clair B, Pourtahmasi K, Laurans F, Arnould O. 2015. CELL WALL THICKENING IN DEVELOPING TENSION WOOD OF ARTIFICIALLY BENT POPLAR TREES. Iawa Journal **36**, 44-57.

Ahn YO, Zheng M, Bevan DR, Esen A, Shiu S-H, Benson J, Peng H-P, Miller JT, Cheng C-L, Poulton JE, Shih M-C. 2007. Functional genomic analysis of Arabidopsis thaliana glycoside hydrolase family 35. Phytochemistry **68**, 1510-1520.

Almeras T, Fournier M. 2009. Biomechanical design and long-term stability of trees: Morphological and wood traits involved in the balance between weight increase and the gravitropic reaction. Journal of Theoretical Biology **256**, 370-381.

Almeras T, Grill J, Clair B. 2012. The origin of maturation stress in tension wood: using a wide range of observations and mechanical considerations to discriminate between hypothetic mechanisms. In: Moulia B, Fournier M, eds. 7th plant biomechanics international conference, Clermont-Ferrand, France, 258.

Anderson CT. 2016. We be jammin': an update on pectin biosynthesis, trafficking and dynamics. Journal of Experimental Botany **67**, 495-502.

Andersson-Gunneras S, Mellerowicz EJ, Love J, Segerman B, Ohmiya Y, Coutinho PM, Nilsson P, Henrissat B, Moritz T, Sundberg B. 2006. Biosynthesis of cellulose-enriched tension wood in Populus: global analysis of transcripts and metabolites identifies biochemical and developmental regulators in secondary wall biosynthesis. Plant Journal **45**, 144-165.

Arend M. 2008. Immunolocalization of (1,4)-beta-galactan in tension wood fibers of poplar. Tree Physiology **28**, 1263-1267.

Aspeborg H, Schrader J, Coutinho PM, Stam M, Kallas A, Djerbi S, Nilsson P, Denman S, Amini B, Sterky F, Master E, Sandberg G, Mellerowicz E, Sundberg B, Henrissat B, Teeri TT. 2005. Carbohydrate-active enzymes involved in the secondary cell wall biogenesis in hybrid aspen. Plant Physiology **137**, 983-997.

Azri W, Ennajah A, Nasr Z, Woo SY, Khaldi A. 2014. Transcriptome profiling the basal region of poplar stems during the early gravitropic response. Biologia Plantarum **58**, 55-63.

Baba K, Park YW, Kaku T, Kaida R, Takeuchi M, Yoshida M, Hosoo Y, Ojio Y, Okuyama T, Taniguchi T, Ohmiya Y, Kondo T, Shani Z, Shoseyov O, Awano T, Serada S, Norioka N, Norioka S, Hayashi T. 2009. Xyloglucan for Generating Tensile Stress to Bend Tree Stem. Molecular Plant **2**, 893-903.

Bamber RK. 2001. A general theory for the origin of growth stresses in reaction wood: How trees stay upright. Iawa Journal **22**, 205-212.

Banasiak A, Ibatullin FM, Brumer H, Mellerowicz EJ. 2014. Glycoside hydrolase activities in cell walls of sclerenchyma cells in the inflorescence stems

of Arabidopsis thaliana visualized in situ. Plants **3**, 513-525.

Barnett JR, Bonham VA. 2004. Cellulose microfibril angle in the cell wall of wood fibres. Biological Reviews **79**, 461-472.

Baskin TI. 2001. On the alignment of cellulose microfibrils by cortical microtubules: a review and a model. Protoplasma **215**, 150-171.

Bentum ALK, Cote WA, Day AC, Timell TE. 1969. DISTRIBUTION OF LIGNIN IN NORMAL AND TENSION WOOD. Wood Science and Technology **3**, 218-&.

Bowling AJ, Vaughn KC. 2008. Immunocytochemical characterization of tension wood: Gelatinous fibers contain more than just cellulose. American Journal of Botany **95**, 655-663.

Busov V, Fladung M, Groover A, Strauss S. 2005a. Insertional mutagenesis in Populus: relevance and feasibility. Tree Genetics & Genomes **1**, 135-142.

Busov VB, Brunner AM, Meilan R, Filichkin S, Ganio L, Gandhi S, Strauss SH. 2005b. Genetic transformation: a powerful tool for dissection of adaptive traits in trees. New Phytologist **167**, 9-18.

Chang S., Puryear J., Cairney. 1993. A simple and efficient method for isolating RNA from pine trees. Plant Molecular Biology Report **11**: 113-116

Chang SS, Quignard F, Almeras T, Clair B. 2015. Mesoporosity changes from cambium to mature tension wood: a new step toward the understanding of maturation stress generation in trees. New Phytologist **205**, 1277-1287.

Clair B, Almeras T, Pilate G, Jullien D, Sugiyama J, Riekel C. 2011. Maturation Stress Generation in Poplar Tension Wood Studied by Synchrotron Radiation Microdiffraction. Plant Physiology **155**, 562-570.

Clair B, Ruelle J, Beauchene J, Prevost MF, Fournier M. 2006a. Tension wood and opposite wood in 21 tropical rain forest species: 1. Occurrence and efficiency of the G-layer. IAWA Journal **27**, 329-338.

Clair B, Almeras T, Yamamoto H, Okuyama T, Sugiyama J. 2006b. Mechanical behavior of cellulose microfibrils in tension wood, in relation with maturation stress generation. Biophysical Journal **91**, 1128-1135.

Clair B, Gril J, Di Renzo F, Yamamoto H, Quignard F. 2008. Characterization of a gel in the cell wall to elucidate the paradoxical shrinkage of tension wood. Biomacromolecules **9**, 494-498.

Cornuault V, Manfield IW, Ralet MC, Knox JP. 2014. Epitope detection chromatography: a method to dissect the structural heterogeneity and inter-connections of plant cell-wall matrix glycans. Plant Journal **78**, 715-722.

Cosgrove DJ. 2015. Plant expansins: diversity and interactions with plant cell walls. Current Opinion in Plant Biology **25**, 162-172.

Crowther TW, Glick HB, Covey KR, Bettigole C, Maynard DS, Thomas SM,

Smith JR, Hintler G, Duguid MC, Amatulli G, Tuanmu MN, Jetz W, Salas C, Stam C, Piotto D, Tavani R, Green S, Bruce G, Williams SJ, Wiser SK, Huber MO, Hengeveld GM, Nabuurs GJ, Tikhonova E, Borchardt P, Li CF, Powrie LW, Fischer M, Hemp A, Homeier J, Cho P, Vibrans AC, Umunay PM, Piao SL, Rowe CW, Ashton MS, Crane PR, Bradford MA. 2015. Mapping tree density at a global scale. Nature **525**, 201-+.

Dejardin A, Laurans F, Arnaud D, Breton C, Pilate G, Leple J. 2010. Wood formation in Angiosperms. Comptes Rendus Biologies **333**, 325-334.

Dejardin A, Leple JC, Lesage-Descauses MC, Costa G, Pilate G. 2004. Expressed sequence tags from poplar wood tissues - a comparative analysis from multiple libraries. Plant Biology **6**, 55-64.

Dejong AJ, Cordewener J, Loschiavo F, Terzi M, Vandekerckhove J, Vankammen A, Devries SC. 1992. A CARROT SOMATIC EMBRYO MUTANT IS RESCUED BY CHITINASE. Plant Cell **4**, 425-433.

Djerbi S, Lindskog M, Arvestad L, Sterky F, Teeri TT. 2005. The genome sequence of black cottonwood (Populus trichocarpa) reveals 18 conserved cellulose synthase (CesA) genes. Planta **221**, 739-746.

Domon JM, Neutelings G, Roger D, David A, David H. 2000. A basic chitinase-like protein secreted by embryogenic tissues of Pinus caribaea acts on arabinogalactan proteins extracted from the same cell lines. Journal of Plant Physiology **156**, 33-39.

Fan D, Liu TT, Li CF, Jiao B, Li S, Hou YS, Luo KM. 2015. Efficient CRISPR/Cas9-mediated Targeted Mutagenesis in Populus in the First Generation. Scientific Reports **5**.

Fisher JB, Stevenson JW. 1981. OCCURRENCE OF REACTION WOOD IN BRANCHES OF DICOTYLEDONS AND ITS ROLE IN TREE ARCHITECTURE. Botanical Gazette **142**, 82-95.

Fournier M, Chanson B, Thibaut B, Guitard D. 1994. MEASUREMENTS OF RESIDUAL GROWTH STRAINS AT THE STEM SURFACE OBSERVATIONS ON DIFFERENT SPECIES. Annales Des Sciences Forestieres **51**, 249-266.

Gantulga D, Ahn YO, Zhou CH, Battogtokh D, Bevan DR, Winkel BSJ, Esen A. 2009. Comparative characterization of the Arabidopsis subfamily a1 beta-galactosidases. Phytochemistry **70**, 1999-2009.

Gantulga D, Turan Y, Bevan DR, Esen A. 2008. The Arabidopsis At1g45130 and At3g52840 genes encode beta-galactosidases with activity toward cell wall polysaccharides. Phytochemistry **69**, 1661-1670.

Gaspar Y, Johnson KL, McKenna JA, Bacic A, Schultz CJ. 2001. The complex structures of arabinogalactan-proteins and the journey towards understanding function. Plant Molecular Biology **47**, 161-176.

Gerttula S, Zinkgraf M, Muday GK, Lewis DR, Ibatullin FM, Brumer H, Hart F, Mansfield SD, Filkov V, Groover A. 2015. Transcriptional and

Hormonal Regulation of Gravitropism of Woody Stems in Populus. Plant Cell **27**, 2800-2813.

Gierlinger N, Goswami L, Schmidt M, Burgert I, Coutand C, Rogge T, Schwanninger M. 2008. In situ FT-IR microscopic study on enzymatic treatment of poplar wood cross-sections. Biomacromolecules **9**, 2194-2201.

Gorshkova T, Mokshina N, Chernova T, Ibragimova N, Salnikov V, Mikshina P, Tryfona T, Banasiak A, Immerzeel P, Dupree P, Mellerowicz EJ. 2015. Aspen tension wood fibers Contain beta-(1->4)-galactans and acidic arabinogalactans retained by cellulose microfibrils in gelatinous walls. Plant Physiology **169**, 2048-2063.

Goswami L, Dunlop JWC, Jungnikl K, Eder M, Gierlinger N, Coutand C, Jeronimidis G, Fratzl P, Burgert I. 2008. Stress generation in the tension wood of poplar is based on the lateral swelling power of the G-layer. Plant Journal **56**, 531-538.

Gritsch C, Wan Y, Mitchell RAC, Shewry PR, Hanley SJ, Karp A. 2015. G-fibre cell wall development in willow stems during tension wood induction. Journal of Experimental Botany **66**, 6447-6459.

Guedes FTP. 2013. Vers l'identification des acteurs moléculaires responsables des propriétés méchaniques du bois de tension de peuplier, PhD thesis, Université d'Orléans

Helliwell C, Waterhouse P. 2003. Constructs and methods for high-throughput gene silencing in plants. Methods **30**, 289-295.

Helliwell CA, Wesley SV, Wielopolska AJ, Waterhouse PM. 2002. High-throughput vectors for efficient gene silencing in plants. Functional Plant Biology **29**, 1217-1225.

Heredia A, Jimenez A, Guillen R. 1995. COMPOSITION OF PLANT-CELL WALLS. Zeitschrift Fur Lebensmittel-Untersuchung Und-Forschung **200**, 24-31.

Hobson N, Deyholos MK. 2013. Genomic and expression analysis of the flax (Linum usitatissimum) family of glycosyl hydrolase 35 genes. BMC Genomics **14**, (23 May 2013).

Hossain MA, Noh H, Kim K, Koh E, Wi S, Bae H, Lee H, Hong S. 2010. Mutation of the chitinase-like protein-encoding AtCTL2 gene enhances lignin accumulation in dark-grown Arabidopsis seedlings. Journal of Plant Physiology **167**, 650-658.

Huang G, Gong S, Xu W, Li W, Li P, Zhang C, Li D, Zheng Y, Li F, Li X. 2013. A fasciclin-like arabinogalactan protein, GhFLA1, is involved in fiber initiation and elongation of cotton. Plant Physiology **161**, 1278-1290.

Isebrands JG, Richardson J. 2014. Poplars and Willows: Trees for Society and the Environment. Poplars and Willows: Trees for Society and the Environment, 1-634.

Jamet E, Canut H, Boudart G, Pont-Lezica RF. 2006. Cell wall proteins: a new insight through proteomics. Trends in Plant Science **11**, 33-39.

Johnson KL, Kibble NAJ, Bacic A, Schultz CJ. 2011. A fasciclin-like arabinogalactan-protein (FLA) mutant of Arabidopsis thaliana, fla1, shows defects in shoot regeneration. PLoS ONE, e25154.

Jourez B. 1997. Le bois de tension, 2. Evaluation quantitative, formation et rôle dans l'arbre. Biotechnologie, Agronomie, Société et Environnement **1** : 167-177.

Jourez B, Riboux A, Leclercq A. 2001. Anatomical characteristics of tension wood and opposite wood in young inclined stems of poplar (Populus euramericana cv 'Ghoy'). Iawa Journal **22**, 133-157.

Kaku T, Serada S, Baba K, Tanaka F, Hayashi T. 2009. Proteomic analysis of the G-layer in poplar tension wood. Journal of Wood Science **55**, 250-257.

Kesari P, Patil DN, Kumar P, Tomar S, Sharma AK, Kumar P. 2015. Structural and functional evolution of chitinase-like proteins from plants. Proteomics **15**, 1693-1705.

Kim J, Daniel G. 2012. Distribution of glucomannans and xylans in poplar xylem and their changes under tension stress. Planta **236**, 35-50.

Kotake T, Dina S, Konishi T, Kaneko S, Igarashi K, Samejima M, Watanabe Y, Kimura K, Tsumuraya Y. 2005. Molecular cloning of a beta-galactosidase from radish that specifically hydrolyzes beta-(1 -> 3)- and beta-(1 -> 6)-galactosyl residues of arabinogalactan protein. Plant Physiology **138**, 1563-1576.

Kumar M, Campbell L, Turner S. 2016a. Secondary cell walls: biosynthesis and manipulation. Journal of Experimental Botany **67**, 515-531.

Kumar S, Stecher G, Tamura K. 2016b. MEGA7: Molecular Evolutionary Genetics Analysis Version 7.0 for Bigger Datasets. Molecular Biology and Evolution **33**, 1870-1874.

Lafarguette F, Leple JC, Dejardin A, Laurans F, Costa G, Lesage-Descauses MC, Pilate P. 2004. Poplar genes encoding fasciclin-like arabinogalactan proteins are highly expressed in tension wood. New Phytologist **164**, 121.

Lamport DTA, Kieliszewski MJ. 2005. Stress upregulates periplasmic arabinogalactan-proteins. Plant Biosystems **139**, 60-64.

Lamport DTA, Varnai P, Seal CE. 2014. Back to the future with the AGP-Ca 2+ flux capacitor. Annals of Botany **114**, 1069-1085.

Lautner S, Zollfrank C, Fromm J. 2012. MICROFIBRIL ANGLE DISTRIBUTION OF POPLAR TENSION WOOD. Iawa Journal **33**, 431-439.

Leple JC, Brasileiro ACM, Michel MF, Delmotte F, Jouanin L. 1992.

TRANSGENIC POPLARS - EXPRESSION OF CHIMERIC GENES USING 4 DIFFERENT CONSTRUCTS. Plant Cell Reports **11**, 137-141.

Li J, Yu M, Geng L, Zhao J. 2010. The fasciclin-like arabinogalactan protein gene, FLA3, is involved in microspore development of Arabidopsis. Plant Journal **64**, 482-497.

Liu H, Shi R, Wang X, Pan Y, Li Z, Yang X, Zhang G, Ma Z. 2013a. Characterization and expression analysis of a fiber differentially expressed fasciclin-like arabinogalactan protein gene in Sea Island cotton fibers. PLoS ONE **8**, e70185.

Liu L, Shang-Guan K, Zhang B, Liu X, Yan M, Zhang L, Shi Y, Zhang M, Qian Q, Li J, Zhou Y. 2013b. Brittle Culm1, a COBRA-Like Protein, Functions in Cellulose Assembly through Binding Cellulose Microfibrils. Plos Genetics **9**.

Love J, Bjorklund S, Vahala J, Hertzberg M, Kangasjarvi J, Sundberg B. 2009. Ethylene is an endogenous stimulator of cell division in the cambial meristem of Populus. Proceedings of the National Academy of Sciences of the United States of America **106**, 5984-5989.

MacMillan CP, Mansfield SD, Stachurski ZH, Evans R, Southerton SG. 2010. Fasciclin-like arabinogalactan proteins: specialization for stem biomechanics and cell wall architecture in Arabidopsis and Eucalyptus. Plant Journal **62**, 689-703.

MacMillan CP, Taylor L, Bi Y, Southerton SG, Evans R, Spokevicius A. 2015. The fasciclin-like arabinogalactan protein family of Eucalyptus grandis contains members that impact wood biology and biomechanics. New Phytologist **206**, 1314-1327.

Macquet A, Ralet MC, Loudet O, Kronenberger J, Mouille G, Marion-Poll A, North HM. 2007. A naturally occurring mutation in an Arabidopsis accession affects a beta-D-galactosidase that increases the hydrophilic potential of rhamnogalacturonan I in seed mucilage. Plant Cell **19**, 3990-4006.

Martin I, Hernandez-Nistal J, Albornos L, Labrador E, Dopico B. 2013. beta III-Gal is Involved in Galactan Reduction During Phloem Element Differentiation in Chickpea Stems. Plant and Cell Physiology **54**, 960-970.

McFarlane HE, Doring A, Persson S. 2014. The Cell Biology of Cellulose Synthesis. Annual Review of Plant Biology, Vol 65 **65**, 69-+.

Mellerowicz EJ, Gorshkova TA. 2012. Tensional stress generation in gelatinous fibres: a review and possible mechanism based on cell-wall structure and composition. Journal of Experimental Botany **63**, 551-565.

Mellerowicz EJ, Immerzeel P, Hayashi T. 2008. Xyloglucan: The Molecular Muscle of Trees. Annals of Botany **102**, 659-665.

Mizrachi E, Maloney VJ, Silberbauer J, Hefer CA, Berger DK, Mansfield SD, Myburg AA. 2015. Investigating the molecular underpinnings underlying morphology and changes in carbon partitioning during tension wood formation

in Eucalyptus. New Phytologist **206**, 1351-1363.

Mokshina N, Gorshkova T, Deyholos MK. 2014. Chitinase-like (CTL) and cellulose synthase (CESA) gene expression in gelatinous-type cellulosic walls of flax (Linum usitatissimum L.) bast fibers. PLoS ONE **9**, e97949.

Mokshina NE, Ibragimova NN, Salnikov VV, Amenitskii SI, Gorshkova TA. 2012. Galactosidase of Plant Fibers with Gelatinous Cell Wall: Identification and Localization. Russian Journal of Plant Physiology **59**, 246-254.

Norberg PH., Meier H. 1966. Physical and chemical properties of the gelatinous layer in tension wood fibers of aspen (Populus tremula L.). Holzforschung **20**: 174-178.

Nishikubo N, Awano T, Banasiak A, Bourquin V, Ibatullin F, Funada R, Brumer H, Teeri TT, Hayashi T, Sundberg B, Mellerowicz EJ. 2007. Xyloglucan endo-transglycosylase (XET) functions in gelatinous layers of tension wood fibers in poplar - A glimpse into the mechanism of the balancing act of trees. Plant and Cell Physiology **48**, 843-855.

Nugroho WD, Nakaba S, Yamagishi Y, Begum S, Marsoem SN, Ko J, Jin Hyun O, Funada R. 2013. Gibberellin mediates the development of gelatinous fibres in the tension wood of inclined Acacia mangium seedlings. Annals of Botany **112**, 1321-1329.

Pauly M, Gille S, Liu LF, Mansoori N, de Souza A, Schultink A, Xiong GY. 2013. Hemicellulose biosynthesis. Planta **238**, 627-642.

Pauly M, Keegstra K. 2016. Biosynthesis of the Plant Cell Wall Matrix Polysaccharide Xyloglucan. Annual Review of Plant Biology, Vol 67 **67**, 235-259.

Persson S, Wei HR, Milne J, Page GP, Somerville CR. 2005. Identification of genes required for cellulose synthesis by regression analysis of public microarray data sets. Proceedings of the National Academy of Sciences of the United States of America **102**, 8633-8638.

Pilate G, Dejardin A, Cornu D, Leple J. 2004. Transgenesis in the poplar: Implications for research on wood development. Biofutur, 49-53.

Pilate G, Guiney E, Holt K, Petit-Conil M, Lapierre C, Leple JC, Pollet B, Mila I, Webster EA, Marstorp HG, Hopkins DW, Jouanin L, Boerjan W, Schuch W, Cornu D, Halpin C. 2002. Field and pulping performances of transgenic trees with altered lignification. Nature Biotechnology **20**, 607-612.

Plomion C, Bastien C, Bogeat-Triboulot MB, Bouffier L, Dejardin A, Duplessis S, Fady B, Heuertz M, Le Gac AL, Le Provost G, Legue V, Lelu-Walter MA, Leple JC, Maury S, Morel A, Oddou-Muratorio S, Pilate G, Sanchez L, Scotti I, Scotti-Saintagne C, Segura V, Trontin JF, Vacher C. 2016. Forest tree genomics: 10 achievements from the past 10 years and future prospects. Annals of Forest Science **73**, 77-103.

Plomion C, Leprovost G, Stokes A. 2001. Wood formation in trees. Plant Physiology **127**, 1513-1523.

Prodhan A, Funada R, Ohtani J, Abe H, Fukazawa K. 1995. ORIENTATION OF MICROFIBRILS AND MICROTUBULES IN DEVELOPING TENSION-WOOD FIBERS OF JAPANESE ASH (FRAXINUS-MANDSHURICA VAR JAPONICA). Planta **196**, 577-585.

Rennie EA, Scheller HV. 2014. Xylan biosynthesis. Current Opinion in Biotechnology **26**, 100-107.

Roach MJ, Deyholos MK. 2008. Microarray analysis of developing flax hypocotyls identifies novel transcripts correlated with specific stages of phloem fibre differentiation. Annals of Botany **102**, 317-330.

Roach MJ, Mokshina NY, Ajay B, Snegireva AV, Hobson N, Deyholos MK, Gorshkova TA. 2011. Development of cellulosic secondary walls in flax fibers requires beta-galactosidase. Plant Physiology **156**, 1351-1363.

Roudier F, Fernandez AG, Fujita M, Himmelspach R, Borner GHH, Schindelman G, Song S, Baskin TI, Dupree P, Wasteneys GO, Benfey PN. 2005. COBRA, an Arabidopsis extracellular glycosyl-phosphatidyl inositol-anchored protein, specifically controls highly anisotropic expansion through its involvement in cellulose microfibril orientation. Plant Cell **17**, 1749-1763.

Roussel JR, Clair B. 2015. Evidence of the late lignification of the G-layer in Simarouba tension wood, to assist understanding how non-G-layer species produce tensile stress. Tree Physiology **35**, 1366-1377.

Ruelle J, Beauchene J, Yamamoto H, Thibaut B. 2011. Variations in physical and mechanical properties between tension and opposite wood from three tropical rainforest species. Wood Science and Technology **45**, 339-357.

Ruelle J, Yoshida M, Clair B, Thibaut B. 2007. Peculiar tension wood structure in Laetia procera (Poepp.) Eichl. (Flacourtiaceae). Trees-Structure and Function **21**, 345-355.

Sanchez-Rodriguez C, Bauer S, Hematy K, Saxe F, Ibanez AB, Vodermaier V, Konlechner C, Sampathkumar A, Ruggeberg M, Aichinger E, Neumetzler L, Burgert I, Somerville C, Hauser MT, Persson S. 2012. CHITINASE-LIKE1/POM-POM1 and Its Homolog CTL2 Are Glucan-Interacting Proteins Important for Cellulose Biosynthesis in Arabidopsis. Plant Cell **24**, 589-607.

Showalter AM. 1993. STRUCTURE AND FUNCTION OF PLANT-CELL WALL PROTEINS. Plant Cell **5**, 9-23.

Showalter AM. 2001. Arabinogalactan-proteins: structure, expression and function. Cellular and Molecular Life Sciences **58**, 1399-1417.

Showalter AM, Basu D. 2016. Extensin and Arabinogalactan-Protein Biosynthesis: Glycosyltransferases, Research Challenges, and Biosensors. Frontiers in Plant Science **7**.

Staehelin C, Schultze M, Kondorosi E, Mellor RB, Boller T, Kondorosi A. 1994. Structural modifications in Rhizobium meliloti Nod factors influence their stability against hydrolysis by root chitinases. Plant Journal **5**, 319-330.

Sundell D, Mannapperuma C, Netotea S, Delhomme N, Lin YC, Sjodin A, Van de Peer Y, Jansson S, Hvidsten TR, Street NR. 2015. The Plant Genome Integrative Explorer Resource: PlantGenIE.org. New Phytologist **208**, 1149-1156.

Takemoto D, Furuse K, Doke N, Kawakita K. 1997. Identification of chitinase and osmotin-like protein as actin-binding proteins in suspension-cultured potato cells. Plant and Cell Physiology **38**, 441-448.

Tan L, Eberhard S, Pattathil S, Warder C, Glushka J, Yuan CH, Hao ZY, Zhu X, Avci U, Miller JS, Baldwin D, Pham C, Orlando R, Darvill A, Hahn MG, Kieliszewski MJ, Mohnen D. 2013. An Arabidopsis cell wall proteoglycan consists of pectin and arabinoxylan covalently linked to an arabinogalactan protein. Plant Cell **25**, 270-287.

Timell TE. 1969. CHEMICAL COMPOSITION OF TENSION WOOD. Svensk Papperstidning-Nordisk Cellulosa **72**, 173-&.

Tuskan G, DiFazio S, Jansson S, Bohlmann J, Grigoriev I, Hellsten U, Putnam N, Ralph S, Rombauts S, Salamov A, Schein J, Sterck L, Aerts A, Bhalerao R, Bhalerao R, Blaudez D, Boerjan W, Brun A, Brunner A, Busov V, Campbell M, Carlson J, Chalot M, Chapman J, Chen G, Cooper D, Coutinho P, Couturier J, Covert S, Cronk Q, Cunningham R, Davis J, Degroeve S, Dejardin A, Depamphilis C, Detter J, Dirks B, Dubchak I, Duplessis S, Ehlting J, Ellis B, Gendler K, Goodstein D, Gribskov M, Grimwood J, Groover A, Gunter L, Hamberger B, Heinze B, Helariutta Y, Henrissat B, Holligan D, Holt R, Huang W, Islam-Faridi N, Jones S, Jones-Rhoades M, Jorgensen R, Joshi C, Kangasjarvi J, Karlsson J, Kelleher C, Kirkpatrick R, Kirst M, Kohler A, Kalluri U, Larimer F, Leebens-Mack J, Leple J, Locascio P, Lou Y, Lucas S, Martin F, Montanini B, Napoli C, Nelson D, Nelson C, Nieminen K, Nilsson O, Pereda V, Peter G, Philippe R, Pilate G, Poliakov A, Razumovskaya J, Richardson P, Rinaldi C, Ritland K, Rouze P, Ryaboy D, Schmutz J, Schrader J, Segerman B, Shin H, Siddiqui A, Sterky F, Terry A, Tsai C, Uberbacher E, Unneberg P, Vahala J, Wall K, Wessler S, Yang G, Yin T, Douglas C, Marra M, Sandberg G, Van de Peer Y, Rokhsar D. 2006. The genome of black cottonwood, Populus trichocarpa (Torr. & Gray). Science **313**, 1596-1604.

Van Acker R, Vanholme R, Storme V, Mortimer JC, Dupree P, Boerjan W. 2013. Lignin biosynthesis perturbations affect secondary cell wall composition and saccharification yield in Arabidopsis thaliana. Biotechnology for Biofuels **6**.

van Hengel AJ, Tadesse Z, Immerzeel P, Schols H, van Kammen A, de Vries SC. 2001. N-acetylglucosamine and glucosamine-containing arabinogalactan proteins control somatic embryogenesis. Plant Physiology **125**, 1880-1890.

Verbelen JP, Vissenberg K, Kerstens S, Le J. 2001. Cell expansion in the epidermis: microtubules, cellulose orientation and wall loosening enzymes.

Journal of Plant Physiology **158**, 537-543.

Wagberg L, Annergren G. 1997. Physicochemical characterization of papermaking fibres. Fundamentals of Papermaking Materials, Vol 1, 1-82.

Wang H, Jiang C, Wang C, Yang Y, Yang L, Gao X, Zhang H. 2015. Antisense expression of the fasciclin-like arabinogalactan protein FLA6 gene in Populus inhibits expression of its homologous genes and alters stem biomechanics and cell wall composition in transgenic trees. Journal of Experimental Botany **66**, 1291-1302.

Yamamoto H. 2004. Role of the gelatinous layer on the origin of the physical properties of the tension wood. Journal of Wood Science **50**, 197-208.

Ye ZH, Zhong RQ. 2015. Molecular control of wood formation in trees. Journal of Experimental Botany **66**, 4119-4131.

Zang LN, Zheng TC, Chu YG, Ding CJ, Zhang WX, Huang QJ, Su XH. 2015. Genome-Wide Analysis of the Fasciclin-Like Arabinogalactan Protein Gene Family Reveals Differential Expression Patterns, Localization, and Salt Stress Response in Populus. Frontiers in Plant Science **6**.

Amra ŠEĆEROVIĆ

Identification et caractérisation des acteurs moléculaires potentiellement responsables pour des propriétés mécaniques du bois de tension

Résumé:

Le but de cette thèse était d'identifier les mécanismes moléculaires responsables des propriétés particulières de la couche G et les propriétés mécaniques remarquables du bois de tension (BT). Trois acteurs moléculaires potentiels (des protéines à arabinogalactane avec domaine fasciclin-like (FLA), une protéine chitinase-like (CTL) et une β-galactosidase (BGAL)) ont été choisis et étudiés dans: analyse phylogénétique, analyses d'expression et caractérisation de peupliers transgéniques affectés dans l'expression de chacun de ces acteurs. La caractérisation fine de ce matériel a révélé que CTL2 et les FLA jouent un rôle dans la régulation de la cristallinité de la cellulose dans le BT. CTL2 apparaît également important dans l'organisation de la paroi cellulaire et des propriétés mécaniques des tiges. BGAL a été avant proposé pour une fonction dans modification de pectine RG-I potentiellement important pour des propriétés mécaniques de BT. Le bois de tension exhibe une activité BGAL plus élevée que dans le bois opposé. L'inhibition par RNAi de l'expression de BGAL7, spécifiquement exprimée dans le BT, n'est pas responsable à lui seul de la forte activité BGAL présente dans le BT. En contrepoint à l'étude menée sur le peuplier, nous avons également évalué la présence d'acteurs moléculaires potentiellement responsables des propriétés mécaniques du BT chez le simarouba qui développe dans leur BT des fibres ayant leurs sous-couches de la paroi intermédiaire entre la G et la S2. Des protéines à arabinogalactanes ainsi que des pectines du type RG-I sont présentes dans les fibres de BT de peuplier et de simarouba et pourraient avoir une fonction dans un mécanisme commun de génération des contraintes dans le BT. Finalement, un modèle est proposé sur le rôle présumé des différents acteurs moléculaires étudié dans la régulation des propriétés de la couche G et la génération des fortes contraintes du bois de tension.

Mots clés: peuplier, simarouba, couche G, FLA, CTL, BGAL

Identification and characterization of molecular players potentially responsible for the mechanical properties of tension wood

Summary:

The aim of this thesis was to approach the underlying molecular mechanisms responsible for the particular properties of the G-layer and the outstanding mechanical properties of tension wood (TW). Accordingly, three potential molecular players (fasciclin-like arabinogalactan protein (FLA), chitinase-like protein (CTL) and β-galactosidase (BGAL)) were chosen and studied through a phylogenetic analysis, expression analyses and most importantly characterization of RNAi transgenic poplars. This multilevel characterization revealed that CTL2 and FLAs have function in the regulation of cellulose crystallinity in TW. CTL2 was also shown to be important both for the cell wall organization and stem mechanical properties. BGAL was studied in a light of the previously reported modifications of RG-I pectin, potentially important for the mechanical properties of TW. Study of BGAL revealed that the enzyme has higher activity in TW than in opposite wood. BGAL7, whose gene was expressed specifically in TW, does not seem to be responsible for the higher BGAL activity in TW. In comparison to poplar, we analyzed the occurrence of molecular players potentially responsible for TW mechanical properties in simarouba, a tropical species, which develops different TW fiber. Arabinogalactan proteins and RG-I pectin potentially targeted by BGAL were localized in TW fibers both in poplar and simarouba and therefore may be involved in a common mechanism of tensile stress generation in different TW types. A model was finally proposed to elucidate a potential function of the studied molecular players in the regulation of G-layer properties and tensile stress generation.

Keywords: poplar, simarouba, G-layer, FLA, CTL, BGAL

AGPF, INRA Val de Loire
2163 Avenue de la pomme de pin, CS 40001
Ardon, 45075 Orléans Cedex 2, France